UNIVERSITEIT VAN PRETORIA
UNIVERSITY OF PRETORIA
YUNIBESITHI YA PRETORIA
Faculty of Engineering, Built Environment and Information Technology

Fundamental Study of Taphole Clay Behaviour with Respect to the Binder System and Evaluation of Alternative Non-Toxic Binders

by

Izak Jian-Pierre Cameron

A thesis submitted in partial fulfilment of the requirements for the degree of

Doctor of Philosophy

in the Department of Materials Science and Metallurgical Engineering,

Faculty of Engineering, Built Environment and Information Technology

University of Pretoria

Supervisor: Professor Andrie M. Garbers-Craig

Co-supervisor: Dr. Shatish Ramjee

May 2024

Abstract

The aim of this study was to determine the critical properties that a binder for use in taphole clay should have, identify alternative non-toxic binders that could potentially replace the currently used toxic high-temperature coal tar (CTht), and evaluate taphole clays in which these alternative non-toxic binders were used.

The work presented in the first part of this thesis investigates the behaviour of the CTht. Analytical techniques were employed to describe the molecular composition and toxicity (Fourier-transform infrared spectroscopy, gas chromatography-mass spectroscopy; targeted and untargeted), thermal behaviour (thermogravimetric analysis, differential scanning calorimetry) and rheological properties of this binder. A set of alternative binders from various sources, including coal sources (a coal tar pitch-merisol oil blend, a low-PAH synthetic coal tar pitch), petroleum sources (a crude waxy oil, a distilled crude waxy oil, a mesophase-forming pitch), wood/plant sources (a beechwood tar, a pinewood tar, a vegetable tar), and a glycerine-resole resin mixture, were then considered and evaluated as non-toxic alternatives to CTht. Using a ranking system based on the results from the analytical techniques, the most suitable non-toxic binders to CTht were identified. The results indicated that the binders had molecular structures that were either cyclic aromatic hydrocarbons (aromatic benzene), chain hydrocarbons (aliphatic), or a combination of both. The toxicity (BE-values) ranged from 0.03-1.67 with the coal-based binders having the highest toxicity values. The thermal analysis indicated an average mass loss of the binders ranging from 0.28-1.79 g/°C with the glycerine-based binders having the highest average mass loss. Rheology results indicated that the vegetable tar and pinewood tar had limited thermal stability to be used as binders and was disqualified as potential alternative binders. The characterization and ranking process indicated that beechwood tar and a glycerine-resole resin mixture were the most suitable replacements for CTht in taphole clay, with BE-values (toxicity) of zero. Pinewood and vegetable tars were disqualified as potential binder replacements due to their limited thermal stability.

In the second part of this thesis, the evaluation of the top two selected non-toxic alternative binders in a taphole clay formulation is discussed. Both non-standardized tests (workability and extrusion pressure ageing, hardenability, strength development) and standardized tests (volatile organic compounds, cold crushing strength, apparent porosity, carbon yield) were used to describe the behaviour of the taphole clay and the changes that occur due to the binder substitutions. Mixing procedures during the pilot-scale manufacturing of the taphole clay highlighted that beechwood tar was not a suitable binder for use in taphole clay. The crude waxy oil and the glycerine-resole resin mixture were selected to be evaluated in the taphole clay. The glycerine and phenolic resin binder caused the lowest decay in plasticity (7%) and smallest increase in extrusion pressure (17.5%) during aging of the THC. Thermal ageing results indicated that glycerine and phenolic resin binder had the lowest hardenability whilst the crude waxy oil had a higher hardenability. The strength development results indicated insufficient strength development for the crude waxy oil-containing clay which was manifested in the fact that the sample could not keep its shape after firing. The glycerine and phenolic resin binder clay had comparative compressive strength values (2.4 MPa) compared to the reference clay sample (3.1 MPa). The clay containing glycerine and phenolic resin binder had a lower volatile organic compound release. The taphole clay evaluations confirmed that the glycerine-

resole mixture was the most suitable replacement for CTht in taphole clay due to similar process parameters (workability and extrusion pressure ageing, hardenability, strength development) as well as standardized test results showing similar performance to the clay with the CTht binder.

ACKNOWLEDGEMENTS

The work presented in this thesis is the result of the collaboration of several individuals and an excellent support network, which made this undertaking a reality. My hope for this work is that it will further advance developments in the field of refractories and contribute to the literature of taphole clay refractory materials. I extend my thanks to the following individuals/organizations:

1. My supervisor: Prof. Andrie M. Garbers-Craig saw a young undergraduate engineer's potential and nurtured and encouraged it to be further developed. I cannot put into words how much your guidance and diligence have contributed towards my professional and personal development. I hope that I can one day provide the same mentorship as you did, to help and promote the new generation of researchers in refractories.
2. My co-supervisor: Dr. Shatish Ramjee. Thanks for your guidance with my experimental work and always being available for me to get your input. Your unwavering devotion to see me advance has greatly contributed to the quality of this thesis. Thanks for the coffee sessions and online chats to help me keep going and have a platform to reflect.
3. My funder: Anglo American Platinum. As a recipient of funding from the Anglo American Chair in Pyrometallurgy (chaired by Prof. Garbers-Craig), I would like to express my gratitude to the organization for providing me with the funding and technical expertise to advance this work and being able to finish the thesis. Additionally, I am thankful for the travel funding that allowed me to present this work at multiple conferences, gaining the needed exposure and facilitating the publication of this work.
4. Language editing: Prof. Kathryn Sole (Sole Consulting). Thanks to Prof. Sole for her contribution to the language editing of this thesis. Your contribution has enhanced the quality of this work.
5. My family. Your unwavering support and encouragement has seen me through tough times during this journey, which without I would not have been able to conclude. Thanks to my parents, Amanda & Izak Cameron for always supporting me in my academic career, and my choices to advance my career. To my partner, Johan van Huyssteen, I also thank you for being my Nr.1 Fan and constantly showing me the light in the long tunnel, which we as PhD researchers travel during our time of study. To all my other comrades, thank you for sharing experiences and having a platform to talk and reflect.
6. My colleagues at Elkem. During my PhD journey, I was fortunate enough to be granted an opportunity to advance my career as a researcher in refractories at Elkem ASA. To all my colleagues, friends and mentors, thank you for your support and constant encouragement to see me through one of the toughest times of transition and to complete my PhD. You are all pillars of support and shall remain so in the near future.
7. *Lastly, but not the least: The Lord. This thesis is a gift to you. I am gifted with talents from Him, which I use to advance the field in which I work but also to help the people around me. Your involvement in my life has shaped me into the person that I am today, and your voice through your parental support has enabled me to continue even in times of doubt. The result of what I have achieved and who I am today, is thanks to you.*

Table of Contents

List of Figures

List of Tables

List of Abbreviations

- AP: Apparent porosity.
- BE: Benzene equivalent.
- BEI: Biological exposure index.
- CCS: Cold crushing strength.
- CMR: Carcinogenic, mutagenic and reprotoxic.
- CP: Coal tar pitch.
- CP-HS: Hexane soluble part of coal tar pitch.
- CP-TI: Toluene insoluble part of coal tar pitch.
- CP-TS: Toluene soluble part of coal tart pitch.
- CT: Coal tar; term referred to general tar produced from the coking process in iron-and steelmaking.
- CTht: Coal tar derived from coking coal furnaces, specifically for use in taphole clay; crude source.
- CTP: Coal tar pitch; term referred to general pitch derived from coal tar source.
- CTPht: Coal tar pitch distilled from coal tar from coking coal furnaces, specifically for use in taphole clay; refined source.
- CTPht-B: Coal tar pitch-oil blend derived from coal tar from coking coal furnaces. Pitch has a high softening point that is lowered by mixing with a coal-source oil to alter the chemical composition and softening point.
- CWO: Crude waxy oil.
- EcoP: Low-PAH synthetic pitch.
- EPA: United States Environmental Protection Agency.
- Gly: Glycerine.
- Gly+XG: Xanthan gum plasticized with glycerine.
- Gly+XG+PFR: Xanthan gum plasticized with glycerine and mixed with phenol-formaldehyde resole resin.
- H-MoR: Hot modulus of rupture.
- MEP: Marshall extrusion pressure.
- MoR: Modulus of rupture.
- MP: Mesophase-forming pitch.
- PAH: Polycyclic aromatic hydrocarbons.
- PCWO: Processed crude waxy oil.
- PEG: Polyethylene glycol.
- PEL: Permissible exposure limit.
- PFR: Phenol-formaldehyde resole resin.
- PG: Propylene glycol.
- PGM: Platinum group metals.
- QI: Quinoline insolubility.
- SDP: Strength development profile.
- Tar-BW: Beechwood tar; Kraft process byproduct.
- Tar-PW: Pinewood tar; Kraft process byproduct.
- Tar-Veg: Vegetable tar; byproduct from vegetable fermentation.
- THC: Taphole clay.
- VOC: Volatile organic compounds.
- WAT: Waxy-appearance temperature.
- WHO: World Health Organization.
- XG: Xanthan gum.

Chapter 1

Introduction

"Do the best you can until you know better. Then when you know better, do better " ~ Maya Angelou

1. Introduction

In the last two decades, refractory materials have been changing, with more emphasis being placed on new product development and strengthening niche market shares that give one refractory manufacturer a competitive advantage over another. One refractory material that has recently received more research efforts is taphole clay (THC). This monolithic composite carbonaceous clay material is used to create a semi-permanent seal in a taphole during smelting. Understanding these materials has become somewhat of an art because fundamental research and intricacies of composition and functionalities have not yet been extensively published compared with those of other refractory materials. Some research entities have taken on the task of reforming and developing taphole clays that are less toxic to the environment and the health of persons handling the materials. Until the last few decades, THC materials made use of very primitive binders, such as coal tar or water (Perez, 2004). Advances that followed used more advanced binders to better control process stability during tapping. These include temperature-sensitive resins (phenolic resins) and/or coal tar (CTht), or distilled versions of coal tar such as high-temperature cold tar pitch (CTPht) (Kageyama et al., 2005; Otsubo et al., 2010; Kitamura, 2014). Although the use of tar is most favoured owing to its wide volatilisation temperature range and carbonising properties, THC manufacturers are being encouraged to reduce or eliminate use of polycyclic aromatic hydrocarbon (PAH)-containing binders due to their associated dangers to the environment and human health.

The composition of cold tar pitch is extremely complex. Some functional groups that have been heavily scrutinised are benzo(a)pyroxene and associated PAH. These liquids are identified as Group I carcinogens by the World Health Organization (WHO) and cause harm to the health of persons who inhale these on a frequent basis (United States Department of Labour, 2012). The use of phenolic resins in THC also poses a risk due to the undesirable release of free phenolics into the environment. Because of these hazards, most research in THC has involved looking for suitable non-toxic alternatives to tar/pitch and phenolic resins. Although there has been a lot of success in eliminating the use of tar and reducing use of phenolic resins, few findings have been published.

The work described in this thesis aims to identify non-toxic alternative binders that can replace CTht/CTPht for use in THC to reduce exposure to PAH of persons working with this material. The investigation assessed the behaviour of a reference binder (CTht) currently used in THC and compared alternative binders. Two groups of binders were investigated: carbonaceous binders and glycerine-based binders. A ranking system was used to identify the most suitable binder to replace CTht based on composition, thermal, and rheology evaluations, and an alternative from each group of binders was proposed. These alternative binders and the reference were used in a THC formulation to characterize the liquid clay behaviour and compare properties of the alternative binder clay formulations. The work presented in this thesis strived to improve understanding of THC and how this can be used to improve functionality of the product; more specifically, this work considered the effect of binders on the THC properties as applicable to a platinum-group metal (PGM) smelting operation.

Chapter 2

Literature

"Go wisely and slowly. Those who rush stumble and fall" - William Shakespeare

2. Literature review

2.1. Constitution of taphole clays

THC, also commonly referred to as a ramming mass, is a composite carbonaceous refractory material that is used to close the taphole of a smelting vessel after tapping. THC is classified as a monolithic refractory and so has similar attributes to those of castables that use hydraulic-setting binders. The material has a high plasticity, adhesion, and non-wetting properties (Otsubo et al., 2010). THC is used in all major smelting operations where containment of a molten fluid is temporary facilitated by closure of an exit stream, primarily through a taphole. THC is used in blast furnace operations, ferrous and non-ferrous smelting, platinum smelting and refining, and many other smelting and refining operations (Geyer & Halifa, 214; Nelson & Hundermark, 2014; Sutherland & Gous, 2018; Steenkamp, 2018).

The composition of a THC consists of aggregates (> 1 mm), a matrix (45 µm to 1 mm), ultra fines (< 45 µm), additives, and binders (Cameron, 2021). The additives form part of the matrix and can be complex, depending on the furnace conditions and corrosivity of the slag. The particle size distribution of a THC is similar to that of a conventional self-flow castable with a particle size distribution coefficient or q-value of 0.21–0.26 (Cameron, 2021). The self-flow nature of the clay lowers the extrusion pressure requirement and assists with flow of the clay during ramming. The resultant non-Newtonian behaviour (de Pretto & Lindstad, 2022) is not affected by the slow extrusion rate, in contrast to the problems of dilatancy experienced with conventional castables, where mixer shear rates are much higher. Aggregate types and different matrix constituents are discussed in Sections 2.1.1 and 2.1.2, respectively.

2.1.1. Aggregate

The aggregate part of a refractory composition has four main functions: 1) structural stability; 2) abrasion resistance; 3) chemical resistance; 4) sintering enhancement (Cameron, 2021). Although the matrix is responsible for most of the sintering strength of a THC, the particle size distribution of the clay influences the sintering properties, which can assist with tap-hole processes (Gupta et al., 2014), such as holding times and drilling practice (discussed in Section 1) (Otsubo et al., 2010). Table 2.1 shows typical aggregates that are used in THC, with their major composition constituents and classification.

Table 2.1: Typical aggregate types used in taphole clays (Cameron, 2021)

Type	Composition (%)	Classification
Sintered alumina	Al_2O_3: > 99	High-grade aggregate
Fused alumina	Al_2O_3: 95–99	High-grade aggregate
Calcined bauxite	Al_2O_3: 75–90	Medium- to high-grade aggregate
Andalusite Sintered andalusite (mulcoa)	Al_2O_3: 35–65	Medium-grade aggregate
Calcined clay	Al_2O_3: 20–40	Low- to medium-grade aggregate
Fused silica	SiO_2: > 99	High-grade aggregate*
Silicon Carbide	SiC: > 97%	High-grade aggregate** Abrasion
Zirconia–mullite (AZS)	Al_2O_3: 50–75 SiO_2: 20–40 ZrO_2: 5–30	High-grade aggregate** Thermal stability Thermal shock resistance

*Specifically, for FeCr taphole; ** Special smelting requirements

2.1.2. Matrix

The matrix of a THC comprises an intricate combination of constituents with different functionalities. Typical matrix components and their functionalities are given in Table 2.2. The specific composition, particle size range, and combination of additives depends not only on the slag chemistry of the smelting vessel, but also on process-related parameters, such as drilling time, THC length, thermal expansion, gas penetration, operating temperature, taphole operations, taphole size, vessel size, and internal pressure (Otsubo et al., 2010; Gupta et al., 2014; Cameron, 2021). Increasing demand on smelting operations to maintain production targets has seen a move to more robust matrix components, such as ferrosilicon nitride, combined with special additives, such as sintered reactive alumina and boron carbide, to further enhance the strength of the THC (Cameron, 2021).

Table 2.2: Typical matrix constituents and additives used in taphole clay (Cameron, 2021)

Matrix constituent	Matrix content (%)	Function
Filler (bauxite, fired andalusite, calcined clay)	15–30	Sintering strength, bulk density increase, volume stability
Metakaolin, bentonite clay	5–10	Plasticizer (workability), sintering aid, volume stability
Coal, coke	5–10	Permeability, sintering strength (carbon network), non-wettability
Silicon carbide	10–15	Abrasion and chemically inert
Zirconia	5–10	Volume stability, corrosion resistance (open porosity)
Ferrosilicon nitride	2	Sintering aid (erosion, strength)
Aluminium, silicon	1–1.5	Antioxidant

2.1.3. Binders

The use of THC materials to close furnace tapholes started from as early as the 19th century. With the progression of processes like iron and steel smelting, more demanding process conditions arose, which initiated development of more technically advanced THC materials. The first THC material utilised in furnaces was primitive, in that it only contained natural clay, which had high concentrations of fluxing alkali oxides, and used water as a binder (Cameron, 2021; Siva et al., 2018). Some countries in Africa still make use of naturally occurring materials, such as bees wax and ants' nests that are mixed with water and used as a tap-hole ramming material (Cameron, 2021). As smelting processes developed, the maintenance of tap holes became more focused and better taphole materials were needed.

The first THC materials that were superior to water-based materials were those containing ceramic aggregate, additives, and CTht (and resin). The use of CTht or CTPht as binders for THC materials started in the early 1900s when byproducts from coke processing needed a use. Their high coking value, viscoelasticity, and gradual volatilisation made these products perfect for use in taphole materials because these are amongst the most important attributes that a binder needs to fulfil. A high coking value ensures that residual carbon remains in the taphole mass after firing to assist with strength of the material; a relatively high viscosity assists with plasticity of the clay; gradual volatile release ensures minimal porosity and avoids abrupt evolution of volatile species in the binder, which could cause a pressure differential inside the taphole and create an unfavourable environment inside the furnace.

The inclusion of a temperature-sensitive resin (such as resole, novolac, or epoxy) (Nelson & Hundermark, 2014; Hsissou et al., 2021; Sharp & Harper, 1993) as part of the binder started when stricter casting, drilling, and holding times needed to be maintained. To ensure shorter turn-around times on the furnaces and increased tonnages of

molten material, development of resin-bonded clays started in the 1980s (Siva et al., 2018). The use of resole resin could ensure low-temperature (< 200°C) green strength, which enables adjusted holding times in relation to furnace requirements, and the formation of a carbon structure on firing, which assists with high-temperature strength.

Although the use of CTht/CTPht and phenolic resins as binders in most THC materials shows satisfactory results during operation, the health and environmental impacts associated with these raw materials are severe. Most CTht/CTPht primarily result from coke processing, which, by nature, contain carcinogens, such as PAH (Andreikov et al., 2008; Wang et al., 2017). These liquids are problematic in the manufacturing of clay materials, during which individuals are exposed to dangerous levels of PAH (Wang et al., 2017; Andreikov et al., 2008) during the ramming process in smelting. The use of phenolic resins, such as resole and novolac, is also problematic in that some contain residual phenol, which, when handled during manufacturing, can be dangerous to the operator (Coutouly & Feng, 2007). During the manufacture of phenolic resin, phenol and formaldehyde are mixed in certain ratios and a resin liquid is formed by condensation (Cameron, 2021). Phenol and formaldehyde are both dangerous: sustained exposure has an adverse effect on the health of persons working with these materials during manufacturing and use in the taphole area (Coutouly & Feng, 2007; Sarika et al., 2020). Formaldehyde that is released into the atmosphere has a negative ecological effect (Sarika et al., 2020). When using a phenolic resin such as resole in THC materials, the resin is only toxic if it contains free phenol and sustained exposure of this chemical occurs (Wang et al., 2017). The use of novolac resin in THC materials is somewhat less problematic because this is in solid form; however, depending on the hardener used to cross-link the resin, it can also be toxic.

The carcinogenic nature of both CTht and CTPht (Lindstad, 2018; Andreikov et al., 2008; Wang et al., 2017) and phenolic resole resin (Coutouly & Feng, 2007) makes these undesirable raw materials for use in carbon refractories. In most of Europe and America, use of CTP is restricted to certain applications, and limitations on exposure exist as permissible exposure limits (PEL). Around one third of the consumption of coal tar/pitch is in the graphite electrode industry, where pitch is used as temporary binder. Phenolic resins are used in many other applications, but their toxic nature makes these undesirable for clay production. According to European legislation, regulations, and administrative provisions for labelling and packaging of dangerous substances, CTht and CTPht and phenolic resins are considered carcinogenic, mutagenic, and toxic for reproduction (CMR). The aromatic structure of CTPht is under scrutiny with regards to carcinogenicity, similar to that of benzo(a)pyrene (Ba-P); for phenolic resins, both phenol and formaldehyde are potentially problematic as raw materials (Coutouly & Feng, 2007). PAH are associated with widespread carcinogenicity owing to their introduction of mutations in oncogenes that may result in tumour formation (Baird et al., 2005). This indicates that any PAH present in CTht/CTPht is considered dangerous. Previous limits of exposure were 100 ppm for BaP (Wang et al., 2017; Coutouly & Feng, 2007), < 1% for phenol, and < 0.2% for formaldehyde (Coutouly & Feng, 2007) over 8 h; as advances in biomass binders progressed and environmental legislation became stricter, these limits have been reduced. The current exposure limits are < 2000 ppb for BaP (Cherrie et al., 2011), < 2 ppm for phenol (Danish Ministry of Environment, 2014), and < 0.3 ppm for formaldehyde (Formacare, 2019). Any precautionary measures for exposure to carcinogens in CTht/CTPht should include the 16 PAH species defined by the US Environmental Protection Agency (16-EPA-

PAH) and eight PAH species defined by the European Union (EU): both regulatory bodies consider these as dangerous (Andreikov et al., 2008). A comparative descriptor known as the benzene equivalent (BE/BEI) is used to refer to the toxic nature of a substance, such as CTht/CTPht, and includes all PAH compounds that are carcinogenic according to 16-EPA-PAH (Andreikov et al., 2008). The BE toxicity coefficient is calculated as shown in Equation 2.1 (Andreikov et al., 2008):

$$BE = 1.00C_{BaP} + 0.034C_F + 0.033C_{BaA} + 0.26C_C + 0.10C_{BbF} + 0.05C_{BeP} + 0.10C_{IP} + 1.40C_{DBA} + 1.00C_{BP}, \quad (2.1)$$

where C_{BaP} is the mass% benzo(a)pyrene, C_F is the fluoranthene content, C_{BaA} is the benzo(a)anthracene content, C_C is chrysene, C_{BbF} is benzo(b)fluoranthene content, C_{BeP} is benzo(e)pyrene content, C_{IP} is the indeno(1,2,3-cd)pyrene content, C_{DBA} is dibenzo(a,h)anthracene, and C_{BP} is the content of benzo(g,h,i)perylene.

The toxic nature of CTht, CTPht, and phenolic resole resins has shifted research of taphole products to design or propose alternative less-toxic (lower exposure to PAH, phenol, and formaldehyde) binders for both the resin and tar/pitch. Some conventional alternatives for CTht/CTPht include distilled CTP, synthetic pitch, biomass pitch (derived from wood and vegetables), lower-PAH petroleum pitch, and waxy-type liquids (Lindstad, 2018; Wang et al., 2017; Murilo, 2009; Mannweiler & Perruchoud, 1997; Acuna & Marzin, 1997; Roder, 1998; Apicella et al., 2017). Alternative biomass raw materials are being used for phenolic resins. Alternative raw materials for both phenol and formaldehyde are expensive and, depending on the source, replacement of either raw material in the resin composition can be varied accordingly. Phenol alternatives include lignin, tannin, and cardanol; alternatives to formaldehyde include hydroxymethylfurfural (HMF), furfural, and glyoxal (Sarika et al., 2020; Siddiqui et al., 2017; Huang, 2019). Unfortunately, due to the reduced reactivity of these alternatives, the eco-friendlier phenolic resins manufactured for these applications only include partial substitution of either or both phenol and formaldehyde (Sarika et al., 2020).

2.1.3.1. Carbonaceous liquid binder

The history of THC using carbon binders is extensive. From as early as the 1980s, low softening-point coal tar or pitch has been the preferred binder for these materials. As phenolic resins gained traction in the refractories industry in the 1990s, introduction of these as binders (resin-bonded) and alternative combinations with coal tar or coal tar pitch became the norm (Nelson & Hundermark, 2014). In the early 2000s, most clay manufacturers in Japan and Canada moved back to CTPht-bonded clays; combinations of resin-bonded and resin-pitch-bonded clay were used in Europe (Nelson & Hundermark, 2014). The playoff between resin-bonded and resin-pitch-bonded clays has been a topic of interest in binder research. Although there are benefits to using phenolic resin as a binder, there are also process drawbacks that can make placement and tap-hole processes difficult. Table 2.3 highlights advantages and disadvantages of tar- and resin-bonded THC materials.

Table 2.3: Comparative advantages and disadvantages of coal tar/pitch and phenolic resin as binders for taphole clay materials (Nelson & Hundermark, 2014; Sarika et al., 2020; Katovic, 1967)

Coal tar/pitch-bonded clay	
Advantages	Disadvantages
1. Thermoplastic 2. High plasticity 3. Improved adhesive strength 4. Form a transition-free union with tap-hole carbon bricks 5. Excellent thermal conductivity 6. Non-wetting by metal or slag 7. Less wastage of clay material (drying ability) 8. Aging of pitch occurs over a long time if temperatures are below 60°C	1. Requires heating to increase workability of clay 2. Cast times are long (> 2 h) 3. Dwell times are long 4. Toxic (PAH) 5. Uncontrolled quality of liquid pitch (byproduct) • Moisture • Viscosity • Softening point • Calorific value or carbon content
Resin-bonded clays	
1. Faster curing times (improved dwell times) 2. Shorter cast times (improved production capacity) 3. Less toxic binder than CTPht	1. Increase drilling time (capacity reduced) if excess resin is used 2. Quick curing clays increase tap-hole temperatures 3. Quick curing clays cause reduced tap-hole clay lengths 4. Quick curing clays have increased wastage 5. Undesirable volatility on heating 6. Only successfully used on blast furnace applications (no PGM or FeCr smelting) 7. Shelf life of resin is shorter than CTPht 8. Sensitive to aging (heat) and oxidation (moisture)

An adapted approach for coal tar/pitch-bonded clay is to use a mixture of phenolic resin and CTht/CTPht as binder. Depending on the phenol:formaldehyde ratio of the resole resin, the curing speed of the clay can be controlled within tolerable limits. For applications that require short dwell- and casting times, resin-bonded clays can be used. These clays are, however, extremely sensitive to temperature and increase sintering strength of the clay, which can cause delays in drilling practice because lancing would be required to assist the standard drilling practice. Other problems, such as shorter taphole lengths, can cause increased temperatures and wear near the taphole area. The hardenability of resin-bonded clays also creates problems in the mud gun because extended thermal aging reduces workability of the clay and increases the extrusion pressure (Cameron, 2021).

The greatest disadvantage of using coal tar/pitch as a binder is the aromatic structure associated with the raw material. The high PAH release has become a health concern for clay manufacturers and incentives are in place to encourage using alternatives that contain less PAH. Although there are many alternatives to coal tar/pitch as a binder, these need to have certain characteristics to successfully be used in THC materials. Important

characteristics of the clay that are directly correlated to the binder include (Otsubo et al., 2010; Nelson & Hundermark, 2014; Dash, 2009; Perez, 2004; Lindstad, 2018):

- High plasticity;
- Viscoelastic behaviour (CTP is viscoelastic but that is not a requirement of the binder, only of the clay);
- High-temperature adhesion;
- High thermal expansion;
- Non-wetting by metal and slag – assists with reduced wear of clay;
- Sufficient residual carbon after firing – assists with strength of clay due to carbon network formation;
- Gradual volatilisation over a temperature range (25–400°C);
- Low volatility for reduced material porosity and cracking in material;
- Low softening point of the clay (< 30°C).

Use of high-temperature coal tar/pitch as a binder for THC imparts certain characteristics or properties associated with the binder. The aromatic structure of the CT/CTPht is one of the main reasons why it is used in THC (Lindstad, 2018). Condensation of the aromatic structures on heating assists with formation of residual solid carbon in the material after firing (Lindstad, 2018). Although other compounds have the same behaviour as binders, pitch produced from coal has a higher degree of mesophase formation (Lindstad, 2018). Inherent chemical properties, such as the broad molecular mass distributions of both coal tar and pitch make these possible to be used over a wide temperature range due to the large number of different PAH species in the liquid and other accompanying species. These include PAH, alkylated PAH, PAH with cyclopentene, PAH that are partially hydrogenated, oligoaryls, hetero-substituted PAH, and polycyclic heteroatomic species (Mazumder, 2012). Specifying alternatives to CT/CTPht is not as simple as saying that any compound containing aromatic structures can be used because this is not the only criteria for a binder. Because the PAH are unwanted in the liquid, a balance between retained properties comparable with CTht/CTPht and eliminated toxic PAH needs to be maintained.

Section 2.1.3.2 introduces the origin of CTPht, some low- and high-temperature properties with reference to THC application, and its reaction mechanism during firing. The discussion primarily focuses on CTPht because this is the most commonly used binder for conventional THC. Proposed alternatives to CTPht for use in THC materials are also introduced.

2.1.3.2. High-temperature coal tar pitch

CTPht is produced as a byproduct from metallurgical-grade coke production for applications such as blast furnace coking coal (Satyendra, 2018; Baron et al., 2016). Tar (CT) that is produced from coke-making contains bi- and polycyclic aromatic hydrocarbons, compounds with heteroatom ring structures, and phenols (Satyendra, 2018). CTPht produced through distillation of the tar predominantly contains anthracene (21–26%), with smaller quantities of naphthalene (8–12%) and an absorbed fraction (5–9%) that are distilled from the tar (Satyendra, 2018). Pitch is the residue portion (non-volatile at 450°C) of the tar that remains after distillation.

CTPht is produced by destructive condensation during high-temperature (700–1000°C) pyrolysis of coal tar that results in a black viscous liquid at room temperature (Bermudez et al., 2018; VROM, SZW, 2008). The viscosity of the liquid depends on the grade or composition of the pitch; hence, CTPht with different softening points can be produced for specific applications (Li et al., 2020). The viscosity of the pitch is dependent on the number of π–π intermolecular bonds due to the presence of heteroatoms in the pitch structure (Li et al., 2020). CTPht that is produced from coking tar accounts for about 2% of the tar (Satyendra, 2018). The large number of different PAH compounds or high aromaticity in CTPht allow it to volatilise over a wide temperature range, depending on the composition (Lindstad, 2018; Gargiulo et al., 2016). Different PAHs in CTPht (Table 2.4) have different boiling points, ranging from 200–600°C, which results in a wide molecular mass distribution (Lindstad, 2018; Gargiulo et al., 2016). Depending on the processing route of the pitch, it will contain different PAH species; the presence of a large number of different species will result in a wider volatilization temperature range and final volatilization temperature. The same is true for the residual carbon content of the binder after firing. Volatilization of a larger average molecular mass pitch will achieve higher operating temperatures and hence higher residual carbon content. The wide temperature range over which pitch volatilises makes it perfect for applications that have rapid heating conditions, like tap-hole environments. Gradual volatile release ensures that porosity within the material is finely dispersed and reduced to a minimum, so prevents crack formation (Lindstad, 2018).

As CTPht is heated, it undergoes certain characteristic changes in microstructure, viscosity, and physical properties. As stated by Lindstad (2018) and Li et al. (2020), the behaviour of CTPht during firing occurs in different stages. These include low-temperature volatilization, polymerization of the pitch, mesophase formation, carbonization, and, depending on the environment, graphitization (Li et al., 2020). The heating process or carbonization of the pitch will differ depending on the composition and, subsequently, the softening point of the pitch. Lower softening-point pitches are semi-liquid at 25–30°C and will, on further heating, start to volatilize smaller molecular mass species or long-chain species (Lindstad, 2018; Li et al., 2020). For CTPht used in THC, the softening point is generally about 20–35°C which is due to modification of the pitch to lower its conventional softening point (100-150°C). To describe the different stages of CTPht on heating (polymerization, carbonization, and graphitization) from its storage temperature, thermogravimetric analysis (TGA) of a high softening-point (> 300°C) meso-phase-forming CTP is used (Figure 2.1) (Lindstad, 2018; Li et al., 2020).

Table 2.4: Polycyclic aromatic hydrocarbon compounds present in high-temperature CTP with associated boiling points (Lindstad, 2018; VROM, SZW, 2008)

Substance	CAS no	Molecular mass (g mol^{-1})	Boiling point (°C)
Naphthalene	91-20-2	128.2	217.9
Acenaphthylene	91-20-3	150.2	270
Acenaphthene	208-96-8	154.2	279
Fluorene	86-73-7	166.2	295
Phenanthrene	85-01-8	178.2	338–340
Anthracene	120-12-7	178.2	340–342
Fluoranthene	206-44-0	202.3	375–383
Pyrene	129-00-0	202.3	393
Benzo[a]anthracene	56-55-3	228.3	425–435
Chrysene	218-01-9	228.3	431–448
Benzo[a]pyrene	50-32-8	252.3	493–496
Benzo[e]pyrene	192-97-2	252.3	493
Benzo[b]fluoranthene	205-99-2	252.3	481
Benzo[j]fluoranthene	205-82-3	252.3	480
Benzo[k]fluoranthene	207-08-9	252.3	480
Indo[1,2,3-cd]pyrene	193-39-5	276.3	534–536
Benzo[ghi]perylene	191-24-2	276.3	542–545
Dibenzo[a,h]anthracene	53-70-3	278.4	524–535
Dibenzo[a,e]pyrene	192-65-4	302.4	592
Dibenzo[a,l]pyrene	191-30-0	302.4	595
Dinezo[a,i]pyrene	189-55-9	302.4	595
Dibenzo[a,h]pyrene	189-64-0	302.4	596

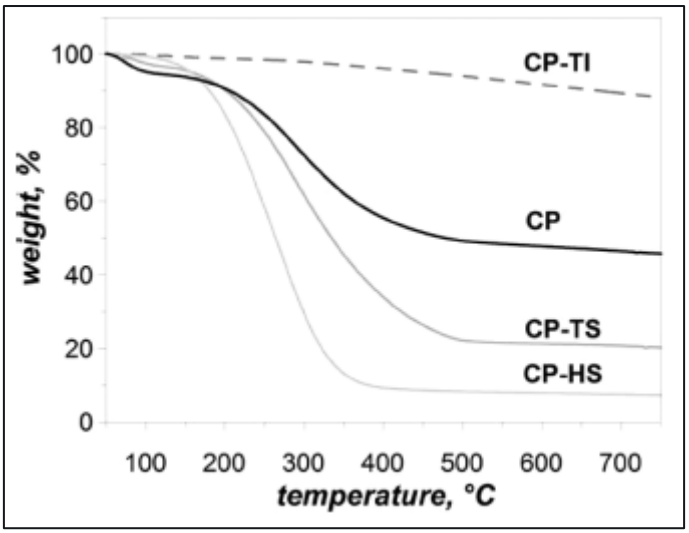

Figure 2.1: Thermogravimetric analysis of a meso-phase-forming pitch (high softening point) produced from coal. Nitrogen atmosphere flow rate of 20 L/min and heating rate of 10°C/min (Gargiulo et al., 2016)

On heating of CTPht from 25°C, the pitch will start to volatilise low-temperature (low molecular mass) species that contain small aromatic or long-chain structures. The sequence usually follows breakage of long-chain molecular species and then ring-type molecular species like benzene (Gargiulo et al., 2016). The increase in temperature causes the molecular structure to vibrate and side chains of the long-chain or ring structures break off. Thereafter, cracking of the long-chain or ring structures occurs. This process proceeds continuously as the decomposition temperatures of the different species in the pitch are achieved. The first heating process involves polymerization of the pitch: this continues until the final mesophase-formation temperature is reached (Lindstad, 2018; Li et al., 2020). The degree or effectiveness of polymerization of the pitch determines the green coke yield or low-temperature strength of the pitch (Li et al., 2020). This involves cross-linking of the pitch as it is heated (Li et al., 2020). During polymerization, cross-linking occurs in the pitch between free radicals from scission of oxygen-containing functional groups (Li et al., 2020). This causes macro-molecules to form and increase the green coke yield of the pitch (Li et al., 2020).

The change from a solid to liquid state (softening point) generally occurs around 25–30°C for CTPht used in THC applications. This means that the pitch is semi-liquid or completely liquid at room temperature. This can be achieved by distillation of the tar or by blending of the pitch with lower molecular mass fluids. Once polymerization has started and the mesophase-formation temperature range is approached (200–400°C) (Yuan & Cui, 2019), the pitch forms anisotropic spheres in an isotropic matrix (Lindstad, 2018; Yuan & Cui, 2019). Mesophase formation is dependent on the pitch quinoline insolubility (QI) content, hydrogen content, and presence of aliphatic side-chains (Li et al., 2020). Both QI and hydrogen content need to be low to have favourable conditions for mesophase formation (QI < 4%, C/H < 1.6) (Li et al., 2020). The growth of anisotropic spheres continues as the temperature increases until the spheres start to coalesce (low QI content) (Li et al., 2020). On further increase of the temperature, the bulk material deforms and disintegrates to form nematic liquid crystals called mesophase. This usually occurs at 350–450°C and

is referred to as liquid-phase carbonization (Yuan & Cui, 2019). The process of bulk liquid crystalline mesophase formation is shown in Figure 2.2.

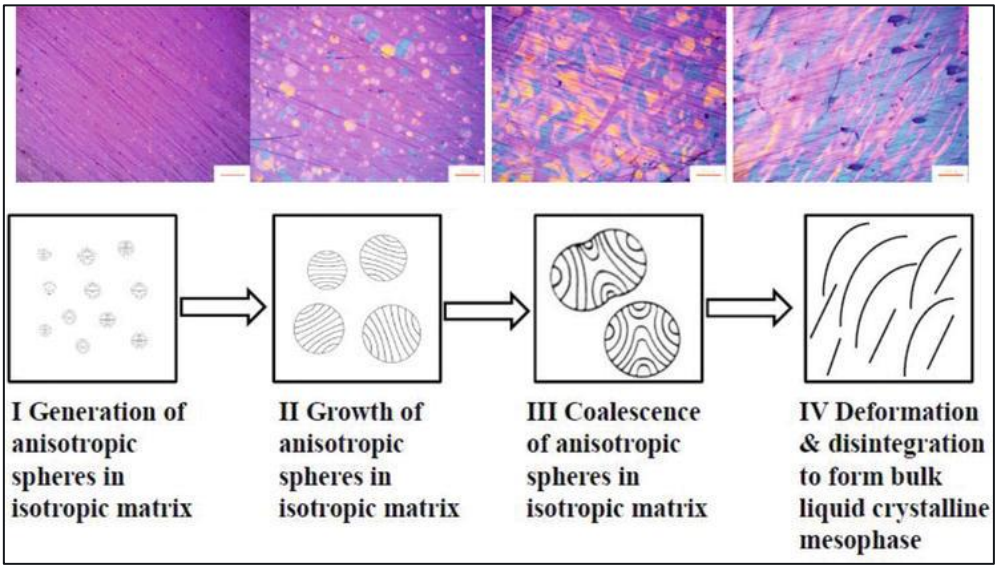

Figure 2.2: Steps in liquid crystalline mesophase formation in liquid carbonaceous compounds such as high-temperature coal tar pitch (Yuan & Cui, 2019)

Once the end of the liquid crystalline mesophase-formation temperature range is reached (~ 450–490°C) (Li et al., 2020), a second process—solid-state carbonization—will start. Depending on the pressure and heating rate, this will occur up to 600°C (Krebs et al., 1995). Alongside mesophase formation, PAH species in the CTPht vaporise and condense as coke (carbonization) and hydrogen gas. The increased condensation of PAH species to coke results in the mesophase structure becoming crystalline, which, upon further heating and favourable conditions, becomes graphitizable (Satyendra, 2018). With further carbonization of the binder after coke formation has taken place, graphene formation can start to occur at approximately 900°C (Wang et al., 2017; Lui et al., 2019). The stability of graphene is dependent on the purity of the CTP and heating rate, which will, if low enough, form graphene (Lui et al., 2019). Slow heating of the pitch will result in higher carbon yield, higher softening temperature, and higher mesophase content, which can also influence the graphitization (Delport, 2015). This is due to evaporation of lower molecular mass species and more effective condensation of ring-type molecular species. If the heating rate is too quick, small carbon cores are formed and graphene formation is not possible (Lui et al., 2019). Owing to the lower operating temperatures of a taphole (up to 1700°C) and fast heating rates, the carbon does not fully graphitize to form a graphite structure. The process of heating the pitch to temperatures above 600°C results in a high-temperature carbon network/structure (coke); if a different binder source, such as fatty acid oil, was heated, the process of transforming organic carbon to high-temperature carbon would occur.

CTPht generally have carbon residues as high as 50% after heat treatment above 800°C, as shown by results of the coal tar pitch (CP) Figure 2.1. Other binders, such as petroleum pitch, do not have the same carbon residue (Satyendra, 2018) after heating and this needs to be supplemented by solid pitch flakes or carbon black in the THC matrix (Menendez et al., 1996). The coke produced from CTPht and other CTht generally exhibits a needle-like

microstructure (Zhu et al., 2020). The type of needle structure that is produced gives certain properties to the coke, such as high mechanical strength, and is dependent on the QI, beta-resin content of the pitch (Zhu et al., 2020), and heating rate. Microstructures of the different types of needle coke that can form from CTP are shown in Figure 2.3.

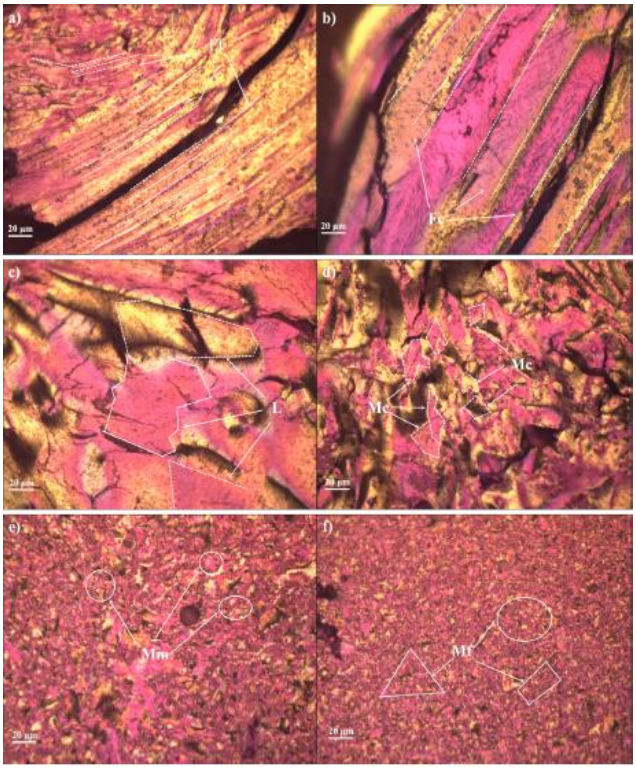

Figure 2.3: Optical microstructures of different types of coke microstructures structures that can form at elevated temperatures: a) fine structure, b) coarse fibrous structure, c) leaflet structure, d) coarse structure, e) medium structure, and f) fine mosaic structure; Nomenclature: Fc – fibrous coarse grain, Ff – fibrous fine grain, L – Leaflet structure, Mc – coarse structure, Mm – medium coarse structure, Mf – fine structure (Zhu et al., 2020)

The formation of mesophase at intermediate temperatures and its transformation to high-temperature carbon structures (coke) improve the mechanical strength properties of the binder and inherent strength of THC. Some standard chemical and physical properties of CTPht are shown in Table 2.5.

There are different variations of CTP: depending on the processing, certain distillation products can be viscous to almost solid at room temperature, whereas others are completely liquid (related to their molecular mass distribution). CTPht used for THC materials is a viscous liquid at room temperature, with a softening point (the temperature at which a liquid can flow a certain distance under certain conditions, such as gravity) of approximately 30°C. The low softening point (Table 2.5) of CTPht is desired for use in monolithic materials, such as THC, due to its high formability and plastic (viscoelasticity) behaviour. The flash points (the lowest temperature at which ignition can occur) of CTPht in Table 2.5 are considered standard when compared with those of petroleum or bio-fuel alternatives. The volatile matter of the binder is usually half of the mass of the liquid and has a desired carbon yield (coking value) of approximately 48–50% if the grade is good. The ash content of the binder after firing is considered

low, with < 1% ash required for these liquids. CTPht is highly viscous at room temperature, with a lowering in viscosity as temperature increases. The behaviour of the binder viscosity is such that the viscosity lowers up to a certain point as temperature increases, after which it reaches a plateau before increasing again as mesophase formation is approached (300–450°C). The decomposition temperature of CTPht is generally low (< 60°C) (Cameron, 2021) before destructive volatilisation starts; thus, CTPht will decompose before it starts to volatilise the largest part of its volatile matter (Cameron, 2021). The carbon/hydrogen ratio for CTPht is generally 0.56–0.59, depending on the aromatic structures of the liquid.

Table 2.5: Chemical and physical properties of high-temperature coal tar pitch (low softening point) (Mannweiler & Perruchoud, 1997; Apicella et al., 2017; VROM, SZW, 2008; Li et al., 2020)

Property	**Range**	**Value**
Softening point (°C)	25–45	32
Melting point (°C)	65–150	90
Density (g/m^3)	1.15–1.40	1.31
Flash point (°C)	> 250	257
Volatile matter (%)	40–50	48
Quinoline insolubility (QI) (%)	4–7	5
Coking value (%)	50–60	59
Viscosity (@25°C, mPa.s)	-	5240
Viscosity (@ 60°C, mPa.s)	-	59.2
Viscosity (@120°C, mPa.s)	-	10.8
Elemental analysis (mass%)		
Carbon	-	92.7
Hydrogen (H)	-	4.4
Nitrogen (N)	-	0.90
H/C Ratio	-	0.58
Ash	< 1	0.75

The proposal of alternative toxic-free binders is a topic of interest in the field of THC materials. Some advances have been made in terms of replacing CTPht with less-toxic alternatives or toxic-free binders. Although this has been successfully implemented, publications concerning specifics of the binders are unknown. CTPht has been used in other products, for which alternatives have been made known. Alternatives that have successfully been used in THC materials are lower-PAH CTP (Wang et al., 2017), synthetically produced lower-PAH pitches from naphthalene sources and similar (Apicella et al., 2017), and lower-PAH petroleum pitch products (Coutouly & Feng, 2007; Mannweiler & Perruchoud, 1997). Possible non-toxic (zero carcinogen) alternatives include bio-pitches produced from vegetable tar and wood tar (Murilo, 2009), byproducts from the Kraft process, such as fatty acid

pitches, e.g., tall oil pitch (Sharp & Harper, 1993), and bio-polymers derived from cellulose or microbial exopolysaccharides (de Pretto & Lindstad, 2022; Azeem et al., 2017; Cano-Barrita & Leon-Martinez, 2016). The common feature of all these liquids is lower aromaticity than CTPht. The high aromaticity of CTPht makes it a well-suited binder for THC application. Although, some of these alternative carbonaceous binders have successfully been implemented, the PAH content was lowered—not eliminated. The use of fatty acid pitch, crude waxy oils, and biopolymers as alternatives can be favourable due to their low softening points, low glass-transition temperature, moderate carbon yield (although lower than CTPht), and lower PAH content.

Selection of an alternative binder for use in THC materials depends on many factors, but the property considered amongst the most important is the rheological behaviour. Rheology of THC is highly dependent on that of the binder system, so changes to stimuli such as temperature, shear, and force to the binder, whether it be only CTPht or a combination of CTPht and phenolic resin, should be studied to understand the behaviour of the binder and how it influences the THC. Rheological behaviours of CTPht and a CTPht modified with phenol–formaldehyde resin are discussed in Sections 2.1.3.2.1 and 2.1.3.2.2, respectively. The behaviour of the binder controls certain characteristics of the THC, including compaction (ramming), extrusion rate/pressure, elasticity, deformation, plasticity, viscous flow, wettability, and volatilization rate and amount.

2.1.3.2.1. Rheology of coal tar pitch

The use of CTPht as a binder system imparts certain properties that are required for optimal performance of the THC. The molecular structure and, more specifically, the amount of high molecular mass compounds in the pitch, largely determine its rheological behaviour. External particulate or chemical additions to the pitch modify certain properties, such as viscosity and Newtonian behaviour. Temperature is another external stimulus that influences the viscoelastic behaviour of the pitch: a change in temperature, depending on the softening point of the pitch, can cause transitional changes in the pitch structure.

The softening point of a pitch is determined by the molecular mass distribution: a higher proportion of larger molecular mass species increase the softening point. The discussion in this section relates to high softening-point pitches, but the behaviour and changes to stimulus can directly be applied to lower softening-point pitches, such as those used in THC materials. Two properties of a low softening-point pitch that determine its suitability for THC are the viscous and elastic responses of the material to temperature and shear rate. The use of low softening-point (high fluidity) pitches for THC materials assists with compaction of the clay, the formation and growth of pores in the matrix, and increases the mechanical strength after carburization (Ciesinska, 2017).

CTP are considered Newtonian fluids because of their ability to maintain a constant dynamic viscosity with an increase in shear rate including at various temperatures (constant power law index) (Mollaabbasi et al., 2018). Pitches that have high softening points are generally considered to behave as Bingham plastic fluids at low temperatures and Newtonian fluids at higher temperatures (Mollaabbasi et al., 2018). The change in dynamic

viscosity of a pitch is not dependent on the change in shear rate, but rather on the increase in temperature that causes a reduction in viscosity, as shown in Figure 2.4 and Figure 2.5.

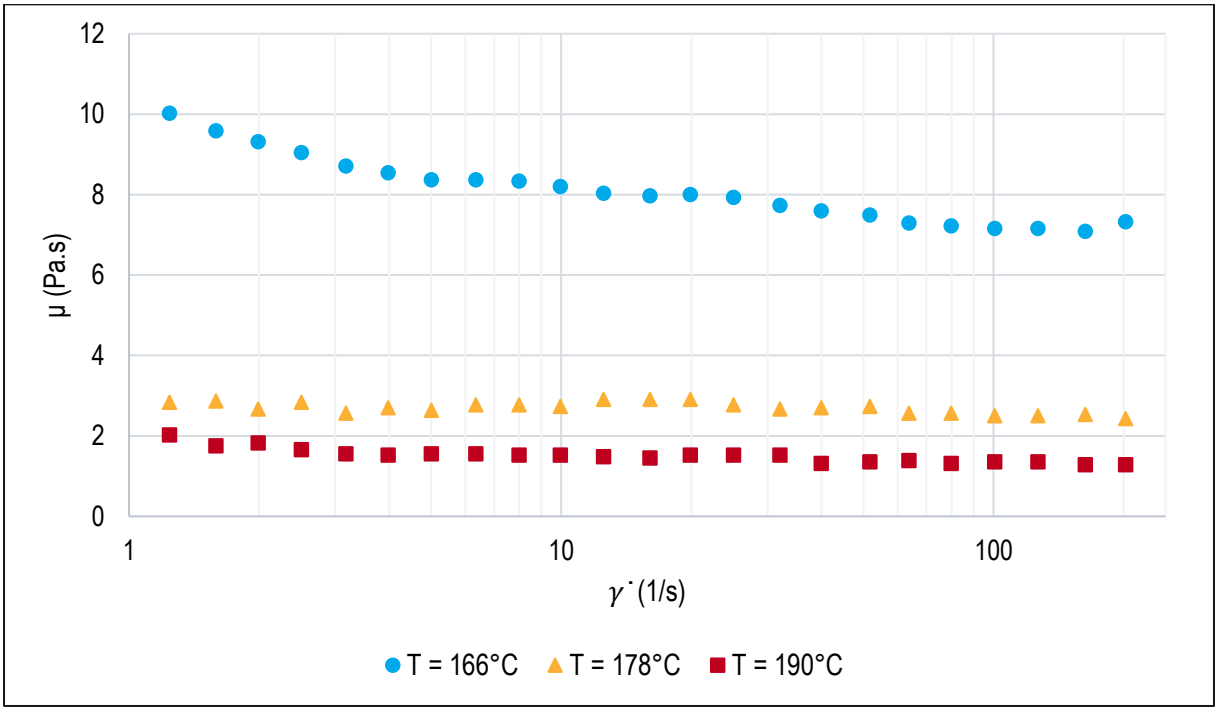

Figure 2.4: Dynamic viscosity as a function of shear rate of high softening-point coal tar pitch at three test temperatures. A two 20 mm diameter parallel-plate configuration with a 1 mm gap in oscillation mode was used (Mollaabbasi et al., 2018)

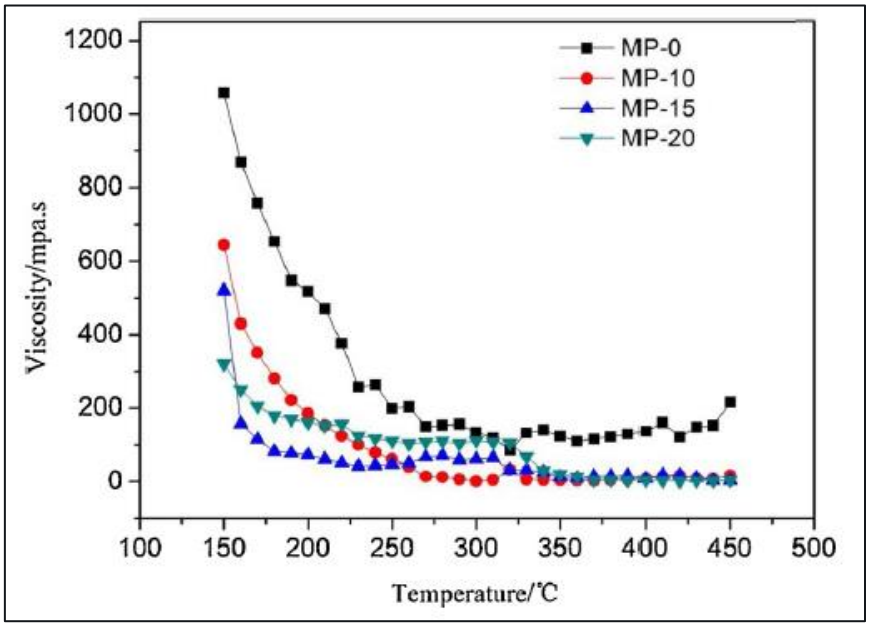

Figure 2.5: Dynamic viscosity as a function of temperature of high softening-point (80°C) coal tar pitch and different mixtures of coal tar and biomass pitches (Li et al., 2020)

The results shown in Figure 2.4 indicate that the pitch was Newtonian, even when the temperature increased. The only change is that viscosity reduced as the temperature increased (thermal stability). This can also be seen in

Figure 2.5, where the zero-mass percent biomass-containing pitch (MP-0) showed a reduction in viscosity as the temperature increased. The viscosity started to reduce once the softening point of the pitch was reached, and continuously decreased as the temperature increased until it starts to plateau, and a constant viscosity range was achieved. The viscosity plateau continued for a specified temperature range until it started to increase again, as occurred at ~ 450°C. This plateau in viscosity and sequential increase in viscosity with increase in temperature is known as the re-solidification process (Ciesinska, 2017). This phenomenon is shown in Figure 2.6 from 180–260°C for a high softening-point (107°C) CTPht (Ciesinska, 2017). With addition of a chemical stimulus, such as phenolic resin, re-solidification did not occur in this temperature range, and probably occurred at a temperature above 300°C (Ciesinska, 2017).

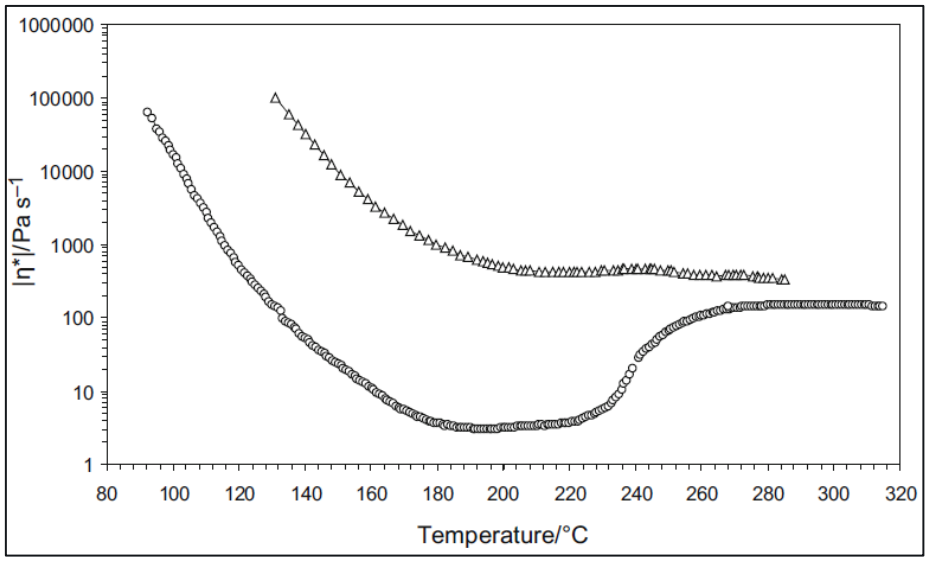

Figure 2.6: Complex viscosity as a function of temperature of high softening-point (107°C) coal tar pitch (open circles) compared with a phenol–formaldehyde resin-modified pitch (open triangles) (Ciesinska, 2017)

The unaltered pitch sample in Figure 2.6 (open circles) showed viscous characteristic behaviour up to 264°C, above which a transition to a viscoelastic response was prominent (Ciesinska, 2017). This also manifested as a decrease in phase angle as temperature increased above 264°C, showing the presence of viscoelastic response of the binder (Ciesinska, 2017).

The viscoelastic response of the binder to a varying frequency (shear rate) should also be discussed. Results of a frequency sweep of unaltered pitch (Figure 2.6) is shown in Figure 2.7: both storage (*G*') and loss moduli (*G*'') are reported. Figure 2.7 shows that the storage modulus of the unaltered pitch was higher than the loss modulus at low frequencies, which implies that pitch can store energy without dissipation at low strain values. As the frequency increased, there was a cross-over point where the loss modulus exceeded the storage modulus (Ciesinska, 2017). This is referred to the glass-transition temperature. With high softening-point pitches, these transitions are prominent; with low softening-point pitches (< 40°C), these transitions are not shown because the pitch is semi-liquid. For the pitch shown in Figure 2.7, the glass-transition temperature was determined to occur at 0.025 Hz and 789 Pa (Ciesinska, 2017). As the frequency increased, the loss modulus increased, which means that more energy

was required to distort the structure of the pitch by deformation and that the pitch structure dissipated energy at higher frequencies for short durations (Figure 2.8). As the temperature increased, the loss modulus decreased until it reached the re-solidification point. As shown in Figure 2.8, the pitch showed more elastic response at frequencies below 1 Hz and a viscous response above this value (Ciesinska, 2017). This is known as viscoelastic behaviour. Addition of phenolic resin to a pitch result in a wide viscous response across the entire frequency range, where the transition to viscous response occurs at lower frequency (0.01 Hz): this means a larger energy dissipation for the mixture is possible compared with unaltered pitch (Ciesinska, 2017).

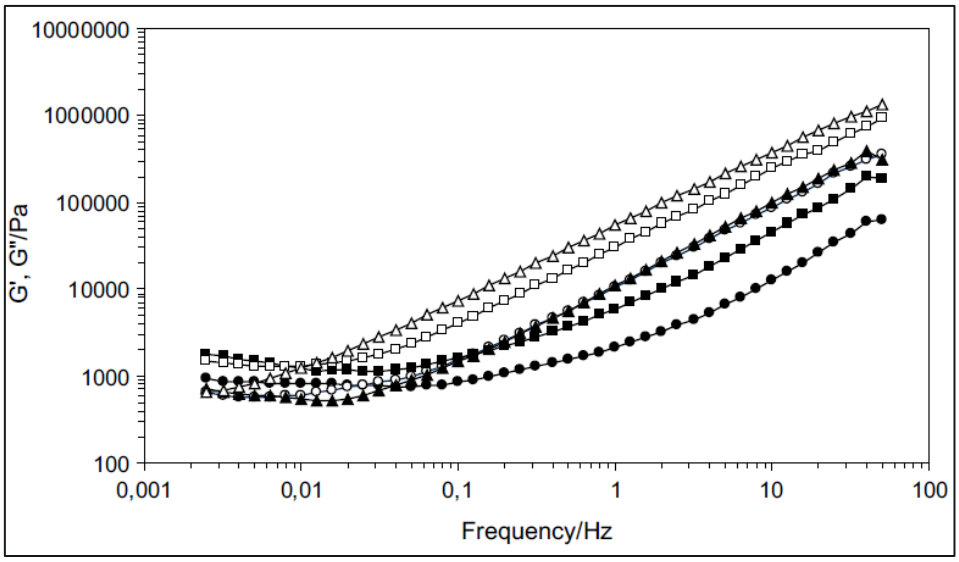

Figure 2.7: Storage (G') (filled symbols) and loss (G'') (open symbols) moduli as a function of change in oscillation frequency of a high softening-point (107°C) coal tar pitch compared with those of various phenol–formaldehyde resin-modified pitches (Ciesinska, 2017)

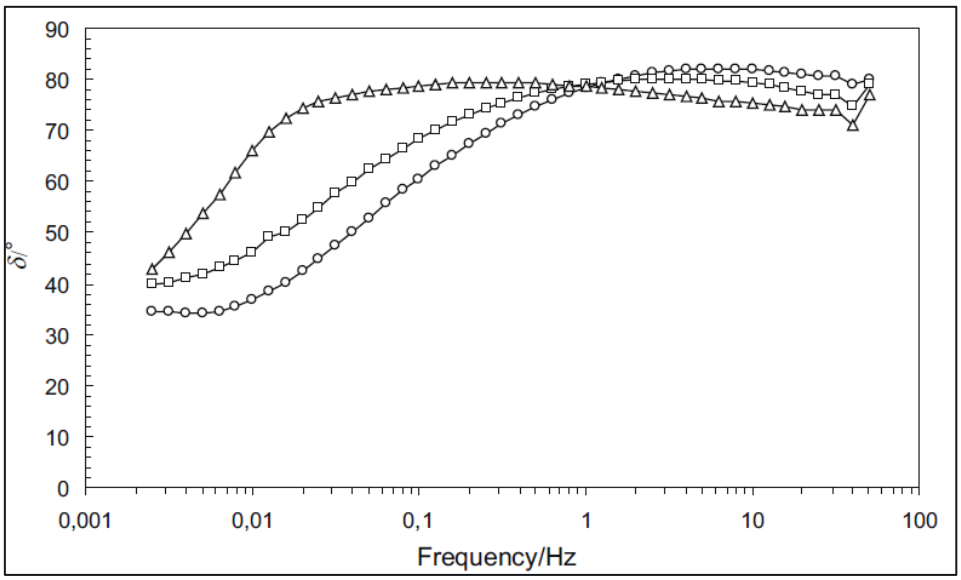

Figure 2.8: Phase angle as a function of change in oscillation frequency of a high softening-point (107°C) coal tar pitch (open circles) compared with various phenol–formaldehyde resin-modified pitches (Ciesinska, 2017)

In addition to temperature, other stimuli also influence the rheology of pitch. With regards to the use of CTPht in THC materials, one such stimulus is the addition of particulate or fine material powder, such as solid pitch, to the binder. Pitch is added in form of flakes or fine powder to assist with filling, dense carbon network formation, compaction, and densification (increased bulk density) of the clay. Addition of particulates to the pitch imparts certain changes to the flow properties, as discussed below.

When mixing a viscous pitch and coke particulates, the binder surrounds the coke particulates and once compacted, the pitch infiltrates the pores of the coke. The binder rheology may be altered by the particle size distribution of the coke, coke content added, and temperature at which mixing and compaction occur (Mollaabbasi et al., 2018). One of the main functions of adding pitch as a binder to THC is that it binds the aggregate and matrix materials together and imparts green strength to the material. THC is considered a granulo-viscoelastic material, in which its behaviour depends on whether the fine powder content is an oxide or carbon, the temperature, particle shape and size of the coke, and the content of pitch added as binder (Mollaabbasi et al., 2018). With additions of fine coke material to CTP, the Newtonian behaviour of the pitch is altered to non-Newtonian by a decrease in the power law index (Mollaabbasi et al., 2018).

Addition of coke particles (−150+38 μm, density 2.057 g/cm^3) to a high softening-point CTPht was conducted by Mollabbasi et al., (2018) who investigated the effects of particle addition and temperature (Mollaabbasi et al., 2018). It was shown that the pitch became increasingly non-Newtonian with an increase in fine coke particles, exhibiting shear-thinning behaviour (more so at low temperatures) (Mollaabbasi et al., 2018). Although shear-thinning diminished with an increase in temperature (Mollaabbasi et al., 2018), the mixture of pitch and fine coke particles (paste) remained non-Newtonian at all temperatures (Mollaabbasi et al., 2018). The pitch elastic properties were enhanced by addition of fine coke particles but were not dependent on the concentration of coke added to the liquid (Mollaabbasi et al., 2018). This means that the pitch used for manufacturing of THC exhibits Newtonian behaviour throughout an increase in temperature and remains viscoelastic. Addition of aggregate and small particulates to pitch changes its behaviour to non-Newtonian and shear-thinning. The THC still showed viscoelastic behaviour even with the change in Newtonian behaviour of the binder. Figure 2.9 shows the change in shear stress as a result of change in shear rate (rotational) of an eco-friendly THC (de Pretto & Lindstad, 2022). This clay utilised a biomass binder: shear-thinning behaviour of the clay is exhibited, whilst still maintaining its viscoelastic behaviour (de Pretto & Lindstad, 2022).

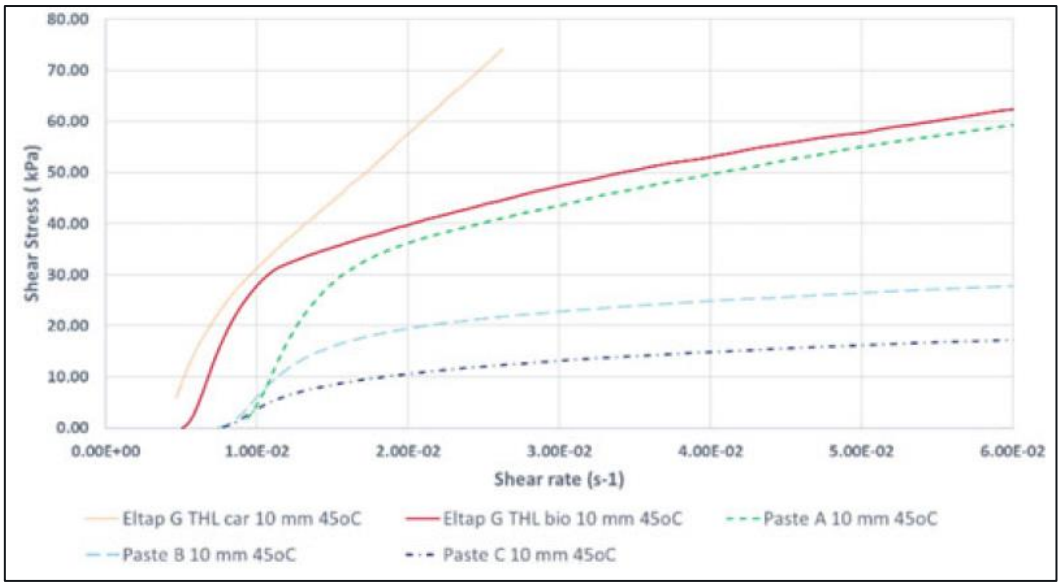

Figure 2.9: Stress–strain response of various eco-friendly taphole clays utilising a biomass binder (de Pretto & Lindstad, 2022)

2.1.3.2.2. Rheology of coal tar pitch modified with phenol–formaldehyde resole resin

The addition of phenol–formaldehyde resole resin to low softening-point pitch has functioned as a combination binder system for THC materials for a considerate time. The amount of phenol resin used depends on its reactivity and operational requirements of the taphole, including the ramming pressure (plasticity), holding time, drilling times heating time, and THC length. Another determining factor for the amount of resin used is the health requirements of the clay, such that increasing the resin content reduces the carcinogenicity (Ciesinska, 2017). THC have been developed to utilise phenolic-only binders and combinations of CTht/CTPht and phenolic resin. Recent trends in THC development have considered lower toxicity binders than CTht/CTPht, including resin-bonded clays. These clays do, however, have limitations and operational constraints, but represent a start towards moving to alternative lower toxicity materials.

CTPht has a distinctive aromatic structure and contains some longer-chain molecular species, depending on the source. Because rheology of the pitch is directly related to its molecular structure, it is worthwhile to understand how the resin addition changes the structure. Modifying agents recorded in literature include phenol–formaldehyde resin, unsaturated polyester resin, and poly(ethylene terephthalate) or polycarbonate (Ciesinska, 2017). Each of these impart different changes to the pitch, such as increasing plasticization and lowering PAH content or improves thermal and mechanical properties (Ciesinska, 2017). The most widely used modifying agent for THC is phenolic resin, specifically phenolic resole resin: this is further discussed.

The pitch molecular structure is altered when mixed with resole resin, owing to formation of higher molecular mass species. This is observed as an increase in QI (Ciesinska, 2017). Changes in the pitch structure can be described by a mechanism that entails reactions between phenol–formaldehyde molecules and methylene species in the pitch, or direct connections between aldehyde carbon in the phenolic resin and PAH in the pitch (Ciesinska, 2017).

The latter can lead to partial cross-linking, which may not be favourable, depending on the cross-linking degree (Cameron, 2021; Ciesinska, 2017). As the resin–pitch mixture is heated, the resin will start a gelation process and finally curing (Cameron, 2021). These molecular structure changes impact rheological changes in the pitch, such as improved thermal and mechanical resistance, increase pitch viscosity, and increased residual carbon content (Lui et al., 2019; Ciesinska, 2017).

Ciesinska (2017) investigated the effect of adding phenolic resole resin to a high softening-point pitch (bitumen source) on the rheological properties (Ciesinska, 2017). Initial changes in the pitch rheology indicated increases in the softening point, initial viscosity after mixing, and storage and loss moduli (Ciesinska, 2017). The rheological measurements were taken under oscillation conditions to observe changes in bitumen colloidal structure. The viscoelastic measurements were performed within the linear viscoelastic region (LVER) of the pitch and at a temperature between the softening point of the pitch and the gelation temperature of the resin to minimize cross-linking (Ciesinska, 2017). Addition of phenolic resin to the pitch resulted in non-Newtonian shear-thinning flow behaviour after mixing but lowered the shear-thinning behaviour as the binder aged (Cameron, 2021). Furthermore, addition of the phenolic resole resin to the pitch reduced the glass-transition temperature to lower frequencies, but higher pressure values, due to an initial increase in viscosity of the binder (Ciesinska, 2017). An increase in resin content assists with energy dissipation, as shown in Figure 2.8, where the viscous transition occurred at lower frequencies and endured over a wider frequency range than that of the unaltered pitch.

The degree of cross-linking during mixing and after inducing gelation is also important because these properties determine whether the resin is suitable for a specific application, such as in THC. Ideally, the degree of cross-linking on mixing should be as low as possible to ensure consistent workability of the clay and with aging. The highest degree of cross-linking occurs on heating, when the resin is cured in the binder to assist with low-temperature strength of the THC. Depending on the resin composition, the decomposition temperature can be closer or further away from the temperature at which liquid carbonization of the pitch starts. The cross-linking degree of resole resin in the pitch mixture increased the pitch-softening temperature and QI (Ciesinska, 2017). The viscoelastic variables also increased with an increase in cross-linking, when samples were cross-linked at 160°C for 2 h compared with 0.5 h and 1 h (Ciesinska, 2017). Addition of resole resin assisted with increasing the re-solidification temperature of the pitch, as shown in Figure 2.6, where the transition from a plateau to an increase in viscosity is not shown due to its probable start at higher temperatures (Ciesinska, 2017). Figure 2.6 also shows that both samples achieved the same starting complex viscosity at higher temperatures, which demonstrates the increase in softening point of the pitch with phenolic resole resin addition. The resin addition also reduced fluidity of the pitch (plateau region), achieving a higher minimum complex viscosity (Ciesinska, 2017). In Figure 2.6, the predominance of viscous behaviour continued until 264°C, after which it transitioned to viscoelastic behaviour as temperature increased. Addition of resole resin to the pitch increased the viscoelastic behaviour of the pitch, shown in Figure 2.10, where a decrease in phase angle with temperature demonstrates an increased fraction of viscoelasticity (Ciesinska, 2017).

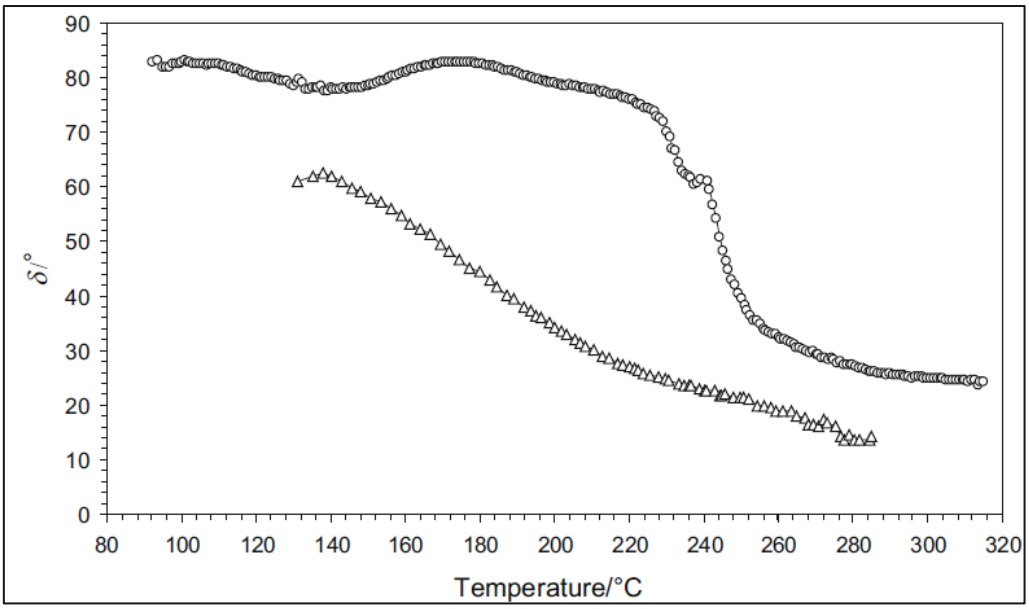

Figure 2.10: Phase angle as a function of change in temperature of a high softening-point (107°C) coal tar pitch (open circles) compared with a phenolic resole-modified pitch, 25% phenol–formaldehyde resin (open triangles) (Ciesinska, 2017)

2.1.3.3. Reduced polycyclic aromatic hydrocarbon high-temperature coal tar pitch

The use of CTPht with reduced PAH as binder for THC materials has been favoured as an alternative to the standard CT/CTPht composition by many clay manufacturers (Kitamura, 2014; Wang et al., 2017; Murilo, 2009; Boenigk et al., 2002). The PAH content is lowered by 80–90% compared with standard CTPht obtained from coke manufacturing. The conventional CTPht is obtained by fractionating the tar produced from coke-making furnaces to yield different products and grades. Although the use of low-PAH CTP is beneficial with regards to human exposure effects and emissions of PAH, processing of the pitch to obtain a lower aromaticity substantially increases the product cost. Lower PAH-modified CTPht is obtained by further fractional distillation or chemical methods (Kaushik et al., 2007) that are carefully controlled to produce an eco-friendly lower-aromaticity and less-carcinogenic product (Murilo, 2009). The distillation process and CTPht composition have a significant influence on the performance of the binder and extent of lowering the PAH content of the binder (Murilo, 2009). This binder can also be used in conjunction with vegetable oils and tars (modifiers) to obtain the desired volatile behaviour and rheological properties. One disadvantage of using these binders is that the carbon yield (coking value) is lowered due to the lower temperature of PAH removal. This can be amended by addition of coke flake (or similar) to the dry aggregate to ensure that the THC maintains its coking abilities and strength at high temperatures. Use of these dry pitch flakes or carbon black (Menendez et al., 1996) also increases the cost of the final product and, because the flakes increase gas permeability (Cameron, 2021) inside the clay, channelling and higher porosity can become a problem. The properties of three different pitch products produced by chemical processing using propylene glycol (PG), polyurethane glycol (PEG), and styrene as modifiers are shown in Table 2.6.

Table 2.6: Properties of CTPht modified by chemical processing to reduce the B(a)P content (Roder, 1998; Kaushik et al., 2007)

Sample	Chemical processing	Softening point (°C)	Coking value (%)	Specific gravity	B(a)P content (%)
1	Crude	112.7	54.3	1.28	1.22
2	With PG	123.4	54.1	1.32	0.43
3	With PEG	129.1	53.1	1.30	0.40
4	With styrene	113.2	51.4	1.30	0.58

The results shown in Table 2.6 are for a CTP with a higher softening point than the CTPht used for THC. Although this is a different product, the rheological modifiers can alter the softening point. The results shown in Table 2.6 are provided for comparison purposes only to assess the changes in properties. The results show that some chemical modifiers can increase the softening point. Changes in the coking values were minimal: the highest deviation was a reduction of 2.9% when using styrene as the modifier. These coking values were still sufficiently high to not alter the performance of the THC product relative to when using crude pitch. The specific gravity also remained consistent with that of the unprocessed sample. Lowering of the PAH content of these products is inferred from the B(a)P content. Although this is only one of 16 PAH present in CTPht, B(a)P generally considered in the industry as the indicating factor for whether a clay is toxic and to what extent (Copetti, 2024). As shown in Table 2.6, the B(a)P content of the CTP was significantly lowered by the different modifiers: the most effective chemical modifier was PEG. The favourable properties of these types of modified CTP are the lowering in PAH content while retaining comparable values of coking values and softening temperatures compared with normal CTPht. The viscosity of these liquids also increases due to the reduction in content of low molecular mass species in the pitch during processing, as shown in Table 2.7 (Cameron, 2021). The viscosity stays high during heating, which means that the flowability of the pitch is lowered; this is why modifying agents, such as carbonaceous oils, can be used to lower the viscosity to desirable values. Other properties, such as the plasticity and adhesivity, are dependent on the overall molecular structure and so these values cannot be determined solely by changes in viscosity (Shmalko et al., 2019).

Table 2.7: Dynamic viscosity differences at various temperatures between a low softening-point CTP and semi-liquid pitch synthetically produced from a coal source (Cameron, 2021)

Binder	Viscosity test temperature (°C)	Viscosity (mPa.s)
CTP – softening point (30–35°C)	30	960
	50	224
	70	106
Synthetic low PAH pitch – semi-liquid at 25°C	30	5240
	50	952
	70	185

2.1.3.4. Petroleum-based fluids or petrochemical pitches

Production of pitches from petroleum crude sources varies depending on the processing stream. Because the processing of crude petroleum is so complex, the products that can be derived from this source far exceed those of coal tar from a coking process. The variety of products include, amongst others, phenolic pitch, intermediate-temperature pitches, waxy liquids, and low-PAH synthetic pitch produced by polymerisation of naphthalene and similar PAH (Apicella et al., 2017). Many feedstock materials can be used as precursors for mesophase pitch manufacturing, including oil from fluid catalytic cracking, pyrolysis tars from naphthalene cracking units, and aromatic extracting units (Srivastava et al., 2012). Although these have all great potential as mesophase pitch-formers, the liquids with higher aromaticity, such as pyrolysis tar, have better coke yield and higher softening points (Srivastava et al., 2012). Petroleum products generally have lower aromaticity (Acuna & Marzin, 1997) (Roder, 1998) (Srivastava et al., 2012) than CTP, which makes them favourable for use in THC products and similar applications due to their lower PAH content. The lower aromaticity does, however, reduce the carbon yield because the polymerization and condensation reactions do not occur as abundantly as in CTP (Srivastava et al., 2012). These pitches are most often referred to as 'aliphatic' pitches, due to their lower C/H ratio, where the structure consists of aromatic molecules with paraffinic side-chains that act as desirable cracking centres to assist with polymerization and condensation of the liquid during heating (Srivastava et al., 2012). The QI, softening point, and coke yield of a pitch indicate its extent of polymerization and condensation. These properties have a direct impact on the mechanical strength of the binder during carbonisation (Srivastava et al., 2012). Although the aromaticities of these liquids are lower than that of CTP, some feedstock materials can produce sufficiently high coke yields, where the coking value remains > 50%, depending on the crude source (Srivastava et al., 2012). The softening point and specific gravity are lower for these liquids than normal CTP, but can be of limited use in binders (Roder, 1998) (Srivastava et al., 2012). The viscosities of petroleum pitch products are generally higher, depending on the process route and conditions (Roder, 1998). The higher sulfur content of petroleum can be problematic when these products are used with liquid phenolic resins because premature or increased vulcanisation can occur.

The results in Table 2.8 compare the properties of a CTPht, a low-PAH chemically modified CTP, and a low/medium-temperature petroleum pitch. The biggest differences are observed with respect to the coking values, sulfur content, softening temperature, and PAH content. The CTPht has a low softening point, which differs from that of both the low-PAH and petroleum pitches: these have relatively higher softening temperatures, which can be lowered if modifiers are added to the binder. The coking value of the low-PAH and petroleum pitches are higher than that of CTPht, which has a direct influence on their coking ability and carburization. The low-PAH and petroleum pitches will have higher coking abilities than the CTPht product shown in Table 2.8, which indicates that the petroleum pitch would be a favourable feedstock to produce a high-coke-yielding pitch (Srivastava et al., 2012). The sulfur content of the petroleum pitch is higher than that of the other two binders. This can be problematic if a phenolic resin is used as low-temperature temporary binder with the carbonaceous binder. The aromaticities of both the low-PAH and petroleum pitches are lower than that of CTPht, which is beneficial for promoting ecological binders in THC materials. It is interesting to note that, although the aromaticity of the petroleum pitch was lower than that of the other two binders, its carbon yield remained high. This might be due to the presence of an additive in the petroleum pitch, such as benzoyl peroxide, that acts as a free radical to initiate polymerization and condensation (Srivastava et al., 2012). The low aromaticity of the low-PAH pitch is due to the chemical processing that it undergoes to remove some PAH functional groups; petroleum pitch, by nature, contains less PAH functional groups than ordinary CTPht (Mannweiler & Perruchoud, 1997). Some petroleum pitches produced from a phenolic source may contain a high phenol content: this can interact with the liquid phenolic resin (resole) and alter the composition cause changes to the curing time, because this is dependent on the phenol/formaldehyde ratio during condensation. Large quantities of free phenol in a phenolic pitch will also be problematic to its use as an alternative to CTPht owing to their environmental and health impacts.

Table 2.8: Typical properties of CTPht, low-PAH chemically modified pitch, and petroleum low-temperature pitch (Murilo, 2009; Mannweiler & Perruchoud, 1997; Acuna & Marzin, 1997; Roder, 1998; Apicella et al., 2017)

Property	**Specification for CTPht**	**Typical values**		
		CTPht	**Low-PAH CTP**	**Petroleum pitch**
Specific gravity	1.15–1.25	1.20	1.32	1.29
Coking value (%)	20.0–35.0	32.30	56.89	53.40
Naphthalene (%)	6.0–10.0	8.70	-	-
Sulphur (%)	0.40–0.80	0.50	0.38	2.90
Carbon (%)	~ 91.0	92.70	93.31	92.20
Hydrogen (%)	~ 5.50	4.40	4.19	5.90
H/C	-	0.57	0.52	0.77
Softening temperature (°C)	25.0–45.0	30.05	112.20	118.00
Viscosity (mPa.s)	@60°C ~20	38.00	4900 @ 150°C	3202 @ 160°C
PAH Index (BEI)	-	1.54	0.65	0.38

The production of petroleum-based pitches is dependent on processing parameters, such as the temperature and pressure, but also on inherent physio-chemical properties of the feedstock (Srivastava et al., 2012). Another petroleum pitch feedstock material that has potential as a THC binder is crude wax oil, primarily due to its viscosity. Waxy crude oil consists of solid paraffin precipitates (waxy crystals) that form once the oil has been cooled to lower than the waxy-appearance temperature (WAT) (Yi & Zhang, 2011). Various products can be produced from waxy crude oil with different processing units and parameters, as shown in Figure 2.11. The oils can be categorised as normal paraffins, isomeric, naphthenic, and aromatic hydrocarbon-containing. The source depicts the type and quantity of the product that can be formed (Yan et al., 2018).

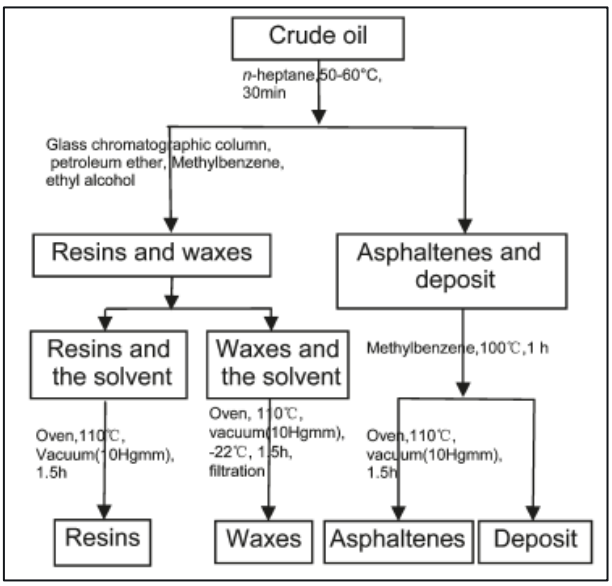

Figure 2.11: Various processing routes of crude oil to form different products, including resins, waxes, and asphaltenes (Yi & Zhang, 2011)

The flow properties of crude wax oil are dependent on the morphology and structure of the wax crystals that form on cooling, as well as on the asphaltene and resin content (Yi & Zhang, 2011; Yan et al., 2018). The wax crystals that form during cooling are long-chain paraffin structures (alkanes) that either crystallise as uniform rod-shaped crystals or shuttle-like structures with higher paraffin content (Yi & Zhang, 2011). The morphology depends on the contents of both asphaltene and resin in the crude oil. Higher asphaltene and resin contents in the crude oil assists with formation of large crystal aggregates that increase fluidity of the oil (Yi & Zhang, 2011). This is because both asphaltene and resin are aromatic hydrocarbon compounds that absorb high carbon alkanes and lower the WAT until saturation is achieved (Yan et al., 2018). The rheological behaviour is largely dependent on the molecular structure of the paraffins contained in the crude oil. These usually comprise long-chain hydrocarbons and a smaller number of lower-carbon-number chains of alkanes or cycloalkanes (Yan et al., 2018). An increase in paraffin content only causes an increase in viscosity and lowers the fluidity (Tarantino et al., 2016).

The effect of paraffin content on viscosity of a wax crude oil is illustrated in Figure 2.12. Both liquids exhibited Newtonian behaviour above 37°C and showed similar thermal stability at temperatures above the WAT (~ 37°C) of the waxy crude oil in question (Tarantino et al., 2016). The paraffin-containing crude oil showed non-Newtonian

behaviour after the start of crystallization of the waxy crystals at temperatures below 37°C (Tarantino et al., 2016); the non-waxy oil exhibited Newtonian behaviour throughout the temperature range.

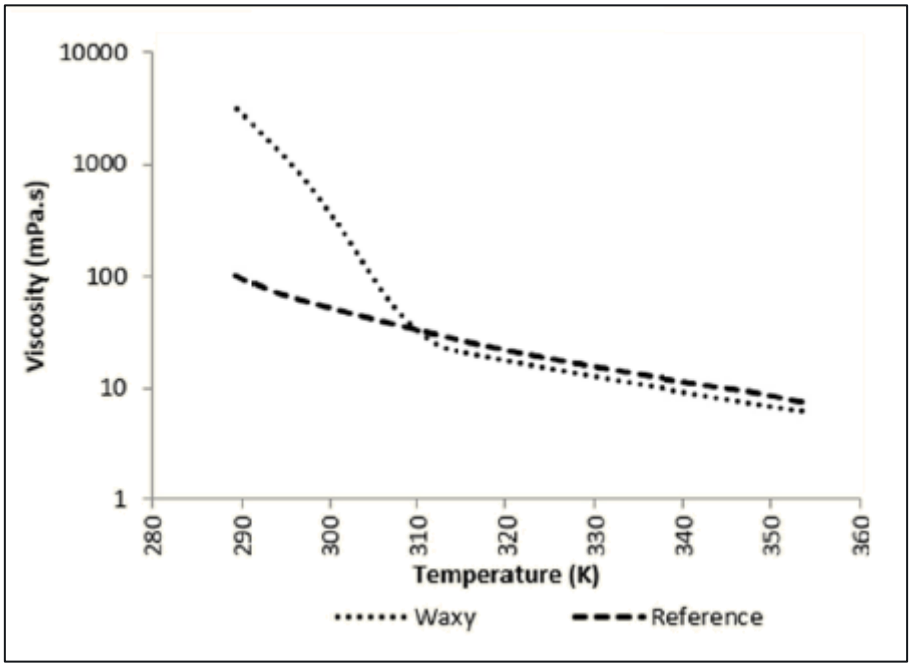

Figure 2.12: Dynamic viscosity changes with temperature of a waxy crude oil compared with a crude oil with negligible paraffin content (reference) (Tarantino et al., 2016)

The effect of aromatics (asphaltene) is also pronounced: an increase in asphaltene content decreases the WAT because asphaltene assists with improving the solubility of alkanes that inhibit precipitation of the wax crystals (Yan et al., 2018). The results shown in Table 2.9 are for different crude wax oil compositions and sources: these illustrate typical values of WAT, asphaltene, resin, and wax contents, and viscosity changes with temperature of these liquids.

Table 2.9: Physicochemical properties of waxy crude oils from difference sources (Yi & Zhang, 2011)

Property	Oil 1	Oil 2	Oil 3	Oil 4	Oil 5	Oil 6	Oil 7	Oil 8
WAT (°C)	30	40	45	45	30	35	55	45
Viscosity 20°C (mPa.s)	505.0	519.5	1164	2278.1	292.3	541.8	2520.1	504.9
Viscosity 60°C (mPa.s)	4.6	6.1	5.7	7.5	6.9	7.4	13.0	7.1
Asphaltene content (%)	0.6	1.4	0.9	1.4	0.6	0.6	1.1	0.5
Resin content (%)	5.2	7.2	3.7	7.1	9.7	6.5	13.5	10.0
Wax content (%)	13.2	12.4	13.8	18.6	5.4	7.2	26.2	11.9

The results presented in Table 2.9 show that the wax contents of the oils were all higher than the asphaltene and resin contents. An increase in wax content caused an increase in viscosity, the effect of which was more pronounced at lower temperatures. At temperatures higher than the WAT, the wax crystals would have already dissolved and did not have the same prominent effect as when the wax formed crystals. The asphaltene contents of the oils were much lower than the resin contents, which assists with removal of the wax from the crude (Figure 2.12) and prevents co-crystallization with asphaltene, because this will increase solubility of the resins in the liquid and prevent successful removal of all paraffin compounds from the crude oil (Yan et al., 2018).

2.1.3.5. Phenol–formaldehyde resole resin

The process of producing phenolic resin is well known and documented. With ever-growing demand, there are ongoing advances in producing resins that are environmentally friendly but maintain equivalent performance. Phenolic resins have been used as binders or binder enhancers in an array of refractory materials, including THC. Depending on the operational requirements of a THC, the resin can either be used as a binder enhancer or as a binder alone. Conventional use of this resin is with a carbonaceous liquid as a binder enhancer. The resin imparts low-temperature strength in the THC, while the condensation reaction of the pitch transforms the hydrocarbons into solid or semi-solid (mesophase) carbon. When phenolic resin is used as a binder enhancer, the main purpose of the resin is to improve the low-temperature (< 300°C) strength of the material while the binder is carbonized. Some clay materials do not utilize a phenolic resin as the enhancer because the binder achieves sufficient strength during ramming.

The second scenario, where the phenolic resin is used as a sole binder, has multiple drivers for its use: elimination of PAH species in the product, increasing corrosion resistance, enhancing the binder strength, and shorter ramming time (increased production capacity). These clay materials are referred to as resin-bonded. When a phenolic resin is used as a sole binder, resole-type resins are more frequently used. These THC can also be used with high-alumina-sintered or fused grains to produce a high-end technical product for high production-throughput furnaces. These binder systems are, however, extremely sensitive to temperature fluctuations, so mud gun operations need to be well maintained if they make use of these products. The shelf-life also greatly reduces when phenolic resins are used as sole binders due to aging and oxidation of the resin once exposed to air and sunlight (Cameron, 2021).

When the phenolic resins are used as binder enhancers, resole resins are generally preferred because they already contain an initiator and hardener; if novolac resins are used, these improvements need to be added to the liquid binder system. Curing of a resole resin results in a solid product with a high strength and endurance at low temperatures in a product such as THC. The phenolic resins are referred to as thermosetting resins and cure through a process called polymerization (Cameron, 2021; Laza et al., 2022). A resole resin starts as a condensation product between phenol and excess formaldehyde under a basic catalyst in a particular ratio, depending on the desired properties of the resin. To produce a phenolic resole resin, the phenol–formaldehyde structure is dissolved into a carrier liquid, most commonly ethylene glycol and, in some cases, glycerol (Rogers, 2007), along with a cross-linking agent, such as hexamethylenetetramine (HMTA), that ensure that the polymer formed during

polymerization is resistant to chemical attack and heating (Laza et al., 2022). Some resole binders also contain initiator agents, such as sodium carbonate, to further enhance the curing time and accelerate the polymerization process (Xu et al., 2009).

The thermosetting nature of the resin allows curing to initiate and proceed on heating. The curing process starts by increased movement of the polymer chains until the start of gelation. During heating, the polymer chains start to attach to one another through cross-linking until a gel-like structure is formed. During gelation, a more viscous polymer solution is formed and is converted to an infinitely viscous liquid with an alcohol-bridged network (gel) in a process called polycondensation/polyesterification (Mulder, 2000). Optimum gelation occurs at a specific temperature, after which the resin will transform from a rubber-like solid to a complete solid, which occurs at the final cure temperature. The resole type resins conventionally used in THC are low-temperature (< 200°C) curing resins (Kageyama et al., 2005). The gelation and final curing temperatures depend on the chemical composition of the resin: generally, gelation occurs at 60–100°C and final cure at 110–200°C (Cameron, 2021; Lee et al., 2003) for phenolic resole resins used in THC. These temperatures also depend on the clay requirement, which is linked to operational requirements, such as ramming, drilling, and casting times. Additionally, the low-temperature strength, high-temperature strength due to carbonization, and corrosion properties of the clay also depend on the type and quantity of resin. Once the resin has fully cured (end of polymerization), the three-dimensional resin structure will be stable up to ~ 300°C: above this temperature, it will decompose and carbonize. The decomposition usually occurs in two stages: the first at 300–600°C, during which gaseous species are volatilized (Knop & Pilato, 1985); the second (> 600°C) stage causes chemically bound water, phenol, and carbon dioxide to be volatilized at up to ~ 800°C, after which the remaining resin is carbonized. The extent of carbonization of a phenolic resin is high and contributes to the carbon network of the THC if pitch is used as the major binding liquid. Although the abovementioned process is important to ensure proper closure of the taphole, the volatile loss or loss on ignition (LOI) of the clay needs to be as minimal possible especially towards platinum smelting operations (Nelson & Hundermark, 2014). Clay containing large amount of volatile matter that is placed into contact with molten material, in platinum smelting case the superheated matte, will result in turbulent gas stirring on the inside of the taphole that causes excessive corrosion due to increase heat and mass transport (Nelson & Hundermark, 2014).

2.1.3.6. Environmentally friendly phenolic resole resin

The two major raw materials in the manufacture of phenolic resins are phenol and formaldehyde. The phenol/formaldehyde ratio will differ depending on whether a novolac- or resole-type resin is manufactured: resole resins require an excess of formaldehyde (Katovic, 1967). Manufacturing of these resins has significant health and environmental impacts because both raw material volatiles pose health risks if inhaled above a certain limit. The risks of spillage and vapours released during manufacturing have initiated a move towards producing resins that make use of natural and bio-degradable raw materials. As stated in Section 2.1.3.1 both the phenol and formaldehyde used in phenolic resins are replaceable by environmentally friendly alternatives.

Research into replacement of phenol and formaldehyde is challenging in supply of the specific raw materials and because initial experimental work showed reduced reactivity of the resin (Sarika et al., 2020). Phenol has been fully or partially replaced with lignin from different sources, such as the Kraft process, corn, enzymic, tannin, and cardanol (Sarika et al., 2020). Formaldehyde has been partial or fully substituted in phenolic resins by hydroxide functional group structures, such as hydroxymethylfurfural (HMF), furfural, and glyoxal (Sarika et al., 2020). Performance of the resin depends on the type of substitution, which raw material is being substituted, and the quality of the natural raw material. Most phenol alternatives are byproducts, so their impurities and source play a big role in determining certain properties of the resin. The type of lignin used will influence the adhesive strength, gel time, viscosity, mechanical properties, and thermal stability (Sarika et al., 2020). Similarly, the type of alternative selected and quantity replacement for formaldehyde will also influence these properties of the resin.

Investigation of the most suitable replacements for phenol and formaldehyde in manufacturing phenolic resin showed that lignin is the favoured replacement for phenol and high-purity furfural is the preferred replacement for formaldehyde (Sarkar & Adhikari, 1999; Sarika et al., 2020; Talabi et al., 2020). Replacements were all favourable with particle substitutions of either phenol or formaldehyde. Complete replacement of either phenol or formaldehyde in phenolic resins is accompanied by reduced reactivity and deterioration of certain resin properties (Sarika et al., 2020; Talabi et al., 2020). The phenol substitute with the highest reactivity towards formaldehyde is lignin (Sarika et al., 2020; Talabi et al., 2020), although only partial substitutions of phenol by lignin have been shown to be favourable. Replacement of both phenol and formaldehyde in the production of phenolic resins is also being pursued. Although the reactivity of lignin towards the formaldehyde is low at high proportions of substitution, some advances have been made to increase the lignin reactivity by demethylation, phenolation, methylolation, and depolymerization (Talabi et al., 2020). These have resulted in phenol replacements of up to 75% of depolymerized lignin with good reactivity (Talabi et al., 2020). This research will assist with producing phenolic resins that can be used with non-toxic alternative binders in THC materials.

Ongoing research and favourable results of these studies have stimulated investment in production sites to produce these products at mass scale and assist with creating a circular economy. One such initiative is by an organization called Viobond that is commercializing a first-of-kind plant to produce bio-based phenolic resins in which phenol is replaced by a wood-based biorefinery lignin (BBI - Bio-based industries, 2018). These initiatives are of cardinal importance for THC materials to move in the direction of being completely eco-friendly: phenolic resin is a current component of the clay binder system that cannot be eliminated: owing to the constraints of producing a fully bio-based phenolic resin, a small part of the binder will remain toxic until such time as a fully bio-based resin is developed.

2.1.3.7. Phenolic resin-enhanced glycerine or glycerine binder

Pursuant to replacing CTPht with less- or non-toxic alternatives, binders have been mentioned in Section 2.1.3.3 and 2.1.3.4 that are considered less toxic than CTPht. The drive towards replacing CTPht with non-toxic alternatives has highlighted that liquids such as glycerine/glycerol, ethylene glycol, and polyethylene glycol could be possible

non-toxic alternatives, although some of these are still considered dangerous to human health (although not necessarily with regards to PAH exposure) and the environment. For this reason, propylene glycol and glycerine/glycerol have shown favour in possible replacement of CTPht with a non-toxic alternative (Xu et al., 2009).

These two liquids are used as binders in other applications and have good thermal stability and flow properties. Their drawback is that they are not as viscoelastic as CTPht and do not impart carbonization during heating. However, the rheological properties of such binders can be adjusted to be more robust for application in THC materials and the carbon yield can be improved by using a carbon-containing phenolic resin or addition of carbon black to the clay matrix or liquid itself. Propylene glycol and glycerine can act as plasticizers for biopolymers, which will assist in altering the rheological properties of the binder (Cano-Barrita & Leon-Martinez, 2016). The use of ethylene glycol with phenolic resin has shown favourable results in application in carbon monoliths, but should also be able to be successfully implemented in THC materials (Xu et al., 2009). Phenolic resole resins also make use of ethylene glycol as a carrier for the resin structure and to plasticize the resin. The idea of extending the plasticizing liquid in the resin and altering the rheological properties of the carrier liquids with biopolymers is a core idea that requires investigation as a suitable non-toxic alternative binder in this study. A change from a phenolic resin to an eco-friendlier version that contains lignin and furfural would ensure that the binder maintains its non-toxic status when used in these products.

Glycerine is an alternative to ethylene glycol because it is also a good plasticizer for the biopolymers that are used to alter the rheology of the liquid (Rogers, 2007). This innovative idea should be investigated to ascertain the likelihood of this non-toxic binder system succeeding and maintaining the critical properties of THC and reduce the variability in tap-hole processes.

2.2. Taphole processes and requirements

The main function of THC is to plug the taphole during smelting. However, there are other taphole processes where THC is also of importance: during ramming, tapping, and when protection of the taphole area is required (Otsubo et al., 2010; Gupta et al., 2014). The requirements for each of these processes are as follows (Otsubo et al., 2010; Gupta et al., 2014; Nolet, 2014; Mc Dougall, 2014, Cameron et al., 2024):

- Ramming
    - Easy ramming of clay mass to properly close the taphole.
- Tapping
    - Easy discharge of molten material from the taphole, including effortless drilling of THC and minimal oxygen lancing during the drilling practice.
    - Stable hearth drainage of molten material during tapping: the molten material needs to drain at a consistent and desired flow rate.
    - Minimal slag splashing and spewing during tapping of molten material.
    - Reduced refractory consumption during storage, transport, and operation.

- Reduced physical workload during tapping, which influences the cost of operation and mitigates the risk of injury during tapping practices.

- Protection (sidewall, taphole blocks, and taphole)
  - Increased furnace life by reduced refractory corrosion inside the furnace.
  - Reduced THC consumption and ensuring that consistent quantities of clays are used in each tap. This is done by designing the clay to erode by only a small amount during tapping to ensure that the THC length is maintained by injection of sufficient, yet consistent, amounts of clay and a constant flow of molten material from the furnace.
  - Reduce the possibility of taphole blow out because of excessive clay usage (high LOI clay).

To align fundamental understanding of the behaviour of a THC with how it performs, it is important to introduce performance indicators that are used for development and research to evaluate performance of the clay. These performance indicators are applicable to all THC applications, i.e., iron and steel, PGM, ferro-alloys, and non-ferrous alloy smelting operations. Figure 2.13 summarises a relationship diagram for the type of operation, the taphole process, and its associated requirements. The performance indicators of each process, and features of the THC that influence these, are shown in Figure 2.13.

Application	Taphole process and requirements	THC performance indicators	Required THC properties for performance indicators

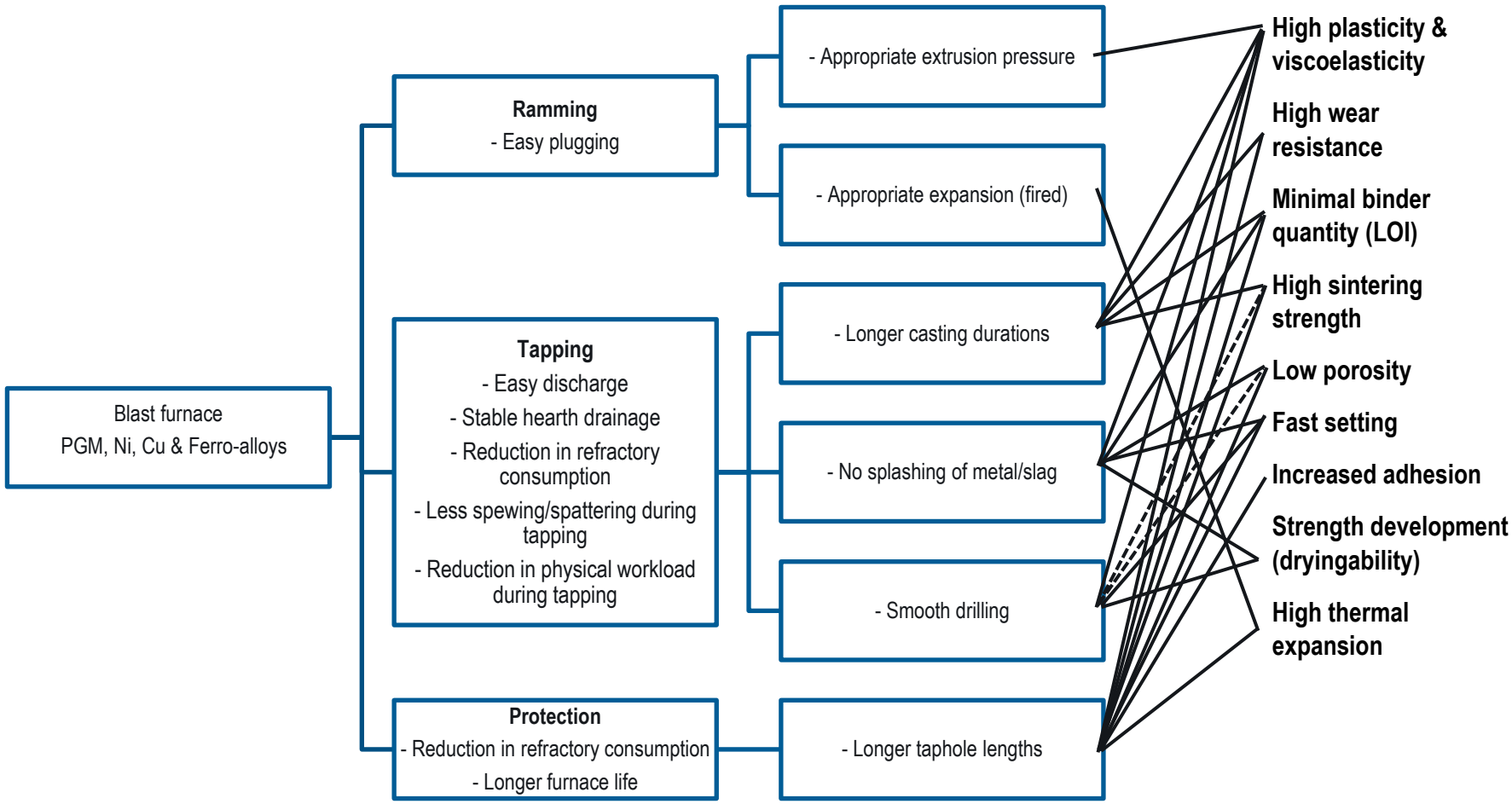

Figure 2.13: Schematic of the relationship between taphole clay application, the tap-hole process, and associated requirements, performance indicators and related taphole clay feature (Otsubo et al., 2010; Gupta et al., 2014; Nolet, 2014; Nightingale et al., 2006; Nelson & Hundermark, 2014; van Beek & Goff, 2014; Dash, 2009; de Pretto & Lindstad, 2022, Cameron et al., 2024)

2.2.1. Performance indicators for the ramming process

The performance indicators for the ramming process, as shown in Figure 2.13, are extrusion pressure and expansion of THC on firing.

2.2.1.1. Extrusion pressure

The extrusion pressure that is applied to the THC when it is rammed into a taphole needs to be sufficiently low to be able to push in the correct quantity of material to ensure that a long enough taphole length is maintained (Otsubo et al., 2010; Gupta et al., 2014). The texture of the THC needs to be smooth to allow for effortless extrusion. The extrusion pressure needs to be within specified limits to allow for a compactable material to form inside the taphole (Gupta et al., 2014). The extrusion pressure required is determined by the type of equipment used: ramming practices can be pneumatic or hydraulic, and, depending on whether the mud gun can heat the material that is placed inside the barrel, the extrusion pressure needed for ramming will greatly depend on the type of mud gun configuration and capabilities (Nelson & Hundermark, 2014). Rheological properties of the binder(s) will determine the necessary extrusion pressure when the clay is heated. An increase in mud gun temperature will generally require lower extrusion pressure for ramming due to the increase in fluidity of the binder. This statement is only valid up to the onset of curing of the resin because curing will cause an increase in the extrusion pressure (Cameron, 2021).

2.2.1.2. Expansion on firing

The second performance indicator is expansion after firing, which gives an indication of how well the THC will seal the taphole. Expansion of the clay occurs in both the ramming direction and perpendicular to the ramming direction (Otsubo et al., 2010; Kitamura, 2014): expansion perpendicular to the ramming direction ensures a proper seal in the taphole to prevent self-openers (Gupta et al., 2014) and eliminate gas escape and liquid penetration; expansion in the ramming direction ensures that a sufficiently long taphole length is achieved during ramming and heating (Kitamura, 2014). Expansion of the THC is dependent on multiple factors: those that have the greatest influence are the aggregate and matrix raw materials. Raw materials such as pyrophyllite, andalusite, and kyanite expand on heating (Figure 2.14) and are therefore used in the manufacturing of THC (Otsubo et al., 2010; Mukhopadhyay et al., 2010; Fortes, 2019). The heating rate of the clay influences how well the product expands and the expansion of the raw material, which influences expansion of the clay (Fortes, 2019); however, owing to the difficulty of controlling the heating rate inside the taphole, the expansion rate is regarded as a constant over a certain temperature range. Although the expansion of the clay in both directions perpendicular and parallel to the tapping channel is important, this should be done with the aim of providing sufficient clay to fill the taphole and prevent excess clay from entering the molten metal or superheated matte as this causes increased corrosion.

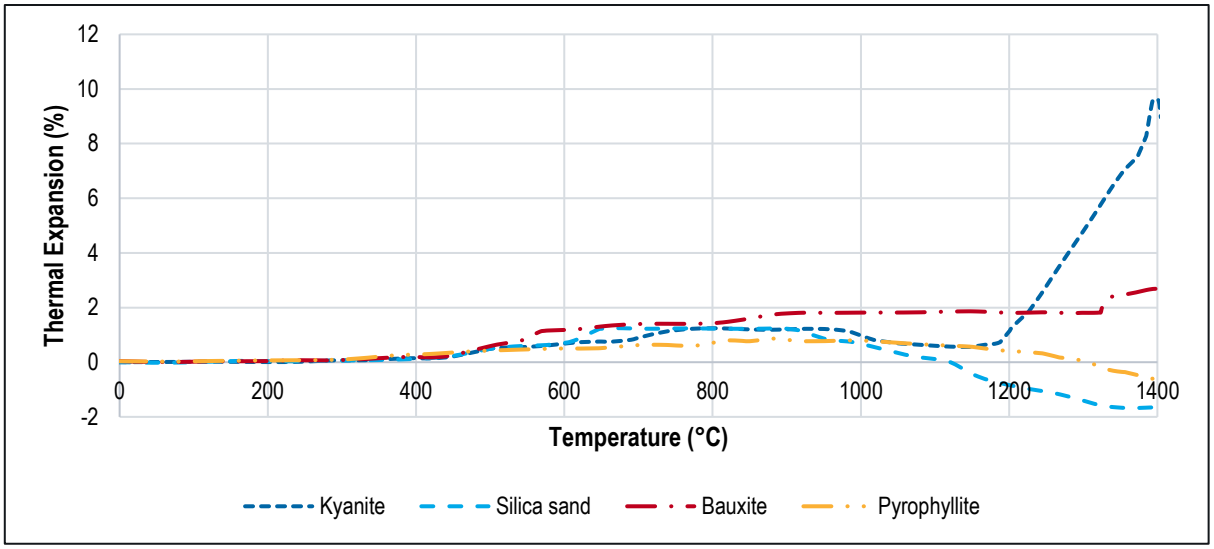

Figure 2.14: Thermal expansion of kyanite, silica sand, bauxite, and pyrophyllite with temperature up to 1400°C (Perez, 2004)

These two performance indicators are related to properties of the THC that can be measured to determine and monitor the performance of the clay (Otsubo et al., 2010). These properties include thermal expansion of the clay on heating and plasticity, as evaluated through workability and extrusion pressure measurements. These properties are discussed in Section 2.2.2.

2.2.2. Performance indicators for the tapping process

Performance indicators (Figure 2.13) for the tapping process are longer tapping times (also referred to as casting duration), no splashing or "spewing" of metal or slag, and efficient drilling practices.

2.2.2.1. Tapping duration

The casting duration refers to the time at which the taphole is opened until it is closed again during ramming. The casting duration significantly impacts the amount of molten material produced per day. The furnace capacity and furnace refractories govern the casting duration. Longer tapping durations are favoured because these allow for less heats per day (Nolet, 2014), lower material (refractory) usage (Gupta et al., 2014; Nelson & Hundermark, 2014), reduced physical workload (Otsubo et al., 2010), and consistent quality material produced from the furnace; however, the taphole will experience more corrosion and erosion during longer tapping times. The taphole experiences an extreme heat flux (which varies between applications (Thomson, 2014)) during tapping, excessive thermal shock due to large thermal gradients along the length of the taphole, sudden changes in temperature at the start of tapping (Nightingale et al., 2006), and increased corrosion and erosion (Nelson & Hundermark, 2014). For platinum smelting the stirring on the inside of the taphole owing to excess clay coming into contact with superheated matte/molten is the biggest contributing factor to taphole corrosion and hence optimized clay quantities pushed into the taphole should be maintained (Nelson & Hundermark, 2014). Any one of these effects may dominate for certain applications; for example, corrosion of the brick material dominates in blast-furnace

applications, which is why mushroom formation is important. The concept of mushroom formation exists only for blast-furnace operations. It comprises extension of the THC into the taphole to connect the taphole to the burden inside the furnace as a way to protect the taphole and act as a heat shield for the heat flux experienced by the taphole during tapping (Van Laar et al., 2003). If the mushroom formation is sufficient and reaches far enough into the furnace, it will allow for longer tapping times because corrosion will preferentially occur on the clay material, which then acts as a buffer to allow for adequate casting times before slag or iron start to interact with the bricks in the tapping channel (Otsubo et al., 2010; Gupta et al., 2014; Nightingale et al., 2006; Nelson & Hundermark, 2014). Smelting operations in the PGM industry are among the most aggressive towards the taphole due to numerous factors, including high slag liquidus temperatures and high heat fluxes that cause increased super-heating of the matte (Thomson, 2014). This leads to corrosion due to chemical interaction between the matte or slag and the clay, and low-viscosity matte penetration and erosion on the inside of the taphole (Nelson & Hundermark, 2014).

For these reasons, there needs to be a balance between the duration of tapping and the degree of taphole erosion that occurs during tapping. Many THC properties are related to the casting duration (Figure 2.13), including its plasticity, wear (corrosion and erosion resistance), binder quantity, and sintering strength. Plasticity is measured by a compressive strength test including the extrusion pressure, ramming, and compacting, and spreadability of the clay during processing. Plasticity of the clay influences the casting duration: a reduction in plasticity reduces mushroom formation in Si-Mn and blast furnace smelting, which will cause excessive wear (Steenkamp, 2014) of the carbon blocks inside the tapping channel. Extrusion pressure, ramming and compaction, and spreadability affect the tapping duration (Otsubo et al., 2010). The increase in extrusion pressure as the clay ages needs to be low enough to still allow proper ramming and compacting of the material in the taphole. Clay aging is defined as the time between production of the clay up to 21 d and more, depending on when the clay is used. Ramming and compaction influence the THC length and mushroom formation (Gupta et al., 2014; Nightingale et al., 2006). If a taphole is not properly rammed with sufficient clay, the taphole length reduces, which impacts casting duration because less time can be spent on tapping material owing to the need to avoid excessive iron and slag heat flux and possible wear near or inside the taphole (Otsubo et al., 2010; Nelson & Hundermark, 2014; Geyer & Halifa, 214). If the required extrusion pressure increases due to aging of the clay, insufficient clay will be rammed into the taphole and will have the same effect.

2.2.2.2. Splashing of metal, matte, and slag

Splashing (also referred to as spitting) of slag, matte, or molten liquid (pig iron or alloy) when tapping is another important performance indicator of a THC. The tapping practice is extremely dangerous: any possibility for spillage of molten material needs to be eliminated because it poses risks for injury to operators on the casting floor and damage to equipment surrounding the taphole. One way in which molten material can escape the runner is by splashing. Splashing can occur on opening of the taphole or during tapping, where molten material is present inside the runner. Generally, the biggest contributor to splashing is THC in contact with molten material outside of the furnace in the tapping launder (Otsubo et al., 2010). From a safety point of view, splashing of molten material

outside of the tapping launder should be avoided. Certain THC properties (Figure 2.13) are required to prevent splashing of molten material outside of the tapping launder, which include high plasticity, optimised binder usage, fast curing speeds of resin in the binder, good adhesion, and good strength development (drying ability) (Otsubo et al., 2010; Cameron, 2021; Sako et al., 2018).

High plasticity of THC ensures that it is properly extruded and rammed into the taphole. If THC plasticity is low, then extrusion through the mud gun would be difficult and this usually leads to wastage of clay. Lowering of THC length due to insufficient ramming of clay into the taphole also increases splashing as the taphole is opened. Low plasticity also causes the clay to prematurely dry inside the mud gun. An increase in extrusion pressure and premature drying of the clay inside the mud gun leads to wastage of THC from the gun. If the THC is not properly extruded during the ramming process, wastage from the mud gun occurs around the taphole area where clay material spills into the runner filled with molten material. This happens because operators extrude the dried clay from the front end of the mud gun to obtain fresh clay material to ram the taphole. Spillage of THC into the runner or surrounding taphole area causes splashing due to reaction of the molten liquid with the liquid binders in the THC. This highlights a second feature that needs to be optimised, i.e., binder/s.

Exposure of a liquid, such as water, to molten material causes a sudden and rapid release of volatiles. This can be explosive, due to fragmentation of the molten liquid and water pressure changes that cause steam where molten liquid and water are in proximity (Nelson et al., 2016). The same applies to binders used in THC, such as oils, high-volatile CTP, and water. These binders all contain moisture, so, with volatilisation of functional groups in the compounds, the volatile release is excessive and causes splashing. The presence of resin in the binder also causes splashing at the start of tapping (Otsubo et al., 2010; Gupta et al., 2014). Splashing of molten material increases if the curing speed of the resin is too short (Gupta et al., 2014); thus, an optimally cured resin will reduce splashing.

The choice of resin to use, or whether to even use resin, depends on the required strength development of the clay and holding times in the mud gun (Cameron, 2021). Where good strength development and green strength are desired, resole resins are included in the binder. The type of resole resin depends on the specified holding time of the furnace for which the clay is designed. The curing rate of a resole resin is dependent on the resin content and its phenol/formaldehyde ratio, which ranges between 1:1 to 1:3, in conjunction with a catalyst (Cameron, 2021). The phenol/formaldehyde ratio in the resin also influences its rheology properties. A higher phenol/formaldehyde ratio reduces the curing temperature and increases the curing rate (Siddiqui et al., 2017). Because the rate of curing influences splashing, it is desired that the THC cures in the specified holding time, but not to the point that it increases the drilling time due to a large increase in sintering strength at high temperatures. To counter this, a small quantity of fast-setting resole is used in the clay to minimise splashing, but still maintain sufficient good strength development and green strength.

Strength development of a THC is a function of the type of resole resin used, quantity of resin, and type of binder. Strength development depends on the type of operation and specified minimum green strength of the clay. The green-strength temperature range of the clay, depending on the composition of the resin, ranges from 25–600°C

(Nightingale et al., 2006): above 600°C, the resin structure starts to break down and sintering of particulates and carbonization of carbon species in the THC become the main contributors to the strength of the material. To control the strength development of THC, the resin/binder ratio needs to be optimised for clays that are not resin-bonded (Otsubo et al., 2010; Nightingale et al., 2006). This is a lengthy exercise because the type of binder, type of resole resin, and their quantities influence strength development. In the case of resin-bonded clays, the curing rate and strength development depend only on the resin used as binder. This means that control of the resin manufacture needs to be done as accurately as possible to ensure that correct quantities are used because there is no other addition to the binder that can assist with lowering or increasing the strength development of holding times.

A further THC feature that influences molten liquid splashing is its adhesion. The adhesion of a THC reflects a combination between the plastic behaviour of the clay and adhesion of the binder. Adhesion determines the degree of sintering between fresh THC and old sintered clay already inside the taphole (Sako et al., 2018). Adhesion of a taphole clay is concerned with the proper formation of a mushroom on the inside of the taphole (excluding PGM and other Cu, Ni matte and blister bath processes) and the sintering of fresh clay material to older clay material already present inside the taphole (Otsubo et al., 2010; Kitamura, 2014; Sako et al., 2018). The formation of a stable and large enough mushroom assists with reducing refractory wear surrounding the taphole (Cameron, 2021). Formation of a stable mushroom is directly related to long taphole lengths that are favourable inside the taphole and to spreadability of the THC (Kitamura, 2014). Another requirement is that the taphole be properly sealed by injection of THC into the furnace (Sako et al., 2018) to prevent molten material from seeping or spilling out of the taphole under specific furnace conditions. To achieve a desired THC adhesion, the resin content of the clay need to be controlled, while also ensuring the presence of expansive raw materials (Otsubo et al., 2010). Use of resin-bonded clays is not desirable for applications where good adhesion is required because such clay has good drying ability that results in poor adhesiveness (Kitamura, 2014). Raw materials such as mullite-forming materials and pyrophyllite assist with improved adhesion properties because these clays expand on heating (Otsubo et al., 2010). Pyrophyllite raw materials have a distinctive expansive nature that assists with increased adhesion and good creep resistance of clay (Otsubo et al., 2010). Good adhesion properties of a THC assist with reducing molten liquid splashing by ensuring long taphole lengths are maintained and ensure lower wear rates while tapping is taking place. The reduced resin content in the clay also assists in lowering the splashing.

2.2.2.3. Drilling

The last performance indicator related to the tapping process is the drilling operation and related THC properties. To achieve correct tapping of molten liquid from a furnace, drilling of the THC from the taphole needs to be quick and efficient. The drilling operation is usually complemented with lancing practices to reduce the drilling time. The drilling practice depends on the drillability of the THC material and the furnace operations. Certain smelting operations are less aggressive, with limited slag and molten material interaction, which assists with opening of the taphole. A large market exists for drilling equipment, and practices differ between applications depending on the operational requirements. To ensure that production targets are met, drilling of a taphole needs to be quick and

efficient, with minimal taphole damage. The ideal drilling practice makes use of a iron drilling rod with tungsten drill bit to gradually open the taphole enough for constant and stable flow of molten material from the furnace. This practice, however, hardly ever occurs because furnace instabilities, taphole material quality, temperature, environmental conditions, amongst others, influence drilling efficiency. In most applications, drilling involves a combination of mechanical drilling and lancing to open the taphole (Nelson & Hundermark, 2014). If drilling practices or equipment are not readily available, lancing practices are implemented. Smelting of PGM material almost always requires both drilling and lancing to remove the matte plug that forms on the inner part of the taphole (Nelson & Hundermark, 2014).

The THC design and properties have an important role in ensuring proper closure of a taphole but also allow for quick and efficient drilling practices. The clay properties that need to be controlled, from a design point of view, are the plasticity, adhesion, and strength development (Figure 2.13) (Otsubo et al., 2010). Strength of the clay and curing of the resin indirectly influence the drilling practice because these alter the material in a way that increases the drilling times and reduces production capacity (Sako et al., 2018). Plasticity of the clay is related to its compressive strength, extrusion pressure, spreadability, and workability. A reduction in plasticity renders the clay less workable and influences its ability to form a good textured mass (Otsubo et al., 2010) (Gupta et al., 2014) (Sako et al., 2018). The ability of a clay to form a stable mass is important for protection and efficient drilling of the taphole. By maintaining high plasticity of the THC, the material effectively spreads to cover not only the inside of the tapping channel but also the inside of the furnace at the end of the tapping channel, the latter part being more important for blast furnace smelting. For any PGM smelting the clay spreadability should be sufficient to fill only the tapping channel and not the back end of the taphole as the contact between clay and superheated matte/molten bath increases wear due to turbulence. An increase in spreadability will ensure maintenance of long THC lengths to prevent molten material from accumulating on the inside of the taphole and penetrating clay in the taphole. This will result in hardening of the molten material inside the taphole due to thermal gradients and increase the difficulty of drilling. The objective is to achieve a long enough THC length to ensure that molten material does not enter the tapping channel or react with the THC to form a hardened plug inside the furnace.

The strength of the clay material also influences the drilling time and practice. If the strength of the material is too high, the specific drilling practice might not suffice, so lancing may need to be implemented or drilling times will increase. Lancing is extremely effective in opening tapholes, but at the expense of taphole longevity. The extreme temperatures experienced by a taphole during lancing promotes exposure of taphole refractory materials to high heat fluxes and oxidation of carbon refractories: this is therefore a less-preferred method of opening a taphole (Nelson & Hundermark, 2014; Thomson, 2014). The curing rate of the clay and strength development are related, and both influence drilling efficiency. To improve drillability, the clay needs to have high adhesion and accompanying strength development. A lower resin content in the binder of the clay delays strength development, but gradual strength formation is achieved at higher temperatures (<300°C). Thus, by using a lower resin content in the clay binder, the material will have reduced drying ability, but improved drillability (Kitamura, 2014).

2.2.3. Performance indicators for protecting the taphole channel

Along with the THC ramming process and drilling practices during tapping, protection of the hearth and taphole refractories are extremely important for successful operation and longevity of a furnace lining. Protection of the furnace refractories reduces the overall cost of refractory replacement due to lower wear rates (Otsubo et al., 2010; Gupta et al., 2014). Longevity of refractory materials is dependent on several THC properties: wear has the largest influence. Thus, refractories need to be maintained in good working order to increase furnace life and operations need to be favourable for reduced refractory wear. There are many ways in which hearth blocks and taphole refractory materials can be protected to reduce wear rates, mainly by ensuring that longer taphole lengths are attained during smelting. The most crucial of THC performance indicators is the taphole length because this is the easiest and most effective way to extend the life of a furnace. The following are consequences of consistent taphole lengths (Otsubo et al., 2010; Gupta et al., 2014; Nightingale et al., 2006; Nelson & Hundermark, 2014; Perez, 2004; Thomson, 2014):

- Quick and effective opening of the taphole;
- Constant stream of molten material tapped from the furnace;
- Reduced wear near the taphole, the hearth blocks, and heat flux dissipation from the taphole;
- Formation of a mushroom on the inside of the taphole (application-specific);
- Increased tapping duration due to less wear and constant molten liquid flow from the taphole;
- Less splashing of molten material from the furnace;
- Proper sealing of the taphole to prevent molten material seepage or excessive gas evolution from the furnace;
- Increased stability of the burden (dead man) formation in blast furnace applications;
- Maintained integrity of the taphole seal during smelting operations.

A longer taphole length is achieved is by multiple contributing factors, such as spreadability of the clay (plasticity), hardening and curing rates (drying) of the resin in the clay, ease of drilling (sintering strength), maintaining a constant taphole diameter while tapping, and sufficient wear of the taphole to ensure that it can be properly closed without compromising the integrity of the taphole material (Otsubo et al., 2010; Nightingale et al., 2006; Nelson & Hundermark, 2014). Problems arise with THC that exhibit lower plasticity when extrusion through the mud gun and ramming of the taphole need to take place. Lower plasticity causes spreading of the clay in the direction of injection, so lower and shorter taphole lengths are achieved. Lower plasticity also reduces the quantity of clay that can effectively move into the taphole by extrusion before reaching the pressure limit of the mud gun. Rapid curing of the resin causes the clay to prematurely dry out inside the taphole, which limits movement of the clay along the taphole, so loss in texture and formability can occur much earlier. The result is that the clay is not pushed all the way to the inner part of the taphole. Reduced drillability resulting from increased strength causes the need for lancing, which damages the taphole refractory, increases the taphole diameter beyond that acceptable for constant molten liquid flow, and shorter taphole lengths are achieved in subsequent ramming processes. Wear resistance

needs to be optimised to allow sufficient wear of the taphole diameter during tapping to ensure that the proper quantity of clay is rammed into the taphole to properly close and maintain the taphole length.

2.3. Required properties of taphole clay

Taphole processes during operation are controlled by the THC properties. The relationships between the various THC properties and the influenced taphole processes are shown in Figure 2.13. The required THC properties discussed in this section are plasticity of the clay, content of binder and its influence on porosity of the clay, sintering strength (which translates to durability of the clay), adhesion of the clay and how this relates to curing of the clay and strength development, thermal expansion, and wear resistance.

2.3.1. Plasticity and rheology (viscoelasticity)

Plasticity is a complex concept. It is described by a combination of tests that include 1) compressive strength after heating at 150°C, 2) extrusion pressure as a function of temperature and time (aging), 3) extrusion pressure thermal aging (drying test), 4) spreadability test and a compactability test that includes aging of the workability, and 5) workability thermal aging (drying test). The combination of these results holistically describes the plastic behaviour of a clay, both in the mud gun and when rammed into the tapping channel (Otsubo et al., 2010; Kitamura, 2014; Perez, 2004).

The compressive strength is evaluated after aging at 150°C in reducing conditions. Different binder viscosities can be used in the clay formulation to simulate the effect on compressive strength of the clay (Otsubo et al., 2010). Figure 2.15 shows the effect of different THC binder viscosities on compressive strength of a clay. The trend shows that, at lower binder viscosities, there is a point where the load on the sample remains constant (stagnant point) as the stroke increases and then reaches a plateau and starts to increase again. Samples with lower binder viscosity experienced a lot of cracking (Otsubo et al., 2010). As the binder viscosity increased, the load continually increased. Samples C and D exhibited a relaxation of load, which means that the sample experienced minimal cracking and exhibited higher plasticity (Otsubo et al., 2010).

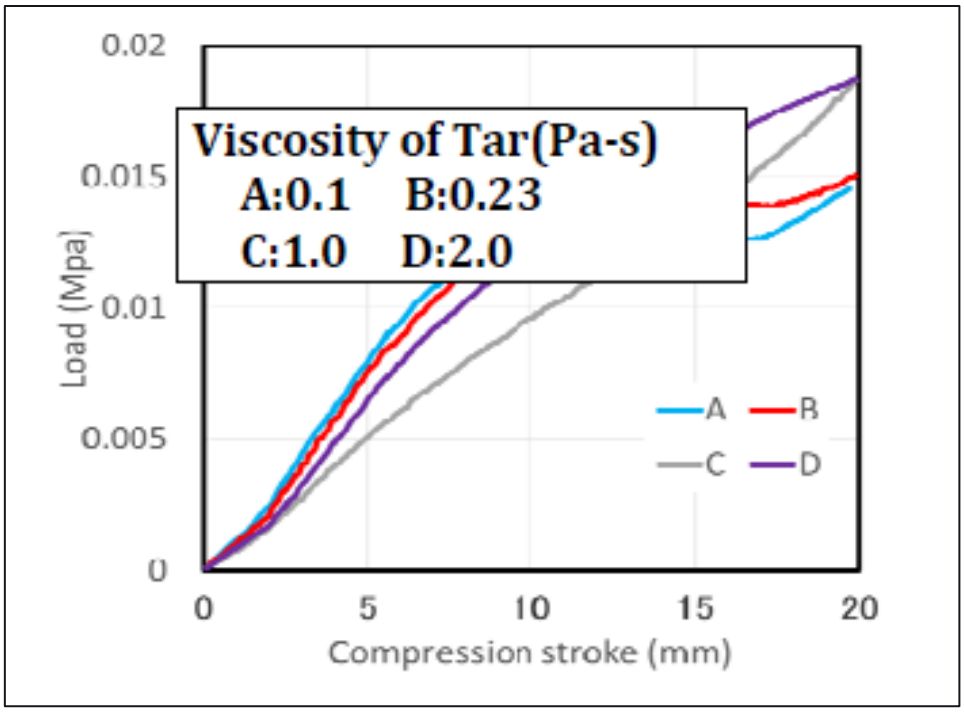

Figure 2.15: Compressive strength test showing the effect of taphole clay binder viscosity on the compressive load (MPa) and stroke (mm) (Otsubo et al., 2010)

The extrusion pressure (Marshall extrusion pressure; MEP) (Cameron, 2021) is evaluated as a function of both temperature and time. The clay sample is heated between 30–70°C in incremental steps of 10°C. This shows any change in extrusion pressure as the binder viscosity increases to develop the green strength of the clay (Otsubo et al., 2010; Gupta et al., 2014). The general trend is that the clay becomes more brittle as the temperature increases, due to low-temperature volatilization of the binder that increases the viscosity, although this can be aggravated due to premature cross-linking of the resole resin in the binder (Cameron, 2021). The increase in temperature and resulting increase in the extrusion pressure reduce plasticity of the clay (Perez, 2004). When evaluating the extrusion pressure at 25°C as a function of time (aging effect), the clay is extruded after aging for 4–60 d at 25°C. An aging test result is shown in Figure 2.16 for a tar and resole resin-based THC, which clearly indicates that the extrusion pressure increased as aging progressed, which resulted in a reduction in the plasticity (Cameron, 2021; Perez, 2004).

The increase in extrusion pressure with age is due to binder penetration into the aggregate raw materials, which reduces the clay rheology with time. Because of the relatively high viscosity of the binders used in THC, penetration of liquid into the aggregate raw materials of the clay is delayed, so the effect is only seen as the clay ages. The results in Figure 2.16 compare the effect of adding resole resin with a synthetic pitch binder to evaluate the effect on MEP aging. The MEP increased in the first 5 d, whereafter it reached a plateau. A continual increase in MEP with aging, as shown by Clay A, is undesirable because this creates problems when the clay needs to be extruded after a period of aging. For this specific difficulty of aging of clays as an effect of the binder viscosity, THC are usually aged for a minimum of 7 d before they are used for ramming.

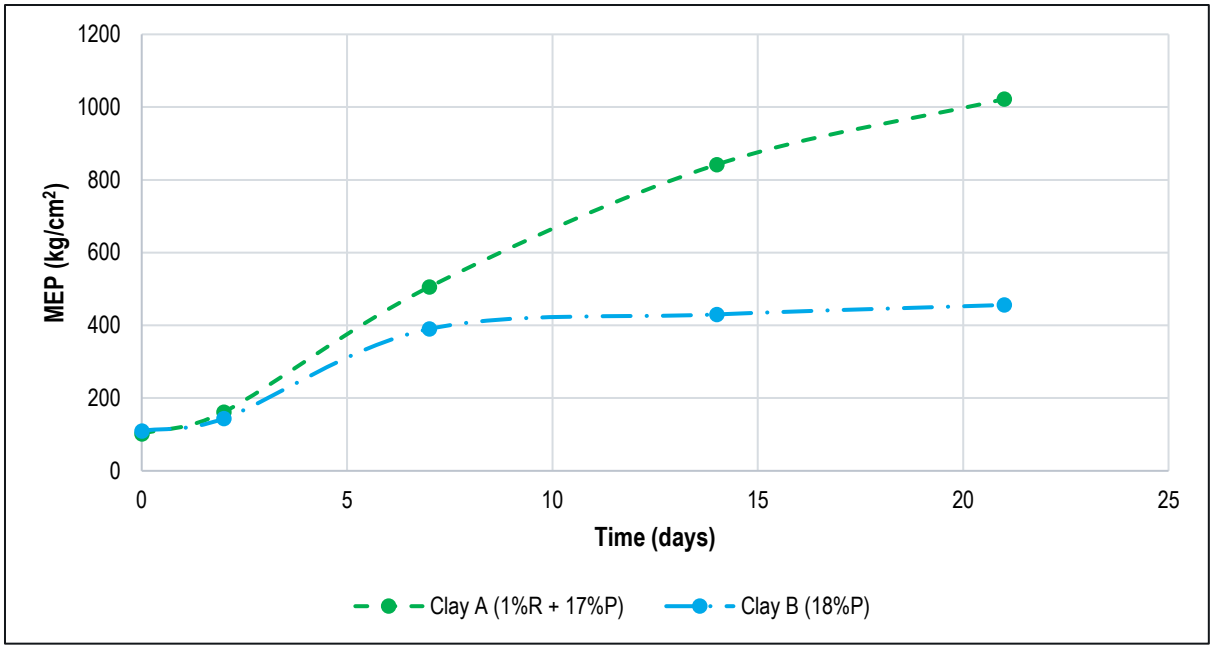

Figure 2.16: Marshall extrusion pressure (MEP) aging of two taphole clays. Clay B contained a synthetic pitch (P) and Clay A contained the same pitch with resole resin (R) (Cameron, 2021)

The third extrusion test that forms part of the plasticity evaluation of a clay is the MEP thermal aging (drying test). This test simulates the dwell time of the THC inside the mud gun. The dwell time refers to the maximum time a THC can be present inside a mud gun at slightly elevated temperature before it becomes difficult or impossible to extrude. The clay is heated in oxidising conditions at 60°C for a period of 48 h, during which the pressure required for extrusion is evaluated after 1 h, 24 h, and 48 h. The change in mass of the sample is recorded because the release of volatiles is related to drying of the clay. Figure 2.17 shows the results of MEP drying tests of tar and resole resin-based THC (Cameron, 2021). THC containing resole resin is prone to drying due to temperature sensitivity of the resin. The clay that only contained tar as binder reached a plateau after 20 h, which means that volatiles were released at temperatures lower than 60°C; the MEP of the clay that contained resole resin and tar continued to increase with time. For the purposes of determining the dwell time, the time at which the tar-only sample reached a plateau was used as the dwell time for the sample that contained resole resin.

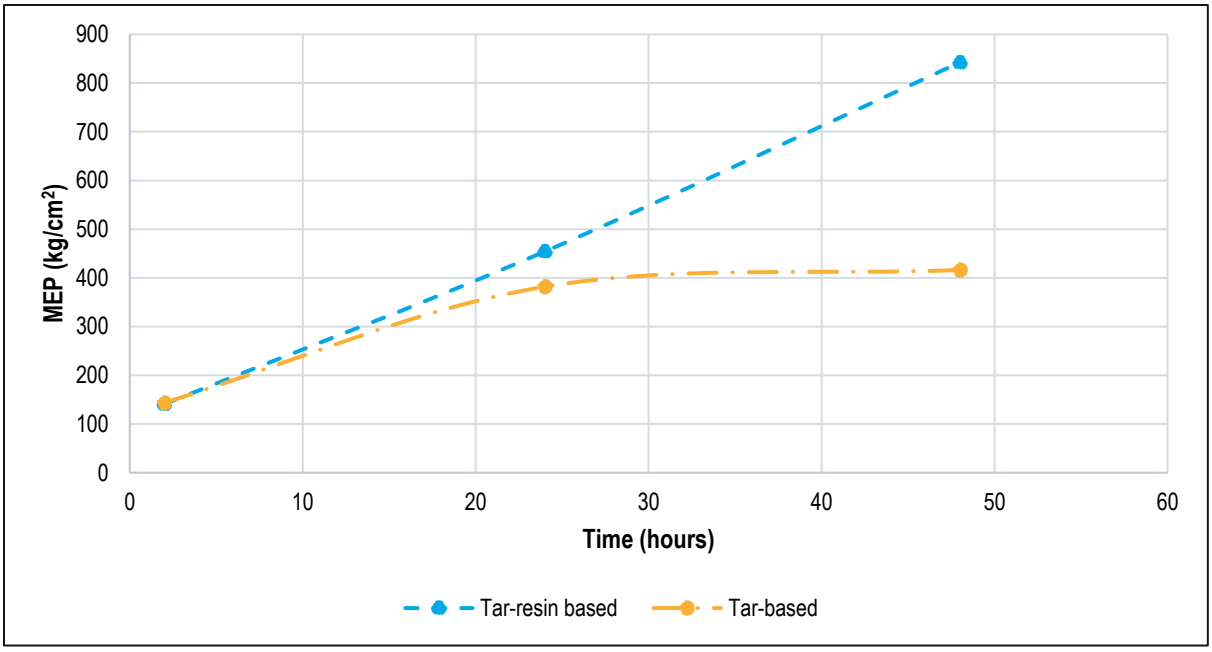

Figure 2.17: Marshall extrusion pressure (MEP) aging test (60°C) results showing the effect of resin addition on the extrusion pressure of a taphole clay

The spreadability test (Figure 2.18) is a visual examination of a THC sample after it has been rammed into a coke-filled furnace taphole: the quantity of clay rammed and extrusion pressure required are recorded during an injection simulation test (Kitamura, 2014). The spreadability test is considered one of the most important when looking at reformulating a THC or designing new clay materials (Kitamura, 2014). Spreadability is examined both parallel and perpendicular to the injection direction. The furnace into which the clay is rammed through the taphole is filled with coke to simulate movement of the rammed clay between the voids in the coke once heated. The simulation gives a good indication of the spreading of the clay into the coke to form a mushroom, but also in the perpendicular direction, which assists with protection of the sidewalls (Mc Dougall, 2014; Nelson & Hundermark, 2014). An example of the spreadability visual examination is shown in Figure 2.18, where the samples have been removed from the coke in the furnace after the injection simulation test. The samples were two different clays for which the effects of different grain size distributions and binders on the spreadability were evaluated. The sample on the left showed greater spreadability than that on the right, which utilised a special tar.

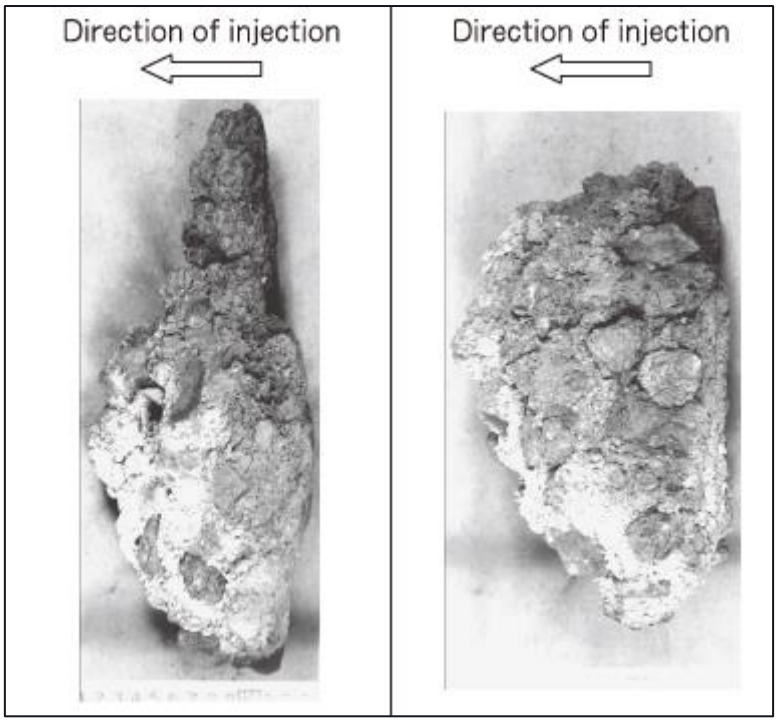

Figure 2.18: Spreadability visual evaluation of two different taphole clays. Left: tar-based clay with 2% less material > 1 mm than right, which utilised a special tar (Kitamura, 2014)

THC that exhibit good spreadability parallel to the injection direction ensure a longer taphole length in a shorter time, but the taphole closure is not stable. THC that show increased spreadability perpendicular to the injection direction tend to be more stable, but do not achieve sufficiently long taphole length due to the sedimentary nature of the deposit that gradually grows in the taphole (Kitamura, 2014). THC that exhibit good spreadability perpendicular to the ramming/injection direction also have good plasticity performance (Kitamura, 2014).

The final set of tests used to describe the plasticity of THC is collectively called a compactability test. This involves workability aging and workability thermal aging tests that are similar to MEP aging and thermal aging tests, respectively. The compactability test gives an indication of how well the THC compacts in the tapping channel after it has been aged and dried in the mud gun. Good compactability of THC is a desired property because it ensures proper closure of the taphole (Otsubo et al., 2010). Compacting of a THC is related to its ramming characteristics (Otsubo et al., 2010), so the workability and extrusion pressure (MEP) are collectively evaluated. Generally, any specific furnace THC will have a desired compactability, expressed as the percentage compaction, and is referred to as workability, i.e., how workable (formable) the clay is. Workability is determined at a specified temperature, which is generally the same as the barrel temperature of the mud gun. The test involves compacting 350 g of THC material with a sand rammer (Figure 2.19) under constrained conditions (inside a cylinder) and applying a load pulse to the sample under unconstrained conditions (removed from cylinder) so that it can deform across the width of the sample as the load is applied. The change in height of the sample is calculated as a percentage, which is referred to as the workability.

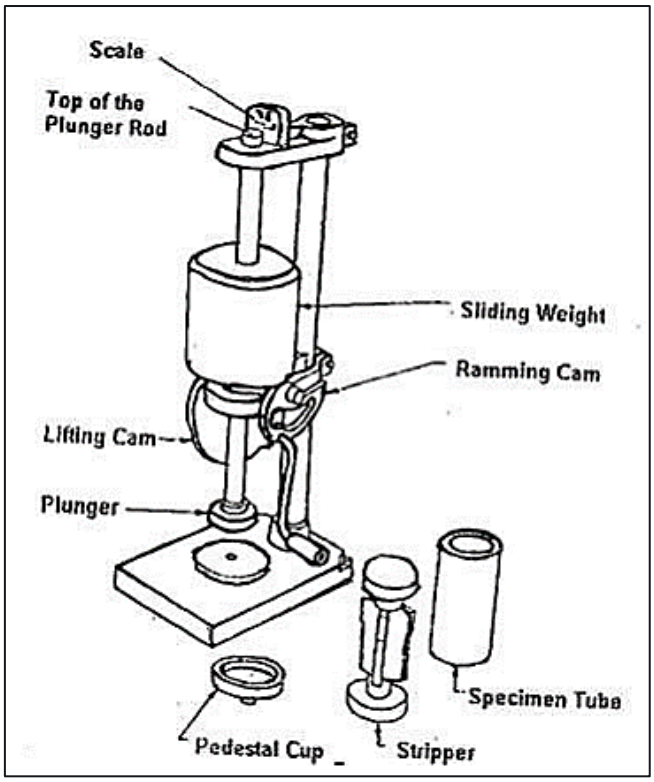

Figure 2.19: Sand rammer used for compacting taphole clay materials during workability testing (JSS Science and Technology University, 2006)

The workability aging test involves aging the clay material at 25°C for a period of 60 d, during which the sample is intermittently evaluated. An example of workability aging test results is shown in Figure 2.20: the samples are the same as used for the MEP test results shown in Figure 2.16.

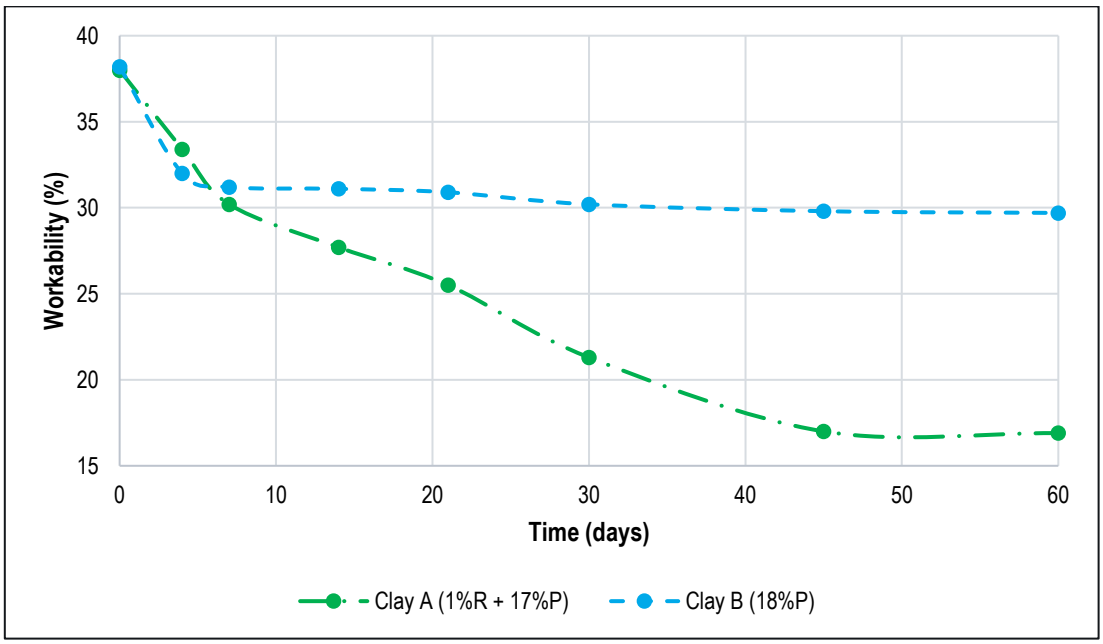

Figure 2.20: Workability aging test results of two clay materials to evaluate the effect of binder on the compacting properties. Clay B contained a synthetic pitch (P) and Clay A contained the same pitch with resole resin (R) (Cameron, 2021)

The workability results of Clay B in Figure 2.20 represent typical behaviour expected of a clay sample as it ages. There was a slight decrease in workability between Day 0 and Day 4 or up to Day 7; thereafter the workability reached a plateau. Some clays, depending on the type of binder used, will only reach a plateau in workability after 14 d of aging. For all THC, a specified percentage reduction in workability is allowed of generally ~ 10–15% in the first 4 to 7 d, dependent on the furnace application. As shown in Figure 2.20, the reduction in workability of Clay B was ~ 15% after 60 d, which is an example of good workability aging. Clay A did not exhibit typical workability behaviour because it continually reduced as the sample aged. This is unfavourable because compacting of this material after 60 would not be possible (reduction of 51%) with the ramming equipment used for this clay. Excessive aging of this sample would also pose a risk for short taphole lengths inside the tapping channel (Perez, 2004) due to the low compactability of the clay that is needed to effectively move the material into the taphole and form a permanent seal. The material only reached a plateau after 45 d, which is due to completion of interaction between the two binders used in the clay, rather than binder movement into aggregate pores (Cameron, 2021).

There is a distinct relationship between the MEP behaviour shown in Figure 2.16 and Figure 2.20. As the clay aged and the workability decreased, the extrusion pressure increased. This means that it would become increasingly difficult to extrude the clay from the orifice of the mud gun. Clay B sample reached a plateau after 4–7 d for both workability and extrusion pressure aging; Clay A showed a continual increase in MEP and reduction in workability. Therefore, when assessing the extrusion pressure changes of a THC material, the compacting characteristics of the clay also need to be taken into consideration.

The plasticity and thermal expansion properties of THC are important for all applications (iron and steel, PGM smelting, ferro-alloys, and non-ferros alloys). It is imperative to make use of a high plasticity clay with high thermal expansion that is adequate to ensure proper closure of the taphole, but also for protection of the taphole (such as by mushroom formation in a blast furnace during in pig iron production). Plasticity influences how well the clay is rammed into the taphole, how well a permanent seal forms inside the tapping channel, how well the clay expands into the taphole and tapping channel perimeter in order for the sintered clay mass in the tapping channel to attain a high sintering strength and influences the corrosion resistance by coating the taphole and in the case of blast furnace, the inside of the hearth with clay material.

2.3.2. Binder quantity and porosity for release of volatiles

Development of a THC requires that various components of the clay design be critically evaluated and closely replicated. The binder is one of the most important components and plays a significant role in overall performance of the clay. The binder composition and quantity alter the rheology and clay physical properties, such as porosity and sintering with tapping channel refractory material (Otsubo et al., 2010). Most binders used for THC materials are organic and consist of different functional groups, so the binder composition determines the rheological behaviour (Cameron, 2021). The types of binders used in taphole clay and their effects on clay performance and process indicators have been discussed in section 2.1.3.

When making changes to binder/s in THC, there are a few important clay properties related to the binder that need to be evaluated. The extrusion pressure and AP need to be as close to those of the original product (Otsubo et al., 2010). Volatilisation behaviour of the binder/s determines the AP of the clay because abrupt or quick volatilisation causes an increase in AP (Otsubo et al., 2010). Volatilisation of the binder is a function of the chemical composition because different molecular mass species will volatilise at different temperatures (Lindstad, 2018). It is generally accepted smelting practice that to reduce volatilisation of the clay, it should contain the minimum binder quantity possible, yet be sufficient to maintain the correct extrusion pressure with time (aging) and desired porosity (Otsubo et al., 2010; Nightingale et al., 2006).

Binder content influences the casting duration (Otsubo et al., 2010). As mentioned, the two most important properties of the clay that are influenced by the binder are the extrusion pressure and AP. These, in turn, influence other features of the clay (Figure 2.1), such as the plasticity, wear resistance, strength, adhesion, sintering strength, and strength development. Hence, changing the quantity or type of binder will influence the casting duration by reduced plasticity, increased wear, and lowering in sintering strength. To ensure longer casting duration, the binder content needs to ensure proper extrusion and ramming inside the taphole and lower AP to assist with reduced wear of the clay and increased sintering strength (Otsubo et al., 2010; Gupta et al., 2014). These guidelines will ensure that the duration of tapping is lengthened, but not to the detriment of the THC refractory.

Evaluation of the extrusion pressure and plasticity are discussed in Section 2.3.1. AP requires simulation over a temperature range following manufacturing and a chosen aging period to determine the change in volatilisation with time. The main aim is to ensure that the AP does not significantly increase and that there is a slow and consistent volatilisation over a wide temperature range (Lindstad, 2018): any abrupt volatilisation could cause large open pores, cracking, or build-up of internal gas in the material. The test involves compacting cores of THC material (50 mm height; 50 mm diameter) that are heated in reducing conditions from 140–1250°C in increments of 100–200°C for 3 h. The maximum temperature of 1250°C ensures that the resin completely volatilizes and both the resin and the pitch carbonizes. A lower AP will benefit sintering strength of the clay by increased durability (Gupta et al., 2014). Figure 2.21 shows an example of the effect of adding ultra-fine matrix powder to a clay on the binder usage and AP of the clay. Voids are reduced by filling with fine powder and liquid binder. Ultra-fine powder is added to the clay matrix to assist with lowering the binder content required and reduce volatilization. Flow properties of the clay are largely dependent on the binder rheology. The results in Figure 2.21 show that AP reduced as the binder content was reduced.

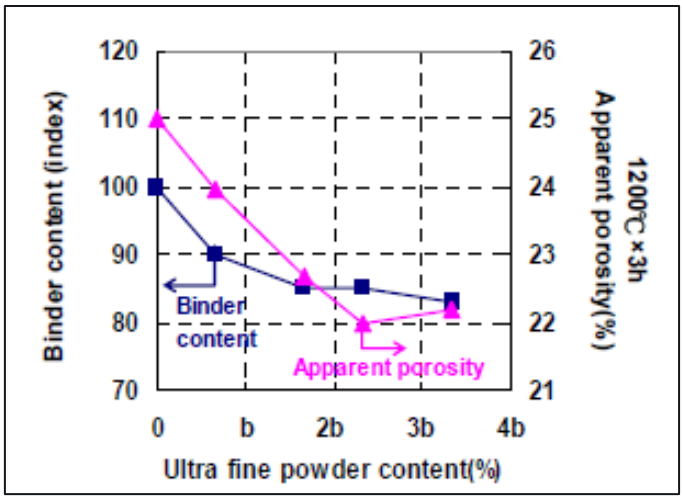

Figure 2.21: Effect of ultra-fine powder addition to the matrix of a taphole clay on the binder content and apparent porosity of the clay (Otsubo et al., 2010)

2.3.3. Sintering strength (durability)

The strength of a refractory material can be reported either as modulus of rupture (MoR) or cold crushing strength (CCS). To understand the true sintering strength of a material, best practice uses a structural integrity test, i.e., MoR (Otsubo et al., 2010; Gupta et al., 2014). This is a three-point bending test in which a rectangular refractory sample is placed on each end on a platform that is open between both points (Figure 2.22). The third contact point and the load finger apply a constant force downwards in the middle of the sample until it fails.

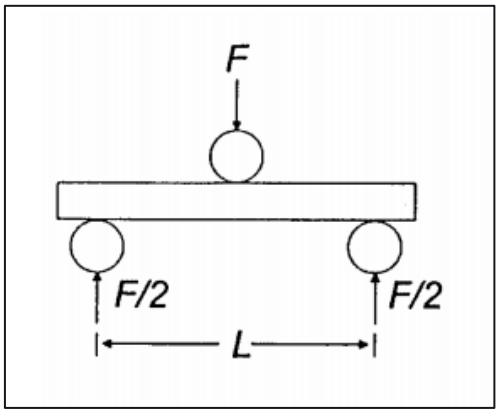

Figure 2.22: Schematic of hot modulus of rupture (MoR) test setup, illustrating the applied force onto the sample and contact points on both ends (Morrell, 1997)

The main factor contributing to strength of a refractory material is the extent of sintering of the clay. Each raw material in the THC will have their own extent of sintering enhancement: the overall effect is evaluated using a sintering strength test. The strength of a refractory material is closely related to AP: as the porosity increases, the sintering strength of the material will generally increase because the structure becomes denser (Otsubo et al., 2010); thus, AP is also evaluated as part of the sintering strength test.

The strength of a refractory material, and how it withstands the environment inside the furnace and the taphole, is referred to as the durability (Gupta et al., 2014). High durability is required to increase the tapping duration. For high durability, a refractory material should have low AP and a densely packed structure (Otsubo et al., 2010; Gupta et al., 2014). There also needs to be a balance between the density of the refractory matrix and evolution of gas to avoid sudden eruptions of refractory materials due to build-up of internal pressure (moisture) or spalling due to thermal cycling. If the matrix of a refractory material is too densely packed, there are not enough crack-arresting sites to prevent crack propagation once cracking occurs and spalling may occur. Drillability of THC is also dependent on durability, although high strength of the refractory materials increases drilling times. To increase the casting duration of a furnace, the durability of the THC needs to be sufficiently high. This is achieved by lowering its AP by effective sintering of the clay matrix by ensuring gradual volatile release of binder as the clay is heated. Reduction of the clay porosity also increases the wear resistance of the refractory: increased sintering strength will increase the erosion resistance as part of the wear process (Otsubo et al., 2010). Improvements in the abovementioned features contribute to increased casting duration.

Methods for evaluating the sintering strength or durability include the hot modulus of rupture (H-MoR) and AP. The AP is described in Section 2.3.2.; however, the maximum test temperature is 1500°C. The results obtained from the standard AP test (1250°C) can be used with an additional two samples tested at 1400°C and 1500°C. The sintering strength test uses rectangular cast THC samples that have been fired at 800°C, 1000°C, 1200°C, and 1500°C in reducing conditions for 3 h and allowed to cool. The samples are then evaluated by a three-point contact load test until failure occurs (Otsubo et al., 2010). The calculated strength is recorded in MPa. Figure 2.23 shows an example of a THC material that was evaluated to determine the effect of nitriding components on AP and MoR. The correlating graph, shown in Figure 2.24, indicates that an increase in MOR of the material will result in reduced wear indexes. The effect of increased MoR—in this example, the H-MoR—due to a reduction in AP of the material is illustrated in Figure 2.25. The nitride additive causes reduced AP that results in densification of the matrix.

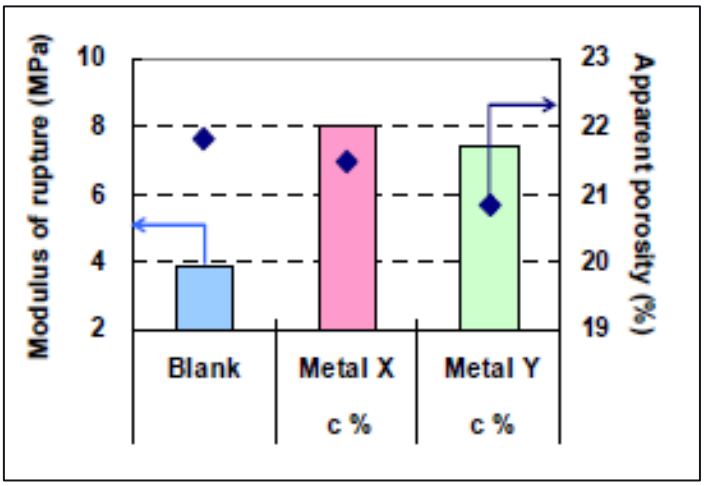

Figure 2.23: Effect of metallic (nitride) additions to matrix of taphole clay materials on the modulus of rupture and apparent porosity (Otsubo et al., 2010)

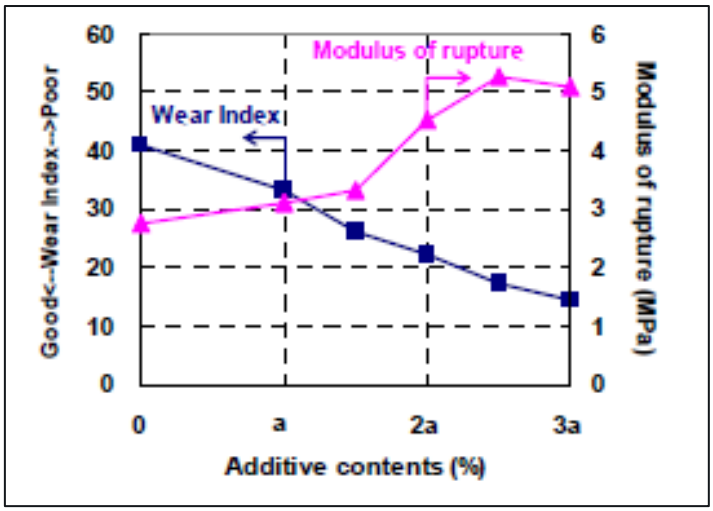

Figure 2.24: Effect of change in modulus of rupture of a taphole clay material on its wear index (Otsubo et al., 2010)

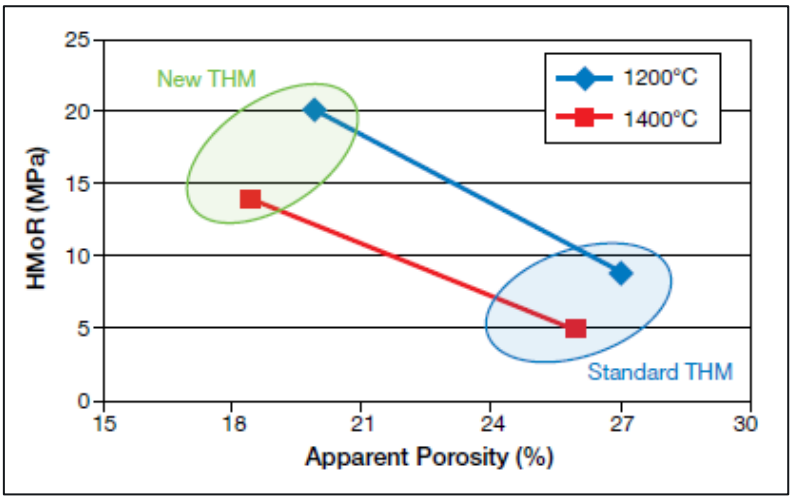

Figure 2.25: Comparison of hot moduli of rupture of two taphole clays as a result of apparent porosity changes (Sako et al., 2018)

2.3.4. Adhesion, resin curing, and strength development (drying ability)

Section 2.2.2.2 and 2.2.2.3 discussed the importance of adhesion and how the resin and binder influences both the adhesion and strength development of the THC. The following discussion continues on this topic with results obtained from clays of different composition to highlight the relationships mentioned in these previously discussed sections.

THC properties related to splashing of molten material during tapping need to be evaluated to understand the behaviour seen in practice. Plasticity and binder optimisation results, discussed in Sections 2.3.1 and 2.3.3, respectively, can be used to assess splashing behaviour of the clay. The strength development evaluation comprises a CCS test with time conducted at a defined temperature. Five core samples (35 mm diameter, 30 mm height, 350 g clay material) are prepared by ramming technique using a sand rammer. The samples are evaluated at 200°C in oxidising conditions and removed after 10, 20, 30, 60, and 120 min soaking time, then cooled to room

temperature and weighed again to determine the mass change. The cores are subjected to CCS analysis, as shown in Figure 2.26, which compares the effect of two binders on strength development of the clay.

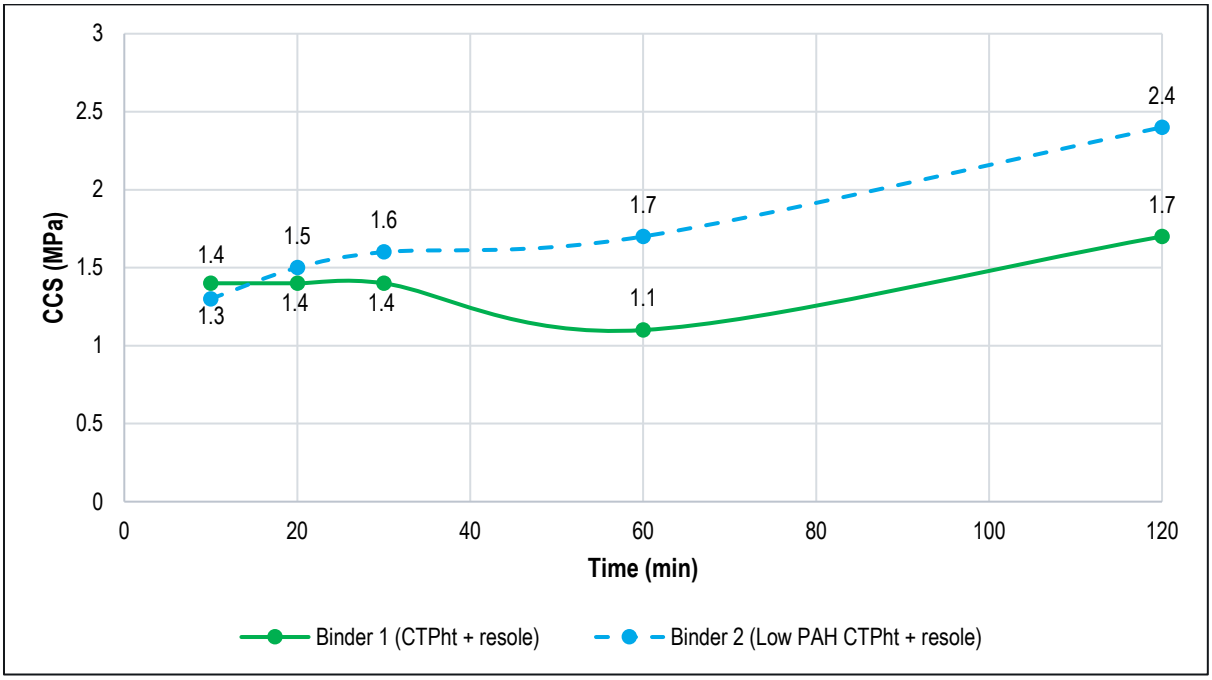

Figure 2.26: Strength development of blast furnace THC with two different binders (Cameron, 2021)

The trend in CCS development followed the same path for both samples, except that the Binder 1 sample showed a decrease in CCS between ~ 28–60 min, after which the compressive strength increased again. This could be due to low-temperature volatilisation of certain functional groups present in the CTPht that evaporated more readily than in the lower-PAH CTP sample (Binder 2) that might not have contained these species. These trends are unique to a specific THC due to the matrix composition and binder ratios used. The objective is to have a continual increase in CCS with heating time. Relaxation of the strength development occurred at 30–50 min. Ideally, the CCS should not drop too much because this may compromise integrity of the clay during heating to form strength through sintering at higher temperatures. When modifying THC binders, it is important to have a similar trend in compressive strength and ensure that the difference with time does not deviate too much: this could cause drying of the clay and compromise other properties, such as spreadability.

Some changes to the THC binder, especially those that contain temperature-sensitive resins, will change the slope of the graph (Figure 2.26) towards longer times if there is a change in the resin structure, such as cross-linking. Such changes could cause premature curing of the resin that increases CCS with time as the resin curing temperature is lowered. In these instances, complete mixing between the binder and chemical interaction needs to be evaluated to ensure their compatibility in the clay (Cameron, 2021).

The adhesion test for THC consists of two parts: a sintering test, which is a structural evaluation where compressive strength tests are conducted under both constrained and unconstrained conditions, and a visual examination, particularly to identify the presence of voids in the sample (Otsubo et al., 2010; Perez, 2004). The sintering and

visual evaluations consider 1) THC adhesion and 2) adhesion of fresh THC to already sintered clay inside the tapping channel (repair property of the THC) (Otsubo et al., 2010).

- Taphole clay and taphole material adhesion

The test makes use of long tubular or rectangular sleeves of refractory material that are filled with THC and fired at a predetermined temperature. The choice of sleeve material depends on the application and the associated refractory used for the taphole and surrounds (Nelson & Hundermark, 2014):

- Blast furnace application: carbon/graphite material;
- PGM, Ni- and Cu-smelting: magnesia chromite ($MgO–Cr_2O_3$) or magnesia (MgO);
- Ferrous and non-ferro alloys: silicon carbide.

Sleeves are manufactured from the desired taphole refractory, like bricks, and a hole drilled through the centre. The sleeve is completely filled with the THC to be evaluated, then fired at 1450°C for 3 h in reducing conditions and allowed to cool to room temperature (Otsubo et al., 2010). The outer surface of the sleeve is examined for crack formation due to THC expansion. The THC is drilled through the centre to expose the inner part of the material and the sleeves sectioned down the middle so that the sintering zone between the sleeve and THC is visible. The sintering zone between the taphole refractory and THC is evaluated for any lack of sintering or drying of clay that would prevent proper spreadability and reduce the sintering effect. The presence of cracks and void formation within the THC are evaluated and recorded as these might be problematic if voids are excessively large or cracking extensive. Visual evaluation of a test conducted on a blast furnace THC and the interaction with the taphole material is shown in Figure 2.27. The taphole refractory used for the sleeves was silicon carbide.

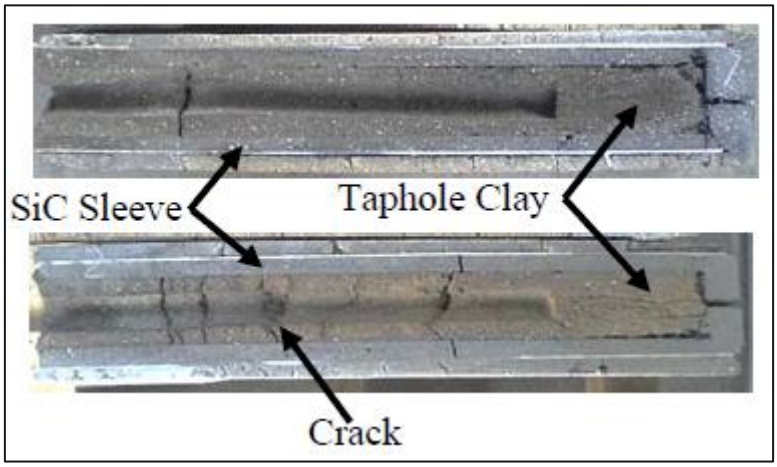

Figure 2.27: Adhesion sleeve test showing the presence of cracking in the taphole clay and improper spreadability at the ends of the sleeve (Otsubo et al., 2010)

- Adhesion between fired- and unfired taphole clays

This test involves the same principle except that a second firing step is involved. To simulate the adhesion between fired THC material inside the taphole and unfired THC material being rammed into the taphole, the test requires a

second firing and ramming step. After the abovementioned test (Figure 2.27) and before sectioning of the sleeve material, another hole is drilled and filled again with fresh unfired THC, and the heating–cooling cycle is repeated. After cooling to room temperature, the outer surface of the sleeve is examined again to evaluate changes in crack size and quantity. The sleeve is then sectioned to expose the sintering zones between the sleeve and fired and unfired clays to show presence of any voids or cracking that occurred.

The desired outcomes of both sleeve tests are to form a proper seal with minimal cracking and void formation within the clay. Expansion of the clay should occur in both the injection direction and perpendicular to ensure a proper seal to maintain the integrity of the taphole seal. The two sintering zones, i.e., between the sleeve and THC, and between the fired and unfired clay materials, need to be dense, with minimal voids or cracking. There should also be a distinct fusion/sintering zone between the respective materials at the interaction zones.

- Compressive strength structural evaluation (constrained conditions)

This test evaluates compressive strength of the THC in contact with the taphole refractory. The choice of taphole refractory is application-specific, as described above. The taphole refractory is sectioned into a cube shape if bricks are used or cast into a cube if a monolithic is used, with sides of 10 mm. A hole is drilled through the centre of the taphole refractory then filled with the THC to be evaluated (Figure 2.28). Five samples are prepared that are heated at 400°C, 800°C, 1000°C, 1200°C, 1450°, respectively, in reducing conditions for 1 h, to evaluate the change in strength with temperature (Perez, 2004). After cooling to room temperature, the samples are sectioned through the centre to expose the clay and taphole refractory (Figure 2.28). The setup in Figure 2.28 is placed on the platform of a compression tester and the top piston that exerts a force onto the sample is aligned with the THC part of the sample. The sample is compressed, and the strength required to disintegrate the taphole material is measured. This is recorded as the compressive strength of the clay material under constrained conditions.

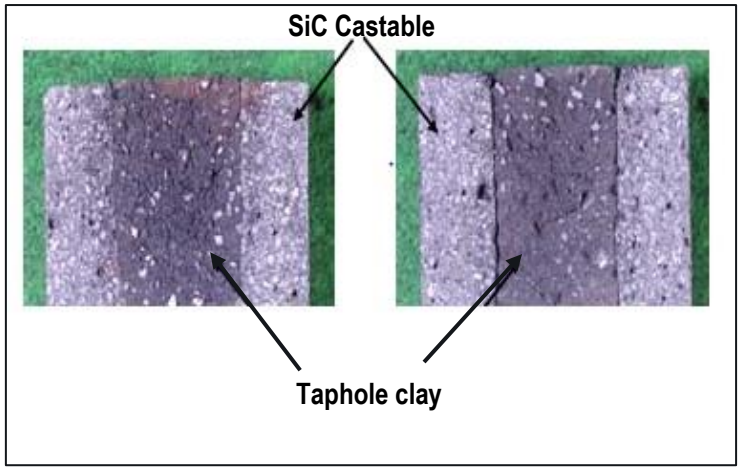

Figure 2.28: Image showing sintered taphole clay within a cube sample of taphole material (SiC) to evaluate the sintering effect (Otsubo et al., 2010)

- Compressive strength structural evaluation (unconstrained conditions)

Evaluation of compressive strength under unconstrained conditions uses cores of the THC sample that are 50 mm in diameter and height. The five samples are heated at 400°C, 800°C, 1000°C, 1200°C, 1450° in reducing conditions for 1 h (Perez, 2004). The samples are allowed to cool to room temperature, after which the compressive strength is evaluated. The strength is recorded as compressive strength under non-constrained conditions because the THC is free to expand and move while heated and tested (Perez, 2004). An example of compressive strength results obtained for a non-polluting THC material, under both constrained and non-constrained conditions, is shown in Figure 2.29. It is evident that this material showed better results under constrained conditions due to self-sintering and simulates a scenario similar to that occurring in an actual taphole.

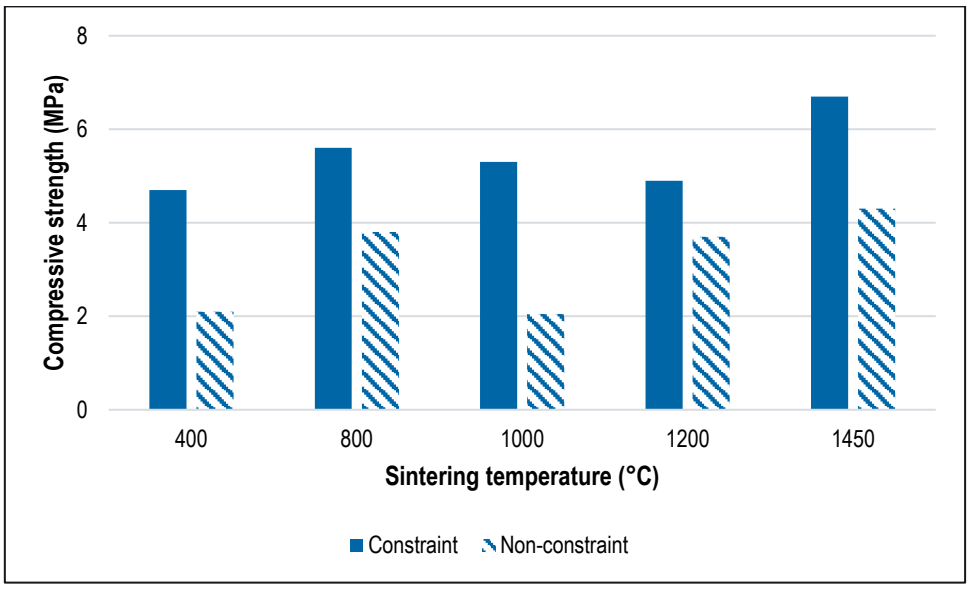

Figure 2.29: Compressive strength results of a non-polluting taphole clay evaluated under constrained and non-constrained conditions (Perez, 2004)

2.3.5. Thermal expansion

Thermal expansion of the clay is evaluated by monitoring the change in dimensions of a rectangular sample. Optimal expansion temperatures differ depending on the raw materials, so the most critical temperature ranges are 600–900°C and 1200–1600°C (Otsubo et al., 2010; Gupta et al., 2014; Perez, 2004): the first temperature range enables evaluation of the simultaneous shrinkage (Figure 2.30) of the clay due to carbon volatilisation (Gupta et al., 2014) and expansion due to heating of pyrophyllite or similar expansive raw materials (Wonderstone, 2020); the second temperature range is to evaluate expansion due to phase formation such as mullite. Formation of primary mullite starts at ~1200°C and can continue up to 1500°C; secondary mullite formation starts at 1300°C (Figure 2.15) (Chen et al., 2000). Examples of results of these tests are shown in Figure 2.31 (100–1600°C) and Figure 2.32 (600–1200°C). Excessive expansion during heating of a clay can lead to cracking and void formation. Visual examination of the sample is required to ensure minimal cracking (deep) and void formation.

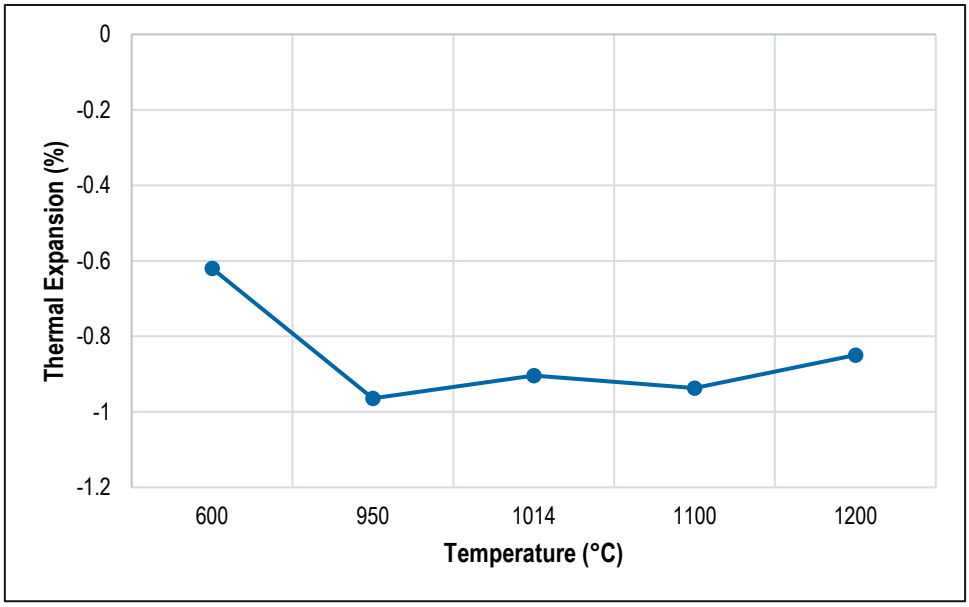

Figure 2.30: Thermal expansion behaviour of a tar-based taphole clay from 600–1200°C (Gupta et al., 2014)

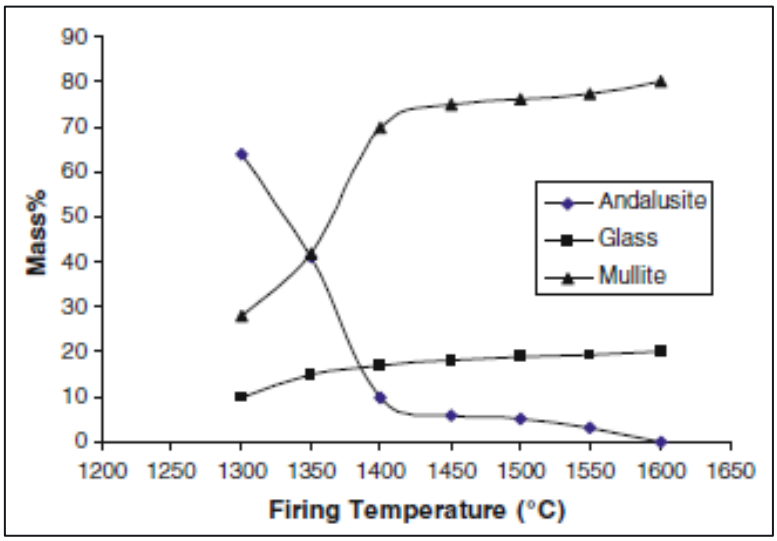

Figure 2.31: Mullite formation from 1300–1650°C, showing the proportion of mullite increasing as the proportion of andalusite reduces (Pooladvand et al., 2011)

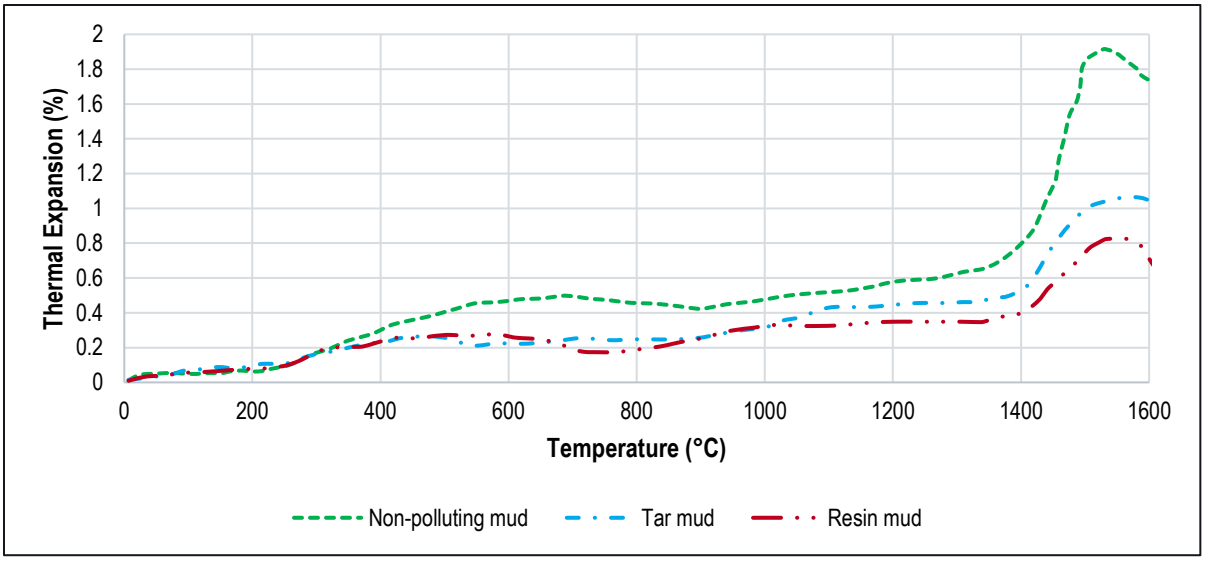

Figure 2.32: Effect of binder composition on thermal expansion of taphole clay at intermediate temperatures (<600°C) (Perez, 2004)

2.3.6. Wear resistance (erosion and corrosion resistance)

The tapping channel and sidewall bricks that surround the taphole experience some of the most aggressive environments in the furnace. Wear can be divided into three successive stages (Figure 2.33): penetration; corrosion; erosion (Nelson & Hundermark, 2014; Campbell et al., 2002).

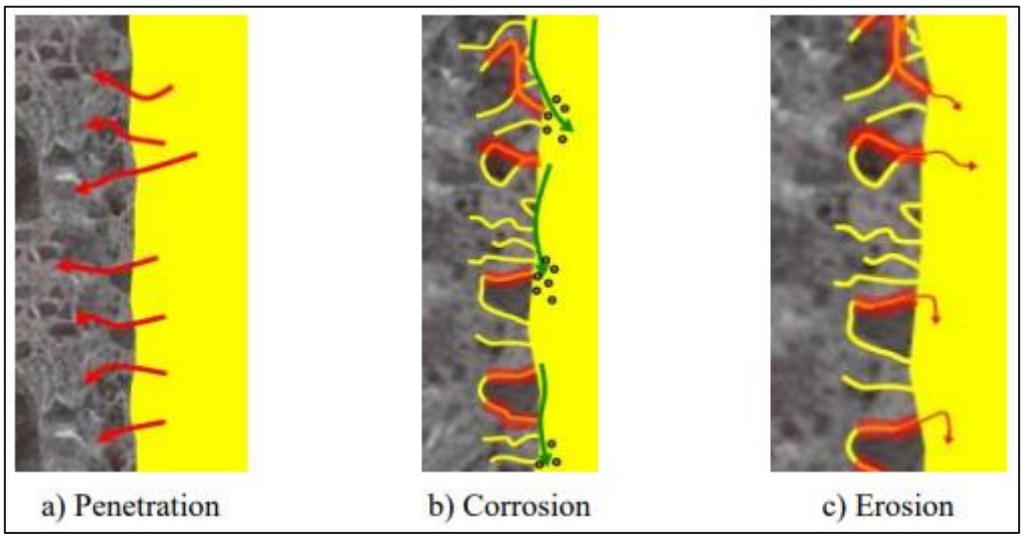

Figure 2.33: Schematic showing the three stages of wear in refractory materials (Campbell et al., 2002)

Penetration is governed by capillary force-driven flow, which is proportional to the capillary radii, the liquid surface tension, the contact angle between the droplets of penetrating liquid, metal, matte, and slag, and the refractory surface. Penetration depth can be determined by Equation 2.2, in which the capillary forces promote flow (Campbell et al., 2002; Chandira et al., 2010):

$$\frac{dl}{dt} = \frac{r\gamma \cos\theta}{4\mu l} = u_{pen}, \quad (2.2)$$

where *l* is the depth of penetration, *r* is the capillary radius, γ is the surface tension in the capillary, μ is the viscosity of the liquid passing through the capillary, and θ is the contact angle. The capillary flow is indirectly proportional to the penetration depth and liquid velocity (Nelson & Hundermark, 2014).

These parameters are all liquid properties, which, depending on the composition of the molten liquid, will change with temperature. If the pore sizes of the refractory material are large and there is chemical incompatibility between the refractory and liquid melt, then corrosion can be expected. The molten liquid properties strongly influence penetration of the refractories, but other factors also need to be considered when evaluating corrosion potential, including chemical interactions (liquid and gas), dissolution, thermal shock, refractory material properties, and operating conditions (Lin et al., 2020; Poirier & Rigaud, 2017) (Figure 2.34).

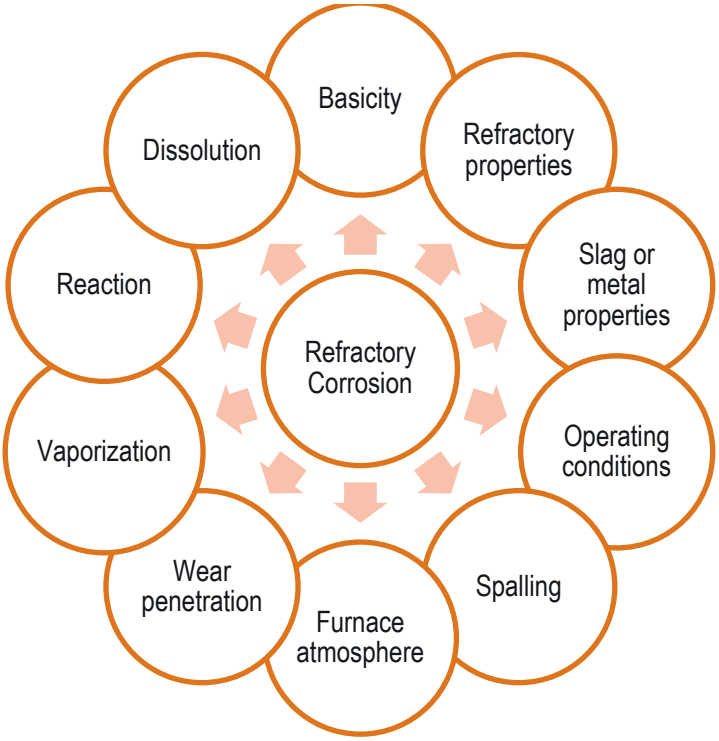

Figure 2.34: Schematic diagram showing causes of refractory corrosion (Lin et al., 2020; Poirier & Rigaud, 2017)

Once a refractory has been infiltrated and the structure weakened by corrosion, erosion is the next wear mechanism. The tendency for erosion depends on whether the shear stress of the corrosive liquid is sufficient to remove refractory material (Nelson & Hundermark, 2014; Campbell et al., 2002). The liquid velocity inside the furnace needs to be high enough to produce a shear force that exceeds H-MoR of the material before it can erode; this is why erosion will only take place once corrosion has weakened the structure (Nelson & Hundermark, 2014; Campbell et al., 2002).

2.4. Test methods used to evaluate properties of taphole clay

2.4.1. Extrusion and ramming

Sections 2.2 addressed the relationships of THC performance indicators to specific properties of the clay and how they can be evaluated. All physical or chemical properties of the clay are independently evaluated—not as part of the composite THC (Otsubo et al., 2010; Kitamura, 2014). This is, however, not a true representation of the overall behaviour of the clay. It is necessary to use simulation to evaluate behavioural changes of the clay with alteration of the composition, such as binder replacement. The performance indicators (ramming process, tapping process, and protection of the taphole) are simultaneously evaluated (Otsubo et al., 2010; Kitamura, 2014). This requires simulation of the extrusion, ramming, and drilling abilities of the THC during tapping (Otsubo et al., 2010). Laboratory simulation tests exist to evaluate these THC processes: examples of ramming and drilling are shown in Figure 2.35 and Figure 2.36, respectively.

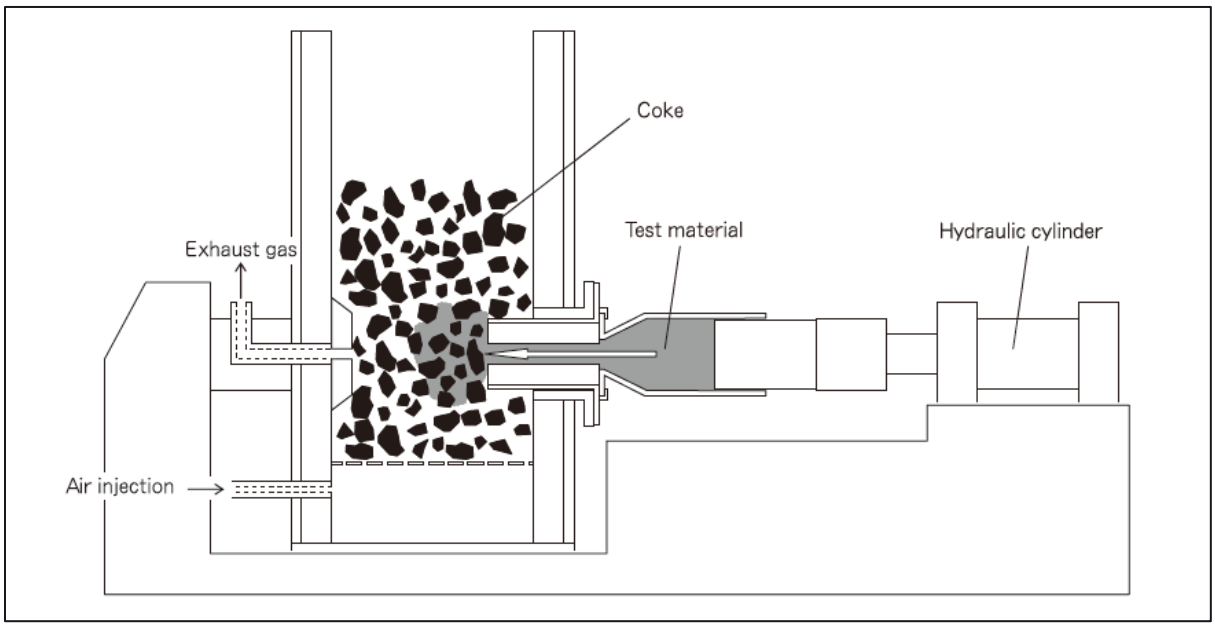

Figure 2.35: Schematic showing a simulation setup for extrusion of taphole clay from a mud gun and ramming configuration (Kitamura, 2014)

The extrusion simulation equipment shown in Figure 2.35 was used to evaluate the quantity of clay material used per taphole closure, the extrusion pressure required to extrude the clay based on a specific mud gun configuration, the taphole length attained, the formation of a mushroom, and spreadability of the clay. The conditions inside the furnace were reducing, obtained by burning of a coal bed in air that was injected into the furnace while heated. This setup is specific for blast furnace applications due to the presence of the coke bed. This equipment can be used to simulate other smelting practices by removing the coke bed and only allowing the clay to move into the furnace to cover the THC. Spreadability in both the injection direction and perpendicular to the tapping channel can be investigated by removing and visually inspecting the clay mass after firing. The orifice configuration that represents the mud gun can be heated and material inside the orifice aged to simulate drying of the clay inside the mud gun

and the resulting changes to the extrusion pressure. Holding time, injection rate, and quantity of clay rammed can be determined. Although this is a laboratory setup, and successful implementation on an industry scale depends on the furnace conditions and the molten material in contact with the clay, this is an effective way to comparatively evaluate design and performance indicators of the clay.

2.4.2. Drilling simulation

The setup shown in Figure 2.36 can be similarly used to evaluate drilling practices and drillability of a clay. The drilling unit can be pneumatic or hydraulic to simulate the practice used in a specific operation. The drilling time can be determined, as well whether the drilling practice will be sufficient or will need to be supplemented by lancing. Strength development, including curing time of the clay, can be investigated if the chamber in which the clay is placed can be heated. In this way, the gradual increase in drilling pressure and dependency on time and temperature can be simulated. Certain drilling tips and practices (Nelson & Hundermark, 2014) can be simulated to evaluate those best suited for the equipment and clay material used.

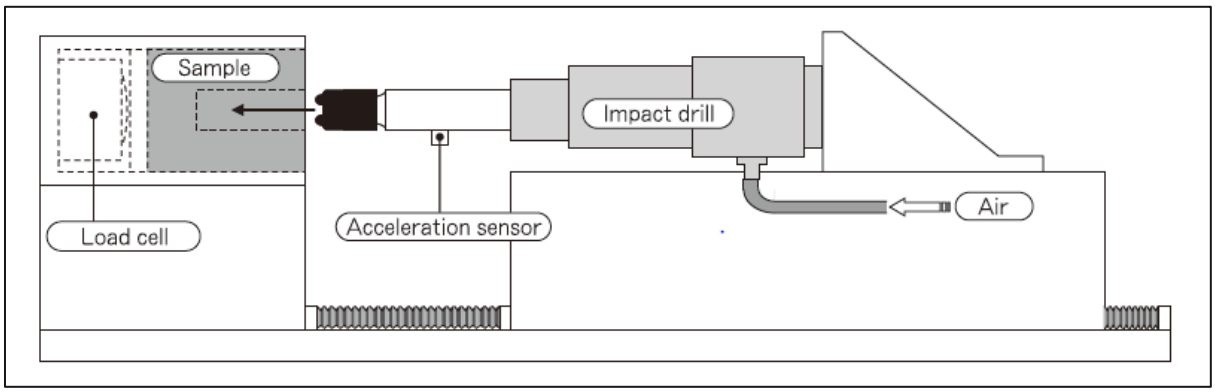

Figure 2.36: Schematic showing a simulation setup for extrusion of taphole clay from mud gun and ramming of a taphole configuration (Kitamura, 2014)

2.5. Conclusion

In this section, various aspects of taphole clay have been introduced, along with the research conducted to understand this composite product, how it can be altered, and consequently, the change in performance. This section introduced the constituents of a taphole clay (aggregate, matrix and binder) and how each of these influences both process parameters such as plasticity change (ramming), extrusion pressure, and protection of the clay, as well as the concept of replacement of binders, which conventionally contain PAH, with lower or zero PAH alternatives. The alternative binders that have been looked at in the past are discussed which include coal-based binders with lower PAH content to CTht, petroleum-based binders such as waxy oils and petroleum pitches and organic binders from plant sources. The literate section showed that with a decrease in PAH (considered toxic), certain changes in the taphole clay need to be addressed from a product design point of view, such as carbon content. The relevant changes in flow properties and how inclusion of a low temperature strengthening agent (phenolic resole resin) can alter both the flow behaviour and intermediate strength of the clay are discussed. Taphole processes including ramming, tapping, and protection are introduced, and a relationship diagram showing

the correlations between clay features and taphole processes, illustrating their interconnected relation to each other. It is discussed how properties like plasticity, adhesion, strength development are related and how changes in the binder affects these properties, leading to related changes in the taphole processes.

Chapter 3

Experimental

"No amount of experimentation can ever prove me right; a single experiment can prove me wrong" - Albert Einstein

3. Experimental

3.1. Materials

3.1.1. Binders

The reference binder selected for the purpose of this investigation was coal tar (CTht), although both CTht and CTP (CTPht) can be used. The binders selected for evaluation as alternatives to CTht are described in this section, as well as the methods for producing the bio-polymer liquids that were also evaluated as alternatives. The selected binders originated from various sources, including coal-based, petroleum-based, wood/plant-based, liquid carbohydrates/polyol compounds that are used as plasticizers, and biopolymers, such as polysaccharides. The binders evaluated are listed in Table 3.1.

Table 3.1: Binders from different sources evaluated as alternatives to conventional pitch

Binder designation	Group	Source
CTht	Coal	Crude coal tar
CTPht-B	Coal	Distilled CTP blend
EcoP	Coal	Synthetically produced pitch
CWO	Petroleum	Crude wax (paraffin) oil
PCWO	Petroleum	Processed wax oil
MP	Petroleum	Bottom from phenolic depitcher – starter material for mesophase pitch
Tar-PW	Wood	Pinewood tar from Kraft process
Tar-BW	Wood	Beechwood tar from Kraft process
Tar-Veg	Vegetable	Tar from processed vegetable discards
Gly	Carbohydrate liquid / polyol compound	Research-grade glycerine
Gly+XG	Biopolymer/carbohydrate	Xanthan gum plasticized with glycerine
Gly+XG+PFR	Biopolymer/carbohydrate with phenolic resole resin	Xanthan gum plasticized with glycerine and mixed with resole resin
CTht+PFR	Coal tar and phenolic resole resin	Coal tar reference binder (CTht) mixed with phenolic resole resin in ratio used in THC
PFR	Phenolic resole resin	Lignin modified to increase carbon yield and lower free phenol content

CTht and CTPht-B are coal-based binders, obtained from the tar-processing unit of the coking furnaces at ArcelorMittal, Vanderbijlpark, South Africa. CTht is a crude tar produced from destructive coal distillation during coke-making before it is distilled to produce various softening-point pitches. CTPht-B is a high softening-point pitch

produced from distillation of CTht that has a softening point of 20–25°C. CTPht-B was adjusted with merisol oil to lower the softening point and produce a blended product for the THC application. EcoP is a synthetically produced pitch with a low softening point (30–32°C) and is lower in benzo(a)pyrene compared with the other coal-based binders. The petroleum-based binders derived from different processing units at Sasol Limited, Secunda, South Africa. CWO is a crude wax oil (alkane composition), which is the starter liquid for producing products such as green coke and diesel. PCWO is a processed version of CWO that has received thermal treatment to remove low-temperature volatiles (< 300°C) before it is used to produce a medium-temperature pitch. PCWO is also alkane-based. The MP petroleum-based binder was a mesophase-forming pitch, derived from a bottom stream of a phenolic depitcher processing unit. The phenolic pitch was a byproduct of the coal-gasification process and MP is the processed version.

The wood-based tars (Tar-PW, Tar-BW) are byproducts from the Kraft process and are generally used for medical purposed in treating the hooves of ungulates. Tar-Veg, a plant/wood-based binder, is a tar produced during vegetable fermentation and is considered a discard. This fluid is used for the same purpose as the above-mentioned wood-based binders. Glycerine was of research grade, supplied by Merck. This is a pure glycerine, which ensured that no impurities reacted with the phenolic resin when mixed or influenced the efficacy of plasticizing the biopolymer. The biopolymer was a food-grade xanthan gum (XG) that was used as a viscosity modifier. It was used to increase the viscosity of the glycerine through plasticizing the biopolymer with the liquid.

The plasticizing of XG with glycerine to produce the Gly+XG sample was carried out using an overhead stirrer with impeller attachment. The glycerine was heated to 60°C on a hotplate whilst stirring at 60 rpm for 30 min. After maintaining this temperature for a specified time, the gum was added in a mass ratio of 1:700 XG:Gly. The stirring speed was increased to 120 rpm and mixing was continued for 30 min at 60°C; thereafter, the mixture was allowed to cool to room temperature. The Gly+XG mixture was used as-prepared and in combination with phenolic resole resin (Gly+XG+PFR) in a ratio of 1:5 (mixture:PFR). The same procedure was used for the preparation of CTht+PFR, where these two fluids were mixed in the ratio 1:5 (CTht:PFR). The phenolic resin chosen as a low-temperature strength development aid for the THC was a resole-type resin with a gelation temperature ranging from 160–165°C. It is phenol–lignin-based, in which some of the phenol is substituted with lignin to lower the free phenol of the resin, which is a health concern, and improve carbonization.

3.1.2. Preparation of taphole clay

The conventional mixing procedure for THC uses a large-scale industrial mixer, such as a Muller or ring-pan mixer. Although this is the preferred method of clay mixing (including for research purposes), the associated cost of raw materials, binder, and energy was not considered economically viable. The alternative is to use a 15 kg Hobart mixer with beater paddle. This option is less efficient owing to the type of mixing action but will suffice for small-scale mixes. The dry raw materials were weighed according to the formulations shown in Table 3.2 to create a 15 kg mixture. The designation '+' in Table 3.2 means that the liquids were added in excess of the dry mixture mass, which sums to 100%. The quantity of CTht used was higher than those of the alternative binders due to the higher

viscosity of the reference binder. The formulation was optimized to a distribution modulus of q = 0.24 according to the Andreasen equation (Equation 1) (Otroj et al., 2009), which is in the range for self-flow monoliths (q = 0.21–0.26) and is the objective of a clay that should flow with ease without the need for vibration, i.e., has self-flow properties.

$$CPFT = 100\ X\ (\frac{d}{D})^{q}; \tag{3.1}$$

where CPFT is the cumulative percentage finer than, d the particle diameter, D the largest particle diameter, and q is the distribution modulus (Otroj et al., 2009).

Table 3.2: Taphole clay formulation and alternative binders

Raw material	Size range (mm)	Percentage (%)	Function
Calcined bauxite	3–5	16	Aggregate, abrasion
Calcined bauxite	1–3	17	Aggregate, abrasion
Calcined bauxite	+0.045–1	24	Matrix, abrasion
Calcined bauxite	−0.045	21	Matrix, sintering
Silicon carbide	−0.045	5	Matrix, abrasion
Clay (high alkali oxide content)	−0.045	12	Filler, sintering (liquid-state sintering), carbon containing
Carbon – coal	−0.045	5	Gas permeability, carbon network (strength)
Lignin/phenol–formaldehyde resole resin	-	+3.5	Low-temperature strength development
Liquid binder: CTht Alternative 1 Alternative 2	-	 +16–17 +13–15 +13–15	Consolidating solid particles into a clay mass, plasticity, flowability

The weighed dry aggregate and matrix solids (bulk sample) were placed in the Hobart mixer and mixed for 3 min to allow the dry mixture to homogenise. The mixture was then wet-mixed by adding half of the liquid binder and mixing for 2 min; thereafter, the total resin quantity was added and mixed for a further 2 min. The temperature of the clay mixture was recorded. The second liquid binder addition was then made while mixing, adding a quarter of the remaining liquid (with a quarter remaining) and mixing for 2 min; CTht = 16.5 mass% liquid addition. The temperature of the clay mixture was again measured to ensure that it did not exceed 45°C. A sample of the clay was removed from the mixer and the workability evaluated to gauge volume required for the last liquid addition to obtain a workability that was within a specified range. For the platinum-smelting application selected for this investigation, the workability specification is > 38%. Depending on the workability result, a last addition of liquid binder to the clay mixture was made. The mixture was then homogenised until the temperature reached 45°C. A

sample was again taken and the workability determined. This result was recorded as the workability after mixing (Day 0). The clay mixture was wrapped in plastic and enclosed in a sealed container prior to further use.

3.2. Analysis techniques

The design of experiments was divided into two main sections: (1) binder characterization and (2) evaluation of THC properties through simulation-type tests. The experimental plan for the binder characterization is shown in Figure 3.1. This study entailed compositional evaluations using Fourier-transform infrared spectroscopy (FTIR), gas chromatography mass spectroscopy (GC-MS), targeted and untargeted analysis, and thermogravimetric analysis (TGA/DTG). Rheology of the binders was evaluated and related to their molecular structures (composition). The biopolymer and liquid carbohydrate binders were characterized by differential scanning calorimetry (DSC) owing to the presence of the phenolic resin in these mixtures. For all analyses shown in Figure 3.1, at least three replicate samples were tested to investigate sampling efficiency, consistency of results, and repeatability. Averages are reported for the compositional analysis (GC-MS targeted); for the rheology results and analyses in which the data are reported in the form of chromatograms or similar (GC-MS untargeted, FTIR, DSC, TGA), the results were compared for consistency, but only a single result is reported.

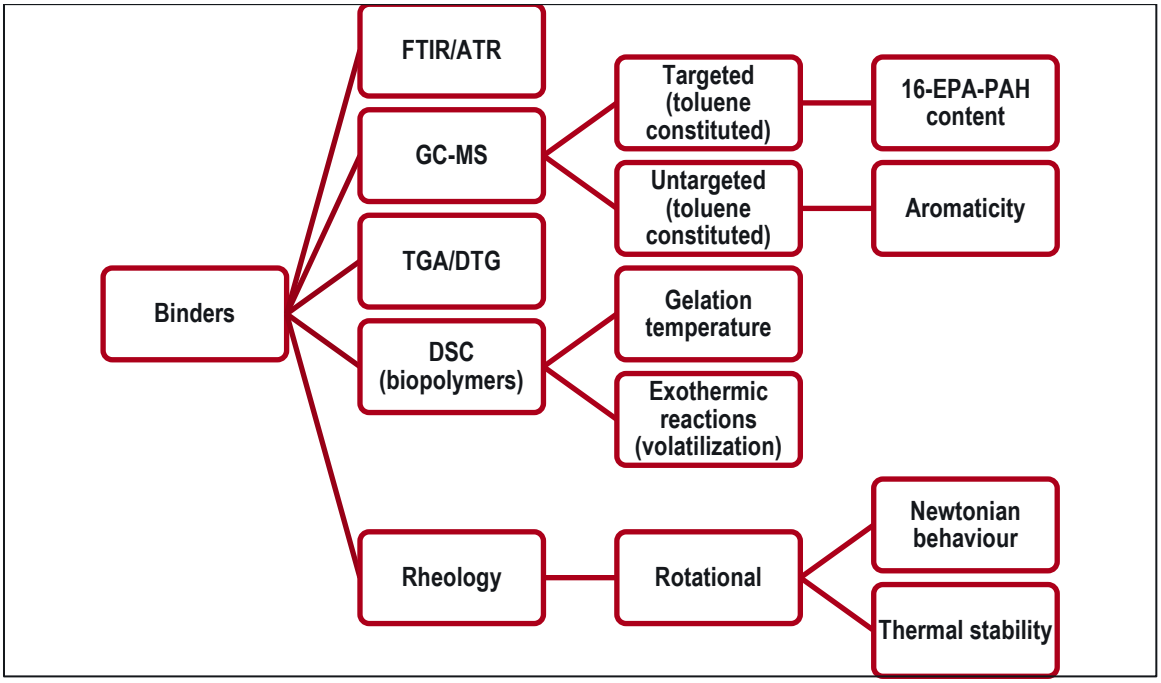

Figure 3.1: Relationship diagram showing the analysis techniques used to characterize taphole clay binders

The techniques shown in Figure 3.1 were used to identify and rank the most suitable alternative binders to replace the conventional binder in THC. For this investigation, a coal tar from a coke-making process was used as the reference to which the other binders were compared.

The two most suitable alternatives identified were selected for subsequent evaluation in the THC. These evaluations included: (i) workability aging (change in clay plasticity as it ages in air); (ii) aging of extrusion pressure (MEP aging)

(extrusion pressure of the mud gun as the clay is aged in air); (iii) strength development profile to simulate the green (< 200°C) strength development of the THC, with the associated change in mass of the sample to simulate the volatilization behaviour at lower temperatures; (iv) strength at higher temperature (800°C) in a reducing atmosphere to investigate how temperature impacted the properties of the clay. The latter tests were carried out at 800°C, as this is the lowest temperature at which strength of the clay develops solely due to carbon network formation. Strength is most crucial at this temperature because solid oxide-phase sintering starts above 1000°C, which then further imparts strength through sintering. Sintering strength (1000°C) derives from both solid- and liquid-state sintering owing to oxide diffusion from the aggregates in the material and liquid-phase sintering due to the high alkali-containing pozzolanic clay used to enhance sinterability and plasticity of the THC. The experimental procedures and conditions used to evaluate changes in binder in THC are summarized in Figure 3.2.

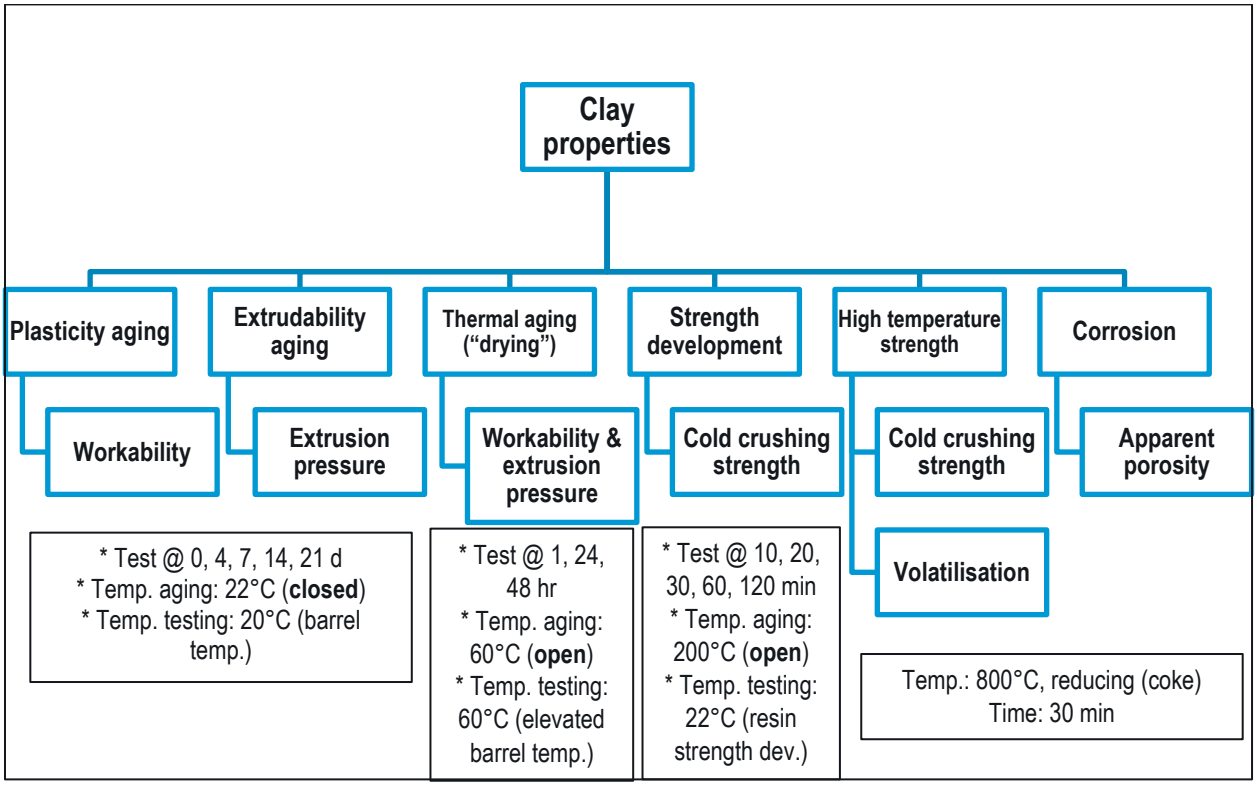

Figure 3.2: Relationship diagram showing the design of experiments and techniques used to evaluate alternative binders in taphole clay

3.2.1. Binder characterization

3.2.1.1. Fourier-transform infrared spectroscopy

FTIR was used in attenuated total reflectance (ATR) mode to measure the absorption of liquid samples at different wavelengths. A Perkin Elmer Spectrum 100 instrument was used, employing a UATR accessory with a diamond/ZnSe measuring system. Spectrum 10 software was used for control and data management. The wavelength range from 600–4000 cm^{-1} was selected; 32 scans per sample were performed. CO_2 and H_2O peaks were excluded from the analyses. Three different specimens of each binder were evaluated to ensure consistency.

3.2.1.2. Gas chromatography mass spectroscopy

GC-MS was used to evaluate the volatile species in the binders. The analysis included both targeted and untargeted identification. In the targeted analysis, a pesticide standard containing the 16-EPA-PAH species was analysed and the concentrations determined using a calibration curve. The 16-EPA-PAH was used as the standard in preference to EU-PAH owing to the larger range of compounds that are considered carcinogenic: this facilitated identification and quantification of each PAH in the examined liquid binders and made the binder selection process more rigorous. In the untargeted analysis, the pesticide standard and three different standards (one for each type of binder: pitch, petroleum, and fatty acid-containing) were used to identify the species in each sample, excluding the 16-EPA-PAH. For the untargeted analysis, only pseudo-quantification of the identified species and isomers was recorded.

The samples were dissolved in both hexane and toluene to determine which solvent offered higher solubility. Toluene and hexane performed similarly for lower molecular mass samples; however, for higher molecular mass binders, such as CTP and some petroleum pitches, hexane did not dissolve the entire sample, so toluene was consistently used throughout. To prepare the binders for analysis, a quantity of 300–1000 mg was dissolved in toluene. The samples were then vortexed and sonicated for 30 min. A volume of 5 mL ultra-pure water was added to the tubes, which were then again vortexed and centrifuged for 1 min at 3000 rpm. The top (toluene) layer was transferred to a 2 mL vial. From this, 1 µL was injected into the GC-MS using a split ratio of 1:20.

Separation of the components was performed using a 6890N Agilent Technologies inert XL EI/CI mass-selective detector (MSD), coupled with a CTC Analytics PAL auto-sampler. The PAH components were separated using a non-polar Rxi-5Sil MS capillary column, with helium as the carrier gas at a flow rate of 1 mL/min, injected into the column at 240°C. The MSD was operated in selected ion monitoring (SIM) mode using electron impact (EI) at an ionization energy of 70 eV and scanning from 30 to 650 m/z.

3.2.1.3. Thermogravimetric analysis

TGA was conducted using a Hitachi STA 7300 TGA equipped with DSC capability, using TA 7000 software. The samples were weighed to two decimal places and placed in 30 µL alumina crucibles: sample masses ranged from 5–10 mg. An automatic sampler was used. The binders were heated in nitrogen atmosphere from 50°C to 800°C at a heating rate of 10°C/min and gas flow rate of 20 mL/min. The corresponding differential curves (DTG) were captured and the DTA results were confirmed by manual calculations. The corresponding DSC analyses showed endothermic volatilization peaks of each binder. Three experiments were performed on each binder and average values are reported.

3.2.1.4. Differential scanning calorimetry

For the binders that were mixed with the phenolic resin, changes in exothermic peaks due to reaction were investigated to identify whether a delay in gelation occurred when the resin was mixed with other liquids (binders) and to characterize the gelation (cross-linking) temperature range of the resin. Endothermic peaks due to volatilization were also identified. The liquid samples were placed in 30 µL aluminium pans. The binder sample

masses ranged between 5–8 mg to avoid spillage inside the heating chamber. The pans were sealed with aluminium lids and an incision made on the middle of the lid to allow gas to escape when the binder volatilized. The DSC was calibrated using a reference pan and a background was run to ensure that peaks identified were only attributed to the sample. The sealed aluminium pan containing the binder was placed inside the DSC heating chamber and closed. The heating rate (5°C/min), maximum temperature (300°C), and sample mass were recorded. A nitrogen purge at a gas flow rate of 20 mL/min was employed.

3.2.1.5 Rheology

Rheological evaluations of the binders comprised three different tests: (1) isothermal rotational test (flow) at 45°C; (2) temperature sweep in rotation that evaluated the change in dynamic viscosity with temperature (thermal stability); and (3) determination of WAT of the waxy oils. An Anton Paar Physica MCR 501 rheometer was used, equipped with a cone-plate measuring system with a 0.5° 50 mm diameter spindle. The rheometer was equipped with a Peltier PTD 200 temperature-control system that can heat liquids up to 200°C in air. RheoCompass™ software was used for capturing and programming the rheometer. All binders were evaluated as-received (without any prior conditioning). The isothermal frequency sweeps were conducted at 30°C, 45°C, and 60°C in the frequency range of 0.1–100 Hz. The isothermal rotation test was performed at 45°C at a shear rate of 0.1–100 s^{-1}. The WAT and temperature-sweep tests employed a shear rate of 1 s^{-1} and heating rate of 5°C/min. In the WAT procedure, the temperature was cooled from 110 to 15°C.

3.2.2. Evaluation of taphole clay properties

3.2.2.1. Workability and thermal aging

The workability (or workability index) of a THC is a measure of the plasticity and degree of compactability when placed under a load, such as when the clay is rammed into a taphole. The sample was placed under a load, in the form of a free mass in a sand rammer and allowed to deform in an unconstrained manner. The sample was prepared according to ASTM C181-11 (2018) (Appendix A). A clay sample of 350 g was taken from the centre of a fresh clay mass (clod), placed in an oven, and heated to the workability temperature (20°C in this investigation). The sample was held at temperature for 60 min to uniformly heat and thereafter removed. The heated sample was placed into a cylindrical sample holder (H = 120 mm, $ø_{inner}$ = 50 mm, thickness = 5 mm, open both sides) and placed under the piston of the AFS (American Foundry Society) sand rammer. The piston was lowered in the cylinder onto the sample until the mass ceased to move under its own weight. The piston was rammed 10 times in 10 s. Thereafter the cylinder was removed and rotated by 180° so that the other open end faced the piston. The sample was rammed again according to the same procedure. After the second set of blows, the compacted sample was gently extruded from the cylinder and placed between two steel buttons under the piston. The piston was lifted, and the sample impacted three times in an unconstrained manner to allow the change in height to occur by bloating of the sample. The change in height of the sample was used to calculate the workability, expressed as a percentage (Cameron, 2021).

Aging of the workability was evaluated over 21 d. Samples were tested after mixing and after 4, 7, 14, and 21 d of aging in air. Aging is typically evaluated at room temperature (21–23°C): this study used a temperature of 20°C. For the thermal aging tests, the samples were aged at 60°C, at which release of low-temperature volatiles hardens the clay. This was used to investigate hardenability of the clay if it is maintained for a long duration inside the mud gun or by continuous heating during ramming practices. The samples were placed in an oven at 60°C, removed after 2, 24, and 48 h of heating, and tested at 60°C.

3.2.2.2. Extrusion pressure (Marshall extrusion pressure) and thermal aging

The extrusion pressure, generally referred to as MEP, measures the pressure needed to extrude clay from an orifice (such as the mud gun) after aging. The detailed setup of equipment for the MEP and calculations to determine the acceleration rate of the sample are described elsewhere (Cameron, 2021). A 450 g sample, taken from the centre of a fresh clod of THC, was heated to the test temperature (20°C) and then extruded at a constant rate (Cameron, 2021) and a chamber temperature of 20°C. The maximum force (N) needed to extrude the sample from the orifice was recorded and used to calculate the maximum pressure (MPa) by using the curved surface area (50.3 mm^2) of the orifice (Cameron, 2021):

$$\text{Maximum pressure at die (MPa)} = \frac{\text{Maximum load (N)}}{\text{curved surface area of die (mm}^2\text{)}} \quad (3.2)$$

Aging and thermal aging of the extrusion pressure samples were carried out using the same procedure as for the workability tests, i.e., aging at 60°C for 48 h, then tested at 60°C after aging for 2, 24, and 48 h.

3.2.2.3. Strength development profile

The strength development profile (SDP) of THC used core samples, prepared using the same method as for the workability samples, that were heated at 200°C for a specified time. The temperature differed depending on the binder system (Kageyama et al., 2005). Five core samples (D = 50 mm, H = 120 mm) were prepared using an AFS sand rammer, weighed, and placed in an oven at 200°C. Samples were removed at intervals of 10, 20, 30, 60, 120 min, placed on a tray to cool down, then weighed again. The cores were evaluated for CCS (unconstrained) in accordance with ASTM C133-97 (2021) (Appendix A) at room temperature.

3.2.2.4. High-temperature properties

The high-temperature properties of the THC evaluated included volatile organic compounds (VOC), retained carbon after firing (carbon yield), CCS, and AP. VOC was determined by mass difference after heating at 800°C for 30 min in a reducing atmosphere (coke bed). The carbon yield was determined in accordance with ASTM C571-81 (Appendix A) using a Leco 844 series carbon and sulfur analyser. CCS was determined in accordance with ASTM C133-97 (2021) (Appendix A) after firing at 800°C in a reducing atmosphere (coke bed) for 30 min. AP was measured in accordance with ASTM C380-00 (Archimedes principle) after firing at 800°C in a reducing atmosphere (coke bed) (Appendix A).

Chapter 4

Evaluation of conventional and lower-PAH alternative binders for taphole clays

"All obstacles are surmountable. Every hill can be conquered" ~ Shonda Shimes

4. Characterisation of binders for use in taphole clay

4.1. Introduction

This chapter is divided into three main sections. The first part covers the characterization of CTht and its selected alternatives as well as screening tests to determine the most suitable alternative binder to CTht. This was based on certain characteristic binder properties of the THC through identification of critical and secondary properties that can be altered. The evaluated binders are liquids that exist as either finished carbonaceous binders, some of which are already used in THC, or byproduct liquids from Kraft processing of different wood sources, that could potentially be alternatives to CTht. These include low softening-point (20–25°C) CTP blend, low-PAH liquid CTP, petroleum-based CWO, refined CWO, petroleum-based phenolic (mesophase-forming) pitch, Kraft process byproducts, and other wood-based tars. This selection of binders was ranked from the most suitable alternative to the least suitable. The ranking holistically considered the performance in all screening test results. The screening tests were used to characterize the behaviour of the reference binder, CTht, with which the alternatives were compared.

The second section discusses the innovative idea of using non-toxic liquids as binders, such as pure glycerine/glycerol/propylene glycol (extender for phenolic resole resin) or plasticizing a polysaccharide biopolymer (xanthan gum) with these liquids to use as a binder in THC. These binders were considered on their own because the glycerine-based binders are innovative for this application.

In the third section, properties of THC containing two selected alternative binders were evaluated against THC containing CTht (the reference sample). Some of the THC features mentioned in Figure 2.13 were evaluated and compared with those of clays that contained the alternative binders. Based on the THC evaluation results, a proposal was for made for most suitable binder alternative (lower/zero PAH) to CTht.

The third section consists of three sub-sections, in which properties of the binders are characterised according to compositional and molecular structure, thermal behaviour, and rheology. Analysis by FTIR and GC-MS was used for compositional and molecular structure analysis. TGA/DTG and DSC were utilized to characterise the thermal behaviour. DSC was only conducted on the phenolic resin-containing binders because these are usually more prone to premature cross-linking, and to assess compatibility of the binder–resin mixture (Cameron, 2021). The rheology evaluation considered the fluid flow properties and thermal stability of the binders. Following characterization and comparison with the reference, the binders were ranked within each sub-section and then on an overall basis. The most suitable binders identified were evaluated in THC compositions described in Section 3.1.2.

4.2. Compositional and molecular structure analysis

4.2.1. Fourier-transform infrared spectroscopy

4.2.1.1. Coal-based binders

FTIR was used to identify the major functional groups present in each sample. This technique cannot be considered as the only indication of the molecular structure because other compounds may be present at concentrations below the detection limit. The reference sample, CTht, is discussed first and all other binders compared against it. The FTIR spectrum for CTht is shown in Figure 4.1, which highlights the major functional groups that were identified.

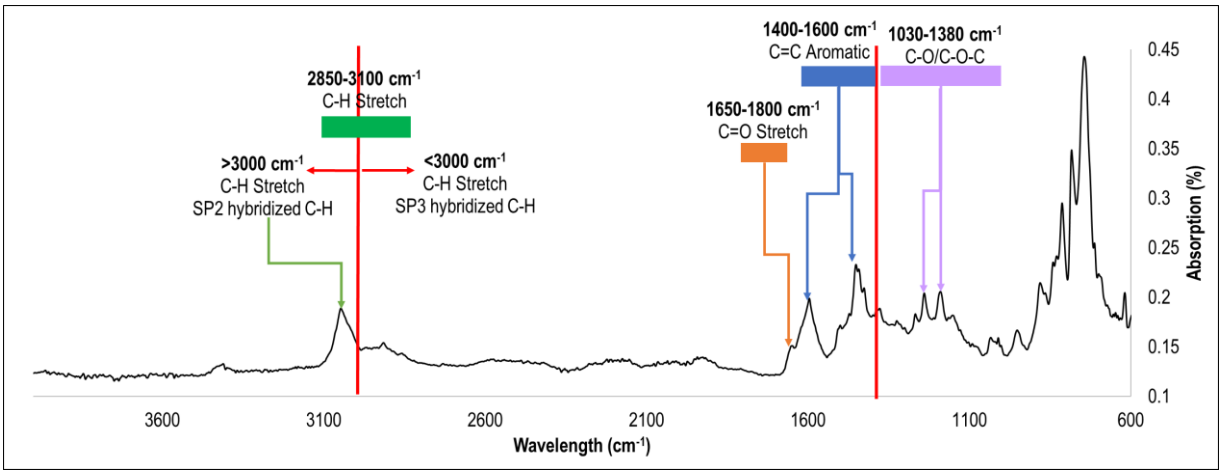

Figure 4.1: Fourier-transform infrared spectrum showing identified functional groups for the CTht reference binder

Functional groups were only identified in the wavelength range of 1400–3600 cm^{-1} because lower wavelengths are considered as the fingerprint region, in which many signals are complex and overlapping appear, which makes identification less accurate. For the reference binder, aromatic C=C stretches were identified at 1444 cm^{-1} and 1592 cm^{-1}. These peaks are usually associated with cyclic aromatic structures that are expected in coal-based tar or pitch samples. Alkylated sp^2-hybridized C–H stretching vibrations were identified at 3040 cm^{-1}, which are present in benzene molecules and complement the aromatic groups identified. The C=O stretch at 1643 cm^{-1} is co-eluted (compound peaks occurring in the same wavelength region that displays as one broad peak): some carbonyl functional groups are expected in coal-based tar samples. Peaks attributed to ester oxygen functional groups with C–O–C bonds were identified at 1236 cm^{-1} and 1185 cm^{-1}. The overall molecular structure comprised benzene or cyclic aromatic hydrocarbons with some ester and carbonyl functional groups. The presence of the ester functional groups could also indicate that the pitch had undergone prior cross-linking (Li et al., 2020) because C–O–C bonds are usually present and form during cross-linking of polymers.

The CTPht-B coal-based binder had an almost identical FTIR spectrum (Figure 4.2) to that of the CTht reference sample. This was expected because the CTPht-B was derived from and is a refined version of CTht. Some of the functional groups became more pronounced with refining of the sample, such as the sp^3-hybridized C–H stretches and C=C aromatics. The C=O stretching vibration was not as pronounced as in the reference binder, which indicates that these functional groups were not as abundant as in the reference CTht. The CTP blend comprised a

high softening-point pitch that was mixed with a lower molecular mass oil to reduce the softening point. The viscosity-modifying oil did not seem to change the molecular composition of the binder, which may be due to the small volume of oil used.

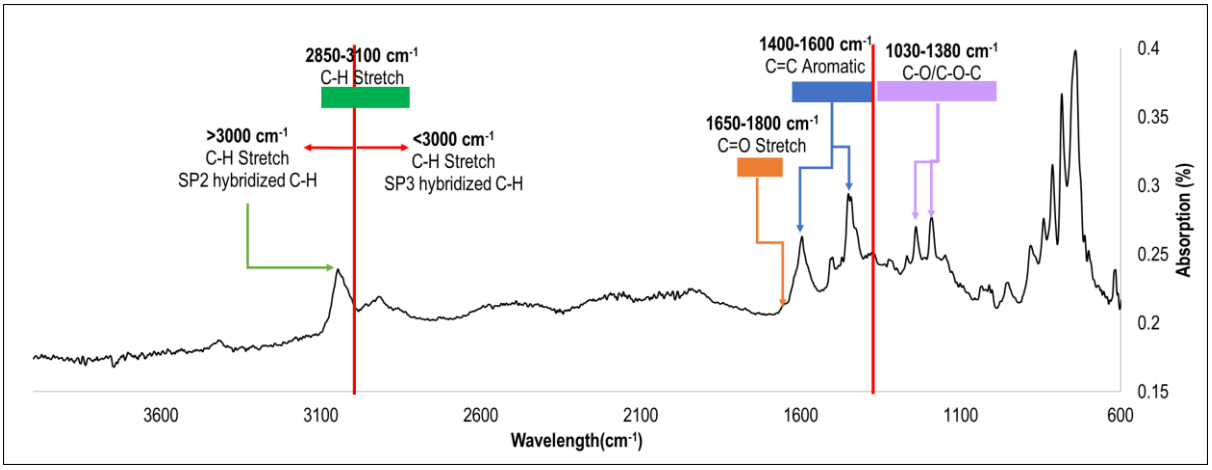

Figure 4.2: Fourier-transform infrared spectrum showing identified functional groups for the CTPht-B low softening-point pitch blend

The EcoP coal-based binder had a combined structure, with both sp^2 C–H stretch (aromatic) and sp^3 C–H (aliphatic) functional groups, as shown in Figure 4.3. Strong intensity of C=C aromatic stretching frequency at 1446 cm^{-1} and 1593 cm^{-1} indicated abundance of this functional group. The aromatic functional groups and sp^2-hybridised C–H stretch peak at 3038 cm^{-1} indicate that the sample contained cyclic aromatic hydrocarbons. The sp^3-hybridized C–H stretch at 2912 cm^{-1} indicates that some long-chained hydrocarbons were present. Accompanying ester functional groups are assigned to the peak at 1187 cm^{-1}, which corresponds with the sp^3 C–H stretches. The presence of these functional groups could also indicate prior cross-linking of the pitch because this was a synthetically produced product.

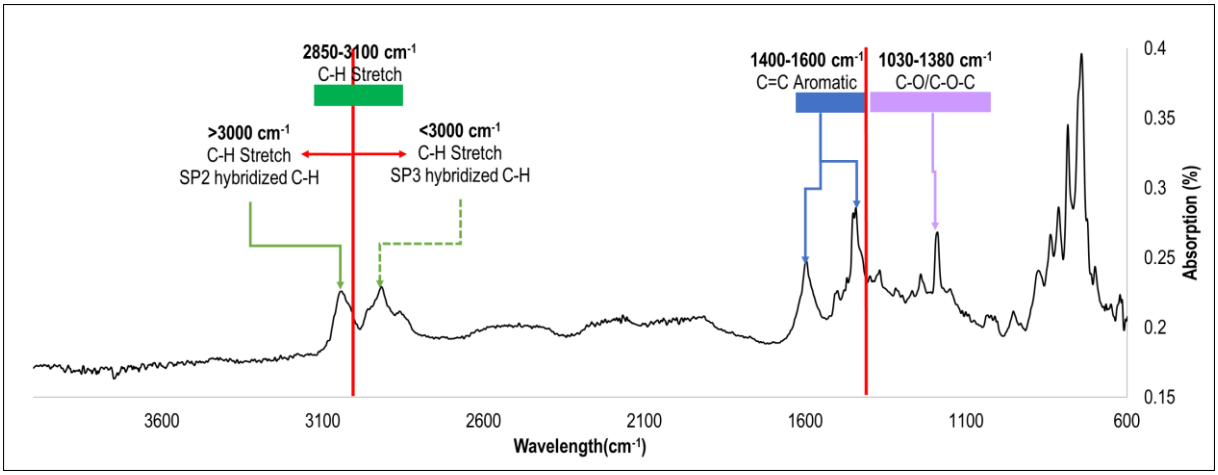

Figure 4.3: Fourier-transform infrared spectrum showing identified functional groups for the EcoP low-PAH pitch

4.2.1.2. Petroleum-based binders

The elementary FTIR spectrum of the waxy oil petroleum-based binder, CWO, is shown in Figure 4.4. Only two main functional groups were identified. The C=C aromatic structure is considered an anomaly, given the paraffinic nature of the binder: paraffinic liquids are aliphatic, which means that C–H stretch and sp^3-hybridized C–H stretch signals would be present in their spectra (similar to shown in Figure 4.4). The presence of C=C aromatic signals in the spectrum in Figure 4.4 may be attributed to its crude nature, i.e., some aromatic species may still be present in the binder. The peaks at 2853 cm^{-1} and 2923 cm^{-1} were assigned to sp^3-hybridized C–H stretches. These functional groups were most abundant in the sample and usually indicate an aliphatic molecular structure with alkanes as the major functional group. The refined waxy crude oil (PCWO) spectrum shown in Figure 4.5, is identical to that of the crude source, also showing an aliphatic structure with some C=C aromatic functional groups at 1459 cm^{-1}. From a qualitative perspective, the CWO and PCWO samples seemed identical, but refining of the oil would be expected to have modified its molecular mass or removed unwanted trace impurities: these would not be detectable by FTIR and require a targeted approach.

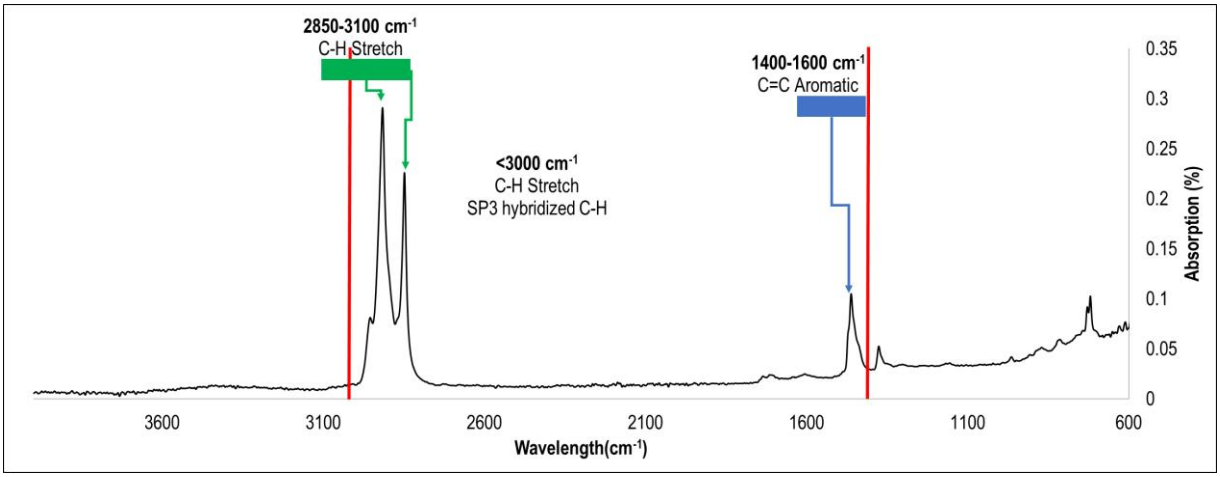

Figure 4.4: Fourier-transform infrared spectrum showing identified functional groups for the CWO waxy crude oil

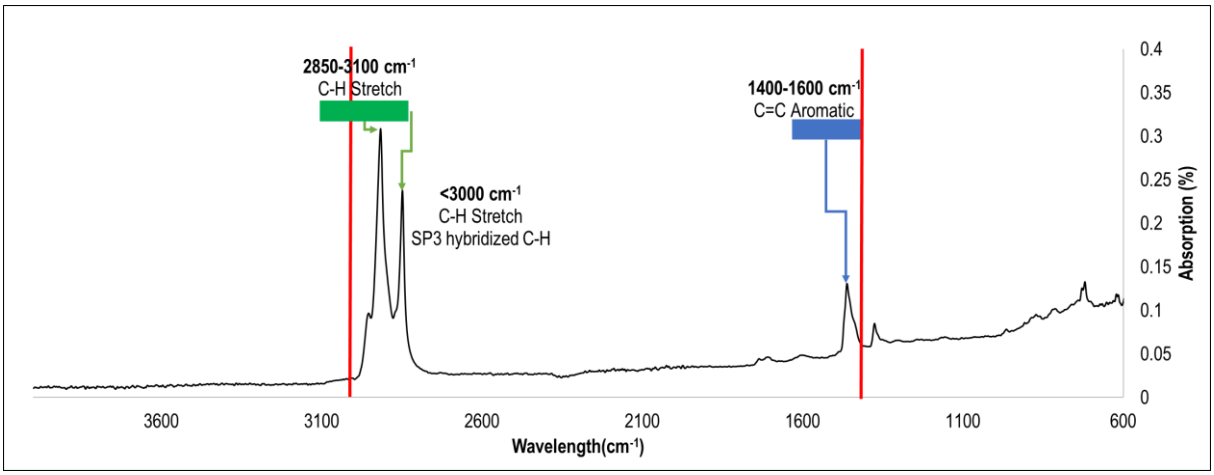

Figure 4.5: Fourier-transform infrared spectrum showing identified functional groups for PCWO refined waxy crude oil

As described by the supplier, the source of the mesophase-forming pitch, MP, is known to be phenolic, originating from a proprietary process. Four main functional groups were identified for this sample (Figure 4.6). C=C aromatic bonds are assigned to the vibrations at 1443 cm^{-1}, 1520 cm^{-1} (co-eluted), and 1586 cm^{-1}. The broad peak at 3334 cm^{-1} is assigned the O–H stretch. C–O bonds were identified from the broad co-eluted peaks at 1100–1324 cm^{-1}. These three functional groups form part of the phenol structure, which also has C=C aromatic content, accompanied by sp^2-hybridized C–H stretches at 3040 cm^{-1}. The peaks below 3000 cm^{-1}, representing the presence of sp^3-hybridized C–H bonds, could be due to the presence of some hydrocarbon chains. Some C=C bonds could be attributed to phenol and the rest to unidentified hydrocarbons. The MP liquid comprised a combination of aromatic benzene hydrocarbons (sp^2 C–H stretch) and aliphatic hydrocarbon chains (sp^3 C–H stretch).

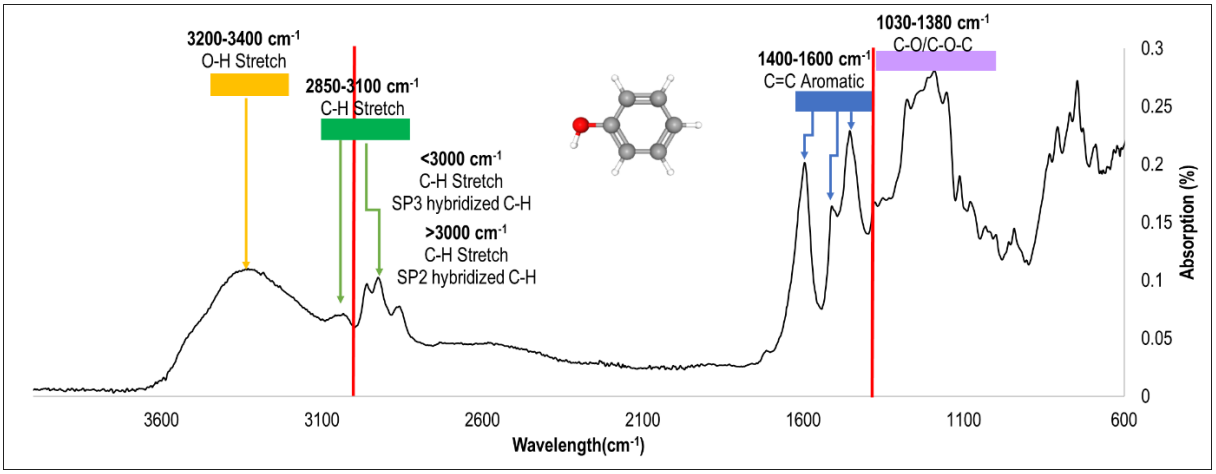

Figure 4.6: Fourier-transform infrared spectrum showing identified functional groups for the MP phenolic-source mesophase-forming pitch

4.2.1.3. Wood and vegetable-based binders

The spectrum of the pinewood tar (Tar-PW) is shown in Figure 4.7. Carboxyl functional groups associated with fatty-acid structures include the hydroxyl, carbonyl, and sp^3 C–H stretch. The broad peak at 3398 cm^{-1} is attributed to the presence of the O–H functional group. The presence of this peak is usually dominant in alcohols, but the presence of the carbonyl (C=O) group at 1700 cm^{-1} favours identification of a carboxyl functional group. Fatty acids are usually long-chain hydrocarbons with a hydrogen on the one end and a carboxyl functional group on the other, as shown in Figure 4.7. The sp^3-hybridized C–H stretch at 2950 cm^{-1} confirmed the aliphatic structure of the binder; the accompanying carbonyl and O–H stretches show a fatty-acid structure. The C–O–C bonds identified at 1204 cm^{-1} and 1102 cm^{-1} could be due to ester groups attached to the main carboxyl structure of the binder.

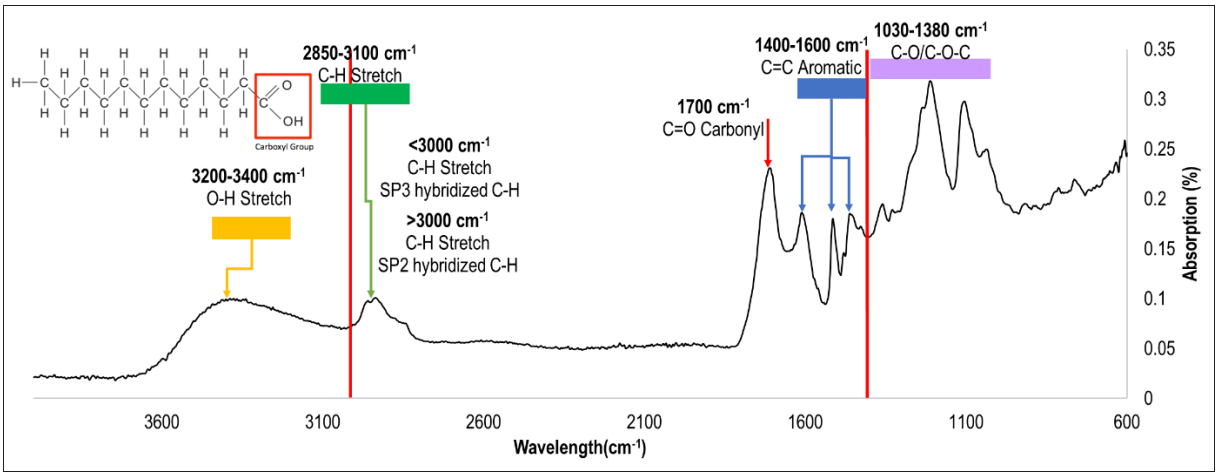

Figure 4.7: Fourier-transform infrared spectrum showing identified functional groups for the Tar-PW fatty-acid tar-based on pinewood source

The Tar-BW wood-based tar originated from the Kraft process of beech source. The spectrum is shown in Figure 4.8. There are noticeably different functional groups compared with the fatty-acid structure of the pinewood tar (Figure 4.7). Strong intensity of the peaks at 1700 cm^{-1} and 1730 cm^{-1} correspond to an abundance of the C=O carbonyl group. The double peak at 2855 cm^{-1} and 2921 cm^{-1} (and some co-elution at 2957 cm^{-1}) are assigned to sp^3- hybridized C–H aliphatic groups. The co-occurrence of these two functional groups suggests an aldehyde or ketone structure, shown in Figure 4.8: they differ in the presence of a C–C or C–H bond at the end of the chain. Some C=C aromatic bonds were identified at 1456 cm^{-1}, which could be due to aromatic bonds attached to the main aliphatic chain. There are also ester functional groups with peaks at 1162 cm^{-1} and 1373 cm^{-1} that could be side chains of the ketone molecular structure.

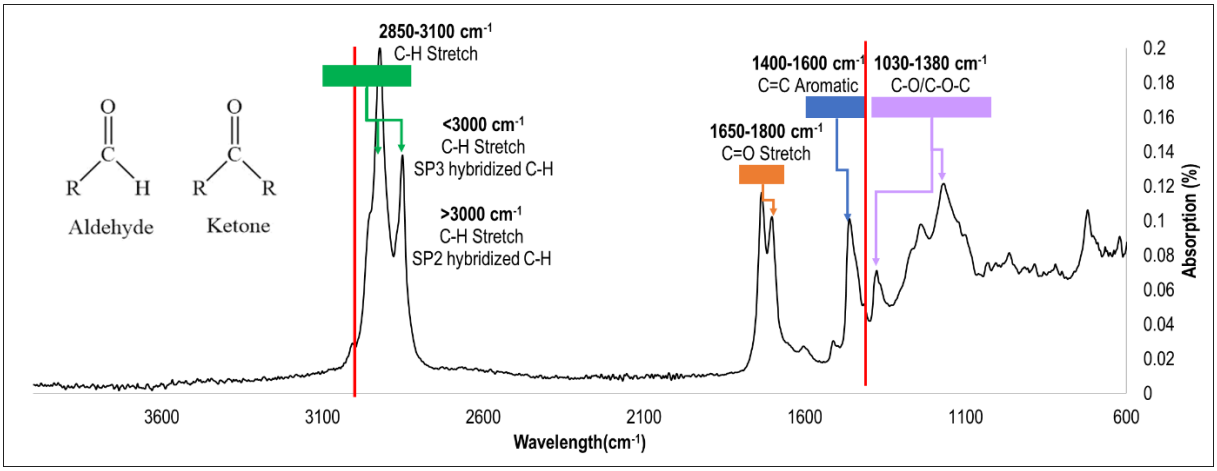

Figure 4.8: Fourier-transform infrared spectrum showing identified functional groups for the Tar-BW beechwood-source tar

The FTIR spectrum of the vegetable tar (Figure 4.9) is similar to that of the beechwood tar (Figure 4.8), showing a predominantly ketone structure with some C=C aromatic rings and C–O ester functional groups possibly attached to the main structure. This binder also contained ester groups, similar to the beechwood tar.

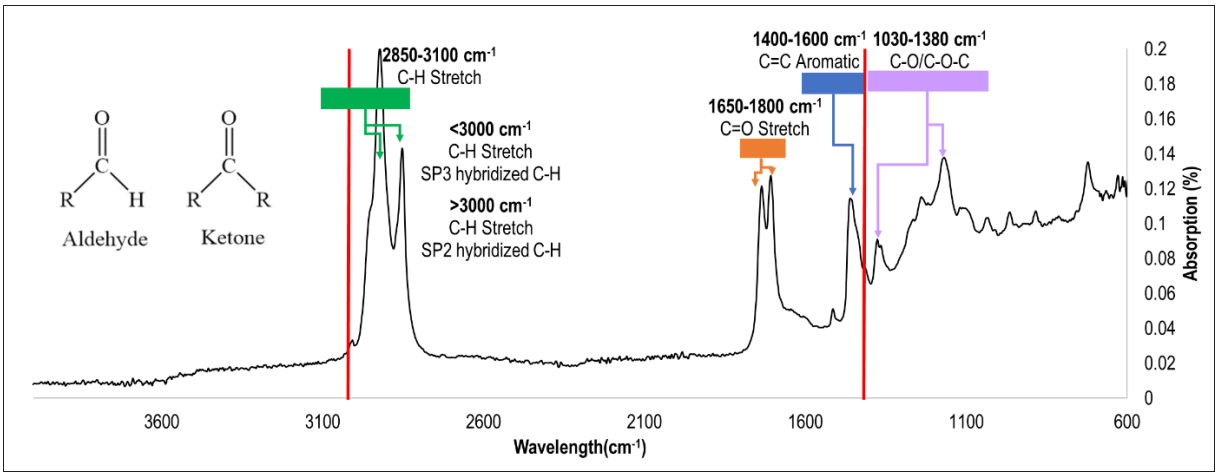

Figure 4.9: Fourier-transform infrared spectrum showing identified functional groups for the Tar-Veg vegetable-source tar

4.2.1.4. Glycerine and polymer-based binders

The binder systems under consideration as non-toxic alternatives to CTht for use in THC have different molecular structure characteristics owing to the presence of reaction products or weak bond interactions that produce a larger molecular structure. The functional groups in each binder and the mixtures were investigated to identify distinctive changes in structure that could explain the evaluation results. The individual materials, i.e., pure glycerine, xanthan gum from source *xanthomonas campestris*, and a phenolic resole resin with a gel time of 12–16 min (> 150°C), were evaluated.

The FTIR spectrum for pure glycerine is shown in Figure 4.10. The identified functional groups are in good agreement with literature. The spectrum shown in Figure 4.10 is of a refined glycerine; indicative peaks for crude glycerine (Danish et al., 2016) are not present. The spectrum shows a distinct broad O–H stretch peak at 3271 cm^{-1} and sp^3-hybridized C–H stretching at 2870 cm^{-1} and 2920 cm^{-1} (Danish et al., 2016). The co-eluted peak at 1400–1420 cm^{-1} is due to C–O–H bending and the C–O stretching (1112 cm^{-1}) region for primary alcohols (Danish et al., 2016).

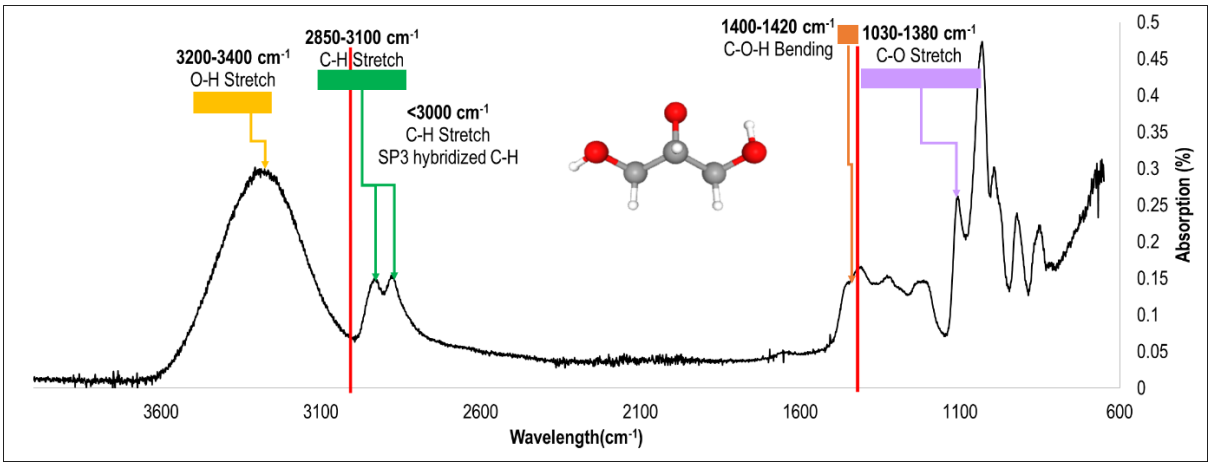

Figure 4.10: Fourier-transform infrared spectrum showing identified functional groups for pure glycerine binder

The XG biopolymer used as plasticizer in the non-toxic binder system is an anionic polysaccharide. This has a branched molecular structure and, depending on the type of fermenting bacteria used, has a different carbon yield. The FTIR spectrum shown in Figure 4.11 is of the XG powder without plasticizer. The gum showed a less-distinct broad O–H stretching peak at 3295 cm^{-1}. As with glycerine and phenolic resin, there were also sp^3- hybridized C–H stretches present, but to a lesser extent. The C=O stretching vibration of acetate was attributed to the peaks at 1650 cm^{-1} and 1700 cm^{-1} and the lower absorption of C–O–O peak at 1400 cm^{-1}. The distinctive peak at 1020 cm^{-1} was assigned to the C–O acetate stretch (Fosu et al., 2016). There was no indication of distinctive peaks at 700–900 cm^{-1} that could be attributed to β-glycoside, as recorded in the literature (Fosu et al., 2016). The presence of O–H functional groups in glycerine makes it a favourable plasticizer for XG (Zhang & Geng, 2020) and ensures a polarity match between glycerine and phenolic resole resin to aid in proper mixing and stability of the mixture.

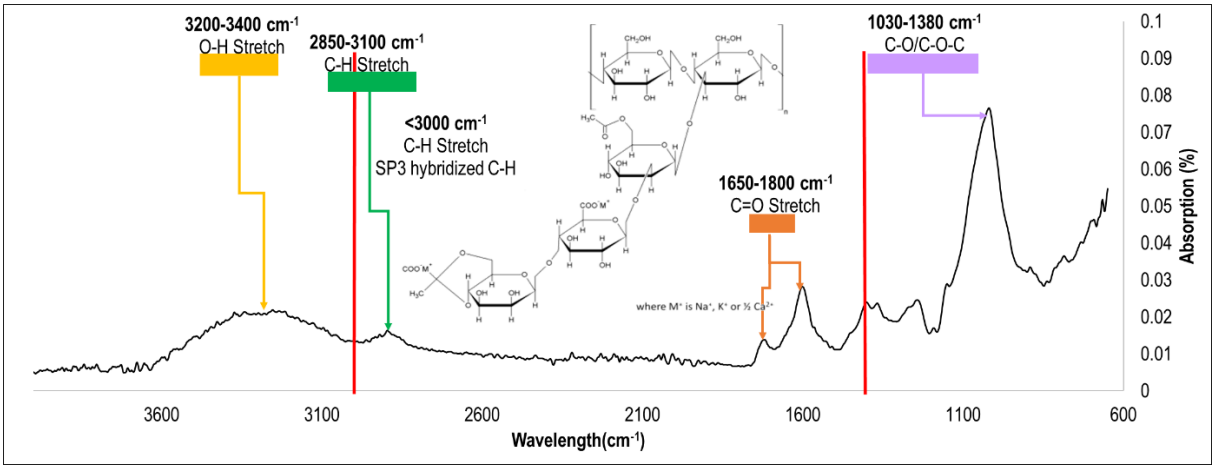

Figure 4.11: Fourier-transform infrared spectrum showing identified functional groups for xanthan gum powder used in combination non-toxic binders

The FTIR spectrum of the pure phenolic resole resin is shown in Figure 4.12. There is a distinct broad O–H stretch peak at 3270 cm^{-1} in the C–OH structure (Bobrowski & Grabowska, 2015). The presence of sp^3-hybridized C–H stretches at 2925 cm^{-1} and 2870 cm^{-1} indicated an aliphatic structure (methylene functional groups) present in the phenolic structure situated between the aromatic rings (Bobrowski & Grabowska, 2015). The resin had a small

amount of residual formaldehyde identified by the low absorption peak at 1645 cm^{-1} that is related to a C=O carbonyl double bond (Bobrowski & Grabowska, 2015). The C=C vibration at 1400–1600 cm^{-1} occurs between the aromatic rings in the resin structure. The possibility of sp^2-hybridized C–H stretching could also be present in the sample with co-elution of the peaks that occurs >3000 cm^{-1} overlapped with the O–H stretch. The two peaks identified in the C–O/C–O–C region are described as vibrations of alkyl phenol (at 1220 cm^{-1}) and deformation vibration of C–H in aromatic rings (at 1080 cm^{-1}) (Bobrowski & Grabowska, 2015).

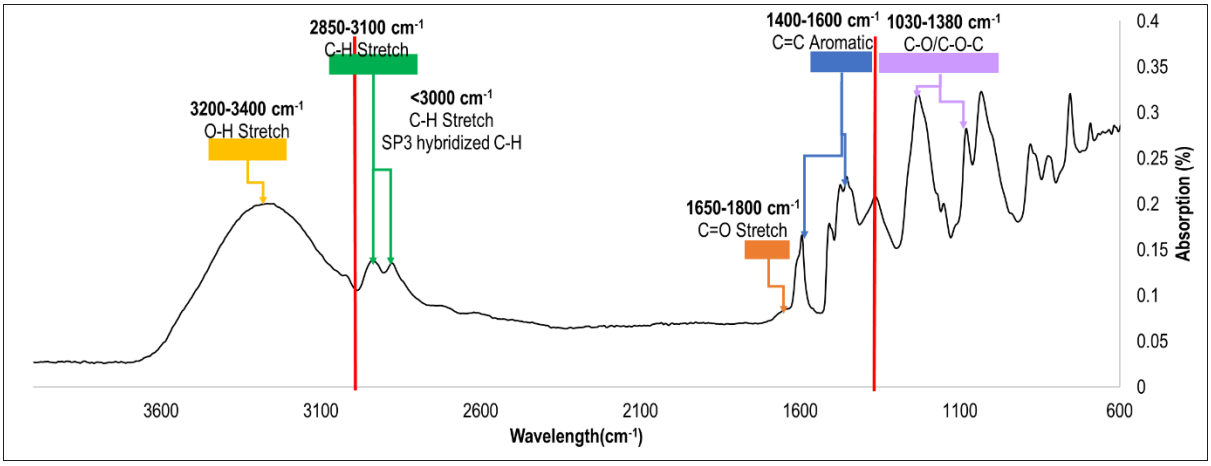

Figure 4.12: Fourier-transform infrared spectrum showing identified functional groups for the phenolic resole resin

FTIR spectra of the mixtures (Gly+XG+PFR = 1:5 plasticized mixture:PFR and CTht+PFR = 1:5 CTht:PFR) are shown in Figure 4.13. Irrespective of whether the glycerine contained XG, phenolic resin or both, the identified functional groups of the combination binders are similar to that of the pure glycerine. The unique peaks for XG and phenolic resole resin are not present due to the small quantities that were present in the sample (Cameron, 2021). The three mixtures (Gly+XG, Gly+PFR, Gly+XG+PFR) all exhibited an aliphatic structure. The presence of the phenolic resole resin in the glycerine binders can result in some carbonization that would increase the carbon yield after firing. Similarly, the type of gum added to the glycerine can increase the carbon yield after firing. The aliphatic nature of these binders will not yield the same degree of carbonisation and would not volatilise in a similar manner to the conventional tar binder used in THC. The volatilization behaviour and residual carbon after firing of these mixtures were therefore evaluated.

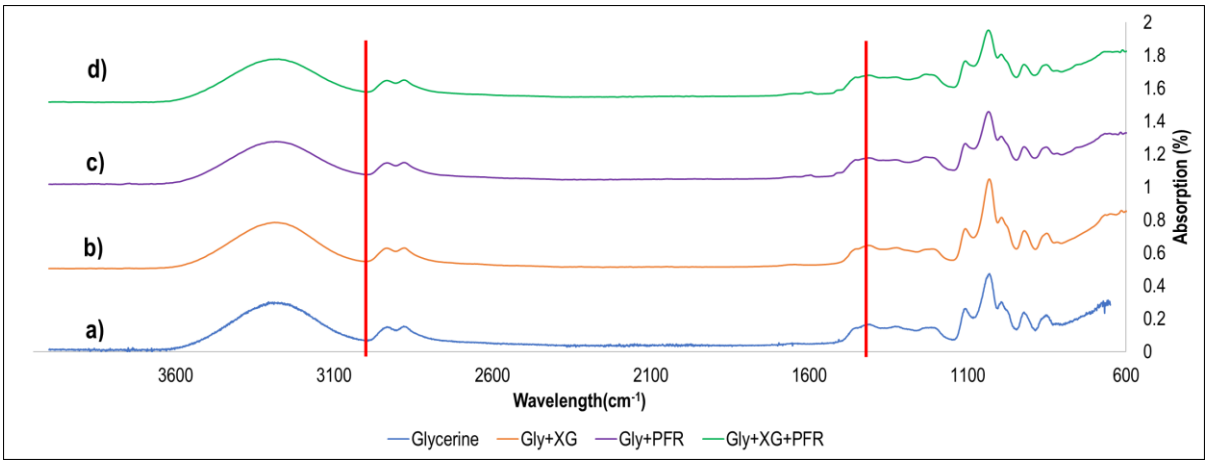

Figure 4.13: Fourier-transform infrared spectrum showing identified functional groups for a) pure glycerine, b) glycerine-plasticized xanthan gum, c) glycerine and resole resin mixture, and d) glycerine-plasticized xanthan gum mixed with resole resin

4.2.1.5. Conclusion

According to the FTIR results, the binders expected to have lower PAH concentrations than the reference are the aliphatic petroleum binders (CWO, PCWO), the wood-based binders (Tar-PW, Tar-BW, and Tar-Veg,) and the aliphatic glycerine-based binders. The coal-based binders are high in aromatic structures, with MP also having some degree of aromaticity, which could directly correlate with the presence of polycyclic aromatic species present in the sample. The phenolic resin has both aliphatic and aromatic species with the main phenol component. GC-MS was employed to confirm and quantify the presence of 16-EPA-PAH species in the binders.

4.2.2. Gas chromatography with mass spectroscopic detection

To enable a holistic view of the performance and correlations between properties of the binders, it was important to understand their composition, specifically the 16-EPA-PAH content. The PAH analysis was used to calculate a toxicity coefficient or benzene equivalent (BE) using Equation 2.1. This allows for the benzene-containing binders to be ranked according to toxicity (BE value and total PAH content) and to distinguish between higher and lower molecular mass PAH species. Species other than 16-EPA-PAH were also identified and a pseudo-analysis was performed to obtain a relative quantification of these species by untargeted analysis. The targeted and untargeted GC-MS analyses are described in Section 3.2.1.2. The respective chromatograms are given in Appendix A. The FTIR and GC-MS results were compared, and characteristic functional groups/species highlighted.

4.2.2.1. Benzene equivalent: coal-, petroleum-, and wood/vegetable-based binders

The targeted analyses, calculated BE equivalent, and total PAH (sum of all 16-EPA-PAH species in ppm) are shown in Table 4.1. The pinewood and beechwood tars did not contain any PAH species. Only the species that are part of the 16-EPA-PAH were considered in this calculation, which excludes Benzo(e)pyrene (BeP).

Table 4.1: Targeted analyses of 16-EPA-PAH in binders (mass%)

Compound	Boiling point (°C)	Formula	CTht	CTPht-B	EcoP	CWO	PCWO	MP	Tar-Veg
Naphthalene	218	$C_{10}H_8$	4.75	6.73	2.99	0.25	-	0.45	-
Acenaphthylene	270	$C_{12}H_8$	1.20	0.07	-	-	-	0.02	-
Acenaphthene	279	$C_{12}H_{10}$	0.07	1.95	1.95	0.37	-	0.42	-
Fluorene	295	$C_{13}H_{10}$	1.03	1.67	1.81	0.28	-	0.40	-
Phenanthrene	338	$C_{14}H_{10}$	2.58	3.08	1.24	0.15	0.01	0.25	-
Anthracene	340	$C_{14}H_{10}$	0.79	3.02	1.21	0.04	-	0.10	-
Fluoranthene	383	$C_{16}H_{10}$	1.64	1.95	0.38	0.03	-	0.09	-
Pyrene	393	$C_{16}H_{10}$	0.95	1.29	0.31	0.02	-	0.07	-
Chrysene	441	$C_{18}H_{12}$	1.11	0.78	0.04	-	-	0.08	-
Benzo(a)anthracene	435	$C_{18}H_{12}$	0.47	0.46	0.03	-	-	0.05	-
Benzo(b)fluoranthene	481	$C_{20}H_{12}$	1.11	0.82	0.03	-	-	0.06	0.06
Benzo(k)fluoranthene	481	$C_{20}H_{12}$	0.19	0.15	0.01	-	-	0.05	0.03
Benzo(a)pyrene	496	$C_{20}H_{12}$	0.65	0.73	0.02	-	-	-	0.01
Indeno(1,2,3-cd)pyrene	524	$C_{22}H_{12}$	0.35	0.49	0.06	-	-	0.06	-
Dibenzo(a,h)anthracene	539	$C_{22}H_{14}$	0.16	0.22	0.04	0.02	0.02	0.15	-
Benzo(ghi)perylene	545	$C_{22}H_{12}$	0.29	0.35	0.07	-	-	0.05	-
BE		**-**	**1.67**	**1.92**	**0.66**	**0.03**	**0.03**	**0.24**	**0.02**
Total PAH (ppm)		**-**	**137 378**	**199 181**	**84 911**	**9 060**	**431**	**15 251**	**1 262**

Based on the results in Table 4.1, all binders had PAH levels above the Permissible Exposure Limit (PEL), as defined by the US Centers for Disease Control and Prevention/Agency for Toxic Substances and Disease Registry (CDC/ATSDR), which stipulates an occupational PEL for total PAH species of 0.2 mg/m^3 (~ 0.04 ppm) per 8-h period (ATSDR, 2013). These values would be higher if additional PAH species are identified that are not described by the 16-EPA-PAH species. A higher PAH level implies more difficulty in complying with PEL regulations.

Owing to the difference in exposure time between an on-site situation (during ramming) and the GC-MS analysis time, the GC-MS result of the reference binder was used as the benchmark against which the alternative binders were compared. An increase in PAH levels, however, implies more difficulties in complying with PEL regulations. The pitch blend (CTPht-B) showed the highest total PAH content of the coal-based binders, with CTht second highest. The petroleum-based fluids had substantially lower PAH content, with PCWO having the lowest PAH content in this category. Its crude counterpart (CWO) had the fifth-highest concentration overall, indicating the effect

of processing of crude waxy oil. The mesophase-forming pitch (MP) had the highest PAH content of the petroleum-based binders; however, there was an order of magnitude difference when comparing this with the coal-based pitch with the lowest PAH content (EcoP).

The reference sample (CTht) comprised an abundance of PAH species, of which naphthalene was in the highest concentration (Table 4.1). BE for the reference sample was > 1.67: this value is comparable with those obtained for similar coal tar liquids reported in literature, with calculated BE values of 1.05 to 1.75 (Andreikov et al., 2008). The BE for the CTP blend (CTPht-B) was above 1.92, which is only slightly higher than the published range of 2.1–2.5 (Andreikov et al., 2008). Published values refer to processed pitches with higher softening points (90–105ºC): CTPht-B was a pitch–oil blend, which had a softening point that had been lowered from 150ºC to between 20–30ºC using merisol oil (as evaluated with a ring-and-ball apparatus). The BE values are nevertheless considered to be comparable.

PAH species of lower molecular mass (naphthalene, acenaphthene, fluorene, phenanthrene, anthracene) were more concentrated in the pitch blend sample (CTPht-B), although higher molecular mass species (chrysene, benzo(b) fluoranthene, indeno (1,2,3-cd) pyrene, dibenzo (a,h) anthracene, benzo (ghi) perylene) were present, as deduced from the higher BE value. The higher BE value of CTPht-B compared with the coal tar (CTht) (which is generally higher in PAH, as previously mentioned) suggests that this is possibly due to the composition of the oil, which could have a higher PAH content than the CTP with which it was mixed. Naphthalene, phenanthrene, and anthracene were the most abundant EPA-PAH species in CTPht-B. Of all the binder compositions considered, CTPht-B had the highest toxicity, with the highest BE value.

Of the alternative binders evaluated, those considered more environmentally friendly with regard to 16-EPA-PAH emissions are the wood-based tars (Tar-PW, Tar-BW), followed by the processed crude waxy oil (PCWO), vegetable tar (Tar-Veg), and the crude waxy oil (CWO). The mesophase-forming pitch (MP) and coal-based binder EcoP were better alternatives than the reference; however, use of these binders in THC is nevertheless considered unfavourable due to their toxicity. These binders contained higher levels of PAH, as indicated by the 16-EPA-PAH results relative to the PEL.

4.2.2.2. Benzene equivalent: glycerine-based binders

The targeted GC-MS 16-EPA-PAH analyses of the binders are shown in Table 4.2 with their calculated BE values (Andreikov et al., 2008). These results are for the three starting raw materials (coal tar (CTht), phenolic resin (PFR), and the two mixtures that contain PFR). The targeted analyses of pure glycerine (Gly) and Gly+XG were identical and did not contain any 16-EPA-PAH species. The values of the identified PAH species were similar for the Gly+PFR and Gly+XG+PFR mixtures. The concentrations in Table 4.2 are given in parts per million (ppm) to compare to the permissible exposure limits (PEL) of each PAH species. The PEL values given in Table 4.2 are stipulated either for 8- or 10-h exposure. Gasification of the binders in the GC-MS is shorter than the PEL exposure

period, so the PEL values were used only as a guideline to compare the binders to one another and identify which PAH species are the most difficult to reduce to adhere to the PEL.

Table 4.2: Targeted GC-MS analysis of binders showing 16-EPA-PAH species, calculated benzene equivalent, and permissible exposure limits (PEL) (United States Department of Labor, 2019; National Library of Medicine, 2023; New Jersey Department of Health, 2016; New Jersey Department of Health and Senior Services, 2001; New Jersey Department of Health , 2010; Agilent Technologies, 2019)

Compound	Boiling point (°C)	Formula	PEL (ppm)	CTht (ppm)	PFR (ppm)	Gly+PFR (ppm)	Gly+XG +PFR (ppm)
Naphthalene	218	$C_{10}H_8$	0.1 (8 h)	37 667	354	12	12
Acenaphthylene	270	$C_{12}H_8$	**	9 480	122	-	-
Acenaphthene	279	$C_{12}H_{10}$	0.03 (8 h)	531	5	4	4
Fluorene	295	$C_{13}H_{10}$	0.1 (10 h)	8162	16	-	-
Phenanthrene	338	$C_{14}H_{10}$	0.03 (8 h)	20 430	19	-	-
Anthracene	340	$C_{14}H_{10}$	0.03 (8 h)	6 270	28	1	1
Fluoranthene	383	$C_{16}H_{10}$	**	12 971	45	1	1
Pyrene	393	$C_{16}H_{10}$	0.025 (8 h)	7 560	31	1	1
Chrysene	441	$C_{18}H_{12}$	0.02 (8 h)	8 773	5	-	-
Benzo(a)anthracene	435	$C_{18}H_{12}$	0.02 (8 h)	3 757	12	-	-
Benzo(b)fluoranthene	481	$C_{20}H_{12}$	0.01 (10 h)	8 777	1	-	-
Benzo(k)fluoranthene	481	$C_{20}H_{12}$	0.02 (8 h)	151	2	-	-
Benzo(a)pyrene	496	$C_{20}H_{12}$	0.02 (8 h)	5 132	1	-	-
Indeno(1,2,3-cd)pyrene	524	$C_{22}H_{12}$	0.02 (8 h)	2 741	1	-	-
Dibenzo(a,h)anthracene	539	$C_{22}H_{14}$	**	1 301	0.1	-	-
Benzo(ghi)perylene	545	$C_{22}H_{12}$	**	2 316	0.2	-	-
BE			-	**1,65**	**0.00**	**0.00**	**0.00**

** no defined PEL for these compounds.

The high concentration of PAH species in the reference binder, CTht, is confirmed in Table 4.2. The BE of this binder (1.65) is in the range observed for similar liquid coal tar fluids (Andreikov et al., 2008). The BE of all other binders, including PFR, was zero. Toxicity of a binder cannot, however, only be determined by the quantity of PAH species that were lower than that of the CTht, because there were some PAH species present in high concentrations that were not included in the BE calculation. The BE value is a good indicator for binders that contain elevated quantities of PAH species. Glycerine did not contain any of EPA-PAH species or aromatic structures, as shown by the FTIR analysis. PFR did, however, contain an abundance of 16-EPA-PAH species and, as shown by the FTIR results, had a primarily aromatic molecular structure. Certain species in the binders are present at concentrations

above the PEL, which indicate that they are unfavourable for human short-term exposure (8–10 h). Comparing the pure glycerine analysis with those of the Gly+PFR and Gly+XG+PFR mixed binders confirms that when phenolic resole resin was added, some PAH species were present in the binder and above the PEL of certain compounds. This means that, regardless of the type of non-toxic fluid chosen as a binder, the toxicity of the binder system will be dependent on the composition and quantity of the phenolic resin.

4.2.2.3. Double-bond equivalent and carbon number

The goal was not only to identify 16-EPA-PAH species in each binder but to also identify their molecular composition, so that they could be ranked in terms of their associated health risks. Other species (non-16-EPA-PAH) in the binders were identified by untargeted (pseudo) analysis. The untargeted analysis results are schematically represented by bubble plots, in which the double-bond equivalent (DBE) is plotted against the carbon number (CN). CN was determined from the theoretical stoichiometry of each molecule that was used to calculate the level of unsaturation (DBE) for that specific molecule. Each individual bubble in a bubble plot represents a type of organic molecule in the sample with a specific CN and DBE. The size of each bubble is an indication of the relative concentration of that species in the sample. The DBE is the level of unsaturation of an organic molecule and can be calculated from the following equation (Bae et al., 2011):

$$DBE = \mathrm{C} + 1 - \left(\frac{\mathrm{H}}{2}\right) + \left(\frac{\mathrm{P}}{2}\right) + \left(\frac{\mathrm{N}}{2}\right), \quad (4.1)$$

where C = number of carbon atoms, H = number of hydrogen atoms, P = number of phosphorus atoms, and N = number of nitrogen atoms. Untargeted analysis was only conducted on the coal-, petroleum-, and wood/vegetable-based binders because their molecular compositions were more complex than the glycerine-based binders. The glycerine-based binders mainly consisted of glycerine, XG, and/or phenolic resole resin, all of which were added as analytical-grade reagents.

4.2.2.3.1. Coal-based binders

The untargeted analyses of the CTht and CTPht-B binders are shown in Figure 4.14 and Figure 4.15, respectively. The EPA-PAH species identified by targeted analysis are represented as black spheres; the untargeted analyses of the remaining species in the binder are depicted as light grey spheres. The conjugated double-bond PAH species follow a linear trend (DBE/CN = 2/3), as indicated by the dashed PAH line. The line for pure aliphatic species is at DBE = 0, extending to higher CN as the chains become longer. Low-PAH alternative binders with fewer species follow the PAH line, but are closer to the X-axis, i.e., have more aliphatic structure, are preferred. Reducing the PAH species, and consequently the 16-EPA-PAH, would lower the toxicity of a binder, but at the cost of the lower carbon yield that would result after firing.

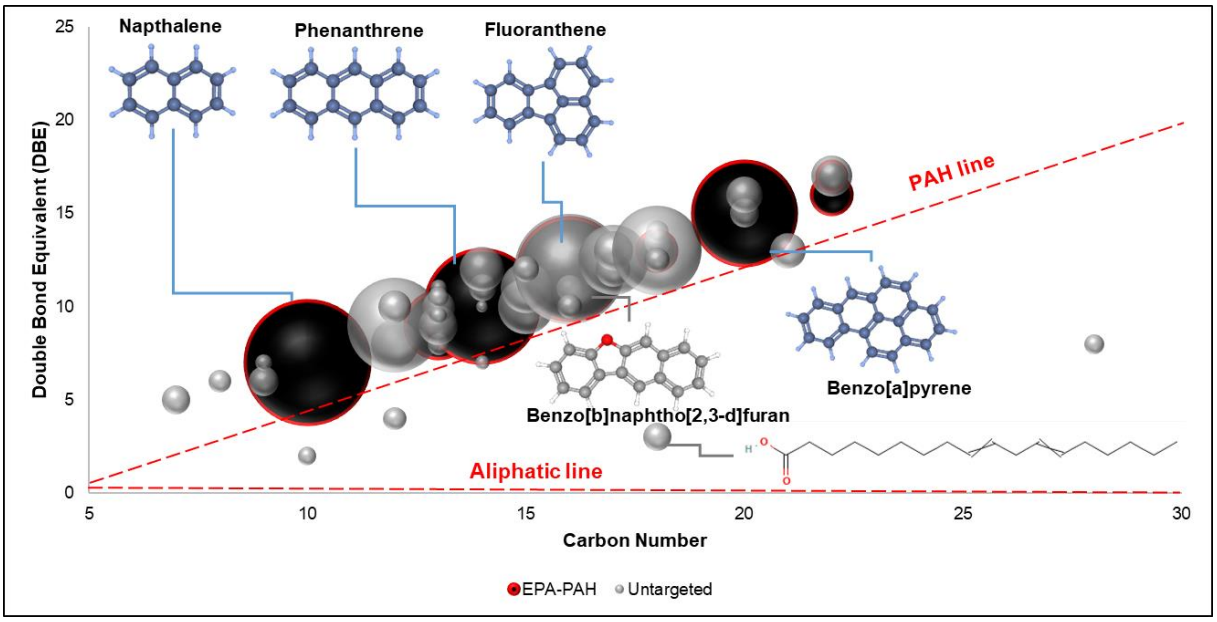

Figure 4.14: Graphical presentation of untargeted analysis results, shown as double-bond equivalents as a function of carbon number for CTht

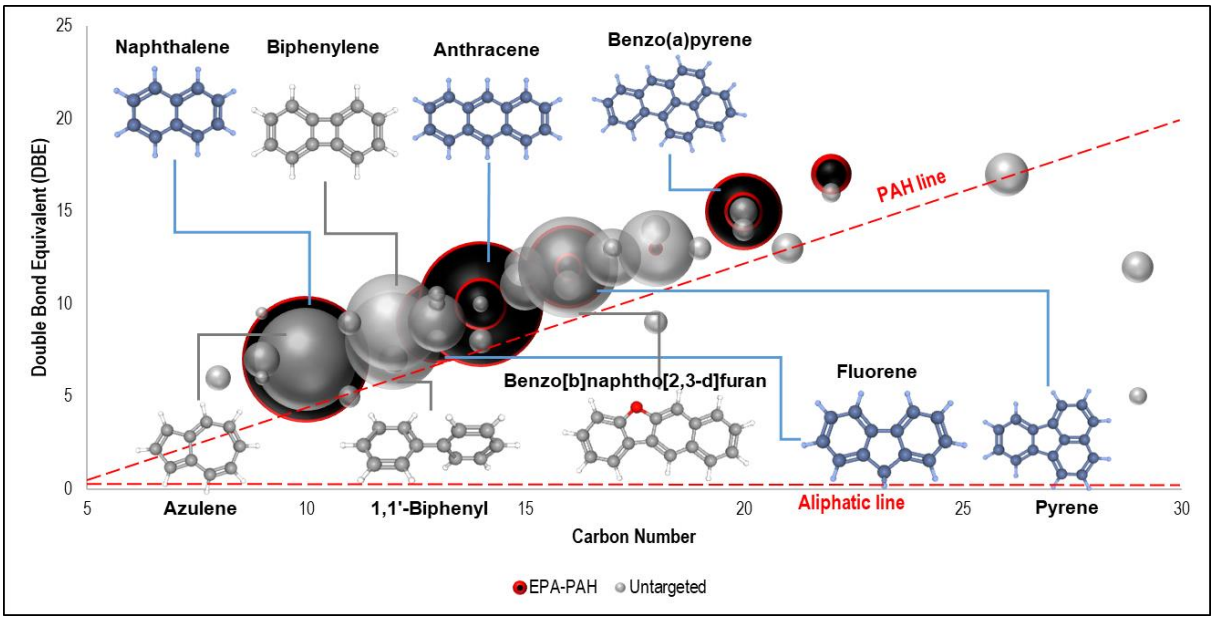

Figure 4.15: Graphical presentation of untargeted analyses of CTPht-B, shown as double-bond equivalents as a function of carbon number

Untargeted analysis of CTht (Figure 4.14) showed the six highest concentration EPA-PAH species (as identified by targeted analysis) as naphthalene, phenanthrene, anthracene, fluoranthene, pyrene, and acenaphthylene. Phenanthrene and anthracene have the same DBE and CN, so were combined as a single bubble with an area equal to their sum. The same was done for fluoranthene and pyrene, with fluoranthene having the larger quantity in the sample. The PAH with highest concentration (untargeted analysis) was benzo(b)naphtho(2,3-d) furan; biphenylene had the second-highest concentration, with DBE = 9 and CN = 12. There were also small amounts of aliphatic species, such as octadecadienoic acid, along the aliphatic line. CTPht-B had a similar composition to that

of CTht, except for a noticeable smaller extent of species with CN = 13–17 compared with the reference sample. The most abundant EPA-PAH species, as shown in Figure 4.15, were naphthalene, anthracene, phenanthrene (DBE = 10, CN = 14), fluoranthene, pyrene, benzo(b)fluoranthene, and benzo(a)pyrene. The highest-concentration species (BDE = 10, CN = 14) were phenanthrene and anthracene, with anthracene being more abundant. Other PAH species identified in CTPht-B were azulene and associated isomers, biphenylene, and biphenyl. The total number of PAH species in CTPht-B exceeded that of the reference sample. CTPht-B did not contain aliphatic species. This was unexpected because this binder was produced by distillation of CTht, which implies that lower molecular mass aliphatic species should have been removed at lower volatilization temperatures. The presence of mainly aromatic species implies that the oil used as the viscosity modifier to produce the pitch blend also had an aromatic structure.

The reduced PAH pitch (EcoP) from coal tar, was synthetically produced and therefore contained higher molecular mass PAH species, such as benzo(a)pyrene (BaP). These were present in lower concentrations than in the reference binder, which will reduce their toxicity (BE value). Untargeted analyses of the EcoP binder are shown in Figure 4.16. This sample contained lower concentrations of high molecular mass PAH species with CN up to 16. The highest-concentration EPA-PAH species were naphthalene, phenanthrene, anthracene, acenaphthene, fluorene, fluoranthene, and pyrene. The overall PAH content of the EcoP binder was higher than that of CTht and CTPht-B. Although EcoP had lower toxicity, this does not necessarily mean that it contained less PAH species: BE calculates the toxicity taking in account only the most carcinogenic PAH species. Some EPA-PAH species present in the sample were not used in the BE calculation: these include naphthalene, acenaphthene, and fluorene. The EcoP binder had a lower concentration of toxic species than the other coal tar-based samples, but considering the carcinogenic nature of EPA-PAH, this material is nevertheless toxic to life and the environment. Other species present in the sample include dibenzofuran (DBE = 9, CN = 12), its associated isomers of biphenyl (DBE = 9, CN = 13) and 1,1'-biphenyl, 2-methyl- (DBE = 8, CN = 13), and small quantities of carboxaldehyde.

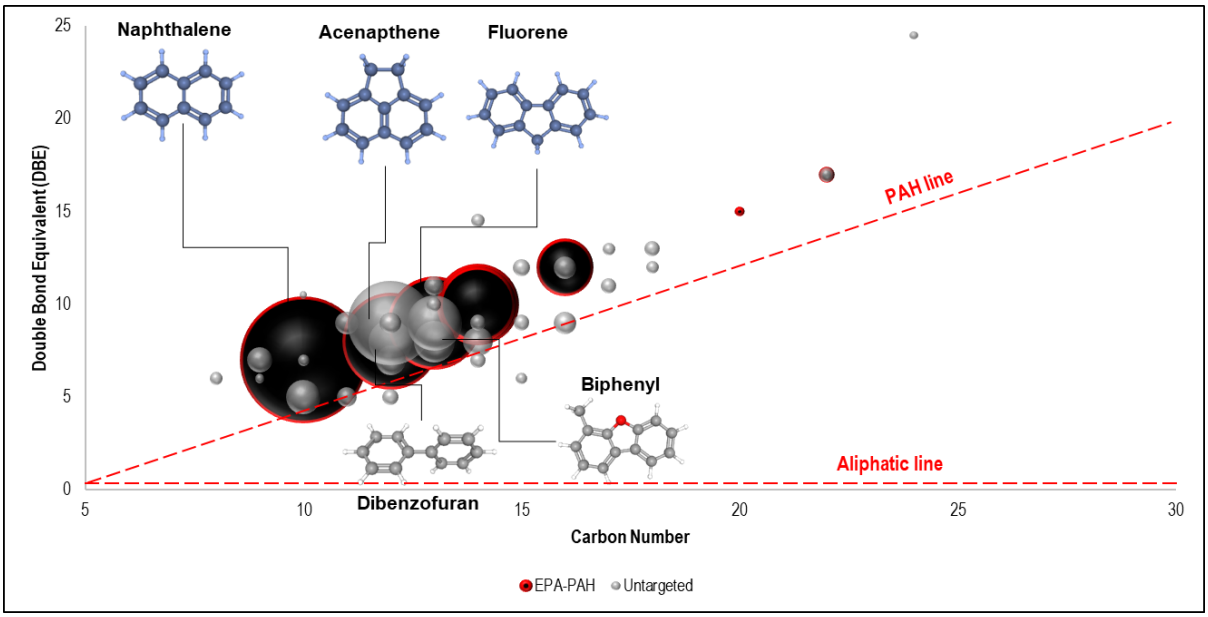

Figure 4.16: Graphical presentation of untargeted analyses of EcoP results, shown as double-bond equivalent as a function of carbon number

4.2.2.3.2. Petroleum-based binders

The CWO sample contained small quantities of acenaphthene, fluorene, and naphthalene, contributing to a BE value of 0.04. When considering the PAH analysis for a toxic-free binder, one needs to ascertain the limits of each individual species: for BE = 0, the binder is considered non-benzene containing with respect to 16-EPA-PAH; however, there are additional PAH species present in the sample. The untargeted analysis of CWO (Figure 4.17) showed the presence of PAH species, including acenaphthene, fluorene, and naphthalene, with trace amounts of phenanthrene and fluoranthene. The C=C stretch identified by FTIR signified the benzene compounds that were identified with GC-MS. There are also hydrocarbon chains (sp^3 C–H stretch from FTIR), as shown by the species near the aliphatic hydrocarbon line in Figure 4.17. Untargeted PAH species identified included dibenzofuran and azulene (isomer of naphthalene), and an abundance of different aliphatic hydrocarbon chains. The combined GC-MS and FTIR results for the CWO binder showed that it comprised a combination of aromatic hydrocarbons and an alkane aliphatic structure.

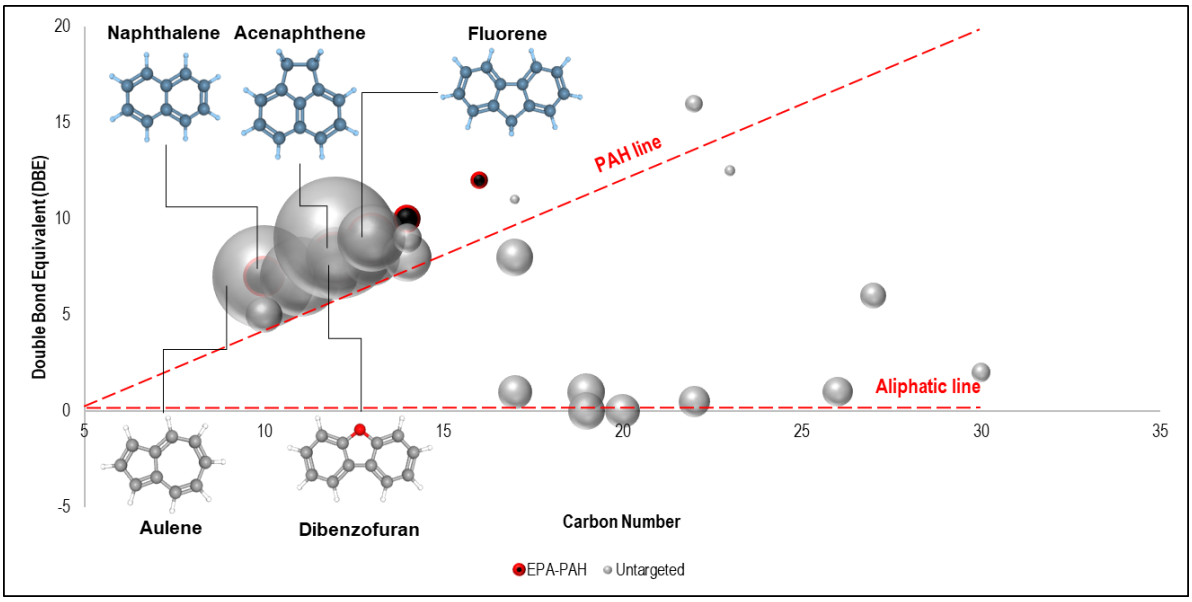

Figure 4.17: Graphical presentation of untargeted analyses of CWO, shown as double-bond equivalent as a function of carbon number

No EPA-PAH species were identified in PCWO, except for a trace amount of phenanthrene (Figure 4.18). The PCWO sample also contained no targeted 16-EPA-PAH species, but mainly aliphatic hydrocarbon chains, the most abundant of which was hexatriacontane, a straight-chain alkane. Other hydrocarbon chains present in lower quantity included 9-hexacosene (DBE = 1, CN = 26), 1-chloro-octadecane (alkane), and dimethyl isomers. Processing of CWO to produce PCWO reduced the aromatic hydrocarbons and linear chain hydrocarbon structure.

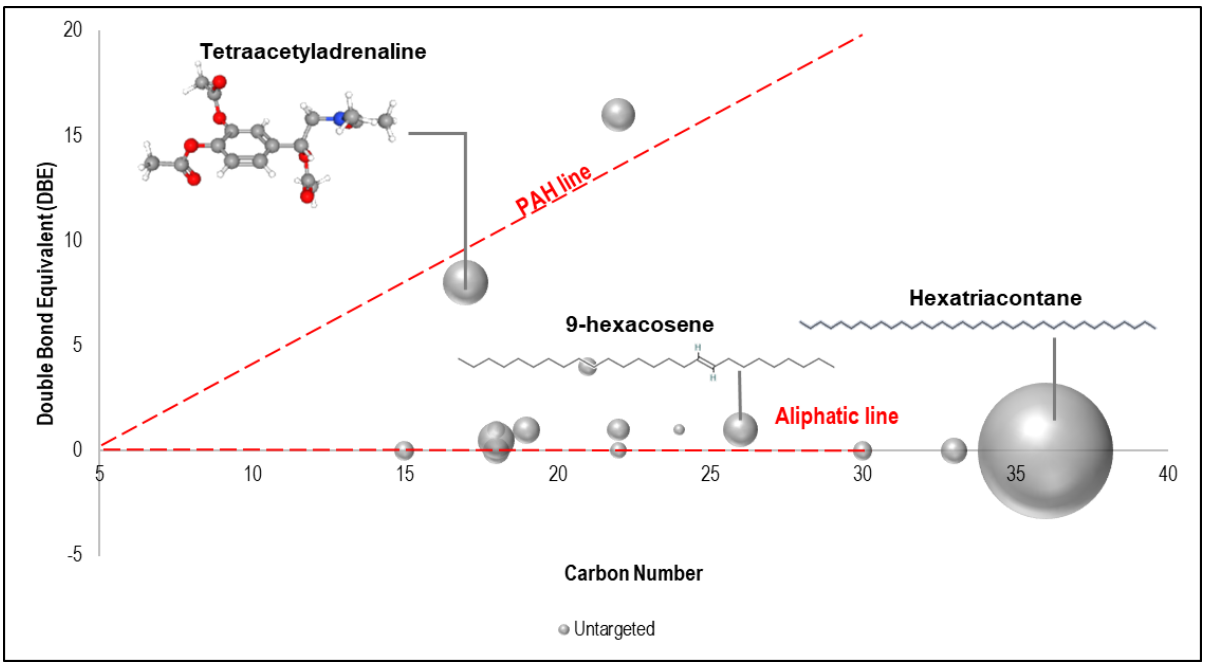

Figure 4.18: Graphical presentation of untargeted analyses of PCWO, shown as double-bond equivalent as a function of carbon number

The phenol-based mesophase-forming pitch (MP) contained naphthalene, acenaphthene, fluorene, phenanthrene, and anthracene (Figure 4.19). Its toxicity coefficient (BE) was 0.24, which is partly due to the presence of

dibenzo(a,h)anthracene, which has the largest coefficient of 1.40 in calculation of the BE value. The identified PAH species are shown in Figure 4.19, in which phenanthrene and anthracene both have DBE = 10 and CN = 14 so are grouped together. Other aromatic species identified in the MP binder include (from highest to lowest concentration) 2,4-dimethylphenol (DBE = 4, CN = 8), 3-ethyl-4-methylphenol (DBE = 4, CN = 9), azulene (CBE = 7, CN = 10), and 4-ethylbenzaldehyde (DBE = 5, CN = 9). The three phenol species are part of a group of aromatic organic compounds called ortho cresols. These are also considered toxic and need to be considered when selecting a suitable replacement for CTht. The presence of both alkyl C–H stretching vibrations (2950–2850 cm^{-}, Figure 4.6) and naphthenic structure are both mesophase promoters, with naphthalene being a better generator of mesophase in petroleum pitches (Li et al., 2018).

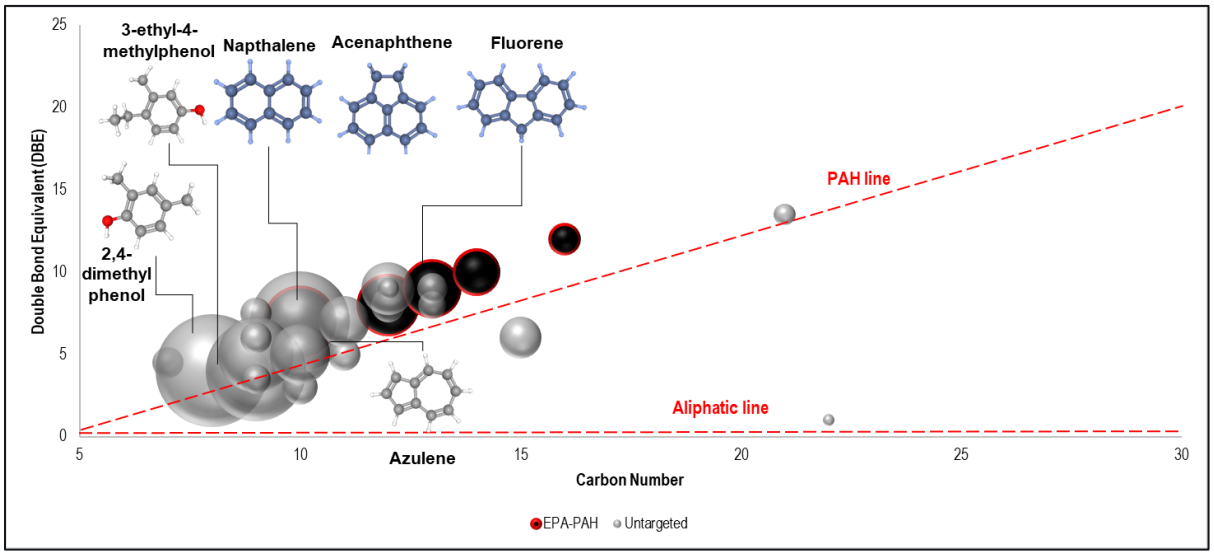

Figure 4.19: Graphical presentation of untargeted analyses of MP, shown as double-bond equivalent as a function of carbon number

4.2.2.3.3. Wood or vegetable-based binders

Tar-PW was a pyrolysis-type oil based on a pine tree-derived byproduct from the Kraft process. PAH analysis of the sample indicated that there were no EPA-PAH species present, i.e., BE = 0. The untargeted GC-MS analyses are graphically shown in Figure 4.20. The binder consisted of some phenol and various methoxybenzene or anisole species, which are organic plant metabolites. Several aliphatic structures were present in the sample. The most abundant species were 4-propenyl-2,6-dimethoxyphenol, 7,8-dimethyl benzocyclobutene (BCB), tetraacetyl adrenaline, and eicosane, which has an alkane structure. Cyclobutene is a benzene ring which is a fused structure with cyclobutene ring that occurs in plants (Dembitsky, 2014). The GC-MS results did not highlight a fatty-acid structure (no O–H functional groups), although some aliphatic molecules were present. The Tar-PW binder mainly (> 85%) contained methoxybenzene species. Investigation of the FTIR fingerprint region identified a co-elusion peak at 1250 cm^{-1}, which shows similar characteristics to compounds like methoxybenzene.

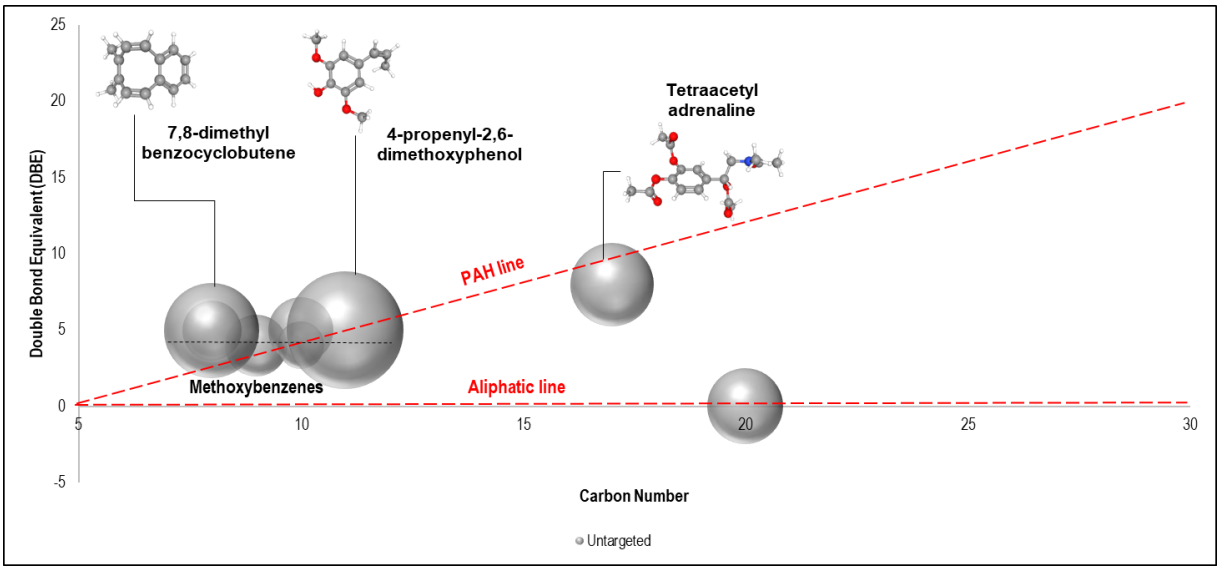

Figure 4.20: Graphical presentation of untargeted analyses of Tar-PW, shown as double-bond equivalent as a function of carbon number

Targeted PAH analysis of the beechwood tar sample (Table 4.1) confirmed that it did not contain any 16-EPA-PAH, i.e., BE = 0. The untargeted analysis results (Figure 4.21) indicated that this sample had a more complex constitution than the pinewood tar although both are plant-based. The major species identified include peri-xanthenoxanthene-4, 10-dione, and 2-,8-bis(1-methylethyl)-quinone, which is a benzoxanthene found in citrus plants and other tropical trees (Asmah et al., 2022; Choi et al., 2010), 9-octadecenoic acid, which is a long-chain fatty-acid hydrocarbon, and smaller quantities of other aliphatic compounds. The FTIR results (Figure 4.8) confirmed the presence of chain hydrocarbons and aromatics, which can be attributed to benzoxanthenes. The ester functional groups can be attributed to the 9-octadecenoic acid molecular structure. The ketone identification by FTIR results aligns with the presence of 9-octadecenoic acid in the binder. The molecular structure of the beechwood tar was more aliphatic in nature (considering both FTIR and BE values) and is considered less toxic than some of the previously discussed binders.

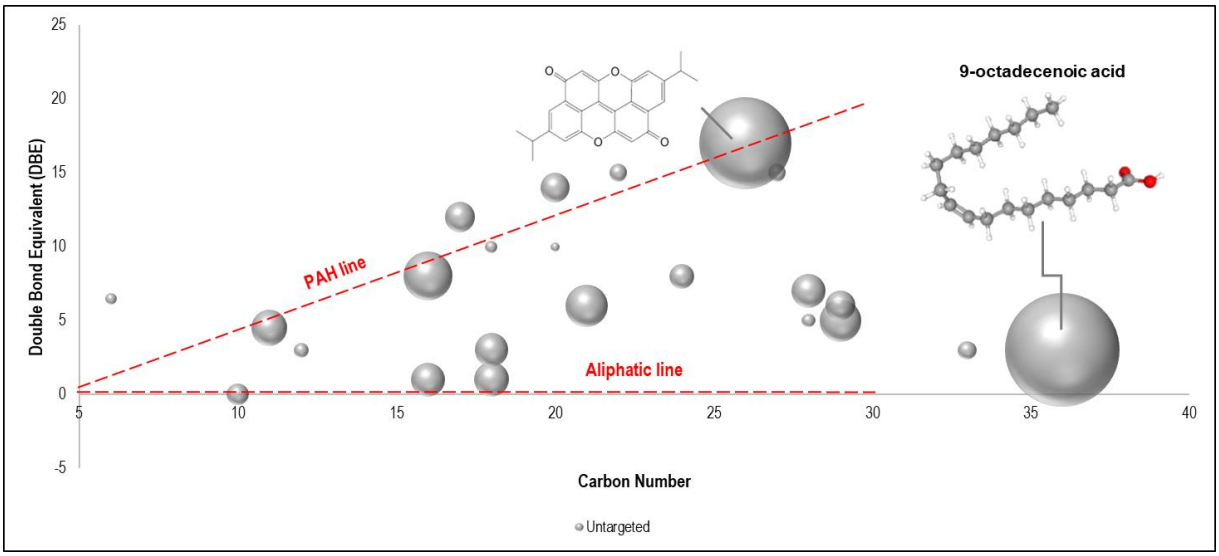

Figure 4.21: Graphical presentation of untargeted analyses of Tar-BW, shown as double-bond equivalent as a function of carbon number

The vegetable tar (Tar-Veg) had a complex molecular constitution, consisting of different organic species, including both cyclic aromatic and chain hydrocarbons. The untargeted GC-MS analysis of Tar-Veg (Figure 4.22) was similar to that of the beechwood tar, with the presence of peri-xanthenoxanthene-4, 10-dione, 2-,8-bis(1-methylethyl)-quinone (DBE = 16, CN = 20), 9,17-octadecadienal (Z), which is a chained hydrocarbon (DBE = 3, CN = 18), and 1,2,4-methenoazulene, decahydro-1,5,5,8a-tetramethyl-, [1S-(1α,2α,3aβ,4α,8aβ,9R*)]- (DBE = 15.5, CN = 15), which has a non-benzene cyclic hydrocarbon structure. The presence of the methenoazulene is dangerous to the environment and aquatic life, and therefore considered hazardous. The remainder of the sample consisted of species with aliphatic structures, which are arranged around the aliphatic hydrocarbon line in Figure 4.22.

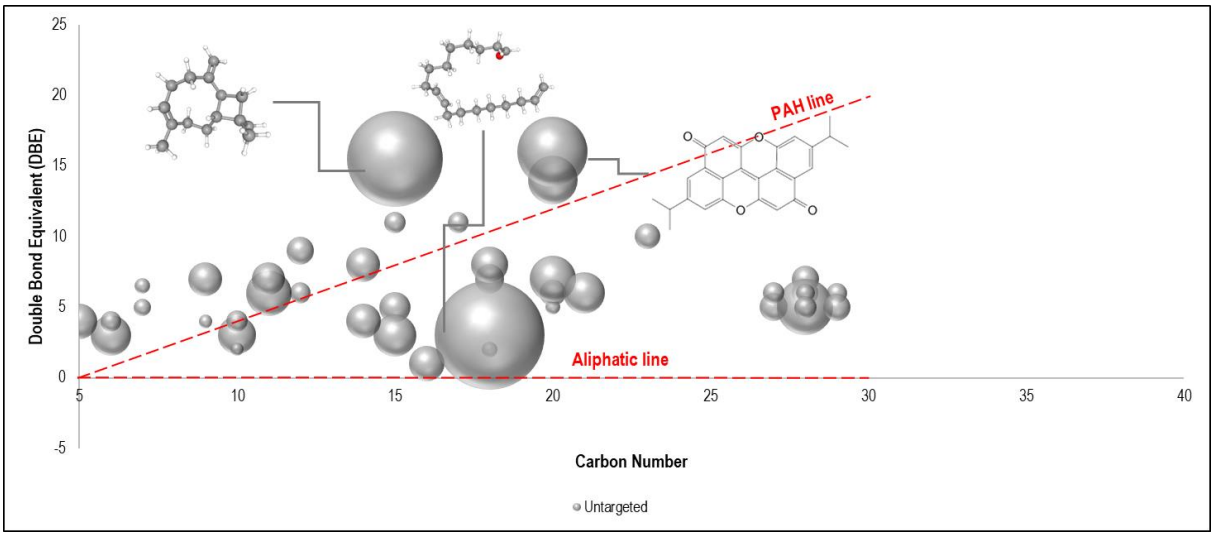

Figure 4.22: Graphical presentation of untargeted analyses of Tar-Veg, shown as double-bond equivalent as a function of carbon number

Analysing the results from the untargeted analysis, binders with a more aliphatic structure, such as PCWO and Tar-BW, would be preferred alternatives to CTht: these binders had low BE values in the targeted analysis.

4.2.2.4. Conclusion

This section assessed the molecular composition of the binders to determine their toxicity, based on BE value and total PAH content (targeted, GC-MS). FTIR and untargeted GC-MS were used to determine the aromaticity of each binder and whether the molecular constitution contained aromatic species. This was used to correlate the performance in terms of thermal and rheological behaviour, described in Sections 4.3 and 4.4.

Targeted analysis results indicated that the pinewood tar (Tar-PW) and beechwood tar (Tar-BW) binders had BE values of zero. The total 16-EPA-PAH values of these binders was also zero, indicating that they are toxicity-free. The vegetable tar contained methenoazulene, which is hazardous for aquatic life and therefore less favourable. The petroleum-based binders had lower BE values than the coal-based binders. Both CWO and PCWO had low BE and total PAH values compared with the mesophase-forming pitch and coal-based binders. The petroleum-based mesophase-forming binder (MP) had a BE value of the same magnitude as the EcoP pitch binder, although the latter had a higher total PAH content. The binders with the highest BE-value and total 16-EPA-PAH (toxicity) were the coal-based binder CTPht-B and the reference (CTht).

FTIR results, confirmed by GC-MS untargeted analysis, indicated that CTht and CTPht-B were mainly aromatic: CTht had higher aromaticity. EcoP had a similar aromaticity (untargeted analysis) to CTPht, although it was more refined and had only a few PAH species in lower quantities, such as Ba(P). FTIR analysis of this binder indicated the presence of some aliphatic species, although these might be chain links between the benzene species, which are weak interactions that dissociated when the sample was heated during GC-MS gasification. The petroleum-based waxy oils seemed to have a combined aromatic/aliphatic structure, based on the untargeted analysis: PCWO was more aliphatic. FTIR results for these binders were the same, indicating both aliphatic and C=C groups. Based on GC-MS analysis, CWO had higher aromaticity than its processed version (excluding 16-EPA-PAH species that showed lower BE values). FTIR results of MP indicated the presence of both aromatic and aliphatic species. Untargeted GC-MS analysis confirmed more aromaticity because there were less species that occurred along the aliphatic line in the untargeted analysis bubble plot for this sample.

The wood/vegetable-based binders comprised a combination of both aliphatic and aromatic species, as shown by the untargeted analysis. The pinewood and vegetable tars showed higher aromaticity (species close to the PAH-line in the untargeted analysis) than the beechwood tar. FTIR results showed the presence of C=C aromatic species and aliphatic functional groups, indicating a combination structure. This was confirmed by the untargeted analysis, which showed that some of these binders had higher-aromaticity species present, excluding 16-EPA-PAH.

The glycerine-based binders were evaluated by targeted analysis and FTIR only. The purities of these binders were such that species other than those identified as 16-EPA-PAH (legislative) were aliphatic, which was confirmed by the FTIR results. Targeted analysis of the glycerine-based binders indicated that all mixtures had BE = 0. Some mixtures that contained phenolic resole resin showed higher concentrations of 16-EPA-PAH than the PEL, as defined by occupational exposure practice. This result indicated that these binders are considered toxic-free based

on their BE value but should be limited in terms of volatile exposure due to the phenolic resin (free phenol and formaldehyde). The toxic-free nature of binders for THC is dependent on the phenolic resin content and composition. This is due to the free phenol and formaldehyde present in these resins as most of the PAH or aromatic species in phenolic resin dissociate during heating and in general do not volatilize as PAH species similar to CTP. FTIR results for these mixtures showed that all binders were aliphatic (no aromatic species; small concentrations identified by GC-MS targeted analysis were not detectable by FTIR).

4.2.3. Ranking of binders based on molecular structure

The binders were ranked based on molecular structure using both FTIR and GC-MS (targeted and untargeted) analysis. The ranking was carried according to the BE value and total 16-EPA-PAH content (toxicity). Binders of the same or close BE values and total 16-EPA-PAH contents were ranked according to their aromaticity (obtained from FTIR results, with untargeted analyses used as a secondary guideline). The ranking of the binders based on their molecular structure features is shown in Table 4.3.

Table 4.3: Binder ranking based on molecular structure features

Rank	BE Value	Total 16-EPA-PAH content (ppm)	Sample
1	**0**	**0**	Gly+PFR, Gly+XG+PFR
2	**0**	**0**	Tar-BW
3	**0**	**0**	Tar-PW
4	**0.03**	**431**	PCWO
5	**0.02**	**1 262**	Tar-Veg
6	**0.03**	**9 060**	CWO
7	**0.24**	**15 251**	MP
8	**0.66**	**84 911**	EcoP
9	**1.92**	**199 181**	CTPht-B

All glycerine-based binders and the beechwood and pinewood tars had BE values and corresponding total 16-EPA-PAH values of zero. These binders were ranked according to their aromaticity. The glycerine-based binders showed the lowest aromaticity (no aromatic species were identified by FTIR). These samples were all aliphatic and pure mixtures. Gly+PFR and Gly+XG+PFR were ranked in first position because addition of the viscosity modifier had no detectable compositional changes. The beechwood tar was ranked in second position ahead of the pinewood tar binder due to the higher aromaticity of the pinewood tar (presence of aromatic species identified by FTIR and confirmed by GC-MS untargeted analysis).

The primary criterion to rank the binders was the BE value: if the values are the same or comparable, the total 16-EPA-PAH content was also taken into consideration, as for PCWO, Tar-Veg, and CWO. The BE of PWCO was higher than that of Tar-Veg and the same as CWO; however, the total 16-EPA-PAH content for the Tar-Veg was higher than that of PWCO, so it was ranked higher. Tar-Veg also contained compounds that are considered toxic to aquatic life, which was considered in the toxicity ranking of this binder. PWCO had a lower total 16-EPA-PAH content than these three binders and so was ranked fourth. The last three binders listed in Table 4.3 all exhibited higher BE, total 16-EPA-PAH, and aromaticities than the beforementioned binders. The ranking according to both the BE-value and total 16-EPA-PAH aligns with a higher BE value corresponding to a higher total 16-EPA-PAH. The mesophase-forming pitch had a lower BE value and total 16-EPA-PAH compared with EcoP and CTPht-B and was ranked 7th. CTPht-B had the highest BE and total 16-EPA-PAH, so was ranked last. This binder had a total 16-EPA-PAH content that was an order of magnitude larger than those ranked in the first position. In terms of molecular structure and toxicity, the glycerine-based binders are the preferred alternatives to CTht for THC.

4.3. Thermal behaviour

TGA, DSC, and DTA were conducted on the coal-, petroleum-, and wood/vegetable-based binders, from 50–850°C. The glycerine-based binders were also subjected to detailed DSC analysis between 30–150°C due to the presence of phenolic resole resin in these binders and to evaluate the potential shift in cross-linking temperature to lower temperatures as a cause of premature cross-linking (Cameron, 2021) in more detail. Thermal behaviours of the alternative binders were compared with that of the reference sample (CTht). All binders transitioned between two regions: pyrolysis (400–600°C) and then gasification (600–800°C). Inflection points in the TGA and DTA curves were identified. The carbon yield, calculated as a percentage of the remaining mass of the sample after heating to 800°C, was also recorded.

4.3.1. Thermogravimetric analysis

As noted in Section 2.1.3.2, important properties of a binder for use in a THC high-temperature application include a high thermal decomposition temperature range, a low degree of volatility over a short temperature range, a gradual volatile release over a wide temperature range (consequently lower porosity in THC matrix), which includes the decomposition temperature of the phenol–formaldehyde resin (~ 300°C), and a high carbon yield to assist with increase in the clay strength by carbon skeleton formation.

4.3.1.1. Coal-based binders

The TGA curve of the reference sample had six inflection points starting at 70.8°C (Figure 4.23). The corresponding changes in mass between two inflection points are annotated on this graph. There was a sharp increase in mass loss at 90.5°C due to volatile release, signalled by the endothermic peak on the DSC curve. The largest change in mass, 49.5%, occurred from 228.2–380.4°C. The inflection points at 150.1°C showed peak overlap on the DTA curve. Two processes occurred simultaneously in the temperature range from 70.8–380.4°C: volatilization of lower molecular mass hydrocarbons at 150.1°C (possibly naphthalene, which was shown to be present in the sample

(Section 4.2.2.3)) and polymerization of the tar, which started at ~ 200°C. Above this temperature, carbonization occurred that resulted in a small change in mass up to 800°C. The CTht binder had a final carbon yield of 10.6%, which refers to organic carbon only or a mixture of organic carbon and mesophase carbon that was transformed to coke at high temperatures. This material was a byproduct from a coke-making process, so it can be assumed that the carbon yield after firing resulted from solid carbon that was present in the sample before heating.

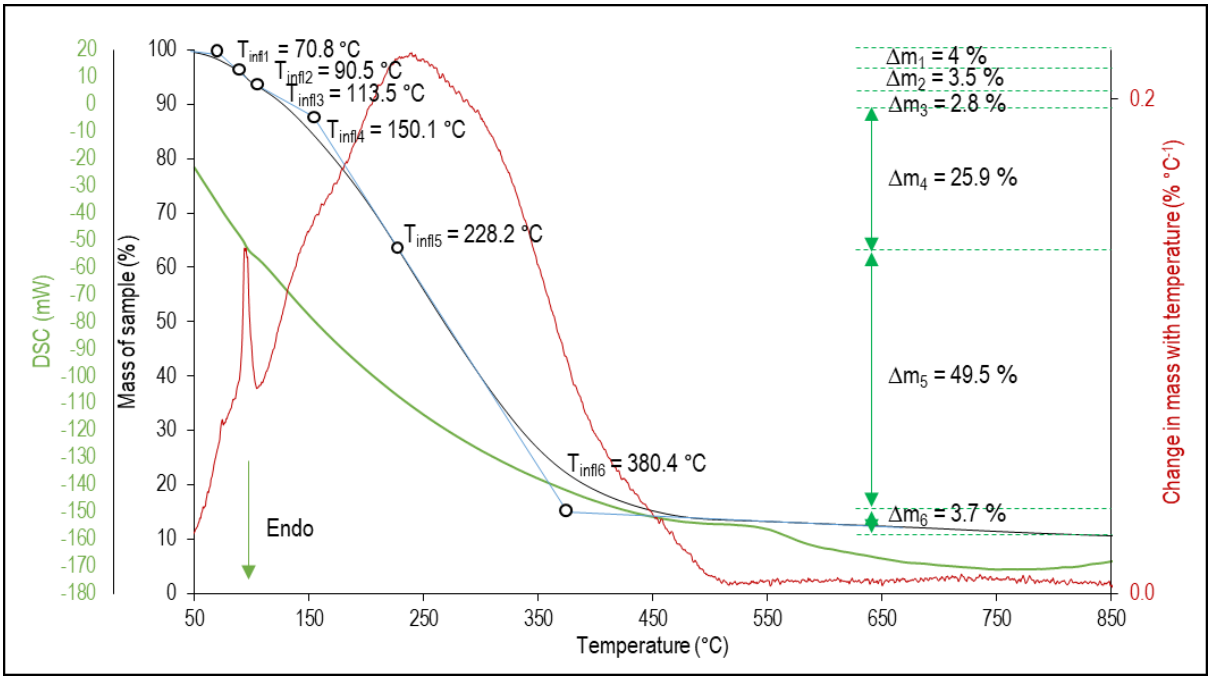

Figure 4.23: Thermal analysis results for CTht (reference) binder, indicating the inflection points and associated changes in mass

Thermal analysis of CTPht-B (Figure 4.24) indicated five inflection points, starting at 116.4°C. The largest decrease in mass occurred at 208.3–306.1°C, with a total mass loss of 39.9% due to volatilization of lower molecular mass hydrocarbons. The mass loss plateaued at the final inflection point at 306.1°C, which is when polymerization started. Above this temperature, the remaining mass of the sample converted to carbon up to 800°C. CTPht-B had a carbon yield of 22.1%, which was almost double that of the reference sample. The largest decrease in mass corresponded to a similar temperature range to that of the reference sample.

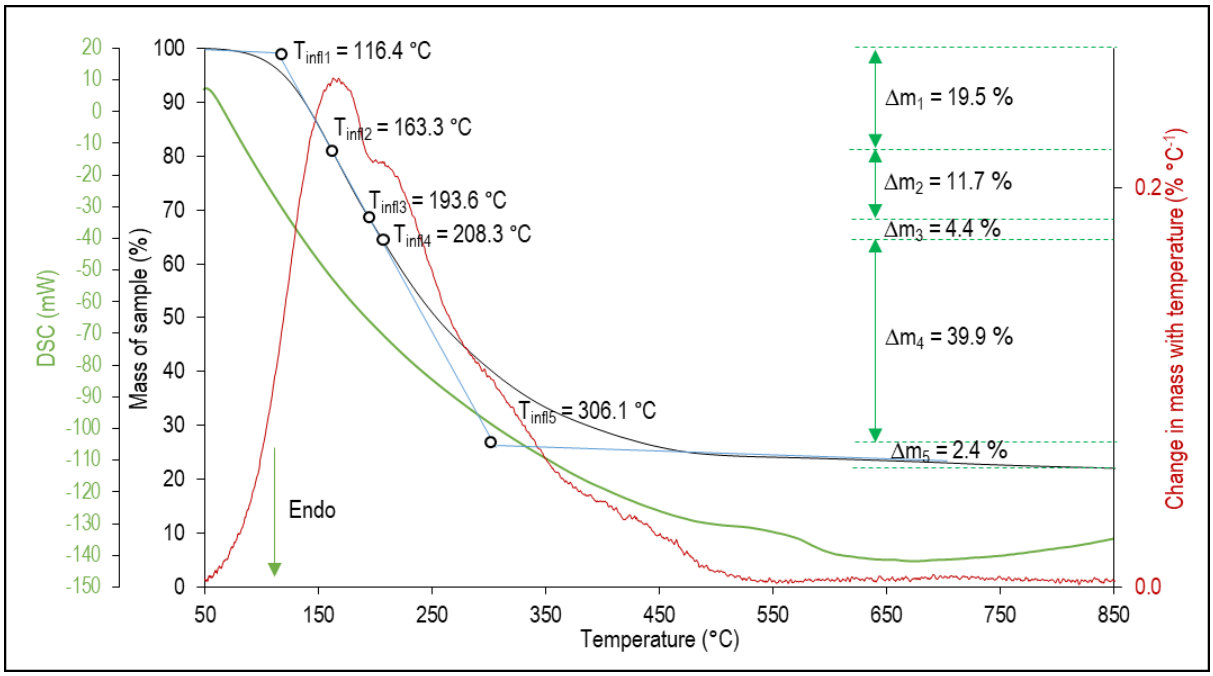

Figure 4.24: Thermal analysis results for the softening-point pitch blend (CTPht-B), indicating the inflection points and associated changes in mass

Thermal analysis of the low-PAH coal-based binder (EcoP) is shown in Figure 4.25. Six inflection points were observed, with a noticeably lower degree of volatilisation with increase in temperature compared with the other two coal-based binders. The largest decrease in mass of 22.1% occurred from 93.4–171.6°C, which was caused by volatilization of lower molecular mass hydrocarbons, presumably naphthalene. Volatile release occurred over a narrower temperature range than CTht and CTPht-B. Polymerization started at ~ 329.2°C, above which the sample pyrolyzed up to 491.6°C. Thereafter, carbonization of the binder resulted in a carbon yield of 30.2%, which is higher than those of CTht and CTPht-B.

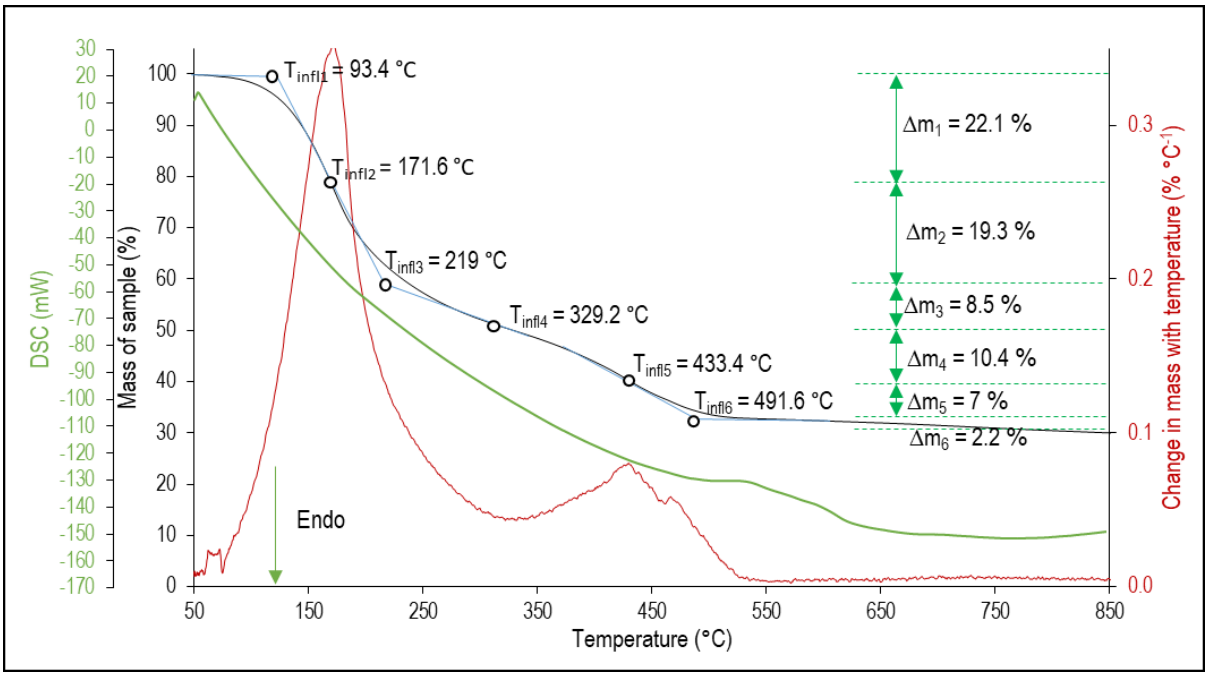

Figure 4.25: Thermal analysis results for low-PAH pitch (EcoP), indicating the inflection points and associated changes in mass

4.3.1.2. Petroleum-based binders

The thermal analysis curve (Figure 4.26) of the CWO sample had five possible inflection points, with a noticeable higher degree of volatilization over a narrower temperature range than the coal-based binders. The first inflection point started at 87.7°C, indicated by a sharp increase in the DTA curve. This could be due to release of moisture in the sample because this was an unrefined binder. Moisture volatilization is also indicated by the corresponding small increase in the endothermic peak on the DSC curve. The largest decrease in mass occurred at 329.3–393.8°C, with half of the binder mass being volatilized within this small temperature range. This would be unfavourable for THC application because a sudden decrease in mass (increase in volatilization) can cause an increase in pore size of the final product that compromises other properties. An increase in porosity lowers the penetration resistance of the clay with respect to gas and liquid, and reduces its strength. Volatilization of lower molecular mass paraffin hydrocarbons proceeded up to 421.6°C. The sample carbonized from 421.6–800°C, giving a carbon yield of 4.9%. This is much lower than those of the coal-based samples, which is expected because the petroleum-based binders had lower aromaticity.

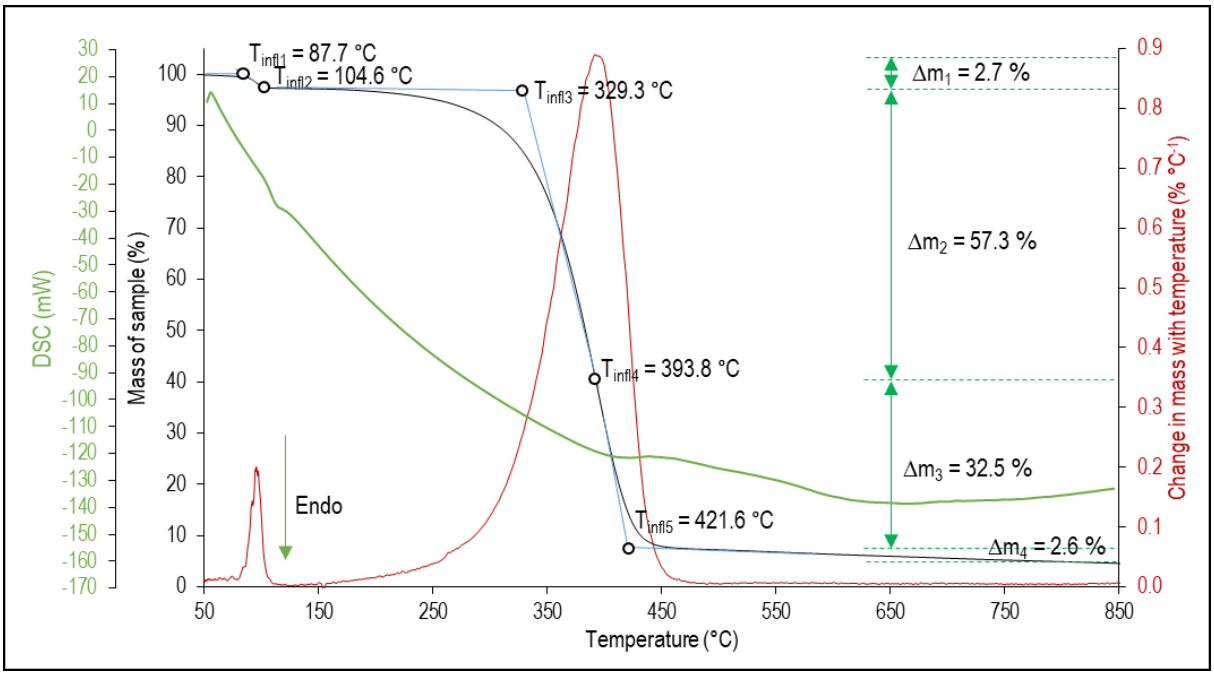

Figure 4.26: Thermal analysis results of waxy crude oil (CWO), indicating the inflection points and associated changes in mass

The refined waxy crude oil showed almost identical results (Figure 4.27) to that of its CWO source material, except for the lower carbon yield of 2.7%. The sample also contained less moisture than the crude sample, with a lower initial mass change of 0.9% compared with 2.7% for the CWO binder. The moisture in this sample is presumably due to moisture pick-up during storage. There were small chemical differences between the samples, but for purposes of evaluating their thermal stability, the two binders were very similar except for the smaller carbon yield of PCWO.

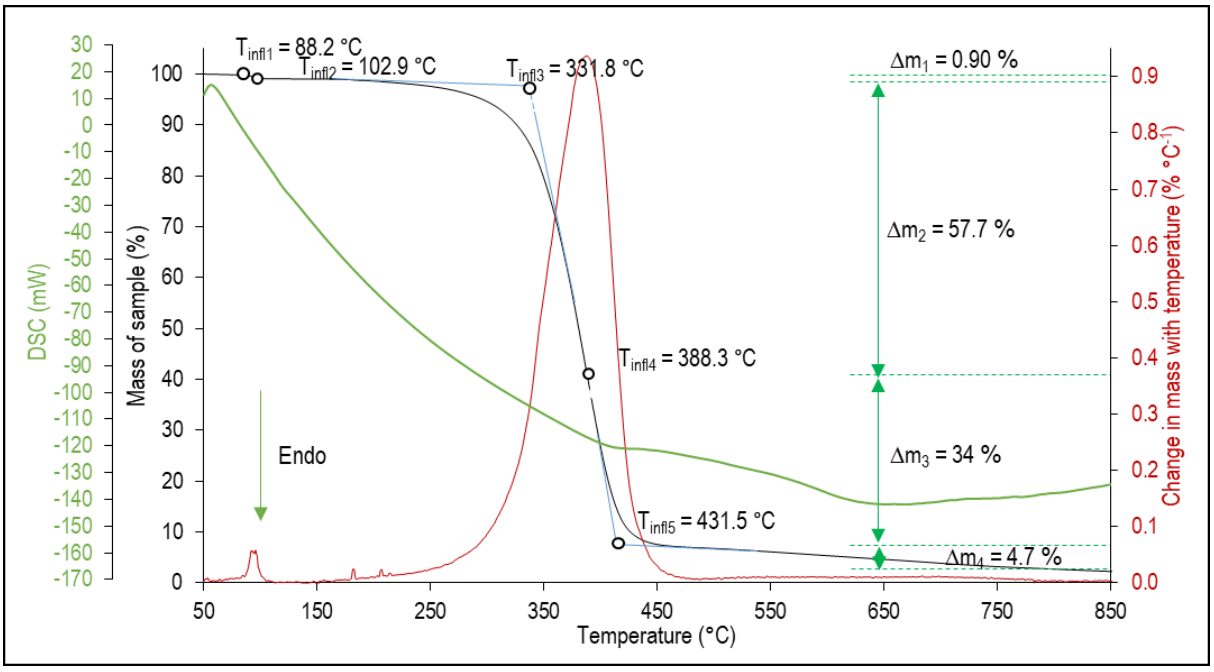

Figure 4.27: Thermal analysis results of refined waxy crude oil (PCWO), indicating the inflection points and associated changes in mass

Thermal analysis of the phenolic mesophase-forming pitch, MP, is shown in Figure 4.28. The volatile release was more gradual than those of the other two petroleum-based binders. Polymerization started at a lower temperature than the CTPht-B binder. The MP sample exhibited two volatilization sequences, evidenced by peak overlap of the peaks at 183.3°C and 257.8°C. Five inflection points were observed between 145.6°C and 317.3°C. The remaining mass at 800°C gave a carbon yield of 5.1%. The sample did not show any decrease in mass during pyrolysis and decomposed at lower temperatures than the other two petroleum-based samples. Thermal behaviour similar to that of CTPht-B was observed from 145.6–317.3°C, where volatilization of lower molecular mass hydrocarbons occurred (although their content was lower than in CTPht-B); thereafter, polymerization occurred at ~ 317.3°C followed by carbonization.

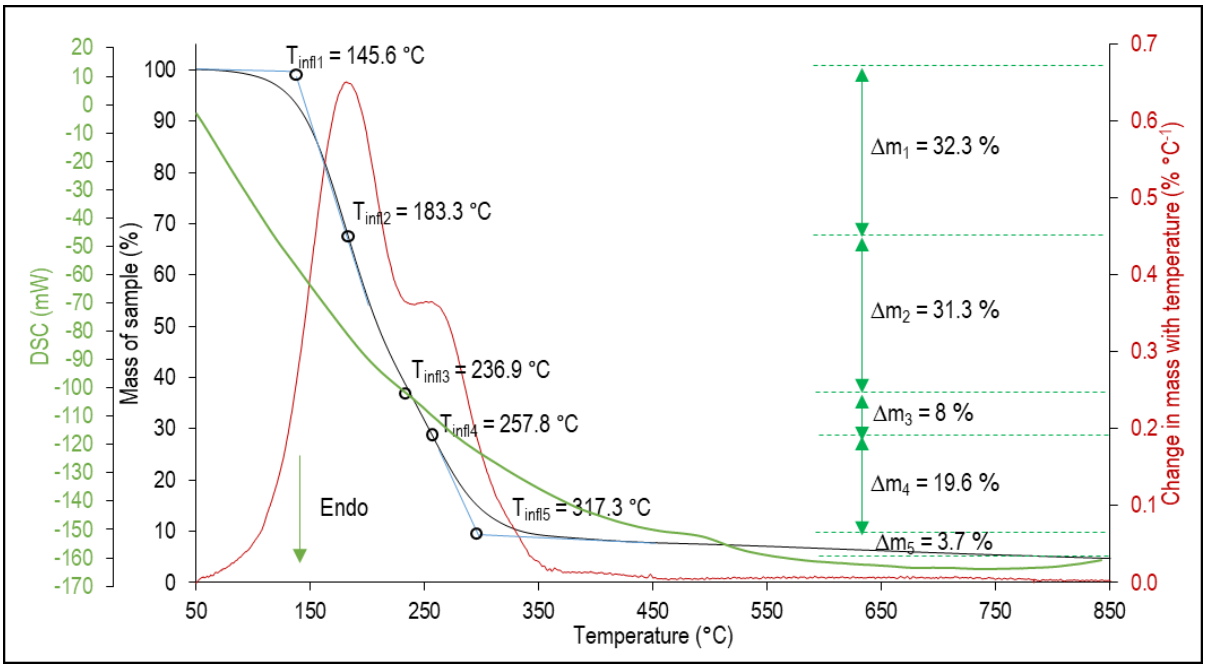

Figure 4.28: Thermal analysis results of phenolic mesophase-forming pitch (MP), indicating the inflection points and associated changes in mass

4.3.1.3. Wood- and vegetable-based binders

Thermal analysis of the pinewood tar (Figure 4.29) indicated five inflection points and a gradual mass loss, similar to that of CTPht-B. Thermal decomposition started at 98.6°C; the largest mass loss (36.8%) occurred on decomposition in the temperature range from 98.6–170.8°C. This is typically due to volatilization of compounds such as moisture, lower molecular mass oxygen-containing species (oxygenates), and lower molecular mass hydrocarbons. There was overlapping of peaks at 170.8°C and 267.6°C with closely related mass losses. Volatilization (31.3% mass loss between 183.3-236.9°C) was due to vaporization of oxygenates and hydrocarbons of higher molecular mass. Decomposition of the sample proceeded up to 300.8°C, after which the remaining mass of the sample carbonized to achieve a carbon yield of 5.8%, which is relatively high for pyrolysis oil samples. The carbon yield was much lower than that of the reference sample, but decomposition occurred over a smaller temperature range. The decomposition temperature range was, however, similar to that of CTPht-B, making Tar-PW a favourable binder except for the lower carbon yield.

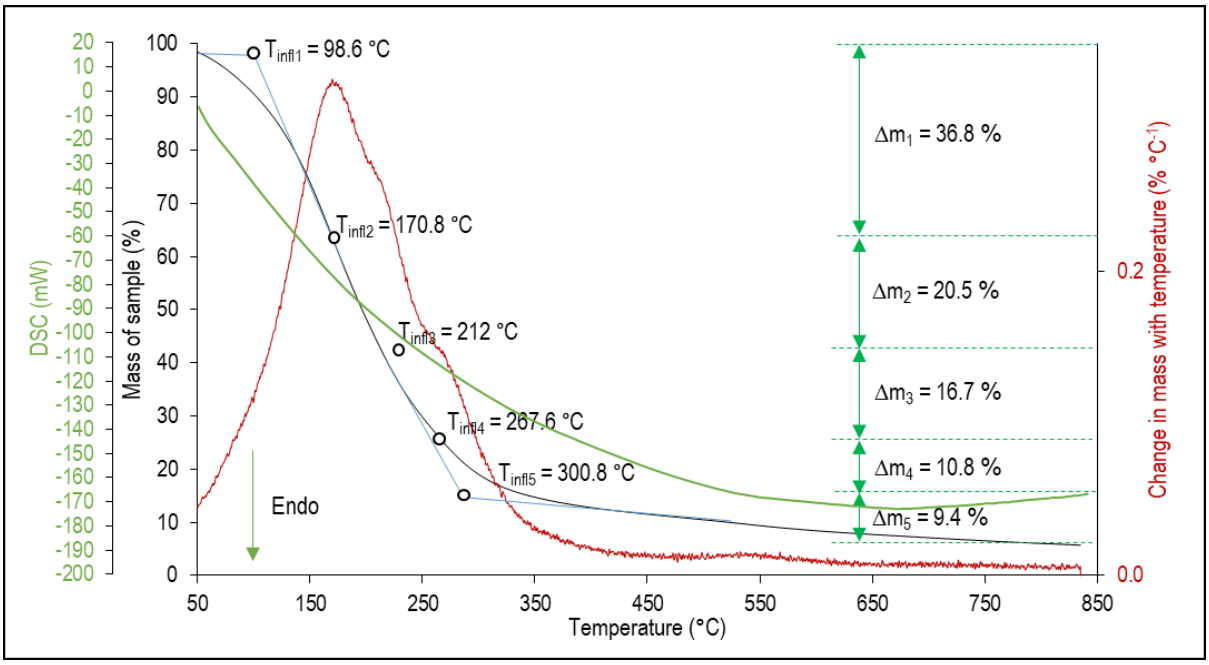

Figure 4.29: Thermal analysis results for pinewood tar pyrolysis oil (Tar-PW), indicating the inflection points and associated changes in mass

The thermal analysis result for Tar-BW is shown in Figure 4.30. Four inflection points, starting at much higher temperatures than the samples previously discussed, were observed. The highest mass loss of almost 50% occurred from 301.5–346.6°C, which is a narrow temperature range. This phenomenon would have the same effect as the waxy oil samples on the physical properties of a THC. The beechwood binder also had a higher degree of volatility over a smaller temperature range, similar to the waxy-containing crude oils. The binder lost mass up to 428.3°C, during which pyrolysis started, resulted in a carbon yield of less than 1%. Based solely on the thermal analysis results, this binder is unfavourable for use in a THC.

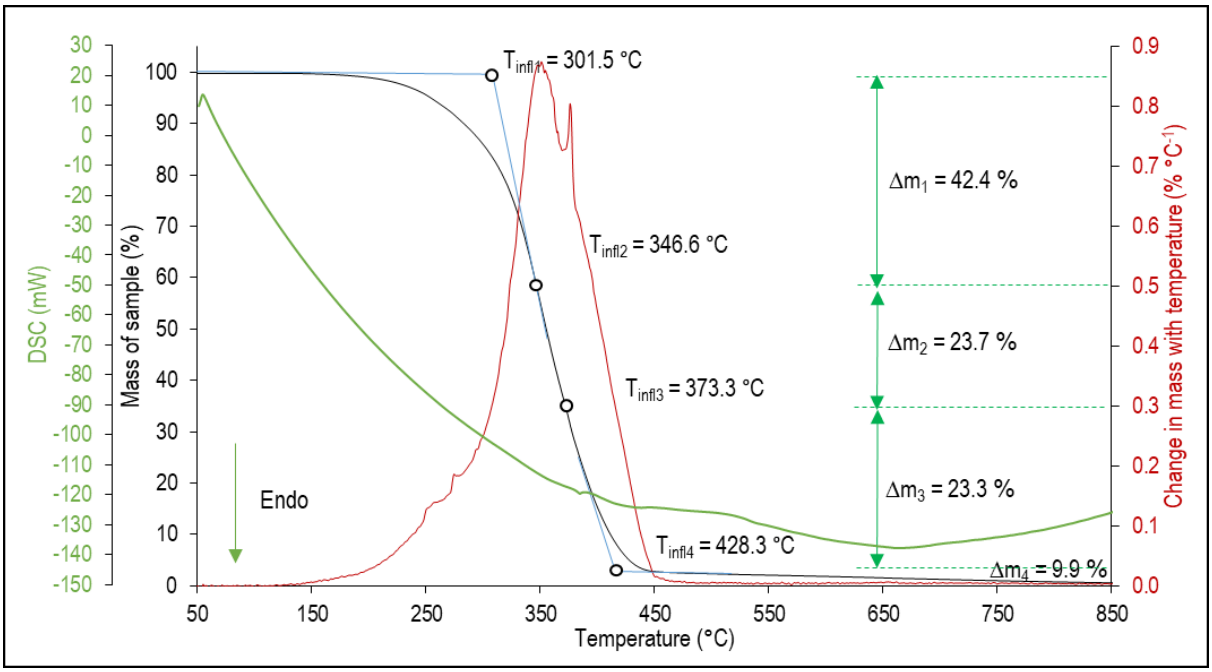

Figure 4.30: Thermal analysis results of beechwood tar pyrolysis oil (Tar-BW), indicating the inflection points and associated changes in mass

The thermal analysis results for the Tar-Veg binder are shown in Figure 4.31. The TGA curve had nine inflection points, indicating the complex volatilization profile of the sample. Decomposition started at a higher temperature (220.8°C) than the other organic binders and reference sample. The largest mass loss (51%) occurred at 220.8–337.5°C. At higher temperatures, gradual mass loss occurred over a wide temperature range. The carbon yield of the binder was 2.7%, which is higher than that of the beechwood tar. Decomposition proceeded to pyrolysis, during which the mass loss continued (mass loss was completed before the pyrolysis temperature was reached for CTht). The mass loss as a function of temperature was similar to that of the Tar-PW and CTPht-B samples. With the exception of the low carbon yield, the vegetable tar is also a possible alternative binder.

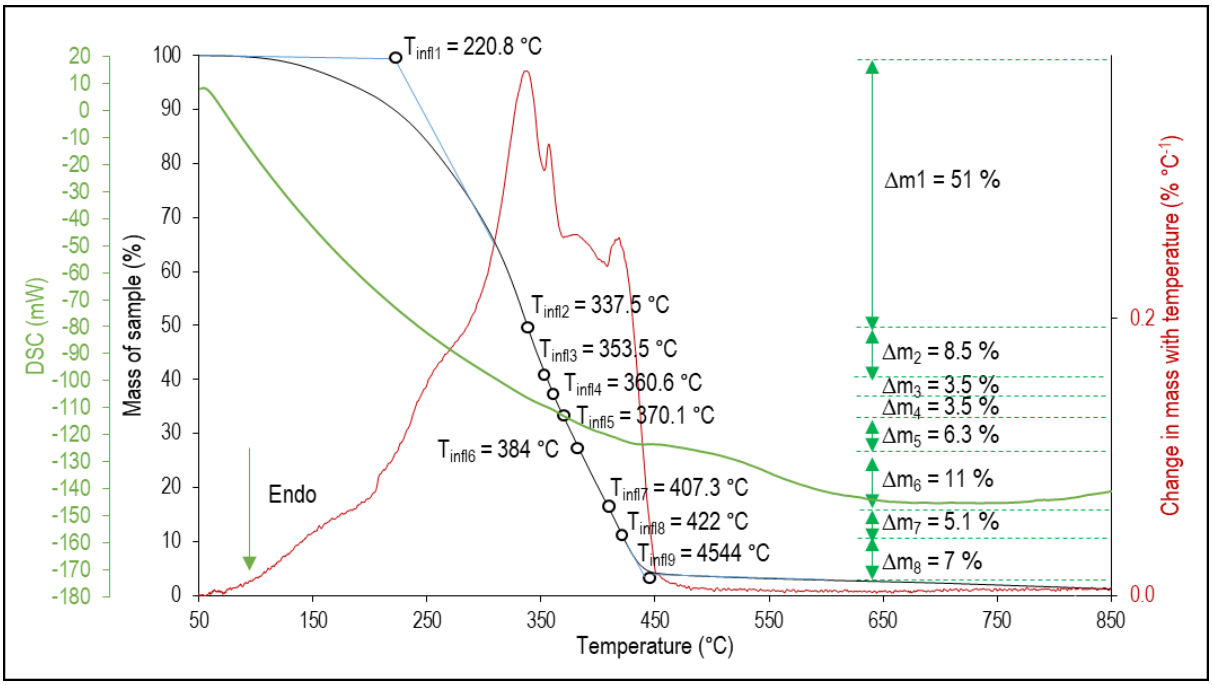

Figure 4.31: Thermal analysis results of vegetable tar pyrolysis oil (Tar-Veg), indicating the inflection points and associated changes in mass

4.3.1.4. Glycerine and polymer-based binders

Evaluation of the average mass loss over a specific temperature range and the carbon yield are of importance when considering the alternative replacements of CTht as binder in THC. The TGA trace of pure glycerine is shown in Figure 4.32. Only two inflection points were observed. Most volatilization occurred above 190°C: the first inflection point was at ~ 192.2°C. The sample experienced an initial mass loss of 8.8% between 25–192.2°C. This is similar to that of the reference binder (CTht), except that volatilization of the latter started at a lower temperature (70.8°C) and another inflection point at 192.2°C with > 10% mass loss was observed. The mass loss of glycerine at the first inflection point was substantial: 91.2 mass% of the binder evaporated at 192.2–236.2°C. The high mass loss coincided with an endothermic peak at 192.2°C in the DSC analysis. No sample remained after heating to 600°C, indicating that this binder did not yield any carbon after firing. The pure glycerine therefore did not exhibit the desired properties of low degree of volatilization over a wide temperature range and some carbon yield after firing. The pore size distribution and porosity of a THC can be affected by excessive volatilization, which will cause insufficient strength of the material and low corrosion resistance to liquids and gases inside the taphole.

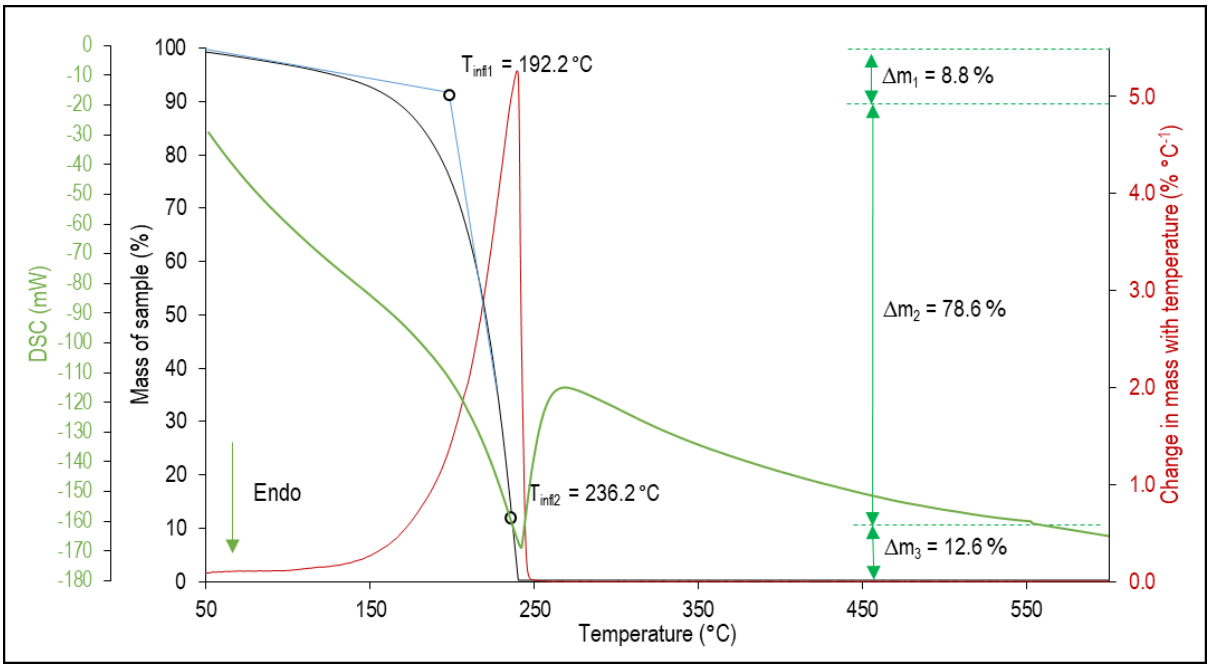

Figure 4.32: Thermal analysis results of pure glycerine, indicating the inflection points and associated changes in mass

Thermal analyses of the mixtures (Gly+XG, Gly+PFR, Gly+XG+PFR) had similar inflection points to that of the pure glycerine (Figure 4.32), but differed in carbon yield. The mixture that contained glycerine and phenolic resole resin did not show any shift or additional inflection points, which was likely due to the small amount of resin used.

4.3.1.5. Conclusion

As previously stated, it is important to use a binder in THC that has a large volatilization temperature range, gradual release of volatiles over the wide temperature range, and allows for a high proportion of the organic material to be transformed into carbon to aid the strength of the clay after firing. Thermal analysis of the binders was conducted in an inert environment with the aim of evaluating the volatilization behaviour of each binder as it was heated from 50°C to 800 °C. The volatilization behaviour was used to highlight the average mass loss, the temperature range of average mass loss, and the inflection points at which the highest mass loss occurred. The carbon yield, calculated as a percentage of the remaining mass of the sample after heating to 800 °C, was also recorded.

A summary of the TGA data, showing the cumulative mass loss of each binder, is presented in Figure 4.33. These curves were used to determine the mass-loss temperature range for each sample, defined as the difference between the volatilization start (onset temperature of critical mass-loss) and end (when mass loss started to plateau) temperatures. This temperature range accounted for most of the mass loss of a sample. The average gradient of mass loss over the temperature range was determined for each curve in g/°C. The carbon yield was determined as mass% of the residue at 800°C (Figure 4.34). The average gradient and mass-loss temperature range of each binder are given in Table 4.4. The temperature ranges given in Table 4.4 represent only the start and end temperatures (range) for the linear slope calculation and do not encompass the entire volatilization range.

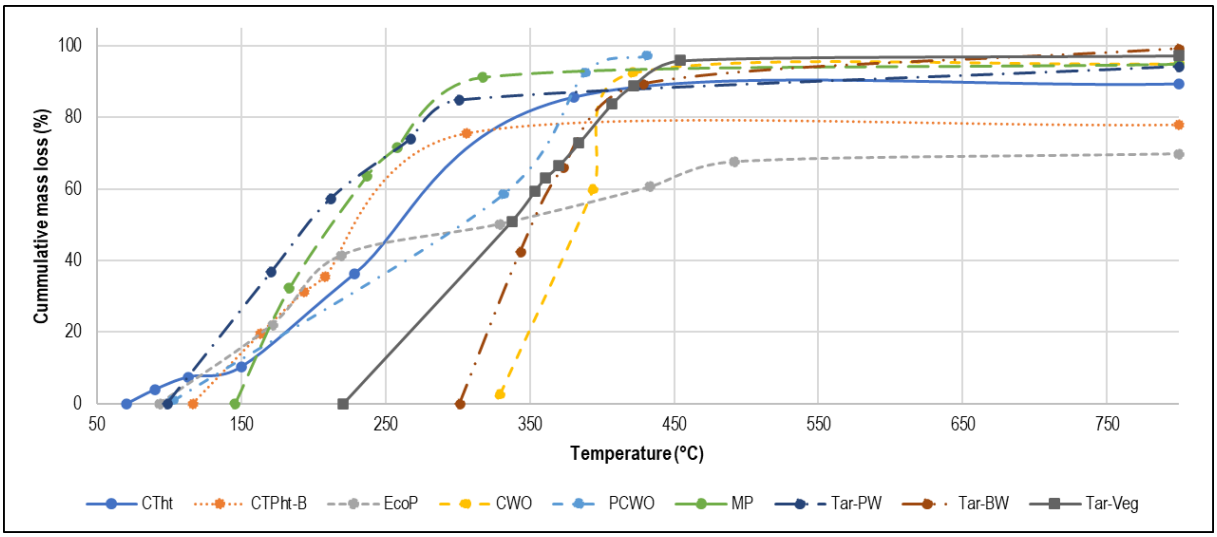

Figure 4.33: Composite comparative thermal gravimetric analysis of the examined binders

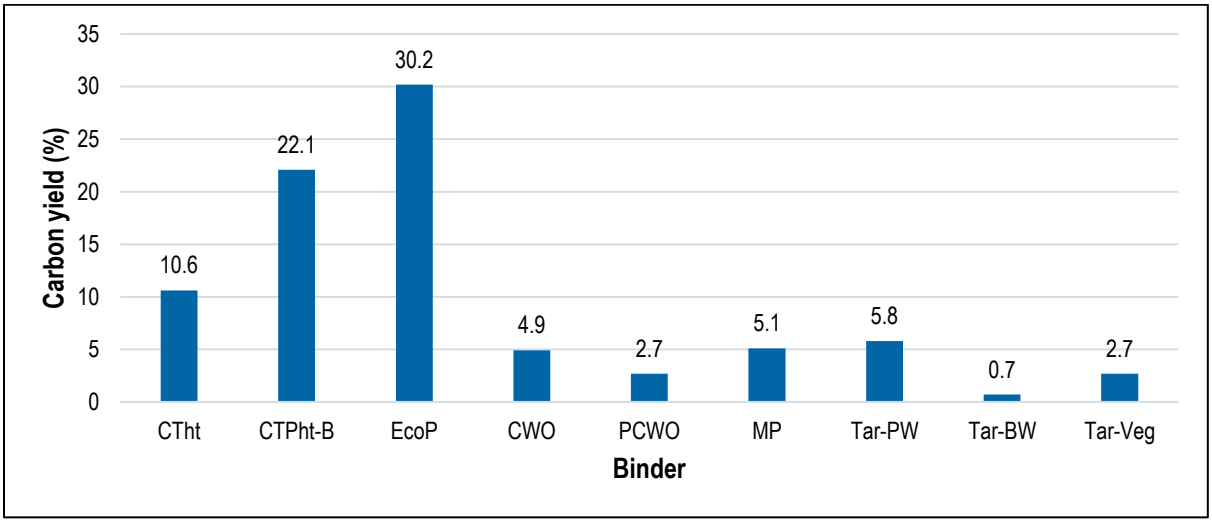

Figure 4.34: Carbon yields of binders on heating to 800°C in a nitrogen atmosphere

Table 4.4: Summary of mass loss over volatilisation temperature range of binders, determined from TGA inflection point results

Binder	Temperatures at inflection point (°C)	Average mass loss per temperature change (g/°C)	Temperature range (°C) (ΔT, °C)
CTht	70.8; 90.5; 113.5; 150.1; 228.2; 380.4	0.28	70.8–380.4 (ΔT ~ 310)
CTPht-B	116.4; 163.3; 193.6; 208.3; 306.1	0.40	116.4–306.1 (ΔT ~ 190)
EcoP	93.4; 171.6; 219.0; 329.2; 433.4; 491.6	0.21	93.4–491.6 (ΔT ~ 398)
CWO	101.3; 329.3; 393.8; 421.6	0.96	329.3–421.6 (ΔT ~ 92)
PCWO	102.9; 331.8; 388.3; 431.5	0.92	331.8–431.5 (ΔT ~ 100)
MP	145.6; 183.3; 236.9; 257.8; 317.3	0.53	145.6–317.3 (ΔT ~ 172)
Tar-PW	98.6; 170.8; 212.0; 267.6; 300.8	0.42	98.6–300.8 (ΔT ~ 202)
Tar-BW	301.5; 343.4; 373.3; 428.3	0.70	301.5–428.3 (ΔT ~ 127)
Tar-Veg	220.8; 337.5; 353.5; 360.6; 370.1; 384.0; 407.0; 422.0; 454.4	0.45	220.8–422.0 (ΔT ~ 201)

The reference, EcoP, and Tar-PW were the only binders that exhibited < 10% mass loss at temperatures below 100°C, which was likely due to evaporation of moisture or low-temperature volatile species. The inflection points at 113.5°C and 150.1°C (CTht) are due to volatilization of lower molecular mass hydrocarbon species. The total mass loss (75.4%) between 150.1–380.4°C is due to volatilisation and decomposition of PAH species. Close to the mesophase-formation temperature, i.e., 380–450°C (Yuan & Cui, 2019), the binder started to phase separate into mesophase and amorphous fractions. The phase separation was a liquid–liquid separation into an emulsion. Solid carbon started forming at 450–500°C during coking. Upon further heating, the binder attained a carbon yield of 10.6%. The average mass loss per temperature change was 0.28%/°C between 70.8–380.4°C, with a total ΔT of 309.6°C and carbon yield of 10.6%. The reference showed the second-lowest average mass loss of the results in Table 4.4. The closest alternative binder to CTht in terms of average mass loss was EcoP, although this had significantly higher carbon yield. The mass loss at temperatures < 100°C was possibly due to species that volatilised at lower temperatures, rather than moisture, because this was a refined fluid.

CWO had the highest mass loss over a small temperature range, with some moisture release close to 100°C. The mesophase-forming pitch (MP) had a higher mass loss over a similar temperature range to the CTPht-B binder.

The pinewood tar binder (Tar-PW) had a higher mass loss over the same temperature range as the reference sample. The vegetable tar (Tar-Veg) lost mass over a wider temperature range than most samples, with a similar mass loss per temperature change to the pinewood tar (Tar-PW). The TGA results demonstrated that the binders that showed thermal properties closest to the reference binder, with reference to application to THC use, were the coal-based alternatives (CTPht-B and EcoP) and, to some extent, MP, and the pinewood tar (Tar-PW). For CTPht-B and EcoP, this is due to the wide range of volatilization temperatures, the low degree of volatilization (close to that of the reference binder), and high carbon yield. Although the volatilization temperature ranges were wide for MP and Tar-PW and their degrees of volatilization low, their carbon yields were also lower.

The average mass losses of the glycerine-based binders are compared with the reference in Figure 4.35. These binders started volatilizing at a lower temperature and had an order-of-magnitude higher average mass loss (1.57–1.79 g/°C) than the reference binder (0.28 g/°C). The temperature range over which the glycerine-containing binders volatilized was 30% smaller (50°C to ~ 230–240°C) than that of the reference binder (70.8–380°C). The wider temperature range of the reference binder can be attributed to the presence of PAH, which have higher molecular mass than the glycerine-containing binders.

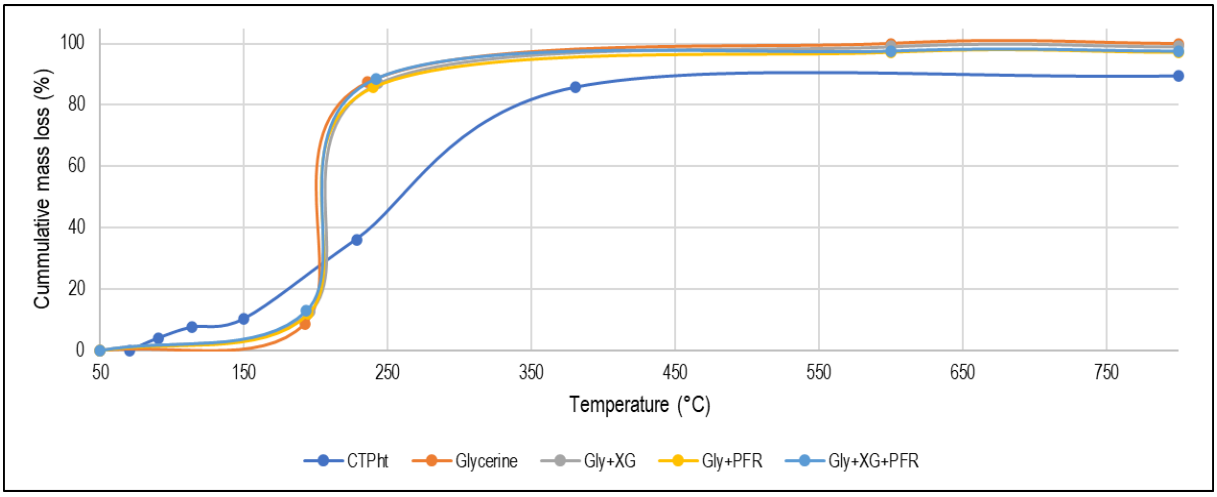

Figure 4.35: Summary the inflection points of the glycerine binders over the specified temperature range

For comparison and purposes of understanding the contributions of XG and PFR resin, the carbon yields of the mixtures were evaluated (Figure 4.36). Addition of the phenolic resin to the glycerine (binder Gly+PFR) increased the carbon yield from zero (pure glycerine) to approximately 2.8%, as expected; addition of phenolic resin to the glycerine-plasticized gum, Gly+XG+PFR, gave a slightly lower carbon yield of 2.5%. These were still considered good results, given that the glycerine alone did not yield any carbon. The contribution of XG to the carbon yield of this binder was not noticeable due to the small quantity of powder that was added to the binder during plasticizing. The carbon yield of the examined resole resin was approximately 80.7%, which is typical of phenolic resins. The carbon yield of polysaccharide biopolymer powders largely depends on their source. As shown in Figure 4.36, the two different XG powders (Sources A and B) differed in carbon yield: Source A had a higher yield of 24.7%. This

XG powder was used in the binders discussed in this study. To achieve a desired carbon yield in a binder, consistency of polysaccharide use is important.

Thermal analysis of XG Source A is given in Appendix A. This confirmed the inflection points and thermal behaviour as recorded in literature, where the thermal decomposition occurs in three stages (Faria et al., 2011; da Silva et al., 2018). The first stage is at 25–100°C, in which ~ 10% of the mass of the powder was lost as moisture; the second stage, at 240–320°C, is due to degradation of the polysaccharide polymer chains as a result of thermal exposure at elevated temperatures (Faria et al., 2011); in the last stage, starting at ~ 600°C, the remaining mass of the sample is converted to carbon.

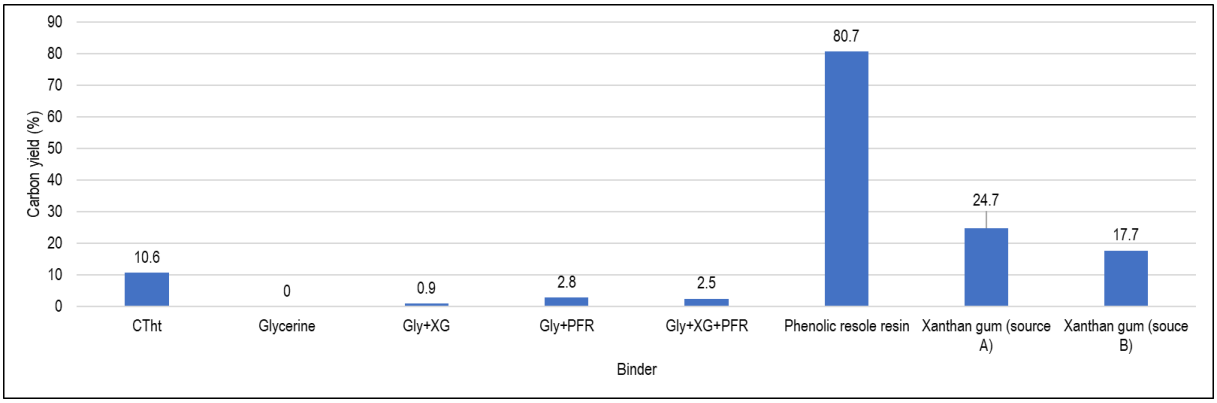

Figure 4.36: Summary of carbon yields of binders on heating to 800°C in nitrogen atmosphere

4.3.2. Differential scanning calorimetry

DSC was used to evaluate the reactions that occur at elevated temperatures in the glycerine-based binders and associated additives (XG and PFR) using the endo- and/or exothermic peaks. Glycerine was used as an extender for the phenolic resole resin when mixed to produce a binder for use in THC. In particular, DSC was used to assess whether mixing of plasticized glycerine (with or without XG) with phenolic resin would alter the gelation temperature of the resin. The gelation and curing processes ensure low-temperature strength development of the clay. Interaction between certain binders and phenolic resole resin can lead to premature gelation, as observed in previous studies (Cameron, 2021). Gelation can also be affected by mixing of the resin with other fluids that can potentially alter its molecular structure and cross-linking during heating. Prior research reported that the combination of glycerol and phenolic resin improved performance by incorporation of the resin into the glycerol molecular structure (Rogers, 2007).

4.3.2.1. Glycerine- and polymer-based binders

Thermal analysis of the glycerine- and polymer-based samples is shown in Figure 4.37. The results for the reference binder are not included because it exhibited no noticeable exothermic peaks and its small endothermic peaks at < 150°C were due to volatilization (Cameron, 2021).

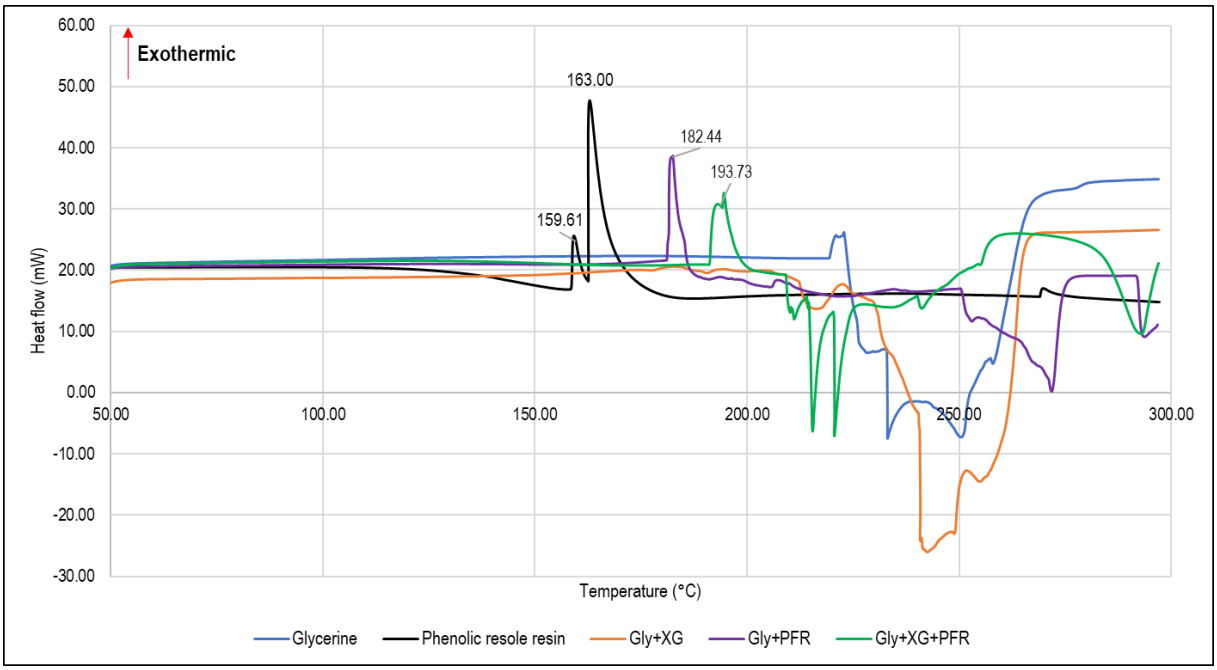

Figure 4.37: Differential scanning calorimetry of binders, showing key endo-and exothermic peaks between 50–300°C

No heat flow was observed in the pure glycerine up to 221°C, after which an endothermic series of peaks was observed, which continued up to 270°C. Considering the TGA results (Figure 4.32), these peaks can be attributed to volatilization of the lower boiling-point hydrocarbon compounds in the binder. The constant heat flow at temperatures below 221°C also indicated that the liquid was refined, so no endothermic peaks occurred due to vaporisation of moisture. The phenolic resole resin exhibited distinct exothermic peaks at 159.6°C. The analysis indicated that heat flow was constant up to 130°C, after which an endothermic reaction started. The exothermic peak at 159.6°C can be attributed to either dehydration condensation of hydrocarbons (further condensation where resin continues to form) or the start of polymerization (Zhang et al., 2016). At 163°C, the resin was completely set due to completion of cross-linking (Zhang et al., 2016). These two processes are well known in phenolic resins and are required to start the curing process. The gelation temperature range and final curing occurred at higher temperatures than shown in prior works in THC (Cameron, 2021), but were still below 200°C. When the phenolic resin was added to glycerine (Gly+PFR), only the peak at 182.4°C attributed to the pure phenolic resin was present. This might be due to the small quantity of resin in the binder, so the first peak may have been too low in intensity to be detected. The peak at 182.4°C is attributed to gelation of the binder because this reaction is generally more exothermic than the final curing. There was a shift in the gelation temperature of this binder system compared with the value of 159.6°C for the phenolic resin alone: mixing of the phenolic resin and glycerine increased the gelation temperature. The second set of endothermic peaks of the Gly+PFR binder occurred at higher temperatures than in the pure glycerine, which means that the resultant molecular structure was more thermally stable and so the volatilization process occurred at higher temperature.

The XG-containing binders were also evaluated (Figure 4.37). Gly+XG had similar thermal behaviour to the pure glycerine. The heat flow of this sample remained constant up to 206°C, above which a small endothermic peak

occurred at 216.5°C. As the sample was further heated, a second broad series of endothermic peaks appeared between 230°C and 270°C. These were similar to those of the pure glycerine, with the first peak occurring at a lower temperature and the second series of broad peaks at a higher temperature.

The Gly+XG+PFR binder exhibited different thermal behaviour to that of the resin and Gly+PFR. The exothermic peak at 193.7°C might be attributed to gelation of the binder system; however, considering the double peaks at 215°C and 220°C, this could correlate with the endothermic peaks of the pure glycerine between 220°C and 270°C, but are more pronounced and occur at lower temperatures. The onset of gelation of this sample occurred almost 30°C higher, at 193.7°C, which is close to the desired resin-curing temperature of 200°C. The Gly+PFR binder had favourable behaviour because curing occurred at a lower temperature than for Gly+XG+PFR and volatilization occurred in a higher temperature range, i.e., 230–270°C.

4.3.2.2. Conclusion

Thermal analysis of the investigated binders revealed distinct behaviour in their heat-flow curves. Pure glycerine exhibited noticeable heat flow up to 221°C, above which an endothermic series of peaks occurred, which can be attributed to volatilization of lower boiling-point compounds in the binder. The constant heat flow below 221°C suggested a refined liquid without moisture-related peaks. The phenolic resole resin showed exothermic peaks at 159.6°C, indicating dehydration condensation or the start of polymerization. Gelation and final curing occurred below 200°C. When phenolic resin was added to the glycerine (Gly+PFR), the gelation temperature increased to 182.4°C, suggesting enhanced thermal stability. XG-containing binders exhibited varied behaviour, with Gly+XG resembling pure glycerine and Gly+XG+PFR displaying a unique DSG curve with gelation onset at 193.7°C. The glycerine- phenolic resin binder demonstrated favourable characteristics, with curing at higher temperatures (close to 200°C) and volatilization in a broader range (230–270°C). This study confirmed the influence of binder composition on the thermal properties, with insight for optimizing binder systems for THC.

4.3.3. Ranking of binders based on thermal behaviour

The high-temperature thermal behaviour of a binder system is a critical feature of THC because the integrity of the clay structure is largely dependent on the volatile behaviour of the binder. This evaluation considered the total volatile release during heating, average mass loss during heating, temperature range over which the mass loss occurred, and carbon yield. These properties depend on the molecular structure and chemical composition of the binder. A liquid binder used in a THC should volatilize over a wide temperature range to ensure fine pore size distribution within the THC matrix, which, in turn, affects the strength and corrosion-resistance properties of the clay. Carbon yield is important for high-temperature strength development. The carbon yield is contributed by both the binder and the phenolic resin used in the THC. For these reasons, ranking of the binders first considered the average mass loss and then the temperature range over which the mass loss occurred. In cases where these values were in the same range, the carbon yield was used as the deciding factor.

According to this ranking (Table 4.5), EcoP was the most suitable alternative binder due to its low average mass loss, wide volatilization temperature range, and high carbon yield. Pinewood tar (Tar-PW) was ranked second, with a slightly higher average mass loss but wider volatilization temperature range. Tar-Veg was ranked lower than CTPht-B, despite their relatively similar average mass losses and volatilization temperature ranges. The carbon yield of CTPht-B was considerably higher than that of Tar-Veg, so this ranked in a higher position. The MP binder was still considered favourable, despite having a higher average mass loss and narrower volatilization temperature range. The beechwood tar and the waxy oils, were considered least favourable due to their high average mass loss within a narrow temperature range. The glycerine-based binder was placed in last position because it had the highest average mass loss, narrowest volatilization temperature range, and low carbon yield.

Table 4.5: Ranking of alternative binders to CTht based on high-temperature behaviour

Rank	Sample	Average mass loss per temperature change (g/°C)	Temperature range (°C) (ΔT, °C)	Carbon yield (%)
1	EcoP	0.21	93.4–491.6 (ΔT ~ 398)	30.2
2	Tar-PW	0.42	98.6–300.8 (ΔT ~ 202)	5.8
3	CTPht-B	0.40	116.4–306.1 (ΔT ~ 190)	22.1
4	Tar-Veg	0.45	220.8–422.0 (ΔT ~ 201)	2.7
5	MP	0.53	145.6–317.3 (ΔT ~ 172)	5.2
6	Tar-BW	0.70	301.5–428.3 (ΔT ~ 127)	0.7
7	PCWO	0.91	331.8–431.5 (ΔT ~ 100)	2.7
8	CWO	0.96	329.3–421.6 (ΔT ~ 92)	4.9
9	Gly+PFR	1.8	175.0–240.0 (ΔT ~ 65)	2.8

4.4. Rheology

Rheological properties of the reference binder (CTht) were characterized according to flow properties (Newtonian behaviour) and thermal stability (temperature up to 150°C as a function of viscosity), and the WAT was determined for the waxy binders. The alternative binders were similarly evaluated and compared with the reference binder.

4.4.1. Coal-, petroleum-, and wood/vegetable-based binders

Results of the isothermal rotational test (Newtonian behaviour) at 45°C of the binders are shown in Figure 4.38. This test temperature is generally the mixing temperature of the THC for optimal binder usage and distribution of binder phase throughout the clay matrix. All binders exhibited Newtonian behaviour, except for CWO. The enhanced shear-thinning at lower shear rate was probably due to higher residual moisture content in this binder because this was an unrefined version of the waxy oil. Water in the emulsion, likely in the form of droplets, was deformed or coalesced. The reference binder had an initial dynamic viscosity of 0.40 Pa.s, which remained constant with an increase in shear rate. Newtonian behaviour, such as that of the reference binder, was exhibited by the vegetable tar (Tar-Veg), the pinewood tar (Tar-PW), and the low softening-point pitch blend (CTPht-B). The latter two had a lower viscosity than CTht. The other binders all had higher viscosity than the reference binder. EcoP and PCWO were the closest alternatives that could still be used in the clay. The beechwood tar (Tar-BW) and mesophase-forming pitch (MP) had the highest viscosities of the alternative binders. Rheological behaviour of the binders is related to their molecular composition: higher average molecular mass binders showed higher viscosity (assuming similar types of molecules in the sample), while larger molecules resulted in increased inter- and intra-compound interactions, which increased the force needed to overcome internal resistance and initiate flow of the fluid (Ciesinska, 2017).

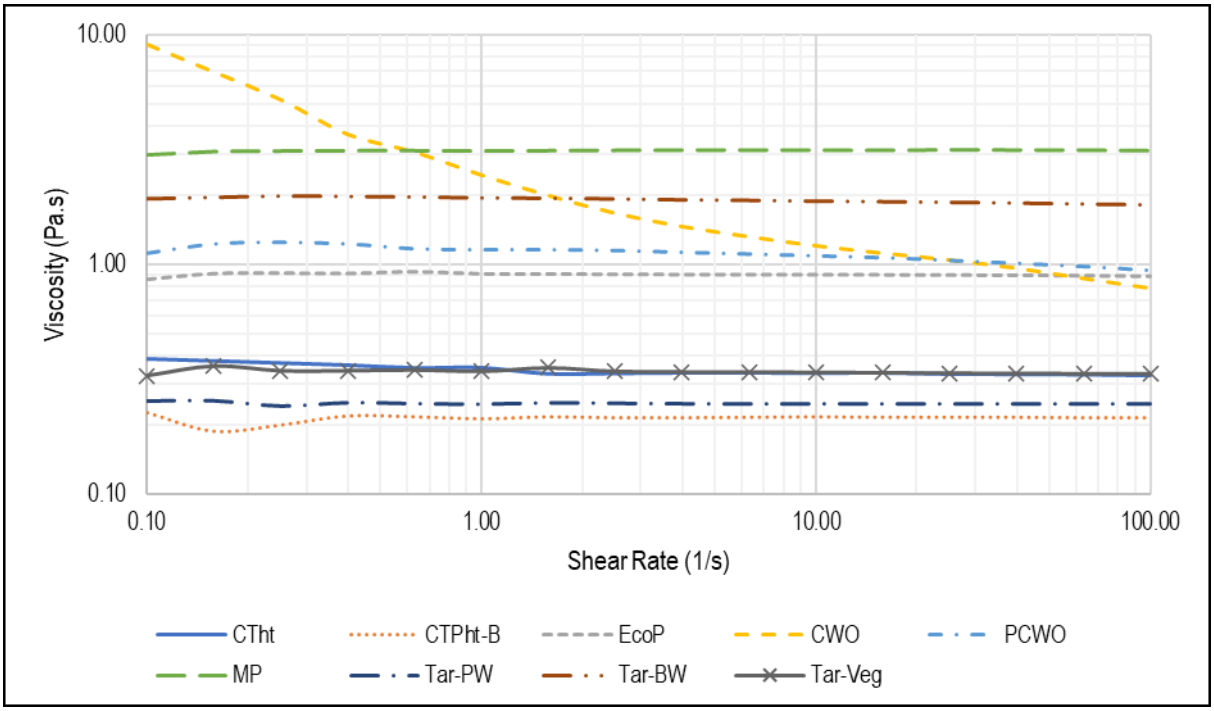

Figure 4.38: Isothermal frequency sweep (45°C) to determine Newtonian behaviour of the binders

Thermal stability of the binders, as depicted by a change in dynamic viscosity (threshold to overcome internal friction) as the temperature increased, is shown in Figure 4.39. The results shown in Figures 4.38 and 4.39 are inconsistent due to variations in the nature of the samples and the sampling process. The results were therefore solely used to observe trends and for comparison between samples. Thermal stability of a binder is described as

the tendency for the fluid to approach a viscosity limit (plateau) and how easily this happens with an increase in temperature. For CTht, CTPht-B, and EcoP, the decrease in viscosity occurred over a wide temperature range. Viscosity of CTht decreased up to 80°C, after which it showed a sudden increase at 80–93°C, and then decreased again with further heating. As the temperature increased (> 93°C), the viscosity remained constant up to 150°C. The sudden increase in viscosity between 80–93°C could be due to rapid volatilization, probably due to lower-temperature volatiles, that affected the manner in which the rheometer measured viscosity. TGA results for this binder (Figure 4.23) indicated a mass loss at 70–90°C, which is a probable cause for the increase in viscosity between 80–93°C. CTPht-B had an initial viscosity of 0.78 Pa.s (lower than that of the reference sample) and showed a similar reduction in viscosity as the temperature increased. The viscosity decreased up to 90°C, after which it remained constant up to 140°C.

EcoP had the highest initial viscosity of the coal-based binders and the degree of change in dynamic viscosity between the starting and final viscosity at 150°C was lower than the reference and CTPht-B binders. The higher viscosity indicated that the binder had a larger attractive binding energy between the molecules in its structure.

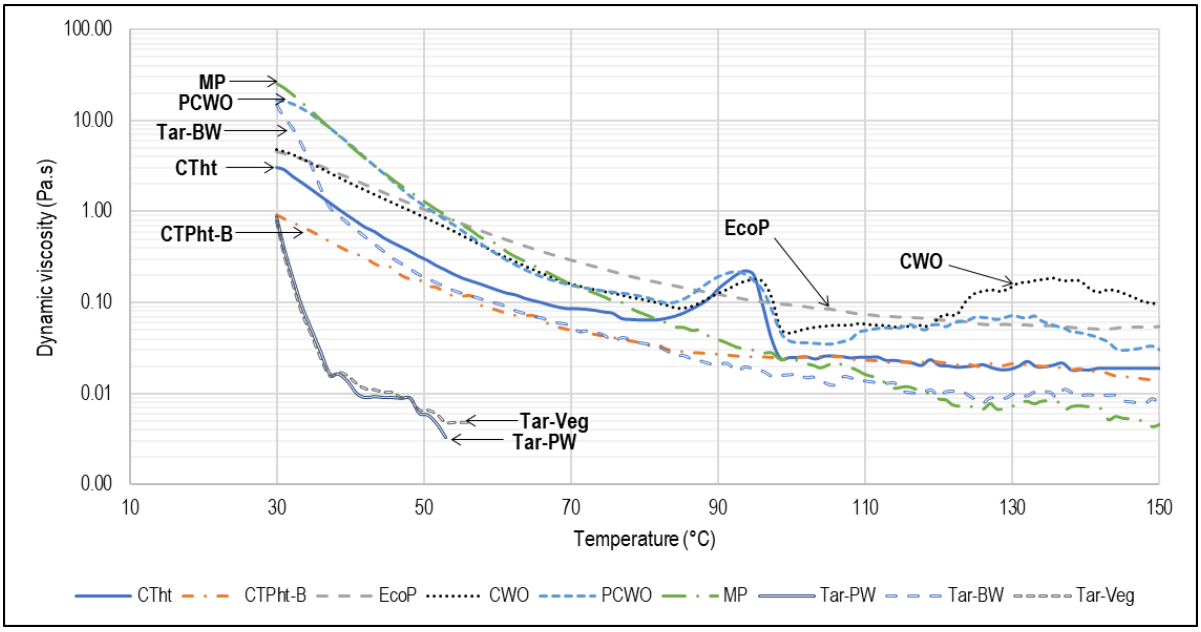

Figure 4.39: Temperature-sweep results between 30–150°C for the binders and influence of change in temperature on dynamic viscosity

The petroleum-based waxy oils (CWO and PCWO) exhibited similar behaviour to the reference sample (Figure 4.39). Both binders showed a reduction in viscosity up to 85°C, with a small increase at 85–96°C, which, for CWO, is attributed to the release of lower-temperature volatiles, including moisture. The increase in viscosity over this temperature range may similarly be due to erratic measurements caused by mass loss. The mesophase-forming pitch (MP) experienced a higher reduction in viscosity and viscosity continued to decrease with an increase in temperature. The thermal stability of this binder was not comparable with that of the reference binder and was lower than those of the aforementioned alternative binders.

The pinewood-based binder exhibited lower viscosity and thermal stability than all other samples. The pinewood tar had an initial viscosity of 0.78 Pa.s, which reduced significantly as the temperature increased up to 35°C. The viscosity decrease slowed down above 35°C (Figure 4.39). The same behaviour was observed for the vegetable tar (Tar-Veg), where the initial viscosity and reduction in viscosity with temperature were similar. These two binders reached considerably lower viscosities, after which no further data could be collected owing to reaching the low-torque region that limited the equipment. The beechwood tar (Tar-BW) binder had an initial viscosity of 15.1 Pa.s, which decreased significantly up to 38°C and then continued to decrease with further increase in temperature. The sample exhibited reduced internal friction up to ~ 110°C and the viscosity remained constant up to 150°C. The Tar-BW binder showed better thermal variability than the other two samples due to its higher molecular mass, demonstrated by the plateau in viscosity up to 150°C. Thermal stability of Tar-BW was comparable with that of the reference sample (CTht).

The waxy oils were heated and then slowly cooled (5°C/min) to determine the WAT temperature (Figure 4.40) (Theyab & Diaz, 2016). Precipitation of wax crystals can cause a sudden increase in viscosity, which, in a THC, affect the extrusion pressure and plastic behaviour. CWO and PCWO had similar WAT of 58–65°C. Precipitation of paraffin crystals started at 65°C (liquidus temperature) and melting (with a reduction in viscosity) occurred at 55°C (solidus temperature). The viscosity measurements for WAT were only indicative of order-of-magnitude changes within a narrow temperature range (~ 5°C). The variability in dynamic viscosity with temperature (Figure 4.40) could be due to sampling errors (not using a composite sample of various lots) or change in homogeneity owing to factors such as impurities (particulate, chemical, moisture) that could influence the sample as it aged.

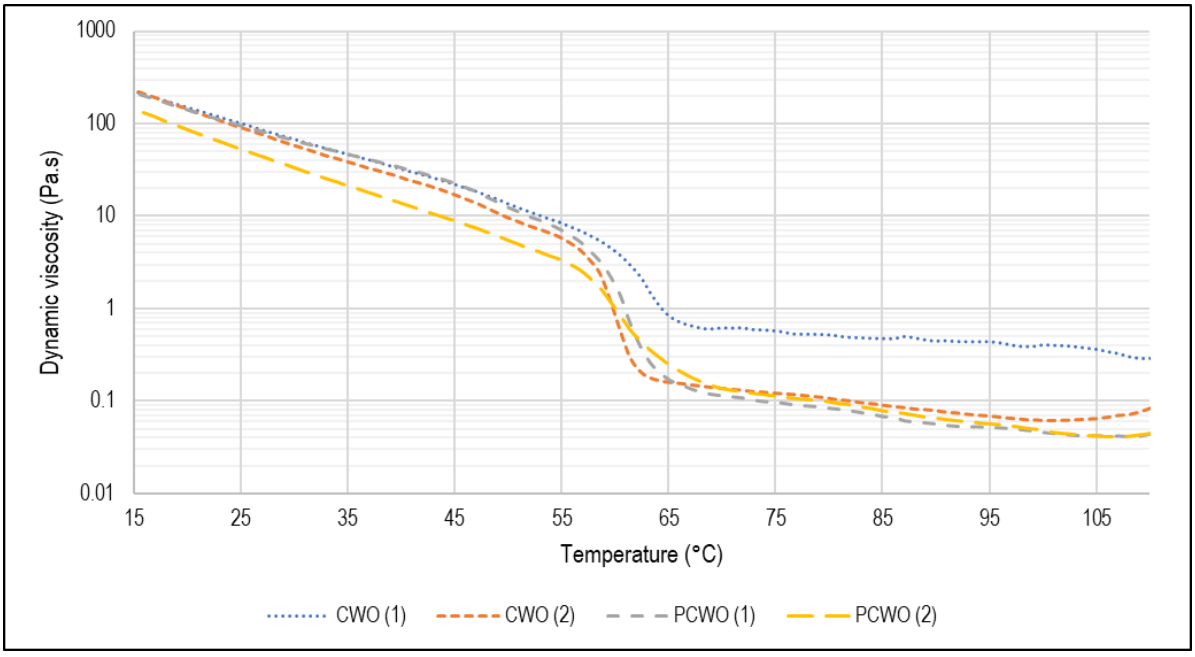

Figure 4.40: Waxy-appearance temperatures of CWO and PCWO between 15–110°C and influence on dynamic viscosity

4.4.2. Glycerine and polymer-based binders

Flow characteristics of the glycerine-based binders were examined by considering the effect of temperature and shear on the flow behaviour relative to the reference binder (CTht). The rheological features evaluated were the Newtonian behaviour of THC at a mixing temperature of 45°C and thermal stability of the binder between 30°C and 150°C, i.e., up to the general gelation-onset temperature region for resole resins.

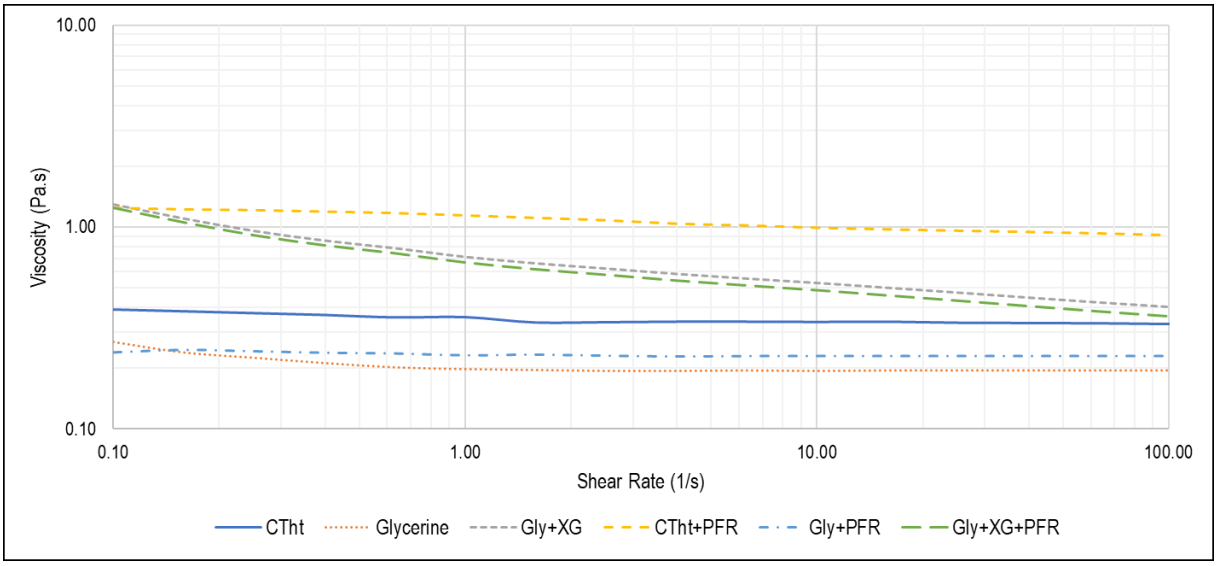

Figure 4.41: Isothermal shear rate (45°C) to determine Newtonian behaviour of the non-toxic binders

Changes in dynamic viscosity with an increase in shear rate, i.e., Newtonian behaviour, of the glycerine mixtures are shown in Figure 4.41. The pure glycerine binder exhibited some shear-thinning at low shear rates of 0.1 to 1.0 s^{-1} (Figure 4.41). At shear rates above 1 s^{-1}, the binder exhibited Newtonian behaviour throughout the frequency range. The initial viscosity was 0.27 Pa.s, then lowered to 0.19 Pa.s, after which it remained constant. The increased shear rate did not alter the molecular structure. The glycerine had a lower viscosity than that of the reference sample (difference of 0.15 Pa.s). A lower viscosity would assist with reducing the quantity of binder required for manufacturing of a clay and also improved its aging; however, if the viscosity is too low and coupled with lower viscoelasticity, it would be unfavourable for use in THC due to reduced plastic behaviour of the clay and associated process difficulties. The lower viscosity and Newtonian behaviour of the glycerine would ensure that the extrusion pressure is low, which would improve extrusion efficiency of the clay.

The initial viscosity of the Gly+XG binder was 1.25 Pa.s, which is an order of magnitude higher than the reference binder (CTht). The binder showed non-Newtonian, shear-thinning behaviour. The plasticizer was incorporated into the molecular structure of the biopolymer by disrupting the strong hydrogen bonding, thereby creating a structure that is not as resistant to deformation as the reference sample (CTht) and pure glycerine. A higher viscosity of the binder and shear-thinning behaviour (de Pretto & Lindstad, 2022) can assist with improved extrusion rate of the clay in the mud gun because the viscosity at higher shear rates was of the same order of magnitude as those of the reference and Gly+XG binders.

CTht+PFR contained a mixture of reference binder (CTht) and phenolic resole resin. The phenolic resin imparted a noticeable increase in viscosity of CTht, from 0.40 Pa.s to 1.25 Pa.s. This is a similar order of magnitude to that observed for the Gly+XG binder. Addition of the phenolic resin contributed to an increase in viscosity of the binder and resulted in non-Newtonian shear-thinning behaviour of the mixture. With an increase in shear rate, some weakening of the molecular structure was observed by the lowering in viscosity, i.e., a change in viscosity from 1.25 Pa. to 0.90 Pa.s from low to high shear rate. This mixture of CTht and phenolic resin is currently being used as a THC binder.

The mixture of PFR and pure glycerine (Gly+PFR) was an exact substitution of CTht with glycerine to evaluate the effect on viscosity, Newtonian behaviour, and thermal stability. The glycerine–resole resin mixture had an initial viscosity of 0.30 Pa.s and exhibited Newtonian behaviour throughout the deformation range. The Newtonian behaviour shown by this mixture, compared with CTht+PFR, can be attributed to polar–polar compounds in the mixtures. Glycerine (Figure 4.10) and PFR (Figure 4.12) have –O–H functional groups, which make them polar: a mixture of these compounds could exhibit possible weak intermolecular forces (van der Waals forces, rather than strong hydrogen bonding), which would result in more uniform distribution of shear forces. The pure glycerine showed an increase in viscosity from 0.20 to 0.30 Pa.s at higher shear rates. This was, however, lower than the comparative sample, CTht+PFR, which had a viscosity of ~ 1.1 Pa.s at the same shear rates. Although Gly+PFR exhibited Newtonian behaviour, the viscosity of this binder remained low, which would have a similar effect than a binder with a high viscosity and shear-thinning behaviour, on the extrusion rate of the clay.

Considering the XG-plasticized glycerine–resole mixture (Gly+XG+PFR), the addition of PFR did not noticeably change the Newtonian behaviour. The initial viscosity was similar to that of the reference, and it also exhibited non-Newtonian behaviour. This mixture achieved a viscosity in the range between those of the reference and phenolic resin-containing reference binders, which are commonly used in THC.

Mixing of a binder with phenolic resin can be problematic because it can cause either an excessive increase in the viscosity or alter the Newtonian behaviour with aging (Cameron, 2021). To evaluate the thermal stability of the molecular structures of the mixtures with time, the Newtonian behaviours of the binders were evaluated at Day 1 (directly after mixing; same samples as shown in Figure 4.42), and after 7, 14, and 21 d of aging. The results of the aging tests are shown in Appendix B, Figures B10–B12. The binder mixtures all showed consistent results on aging: there was only minor changes in the viscosities of the Gly+XG and Gly+PFR samples. There were no detectable changes in the molecular structure with time that could be attributed to reaction of the phenolic resin with either XG or glycerine.

Dynamic viscosity was also evaluated as a function of temperature, i.e., thermal stability of the molecular structure of the binders/mixtures. The samples were heated from 30°C to 150°C at a heating rate of 5°C/min (Figure 4.42). Glycerine had a lower initial viscosity than the reference binder (CTht), as highlighted in Figure 4.42. As the temperature increased, the viscosity decreased up to ~ 85°C then started to plateau (reduced by more than an order of magnitude). The viscosity then increased from 85°C to 150°C. This was attributed to volatilization of the

sample, which caused an erratic instrument reading above 100°C, as shown in Figure 4.42. Gly+XG had a higher initial viscosity at 2.44 Pa.s than pure glycerine due to the plasticizing nature of the polysaccharide. The viscosity reduced up to ~ 114°C, after which it reached a plateau. The viscosity reduced by more than an order of magnitude. The glycerine-plasticized XG showed similar thermal stability but lower reduction in viscosity in the initial heating stages compared with the reference binder. The non-Newtonian, shear-thinning behaviour of this binder and its thermal stability over this temperature range made it more favourable as an alternative binder than pure glycerine.

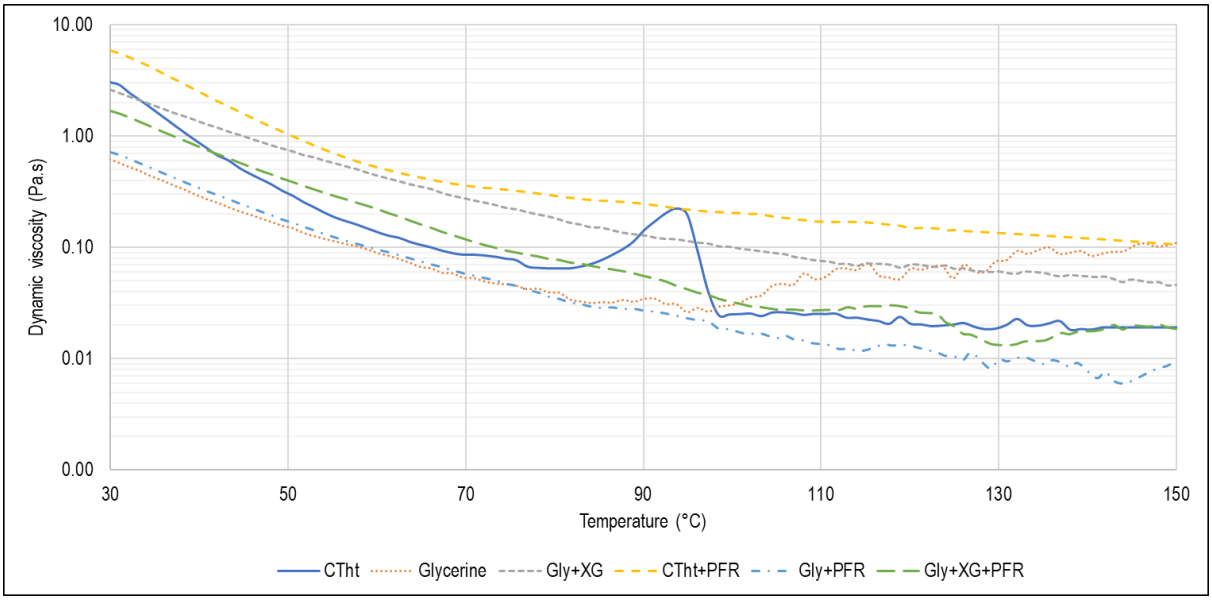

Figure 4.42: Influence of change in temperature from 30°C to 150°C on dynamic viscosity of glycerine-based binders

The CTht+PFR binder had a higher initial viscosity than the CTht binder, with no indication of onset of curing of the phenolic resole resin (gelation temperature for this resin is usually 160–200°C). This was confirmed by the DSC results (Figure 4.37), which indicated that gelation started at 159.61°C. Viscosity of the mixture reduced as the temperature increased from 30°C to 65°C. Above 65°C, an inflection was reached, which demonstrated good thermal stability of the binder because the viscosity slowly decreased even at higher temperatures. The change in dynamic viscosity of this binder (CTht+PFR) compared with the binder that did not contain phenolic resin (CTht) was lower by an order of magnitude. Addition of the phenolic resin to glycerine resulted in an increase in viscosity (higher molecular mass structure), but the product had lower thermal stability (weak bonding strength of the resultant structure). Although this mixture maintained its Newtonian behaviour over the deformation range, subjecting the same molecular structure to a thermal stimulus yielded a less stable result than the mixture that is used in THC (CTht+PFR).

The Gly+XG+PFR binder had lower initial viscosity than Gly+XG (Figure 4.42). Thermal stability of this binder was better maintained over this heating range compared with that of Gly+PFR. Addition of the phenolic resin altered the molecular structure of Gly+XG, but it retained thermal stability compared with the other glycerine-based binders. The decrease in viscosity was an order of magnitude lower. The viscosity range in which this binder showed stability

was close to that of the reference binder. Results for the effect of aging on the binder thermal stability are shown in Appendix B, Figures B13–B15. All glycerine-based binders were thermally stable, and their structures did not noticeably alter with time.

4.4.3. Conclusion

The rheology properties evaluated were flow behaviour and thermal stability; WAT was determined for the petroleum-based waxy oil binders. The results indicated that the reference binder (CTht) had Newtonian behaviour and exhibited good thermal stability between 30°C and 150°C. The alternative binders showed a combination of Newtonian and non-Newtonian shear-thinning behaviour: those from coal-based sources (EcoP, CTPht-B), petroleum-based sources (PCWO, MP), and wood/vegetable-based binders (Tar-BW, Tar-PW, Tar-Veg) exhibited Newtonian behaviour; the crude waxy oil showed non-Newtonian shear-thinning behaviour; all glycerine-based binders showed shear-thinning behaviour. WAT of the waxy oil binders (CWO, PCWO) were 58–65°C.

The coal-based binders had good thermal stability compared with the reference binder. CWO and PCWO showed comparable thermal stability. The MP and Tar-BW binders had lower thermal stability above 85°C. Tar-PW and Tar-Veg had limited thermal stability up to 50°C, confirming that these two binders are not good candidates for use in THC. The glycerine-based binders showed good thermal stability, comparable with the reference binder, except for Gly+PFR: thermal stability of this binder was lower and comparable with MP and Tar-BW.

The binder properties considered important for THC include flow behaviour that results in a solid rammable mass after mixing (high viscosity), low extrusion pressure during ramming (shear-thinning), and maintenance of the rammable shape during heating (thermal stability) up to the cross-linking temperature of the resin (if resin-containing) to develop low-temperature strength in the tapping channel. From the first set of binders, the most suitable replacements for CTht are the CWO and Tar-BW coal-based binders; from the glycerine-based binders, the most suitable are pure glycerine, Gly+XG (if no resin is used), and Gly+XG+PFR (if resin is used).

4.4.4. Ranking of binders based on rheology

Rheological requirements of a binder system for THC include: 1) allowance for continuous flow of the clay with minimal variability in extrusion pressure and ability to maintain a low extrusion pressure; 2) formation of a homogeneous mixture (not an emulsion that will separate during aging) when strengthening agents, such as phenolic resin, are added; 3) maintenance of molecular structure when heated. THC exhibits shear-thinning behaviour during extrusion (de Pretto & Lindstad, 2022) due to aggregate in the material that rearranges to orient with the flow. Any non-Newtonian behaviour will favour both the extrusion and quantity of binder used for mixing of the clay during production. Non-Newtonian shear-thinning behaviour of binders is favourable if the viscosity is high, because this requires a lower extrusion pressure. In the case of THC, an increase in workability results in a decrease in extrusion pressure, and vice versa (Cameron, 2021). An increase in binder viscosity during aging reduces workability and consequently increases extrusion pressure; therefore, binders with high viscosities will

require higher extrusion pressures (Cameron, 2021). This can be alleviated by using a low-viscosity, non-Newtonian, shear-thinning liquid to assist with increased flow during extrusion.

The binders were ranked based on the rheology results (Table 4.6) according to their thermal stability and Newtonian behaviour. Thermal stability is a critical property and was considered in preference to Newtonian behaviour, where shear-thinning was favoured. In cases where thermal stability was limited or close in comparison, the Newtonian behaviour (shear-thinning) was used as a determining factor. Ranking of the glycerine-based innovative binders was determined with regards first to gelation temperature (DSC) and then rheological thermal stability. These properties are equally important for maintaining the shape of the clay sample and enabling adequate strength development at temperatures < 300°C. A secondary property, the Newtonian behaviour, was used in cases where behaviours were similar. Gly+XG+PFR was not selected for ranking because the shift in the first exothermic peak (Figure 4.37) of this binder to 193.73°C compared with that of the pure resole resin (159.61°C) signified the onset of gelation. Gly+XG could be a suitable binder for operations that do not require resole resin for low-temperature strength development, but this binder was also not ranked because the application of this study required a phenolic resole resin.

EcoP had iso-viscous and thermally predictable behaviour, followed by CTPht-B, due to its smaller decrease in viscosity with temperature. Gly+PFR was ranked above CWO due to its lower decrease in viscosity between 30°C and 150°C, which signified higher thermal stability. CWO showed better thermal stability and shear-thinning behaviour than its processed version, PCWO. PCWO was ranked lower due to its high initial viscosity that would make it more difficult to extrude than CWO, which has some shear-thinning behaviour. Tar-BW and MP were ranked in 4th and 5th positions (above PCWO), respectively: Tar-BW had a lower viscosity and would result in a lower extrusion pressure. Tar-PW and Tar-Veg were placed in the last two positions because of their limited thermal stability. These binders, according to rheology measurements, were disqualified as potential replacements for the CTht reference binder in THC.

Table 4.6: Ranking of alternative binders based on rheology results

Rank position	Sample
1	EcoP
2	CTPht-B
3	CWO
4	Gly+PFR
5	Tar-BW
6	MP
7	PCWO
8	Tar-PW
9	Tar-Veg

4.5. Overall ranking of alternative binders

Individual rankings of the examined binders, based on molecular composition, thermal analysis, and rheology, as well as the overall ranking, are summarised in Table 4.7. The criterion for determining the overall ranking was a combination of the lowest total PAH value, good dynamic viscosity (preferably non-Newtonian, shear-thinning), and thermal stability suitable for manufacturing and green-strength development, compared with the CTht reference binder. To select the most suitable binder replacement, a contribution calculation (C_1) was carried out using the sum of products in Equation 4.2:

$$C_1 = \sum S_n n_n, \tag{4.2}$$

where S_n is the significance coefficient according to the most critical features required from the binder and n_n is the massed coefficient based on the ranking position. For total PAH and rheology, the significance coefficient (S_n) was 2, because both are considered equally important for the purpose of this study; the high-temperature thermal analysis (TGA) was denoted with an S_n value of 1. The massed coefficients are only based on their position in the ranking, i.e., if a binder ranked in the first position of a group, then the S value was multiplied by 0.9. The calculated contribution (C_1) is the sum of all the products ($S_n n_n$).

Table 4.7: Overall ranking of alternative binders based on molecular structure, thermal analysis, and rheology

Rank	Molecular composition (total PAH) $S_1 = 2$	Thermal analysis (volatilization) $S_2 = 1$	Rheology (viscosity & thermal stability) $S_3 = 2$	Overall rank	
				C_1	Binder
1* (n_1 = 0.9)	Gly+PFR	EcoP	EcoP	3.1	EcoP, Gly+PFR
2 (n_2 = 0.8)	Tar-BW	Tar-PW	CTPht-B	3.0	Tar-BW
3 (n_3 = 0.7)	Tar-PW	CTPht-B	CWO	2.5	CTPht-B
4 (n_4 = 0.6)	PCWO	Tar-Veg	Gly+PFR	2.4	CWO
5 (n_5 = 0.5)	Tar-Veg	MP	Tar-BW	2.1	PCWO
6 (n_6 = 0.4)	CWO	Tar-BW	MP	1.9	MP
7 (n_7 = 0.3)	MP	PCWO	PCWO	-	Tar-PW
8 (n_8 = 0.2)	EcoP	CWO	Tar-PW	-	Tar-Veg
9** (n_9 = 0.1)	CTPht-B	Gly+PFR	Tar-Veg	-	-

Based on the ranking from the three groups, i.e., molecular composition, structure, and toxicity (PAH content), thermal analysis, and rheology, as shown in Table 4.7, the most favourable binders according to this investigation are the low-PAH pitch (EcoP) and glycerine–resole resin mixture (Gly+PFR). The bio-based binder, Tar-BW was ranked second. Tar-PW and Tar-Veg were ranked lowest; although these binders had C_1 values of 2.6 and 1.8, respectively, they were ranked last due to their failure to maintain thermal stability (rheology). This is a critical property for use in THC, because low viscosity would not only impede clay flow and compromise the integrity of the clay, but also cause the clay to lose shape during extrusion. The coal-based binder (CTPht-B) was placed third, primarily because of its high total PAH. Coal-based binders, including EcoP, are conventionally used, but present the well-known dilemma (Table 4.1) that their high carbon yield, wide volatilization temperature, rheology (viscoelasticity), and thermal stability make them excellent binders for use in THC; however, they have the disadvantage of high total PAH content, which is the reason for their high carbon yield and good rheological characteristics. Industrial use of CTPht-B can be justified due to its excellent thermal and rheological characteristics; however, the aim of this study was to identify suitable non-toxic (zero 16-EPA-PAH) or lower-toxicity binders as alternatives to conventional CTht. When compared with other alternatives, such as the petroleum-based fluids, EcoP and CTPht-B are considered less favourable.

The highest-ranked petroleum-based binder in Table 4.7 was CWO in fourth position. MP and PCWO are ranked lower than the coal-based binders. This decision was taken by first examining which of the petroleum-based binders consistently received a higher ranking. The crude wax oil (CWO) consistently ranked higher than the mesophase-forming pitch and PCWO because it has a lower total PAH than the MP and is a more shear-thinning liquid than PCWO. Similarly, the thermal analysis performance and rheology of PCWO allowed it to rank higher than MP.

Considering the top three non-toxic alternative binders to CTht were Gly+PFR, Tar-BW, and CWO. Although EcoP is a refined version of normal CTP, the objective of this study was to investigate the best-suited non-toxic binders (zero 16-EPA-PAH) or the closest possible replacements for conventional CTht. These three non-toxic binders derived from this selection process all have low carbon yields, which, when considering the function of a binder, lack the property of having residual solid material (generally carbon) after heating at high temperature. However, these non-toxic liquid binders can be used with a phenolic resin (Hiroaki, 1982), such as resole, which has a significantly higher carbon yield (Borrego et al., 2022). This type of resin is one of the main reasons for binder strength when used in THC. The liquid (without resole) serves as a binding agent up to the polymerization temperature of the resin (~ 200°C), after which polymerization of the resin provides low-temperature strength for the clay, which is maintained up to the sintering temperature of the ceramic components in the THC. Various ratios of phenolic resin to liquid binder can be implemented to ensure that modification of a high-carbonizing liquid binder, such as CTht, to a lower-carbonization liquid binder, such as Tar-BW and CWO, will attain the same low-temperature strength of the resulting THC.

Chapter 5

Evaluation of taphole clays with alternative binders

"There is value in doing things that scare you " ~ Roald Dahl

5. Evaluation of taphole clays that contain CTht and alternative binders

5.1. Introduction

Proposed alternative binders to CTht for use in THC materials were evaluated in Chapter 4. The most favourable alternatives of the coal-, petroleum-, wood/vegetable-based and glycerine-based binders were identified as CWO, Tar-BW, and Gly+PFR. This chapter examines processabilities of clays using these identified alternative binders. The use of pure glycerine and CWO in mixtures with phenolic resole resin for use in a THC formulation is also discussed in this chapter. Changes that occurred in the process parameters and clay properties were monitored and reported. CTht was mixed in the same formulation (Section 3.2) and tested as the reference sample for comparison with the two alternative binders. For explanation purposes, the designations are Gly+PFR for glycerine mixed with phenolic resin, CWO+PFR for CWO mixed with phenolic resin, and CTht mixed with phenolic resin as in Chapter 4.

5.2 Mixing tests

The three binders chosen for evaluation (CWO, Tar-BW and glycerine) were first evaluated in terms of their mixing properties according to the method described in Section 3.1.2. Initial THC mixing tests showed that Tar-BW was extremely problematic to use: the mixture did not form a clay mass, but a viscous layer on the inside of the mixer bowl. This was attributed to its ketone/ester structure, because C=O carbonyl and C–O–O–R ester functional groups identified through FTIR that increase the adhesive properties (stickiness) of a binder (Lu et al., 2020; Hussein et al., 2020). Mixing of the clay using CWO as binder did not show the same behaviour, but formed a solid clay mass that could be moulded. The CWO binder did not contain any oxygenated functional groups, so showed reduced adhesion compared with Tar-BW. According to the literature the oxygen content of wood-based binders is much higher than that of petroleum or coal alternatives (Lu et al., 2020; Hussein et al., 2020), which influences adhesion of the binder during mixing. Possible working alteration of Tar-BW could be obtained by mixing with a compound that has a lower content of hydroxyl (O–H) or carboxyl (HO–C=O) groups, whereby the overall polarity can be reduced, and adhesion lowered. The aim of this investigation was to evaluate direct substitution of CTht with the alternatives evaluated, so CWO was directly substituted in the clay formulation. This resulted in similar mixing and aging practices to those of conventional THC mixing. CWO has a lubricating nature because it is paraffinic in nature, which also assists with processability of the clay.

5.3 Non-standardised tests

Specific requirements for clays for different smelting operations need to be considered. The performance indicators include workability of the clay, strength development, holding time, casting duration, quantity of clay used per ramming, and taphole length. A PGM smelting operation was selected for the comparison of alternative binders in THC: the associated performance requirements for this smelter were used as the baseline.

Non-standardized tests were used to assess the suitability of the clays produced from these binders for application in a THC. These included:

- Workability aging test,
- MEP aging test,
- Workability thermal aging test (hardenability),
- MEP thermal aging test (hardenability),
- Strength-development test,
- Volatilization profile of the material up to 200°C.

Standard high-temperature tests were conducted on pre-fired samples that were heated under reducing conditions at 800°C for a specified time. These tests included:

- CCS,
- VOC,
- AP,
- Carbon yield/retained carbon.

Each test assessed the performance indicators and desired behaviour of the clay that are required for successful usage.

The workability and MEP aging tests evaluated the change in plasticity and required extrusion pressure (mud gun) of the clay with time. THC is considered a consumable refractory product and is not generally aged for longer than 30 d. These tests simulated the period from when the clay is placed inside the mud gun and heated at the barrel temperature (20–30°C) for an extended period. This simulates the heating and cooling cycles of the clay in the gun because it is used during every ramming turn to close the taphole. THC practices involve filling the mud gun to full capacity and ramming until the barrel is empty before adding new clay. The practice of filling the mud gun to capacity is to ensure excess clay availability in case of non-closure of tap hole. The mud gun barrel is also exposed to elevated temperature cycling (heat radiation from tapping launder to the mud gun barrel during ramming) during which the inside temperature of the barrel may exceed 45°C (maximum specific temperature for the phenolic resin). This can cause volatilization of the clay; more specifically, low-temperature volatiles in the binder. Using a full mud gun for extended heating cycles increases the extrusion pressure and lowers the plasticity of the clay (Cameron, 2021). The thermal aging tests simulates this scenario and evaluates changes in clay properties after heating for an extended period.

The SDP simulates the increase in green strength of the clay as it is heated up to 200°C, at which temperature the phenolic resin is responsible for imparting green strength to the clay, and then up to the sintering temperature of the ceramic oxide aggregates. The SDP provides a guide to whether the clay is achieving the desired strength to maintain the specified holding time and efficient drilling practices. The degree of volatilization of the samples used for the SDP test is correlated with volatilization of the resin in the binder. SDP data can also be used to explain high-temperature strength properties of the clay, such as CCS and AP after firing.

5.3.1. Taphole clay workability aging

Workability (plasticity) of the THC was measured by evaluating the percentage change in height of a cylindrical sample that was compacted using a sand rammer and allowed to deform under unconstrained conditions. The workability results of the three clay samples that contained the reference binder (CTht) and alternative two binders (glycerine and CWO) are shown in Figure 5.1 (values for workability and MEP are average of three samples per clay variant). The workability specification for the mud gun used in the selected PGM operation as communicated through technical interactions with Anglo American Platinum is 38–45%. The liquid additions of CWO and glycerine were 13.8 mass% and 13.5 mass%, respectively (Table 3.1). The specification was used as a guide to ensure that the workability of the clay was maintained above this value. Extrusion pressure increases with reduced workability (plasticity) (Cameron, 2021), which limits operation of the mud gun. The barrel temperature for this specific furnace operation is 20–25°C, so a temperature of 22.5°C was selected for the workability and MEP aging tests.

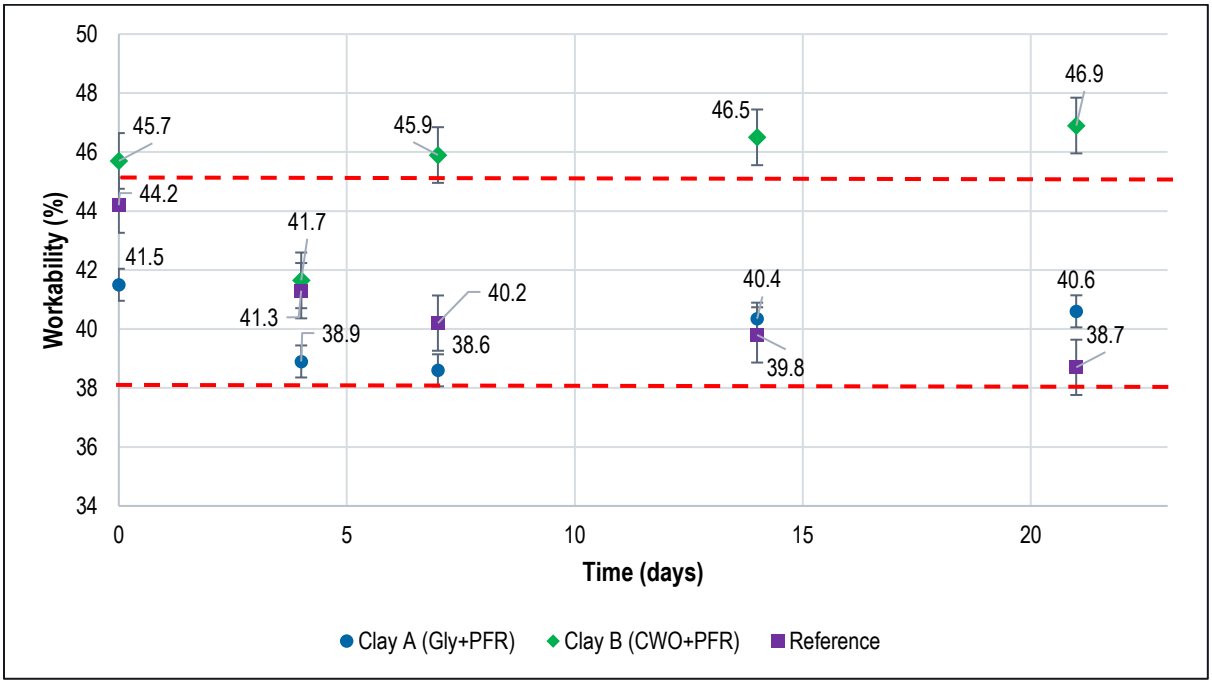

Figure 5.1: Workability aging test results from clay samples with alternative and reference binders

The results in Figure 5.1 show that the reference clay sample had high workability, close to the upper limit of the specification. The workability reduced with time up to 7 d, after which it steadily decreased to a plateau at 21 d. At 21 d, the workability was close to the lower limit of the specification, at 38.7%. Clay A (Gly+PFR binder) had a workability of 41.5% after mixing, which also reduced during the first 7 d to 38.6%. From 7 to 21 d aging, the workability increased to 40.6%. Although the workability at 7–14 d aging was within the specification, the value can be increased by increasing the liquid content of the clay during mixing. It is difficult to determine the exact liquid content of a THC; variability in binder quality and limitations to the frequency of addition to the clay mass contribute to the difficulty. The general practice for manufacturing a wet mixed clay is that after the first addition of liquid, a correction can be made by adding a second aliquot of liquid. After the second liquid addition, the clay should have a workability close to the desired value or it is discarded. Workability (plasticity) should be evaluated after the first

binder addition; if additional binder is required to increase the workability, then the second (final) addition can be made. If the resulting workability is still inadequate, a new sample needs to be prepared. Continuous shear heat generation during mixing of the clay alters the structure of the binder, which affects its behaviour in the clay: for this reason, the THC can only be wet-mixed twice.

An unusual phenomenon was observed for Clay B (CWO+PFR binder), in which the workability decreased (from 45.7% to 41.7%) and then increased after 4 d aging (up to 46.9%). The initial decrease in workability up to 4 d of aging for all samples was due to progressive penetration of the binder into open pores of the ceramic oxide particles in the matrix and aggregates of the clay (Figure 5.1). Owing to the high viscosity of the binder, this process takes longer than for conventional monolithic refractory materials or clays that use water as binder. For this reason, THC is only used after 4 d of aging (Nelson & Hundermark, 2014). Desired behaviour of the clay is that the workability reduces to a small extent due to the abovementioned process, but is stable (workability reaches a plateau) after 7 d, as shown in Figure 5.1 (Kageyama et al., 2005). The Gly+PFR binder showed a workability decay closest to that of the reference binder. The reference binder clay workability continually decreased after 7 d of aging; Clay A reached a plateau after 14 d. The increase in workability after 4 d of ageing could potentially be due the inherent lubrication nature of the binder that after penetration of liquid into the pores, the excess liquid between the matrix particulates move relative to each other which caused the increase in workability.

5.3.2. MEP aging

The MEP aging results of the reference and alternative binder clay samples are shown in Figure 5.2 (standard deviation as error bars plotted for all samples). Considering the results shown in Figures 5.1 and 5.2 together, a correlation between workability and MEP is observed, in which a decrease in plasticity of the clay resulted in an increase in the extrusion pressure (Cameron, 2021). The results showed that the MEP of the reference binder clay increased up to 7 d and thereafter decreased: once the clay reached a plateau in workability, the MEP decreased. The desired behaviour of the extrusion pressure should be the same as that of workability, in that the MEP should remain as constant as possible: where there is an increase in the MEP, this should remain lower than the ramming pressure of the mud gun. The MEP aging of both Clay A and Clay B were less variable than the reference sample, although Clay B showed an increase in extrusion pressure up to 7 d. Both Clay A and Clay B showed the desired MEP aging behaviour, with Clay A showing a more constant extrusion pressure during aging. This would ensure stable mud gun operation, with little variability in the product and improved ramming efficiency. A continued decrease in workability of the reference material should be anticipated during ramming operations because a specific amount of clay should be extruded at a given mud gun extrusion pressure. A continued decrease in MEP of the clay could result in material bypass occurring when excess clay accumulates in the mud gun. Bypass of clay material into the furnace is highly unfavoured because this creates a turbulent environment inside the taphole and generates a significant amount of volatiles. This scenario has associated risks in terms of furnace operations (Hundermark et al., 2014).

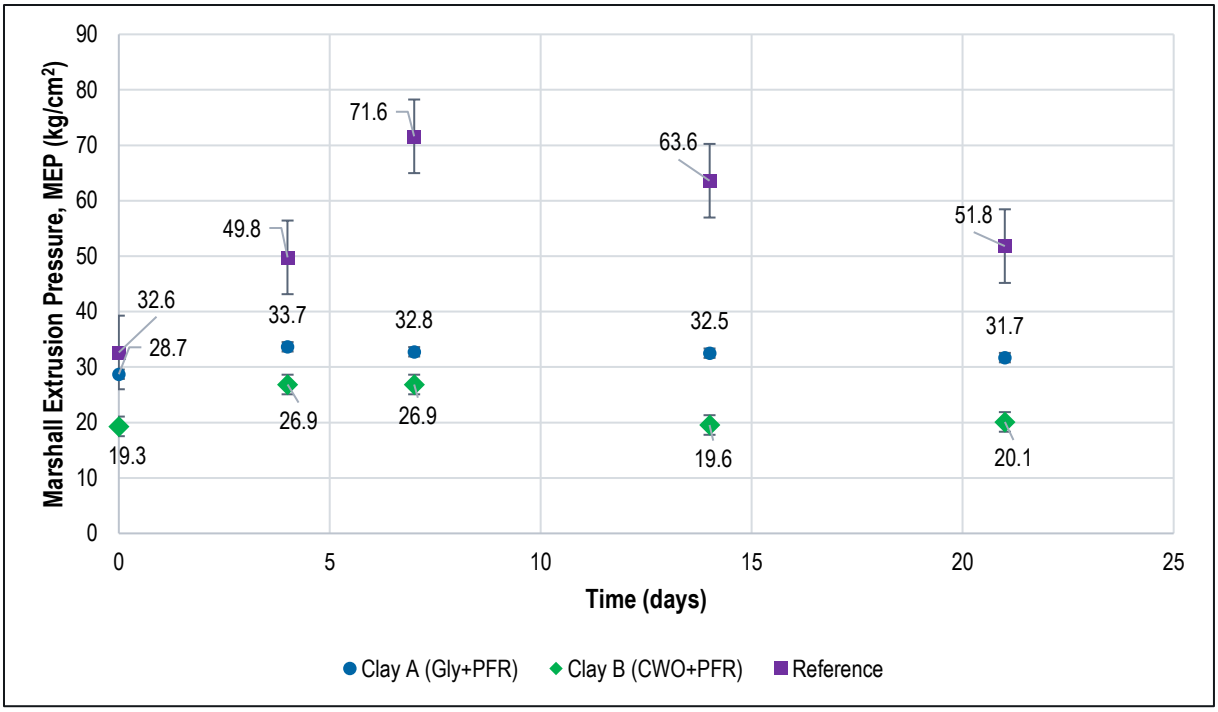

Figure 5.2: Marshall extrusion pressure aging test results from clay samples of alternative and reference binders

5.3.3. Taphole clay thermal aging (hardenability)

Hardenability of the clay is an important part of the ramming process during casting operations. The ability of the clays to be heated at an elevated mud gun barrel temperature (60°C) for a period was evaluated. This simulates heating of the clay in the mud gun during ramming. The barrel is usually filled with clay after it has been emptied, which means that clay in the mud gun is continuously heated until it is extruded into the taphole. This heating causes lower-temperature volatiles to be released from the binder and increase its viscosity, which further causes plasticity to decrease and extrusion pressure to increase (Cameron, 2021). Increased extrusion pressure can be inferred from the hardenability of the clay. The workability (plasticity) results from thermal aging at 60°C for 48 h are shown in Figure 5.3.

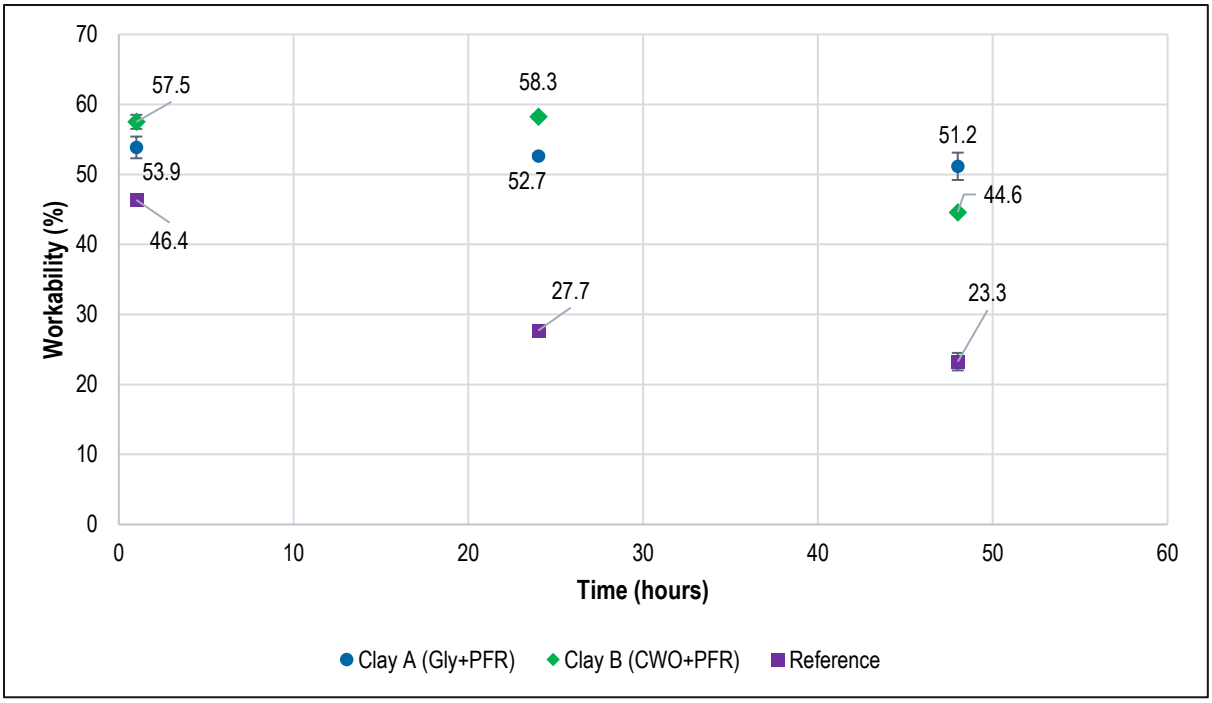

Figure 5.3: Workability thermal aging of clays produced with alternative and reference binders

The reference clay had the lowest initial workability (Figure 5.3 – standard deviation as error bars plotted for all samples). Aging revealed that temperature alter the viscosity of the reference binder more than it did for the alternative binder clay samples. Workability of the reference clay reduced significantly (40%) as the clay was heated up to 24 h, and then tended to plateau. Lowering in workability can be attributed to low-temperature volatilization that increased the viscosity of the binder (Cameron, 2021). The desired behaviour of a binder is that the workability should reach a plateau after continuous heating. This is not shown by the results for Clay B (Figure 5.3), which showed constant workability up to 24 h followed by a decrease. Results of the WAT (Figure 4.40) showed that the viscosity decreased as the wax crystals melted. The rheology results in Figure 4.41 show that as CWO was cooled below ~65°C, the liquid become viscoelastic from its original viscous state. Melting of the wax crystals reduced the viscosity of the binder to allow the liquid to penetrate open pores of the matrix constituents of the clay. This resulted in accelerated aging of the clay, observed from the reduction in workability after 24 h. Workability continued to decrease with heating until all wax crystals had melted. Adhesion of clay inside the mud gun can become problematic when this occurs and can lead to spontaneous breach of the integrity of the clay (self-openers). The glycerine-based clay (Clay A) had constant workability throughout the aging period and the most desirable thermal aging behaviour for application to THC.

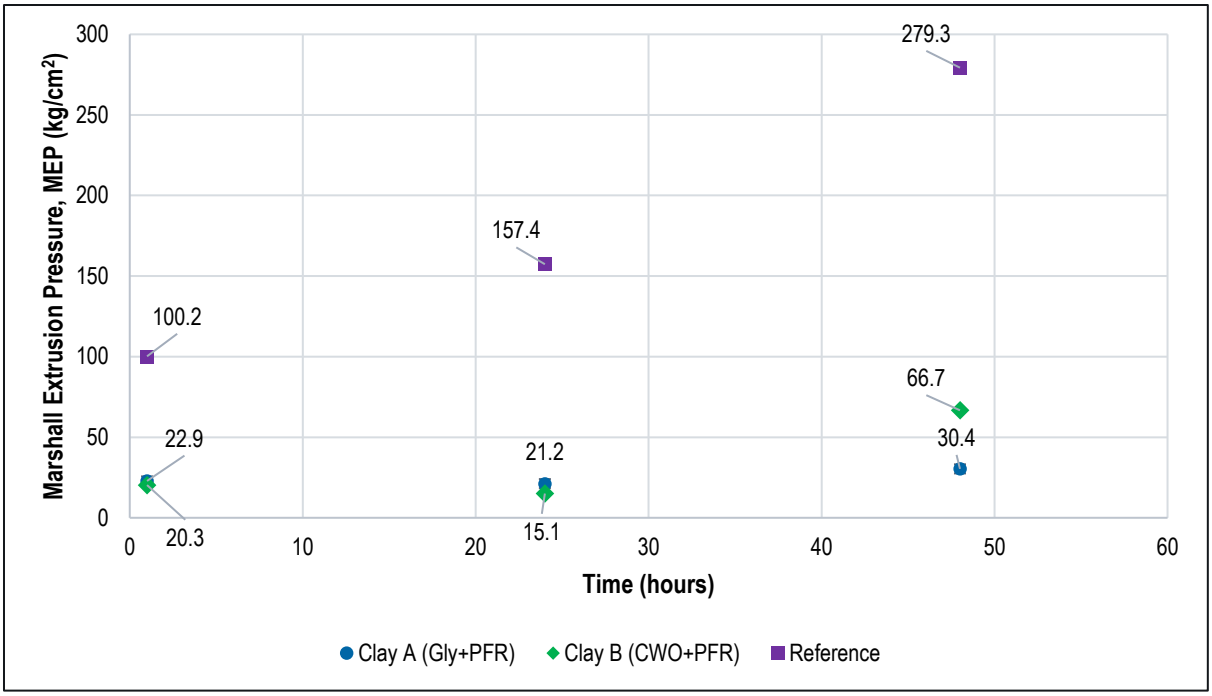

Figure 5.4: Marshall extrusion pressure thermal aging of clays with alternative and reference binders

5.3.4. MEP thermal aging (hardenability)

Results for extrudability, as determined from MEP measurements, are shown in Figure 5.4 (standard deviation as error bars plotted for all samples). As the reference clay sample was aged at 60°C, the extrusion pressure continuously increased up to 48 h. The extrusion pressures of Clay A and Clay B showed similar behaviours and the MEP remained relatively constant. There was a small increase in the MEP after 24 h for Clay B, but not comparable with that of the reference binder clay sample. The results for Clay B showed that the MEP increased with the decrease in workability after 24 h. This suggests accelerated aging of Clay B due to substantial lowering in viscosity of the binder. Although the viscosity of glycerine decreases with an increase in temperature, there was a larger decrease in viscosity of the CWO. Clay A showed a relatively constant MEP throughout thermal aging, which also correlated with the workability results for this sample. Considering a preferred alternative binder to CTht, the glycerine–phenolic resin mixture showed less variability in thermal aging and easier taphole operations would be expected. The workability measurements at lower temperatures (22°C, Figure 5.3) showed higher variability (larger error) than the samples valuated at higher temperature (60°C). This was partly because the binder viscosities decreased with heating, which improved initial workability (plasticity) and improved extrusion of the clay.

5.3.5. Strength development of taphole clay

Strength development of THC is an important feature. Strength development, also referred to as the hardening rate of the clay, depicts the rate at which the green strength increases with an increase in temperature (Kageyama et al., 2005). Contributing influencing factors include the binder volatilization behaviour, and type and quantities of the binder and resin (Kageyama et al., 2005). When the binder volatilizes, the viscosity increases and the liquid

becomes solid or semi-solid, depending on the composition. This increase in viscosity will proceed until the binder imparts green strength to the clay.

Strength development of the three clay samples is shown in Figure 5.5 (results reported are averages of three samples; standard deviation shown). Samples for strength development are usually heated between 200°C and 400°C, depending on the resin composition (Kageyama et al., 2005): for the resin used in this study, the curing temperature was chosen as 200°C based on the DSC results (Section 4.3.2.1). Owing to volatilization of the binder, which influences the viscosity and strength development of the clay, the volatile releases of the samples evaluated in Figure 5.5 are reported in Figure 5.6.

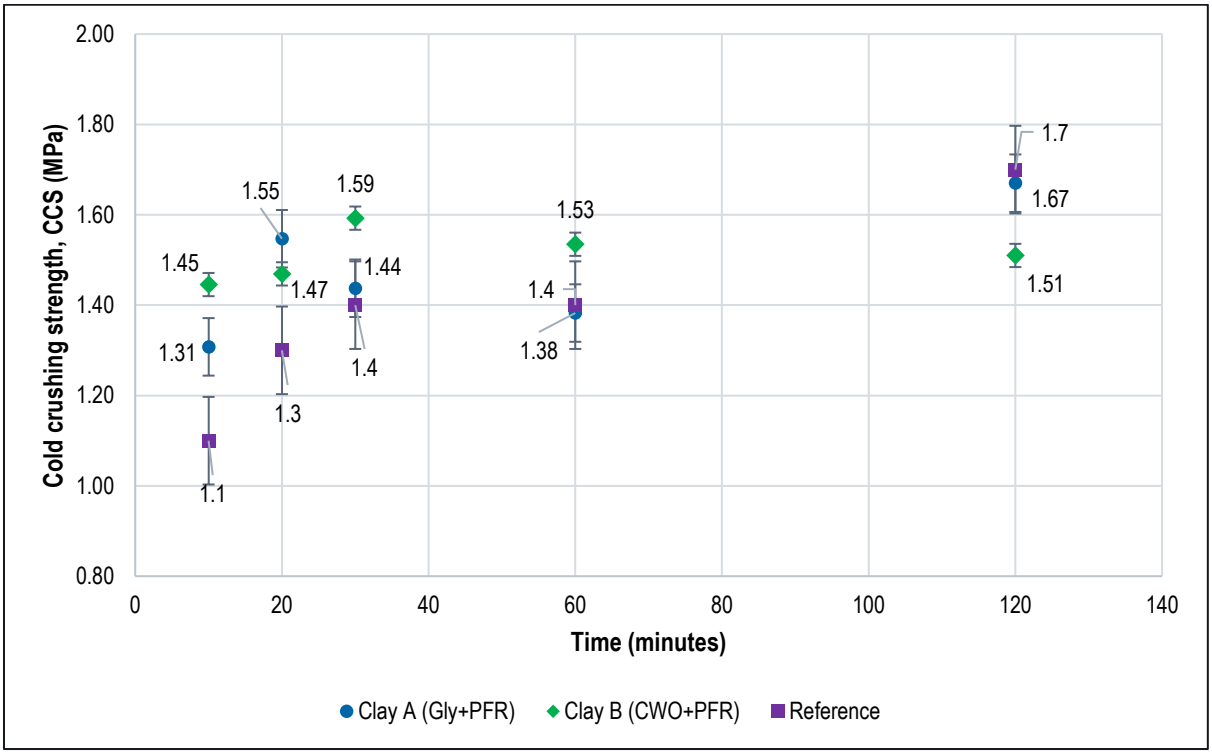

Figure 5.5: Strength development profiles of taphole clays produced with alternative and reference binders, evaluated by cold crushing strength after firing at 200°C

The SDP of the clays showed similar trends except for Clay B. CCS of the reference sample gradually increased up to 30 min, remained constant at 30–60 min, and then increased up to 120 min. This is a typical SDP for THC. Several reasons may explain the relaxation at 30–60 min. Phenolic resole resin generally undergoes various steps during volatilization up to final cure and a carbonized solid. Two of these steps, cross-linking and solidification, are responsible for the increase in strength during heating. The exact step responsible for this relaxation stage is not well understood; this is considered as scope for a separate study. The cross-linking step was slow because the temperature was close to the curing temperature of the resin, so the relaxation could also be due to slow cross-linking kinetics.

The desired SDP of a clay can be described as a gradual increase in strength to fulfil two requirements: 1) ensure a plug is formed on the inside tapping channel as quickly as possible to contain molten material in the smelting

vessel; 2) ensure quick and efficient drilling practices during tapping. The latter implies that the strength development of the clay should be limited since too high CCS after heating could cause difficulty in drilling, wear of drilling tips, and possible damage to the taphole bricks due to transfer of vibration from the drill to the surrounding bricks. For the PGM smelting furnace considered for this study, the desired compressive strength after firing to 800°C is 2.1–3.0 MPa. Difficulty in drilling during these taphole operations requires lancing, even if the clay is easily drilled (Nelson & Hundermark, 2014), because a molten scab forms on the back end of the tapping channel inside the furnace that needs to be removed. Lancing problems, such as incorrect movement of the lance down the tapping channel, could cause taphole damage and compromise integrity of the tap hole (Nelson & Hundermark, 2014).

The SDP of the reference sample (Figure 5.5) showed that the final strength of the clay at 200°C was closer to the lower bound of the specification (2.1 MPa). Clay A showed a similar SDP, with an initial increase in CCS, relaxation at 20–60 min, and then steadily increasing in strength up to 1.67 MPa. The only difference between the reference binder clay and Clay A was the increased relaxation period for the latter. Clay B showed the same initial strength development at 15–30 min, but thereafter reduced in strength up to 120 min. This decrease in strength affects the green strength of the clay, which could influence the sintering strength of the clay at higher temperatures. This decrease in CCS during heating could be due to the high initial workability (Figure 5.1). Although the workability of Clay B after mixing was only 1.5% higher than Clay A, Clay A did not experience the same effect. The sudden decrease in viscosity after heating the binder above 60°C could also have influenced the viscoelastic properties of the clay to maintain structural integrity during heating. Another possible reason for the decrease in CCS could be due to poor adhesion between the ceramic oxide particles and the binder to form a homogenous clay as described by earlier works assessing the wettability of binder phase to the oxide and carbon particles in the clay matrix (Cameron, 2021).

5.3.6. Volatile release

The mass loss results due to volatilization shown in Figure 5.6 are for samples used for the strength development. The differences in mass of each sample before and after heating to 200°C are shown (Figure 5.6). Volatilization losses of the samples represent the combined contributions from the binder, i.e., CTht, CWO, and glycerine, and the phenolic resin. Owing to the small quantity of the resin that was added to the clay, most of the mass loss is attributed to the binder. The volatilization curves of the clay samples correlate with the strength development results. It has been shown that gradual volatile release from the clay samples results in good strength development (Kageyama et al., 2005). This is observed from the data in Figure 5.5 and Figure 5.6. The reference sample exhibited a continuous increase in volatilization as the sample mass decreased with time: the mass loss increased up to 30 min, before increasing up to 120 min. This relaxation effect was also observed with the strength development (Figure 5.5): after 30 min, the CCS entered a relaxation stage, and then started to increase. The relaxation observed in the volatilization results (Figure 5.6) confirmed the slow phenolic-resin cross-linking kinetics linked to volatilization of the resin, where reduced volatilization of the binder resulted in relaxation in the strength development of the clay.

The total mass loss of the reference sample after 120 min heating was 2.60%. A similar trend was shown for Clay B, where the initial mass loss increased up to 30 min, reached a relaxation period, and then slowly increased again. The total mass loss of Clay B after 120 min was 1.54%. The strength development was dependent on the rate and extent of volatilization. The lower CCS of Clay B (Figure 5.5) was related to the lower volatilization of the sample, as observed in Figure 5.6, compared with the other clay samples. This is linked to the lack of increased viscosity of the binder that would assist with its conversion from a liquid to a semi-solid and finally to a solid. The mass loss of Clay A after 120 min was 3.3% which is twice that of the Clay B. Although the mass loss of Clay A was higher, the CCS was also higher after 120 min for this variant indicating an improved strength development compared to Clay B.

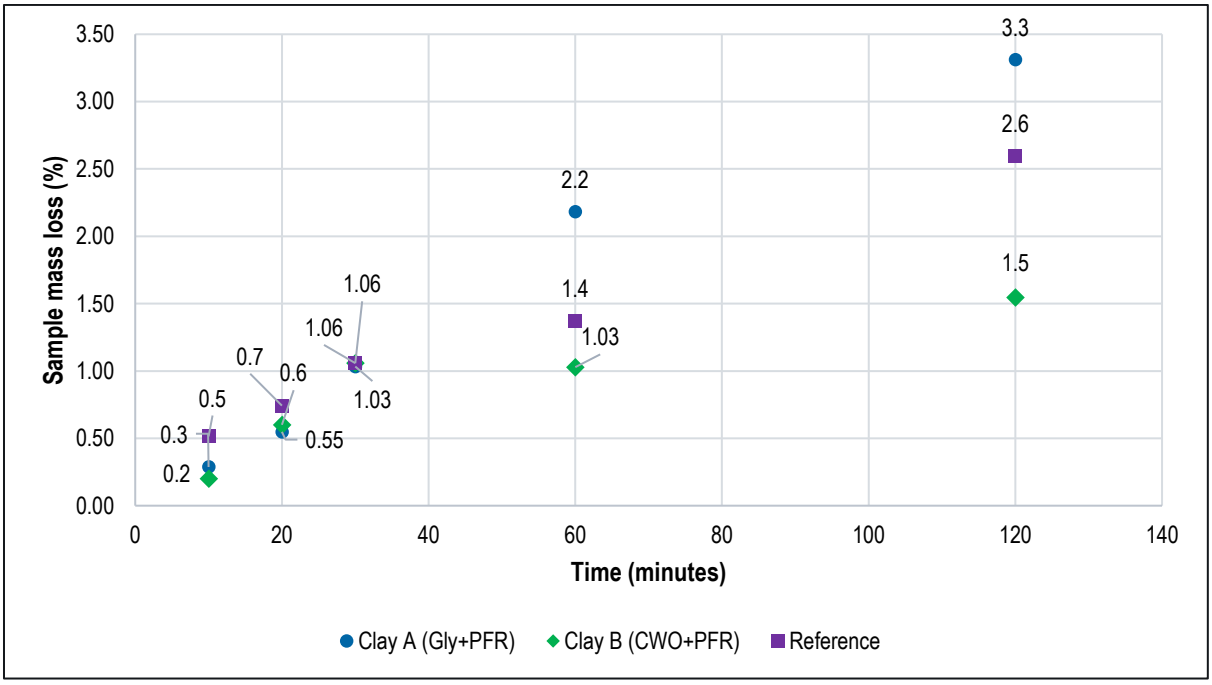

Figure 5.6: Volatile release of taphole clays produced with reference and alternative binders during strength development profile analysis, fired at 200°C

5.4. Standard high-temperature property tests

The high-temperature properties selected for evaluation were VOC analysis, carbon yield, CCS, and AP: the latter two parameters were measured after firing at 800°C in reducing conditions for 30 min. The results in Table 5.1 show the compromised integrity of the Clay B sample, which was anticipated based on the results for strength development (Figure 5.5) and degree of volatilization of the binder system (Figure 5.6). The contributions of both the binder and resin in the carbon yield in each of the clays is also shown in Table 5.1. The binder carbon content and resin carbon content is calculated based of the carbon yield determined for each binder in Section 4.3.1.5 and how much of these binders were used when the clay was mixed. The calculated remaining carbon in clay dry mix (residual carbon) is calculated as the difference between the clay carbon yield determined in Table 5.1 and carbon content of both the binder and resin in the clay formulation. The residual carbon in the clay originates from the coal

fines and sintering clay dry raw material that was used in the taphole clay. The source of sintering clay dry raw material is an organic source which contains carbon (Table 3.2).

Table 5.1: High-temperature properties (pre-fired temperature 800°C in reducing condition, testing temperature 25°C) of taphole clays with different binders (including phenolic resole resin)

Property	**Reference (CTht)**	**Clay A (Gly+PFR)**	**Clay B (CWO+PFR)**
Volatile organic compound (VOC) (%)	21.3	14.6	13.8
Carbon yield (%)	12.4	10.3	11.2
Cold crushing strength (CCS) (MPa) (> 2.1 MPa)	3.1	2.4	-
Apparent porosity (AP) (%)	12.3	12.0	-
Carbon content			
Clay sample	**Binder carbon content (%) (Section 4.3.1.5)**	**Resin carbon content (%) (Section 4.3.1.5)**	**Calculated remaining carbon in dry clay mix (%)**
Reference (CTht) – CTht addition = 17%, resin addition 3.5%	1.8	2.8	7.8
Clay A - Glycerine addition = 13.5%, resin addition 3.5%	0	2.8	7.5
Clay B – CWO addition = 13.8%, resin addition 3.5%	0.7	2.8	7.7

The VOC results were obtained by measuring the clay mass before and after firing in an oxidising environment at > 1000°C. The carbon yield was determined by analytical methods that reflected the combined yield from the binder and carbon raw material added to the clay (a constant value for all three clay samples). The reference sample showed higher VOC than the other clay samples. Clay B had lower volatilization than the glycerine alternative binder. The reference sample had the highest carbon content (12.4%), as expected because of the high carbon yield of the binder (10.6%), shown in Figure 4.34. Clay B exhibited the second-highest carbon yield of 11.2%. The lower carbon yield of this binder (2.7%) resulted in the overall lower carbon yield of the clay. The glycerine-based Clay A gave the lowest carbon yield: this binder did not contain any residual carbon after firing (Figure 4.36).

The integrity of Clay B after firing was poor (Table 5.1): firing yielded a brittle clay that disintegrated on touch, so this sample could not be evaluated. The binder combination of CWO and phenolic resin did not perform well at this temperature. Clay A maintained its integrity and results of the evaluations are shown in Table 5.1. The strength of Clay A was lower than the reference sample, although still exceeded the requirements for the specific furnace (> 2.1 MPa). These properties of Clay A would also promote easier drilling operations before lancing. This can reduce the drilling time and improve productivity of the furnace. AP of the reference and Clay A samples were

similar, with the latter having a slightly denser structure after firing and consequent lower AP. Although the volatility and degree of mass loss of this binder (glycerine) were high (Figure 4.33), the effect was not noticeable in the clay.

The carbon content results in Table 5.1 are for comparison purposes to highlight the effect of making direct substitutions of alternative binders to CTh in the clay based on viscosity and processing parameters requirements. The calculated remaining carbon in the dry clay mix is comparable to the carbon content of the dry raw materials (coal fines and sintering clay) in the taphole clay. The effect of changing the binder to a non-toxic alternative lowers the overall carbon content of the taphole clay due to the reduction in the carbon content of the binder. This is a drawback of changing binders and making direct substitutions. To correct this reduction in carbon content, optimization of the binder to resin ratio or increases in carbon-based dry raw materials need to be made to compensate for the change in carbon content of the clay. However, this was not part of the scope of this investigation. This study only investigated the feasibility of making direct substitutions of the alternative binders to CTht and how this would affect the behaviour and performance of the clay.

These high-temperature properties in combination with results of the simulation tests, i.e., workability and MEP aging, thermal aging, and strength development profile, indicate that glycerine is a suitable non-toxic alternative to CTht that could be used in THC. The toxicity of the binder system, if phenolic resin is used with glycerine, will depend on the resin (free phenol and formaldehyde). There is currently limited choice with regards to bio-based non-toxic phenolic resins that could be used in THC and maintain their reactivity. Studies to produce 100% bio-based phenolic resin for toll-manufacturing are currently being researched (BBI - Bio-based industries, 2018).

5.5. Summary of non-standardised test results

5.5.1. Workability and extrusion pressure aging

The alternative binder clays (Clay A and Clay B) had lower workabilities of 7.5% and 10.6%, respectively, than the reference sample (12.3%) (Figure 5.1). The reference binder showed the largest decrease in workability, corresponding to a higher extrusion pressure (MEP). The alternative binders did not show significant increases in MEP during aging, which implies better anticipated control over operating parameters, such as extrusion pressure on the mud gun and constant THC length. With all three clay compositions, the workability remained above the specified minimum of 38%: the reference clay approached this limit after 21 d of aging. The reference clay showed a decrease in extrusion pressure after 7 d of aging, which can cause process instabilities, such as variable extrusion pressure leading to possible bypass of clay materials into the furnace, which would create a volatile and dangerous environment during tapping. Second to that is also material waste from the mud gun and clay deporting to the tapping launder.

5.5.2. Workability and extrusion pressure thermal aging (hardenability)

The hardenability test results showed that the glycerine-containing clay (Clay A) had minimal changes in either workability or MEP during thermal aging, indicating that the clay was not hardenable. Clay B showed a 22.4% decrease in workability after only 24 h aging, with an increase in MEP. The reference clay showed a decrease in

workability of ~ 50% after 48 h of aging,-with 40% of the clay plasticity that would be lost in the first 24 h in the mud gun. This loss of plasticity can cause difficulty with extrusion of the clay and adhesion losses that will result in reduced sintering capabilities. Workability of the reference sample started to plateau after 24 h of aging, but the extrusion pressure continued to increase, which indicated that clay was extremely hardenable. Loss of the binder lowered the plasticity. A continuous increase in MEP could result in shorter taphole lengths, clay material wastage, waste deporting to the launder, and reduced adhesion to form a seal on the inside of the taphole, with consequent increased corrosion and increased exposure of the tapping channel to heat flux due to shorter taphole lengths. Clay A would be preferred over Clay B and the reference material for this application due to its lower hardenability.

5.5.3. Strength development of taphole clay

The increase in CCS in the first 5–10 min is important for low-temperature strength development because a taphole generally attains temperatures of 300–500°C in the first 10 min (Hloben, 2000). The glycerine-containing clay (Clay A) showed an increase in CCS in the first 20 min, compared to waxy oil-containing clay (Clay B). There was a period of relaxation after the initial increase in CCS, after which it increased again after 60 min of heating: this was attributed to slow cross-linking kinetics of the resin in the binder system. Both the reference and glycerine-containing clay demonstrated an increase in CCS up to 120 min, which is the desired profile for continuous strength development. Clay B exhibited a decrease in CCS after achieving a maximum at 30 min, and continued to decrease up to 120 min. This is not favourable for low-temperature strength development to assist with maintaining the integrity of the rammed mass inside the taphole. A decrease in CCS during low-temperature strength development can cause lower sintering strength at high temperatures and possibly result in self-openers, where the clay does not have sufficient strength to carry the burden and gas pressure inside the furnace (applicable to ironmaking). The occurrence of bypass of taphole mass into the smelting vessel due to insufficient strength development can also be problematic (Nelson & Hundermark, 2014). This is caused by insufficient green-strength development, similar to that observed for Clay B. A higher mass loss of the sample should correlate with an increase in CCS as more of the resin cross-links and decomposes (Kageyama et al., 2005). The glycerine-containing clay showed the highest decrease in mass at 60–120 min after heating at 200°C, followed by the reference sample, although Clay A and the reference clay had similar rates of mass loss over this time interval. Although these samples had a higher mass loss than Clay B, which contained the waxy oil binder, the strength of the clays continued to increase. Low-temperature mass loss of the binders resulted in stiffening due to the increase in binder viscosity, which imparts physical strength to the clay in combination with cross-linking of the resin. Clay B showed reduced strength at 30–120 min, when the loss in mass of the sample ceased, and resulted in a decrease in strength of the clay on further heating.

5.6. Summary of standardised test results

5.6.1. Thermal properties of taphole clay

The reference sample exhibited the highest volatile loss of the three clay samples because its binder contained more organic species that could volatilize and carbonize at high temperatures. The alternative binders had lower

VOC and consequently lower carbon yield. The carbon yield derives from the carbon source in the clay (coal as dry raw material, sintering clay, tar binder in reference clay, petroleum binder in Clay B and glycerine binder in Clay A) and residue after carbonization of the resin. Very little carbon from the binders (glycerine and wax oil) contributed to the carbon yield in these samples (0% and 0.7%). Clay B did not attain any high-temperature strength, as shown from the SDP results. The reference clay sample showed higher CCS (3.1 MPa) than Clay A (2.4 MPa); both samples met the specification for compressive strength (2.1 MPa). The lower CCS of Clay A was attributed to the higher mass loss during strength development, which manifested as lower high-temperature strength and lower carbon yield. The glycerine-containing clay showed a relatively lower, but comparable, AP than the reference sample.

Chapter 6

Summary of Results

"Any intelligent fool can make things bigger and more complex. It takes a touch of genius - and a lot of courage to move in the opposite direction " - E.F. Schumacher

6. Summary of results

The aim of this investigation was to characterize the behaviour and performance of a reference binder (CTht) that is used in taphole clay and compare possible non-toxic alternative binders to the reference. The binders that were successfully selected through a ranking process as possible non-toxic alternatives, were used to prepare laboratory-scale clay mixtures to evaluate the changes in taphole clay properties with direct substitutions of these alternative binders.

In Chapter 3 the characterization of the reference binder (CTht) was executed by evaluating molecular composition, thermal behaviour, and rheology, against which the proposed alternative non-toxic binders were assessed and compared. The binders selected for evaluation as alternatives to CTht were grouped as coal-, petroleum-, wood/vegetable tar-, and glycerine-based, and are discussed in Chapter 3. The coal-based binders comprises a reference coal tar (CTht), a coal tar and merisol oil pitch blend (CTPht-B), and a lower B(a)P synthetic pitch (EcoP). The petroleum-based binders comprised a crude wax oil (CWO), a distilled version of the crude wax oil (PCWO), and a phenolic-based mesophase-forming pitch (MP). The plant/wood tars included pinewood (Tar-PW) and beechwood (Tar-BW) tars, which were byproducts from a Kraft process, and a vegetable tar (Tar-Veg). The glycerine-based binders included a plasticized mixture with xanthan gum (Gly+XG) and a mixture with xanthan gum and a phenolic resole resin (Gly+XG+PFR).

Chapter 4 discussed characterization and ranking of lower-PAH and non-toxic glycerine-based alternative binders to CTht, followed by selection of the most appropriate alternative binders for application in THC. Characterization and evaluation of these alternative lower-PAH and non-toxic alternative binders employed compositional and molecular structure evaluation using FTIR and GC-MS, evaluations of thermal behaviour using TGA, and rheology tests to identify the flow and thermal stability of the binders.

Chapter 5 discussed characterization of the binders in simulated THC applications and evaluated their performance in THC.

The main findings are summarized in this chapter.

6.1 Compositional and molecular structure analysis of the reference and selected binders

6.1.1. Fourier-transform infrared spectroscopy

Analysis of the binders by FTIR revealed that they predominantly consisted of cyclic aromatic or aliphatic (chain) hydrocarbons, sometimes with additional functional groups. Peaks at characteristic wavelengths on the FTIR spectra were used to identify functional groups and structures. The CTht and CTPht-B coal-based binders showed a cyclic aromatic hydrocarbon structure with some C-O cross-linking functional groups; EcoP had a combined structure of aromatic and aliphatic hydrocarbons. Both petroleum-based waxy oils (CWO, PCWO) showed identical structures that primarily consisted of alkanes. The mesophase-forming pitch had a combination structure, similar to EcoP, that consisted of both aromatic and aliphatic hydrocarbons. Phenol was also identified as a major constituent. The pinewood tar showed a saturated fatty-acid structure; the beechwood and vegetable tars had

ketone/ester functional groups. FTIR results for glycerine revealed an aliphatic structure; its mixtures (Gly+XG, Gly+XG+PFR) showed similar functional groups. Addition of XG and PFR did not alter the molecular structure that was detectable by the FTIR, which suggests minimal changes to the structure of the glycerine due to the addition of these compounds. This could also be a concentration effect that results in the undetected presence of these species in the sample due to the detection limit of the FTIR.

Binder molecular structures were differentiated as either cyclic aromatic hydrocarbon (CTht, CTPht-B), chained hydrocarbon (CWO, PCWO, Tar-PW, Tar-BW, Tar-Veg, Gly+XG, Gly+XG+PFR) and a combination of cyclic aromatic-and chained hydrocarbon (EcoP, MP).

6.1.2. Gas chromatography mass spectroscopy

The GC-MS evaluation encompassed both targeted and untargeted analyses. Untargeted analyses were only conducted on the coal-, petroleum-, and wood/vegetable tar-based binders The aim of the untargeted analyses was to identify and quantify the 16-EPA-PAH species and total PAH content in each binder. Species other than 16-EPA-PAH were identified and graphically depicted to enable differences in aromaticity between the binders to be distinguished. The targeted analyses enabled toxicity characterization of each binder based on the calculated BE value and total 16-EPA-PAH content.

6.1.2.1. Targeted analysis

The CTht and CTPht-B binders had the highest BE values of 1.67 and 1.92, respectively, which are typical values for coal-based binders. EcoP had the lowest BE (0.66) of the coal-based binders. The petroleum-based and wood/tar binders had much lower BE values, some by an order of magnitude. The refined (PCWO) and crude (CWO) waxy oils had the same BE (0.03), but their total PAH content differed (PCWO: 43 ppm; CWO: 906 ppm). The mesophase-forming pitch had a higher BE (0.24) than CWO and PCWO, but was comparable with that of the EcoP binder. Both pinewood and beechwood tars had BE and total PAH values of zero. The BE of the vegetable tar was low (0.02), and this binder was comparable with CWO and PCWO, but with a total PAH of 126 ppm. All glycerine-based binders had BE values of zero; however, some had low concentrations of 16-EPA-PAH species (total PAH of 19 ppm). Pure glycerine contained no 16-EPA-PAH species, while its mixtures with phenolic resole resin had low concentrations of 16-EPA-PAH. It was observed that the non-toxic nature of the glycerine-based binders is dependent on the phenolic resin composition and quantity used. Permissible exposure limits (PEL) were used to compare the examined alternative binders with the reference and criteria for adherence to the PEL were used for selection between the binders in this category.

Calculated BE-values indicated the toxicity of the binders from most toxic to least toxic as coal-based binders, petroleum-based binders, wood/plant-based binders, and glycerine-based binders.

6.1.2.2. Untargeted analysis

The GC-MS results were visually represented on plots of double-bond equivalent (DBE) as a function of carbon number (CN), which indicated the presence of PAH or aliphatic compounds, and therefore the aromaticity of each binder. All three coal-based binders exhibited the presence of PAH species and limited aliphatic compounds. CWO showed some PAH species and a smaller content of aliphatic species; PCWO primarily contained aliphatic hydrocarbons and trace PAH content. The mesophase-forming pitch (MP) contained only PAH species. Tar-PW and Tar-BW had PAH and aliphatic species in addition to the 16-EPA-PAH. The vegetable tar had a complex structure with various identified compounds, including methenoazulene, which is deemed harmful to aquatic life. The GC-MS results compared well with the FTIR results in terms of aromaticity of the binders.

6.1.3. Thermal behaviour

Thermal behaviour of the binders was evaluated using two different methods. All binders were evaluated by TGA/DTG-DSC analysis from 50–850°C in an inert atmosphere. The glycerine-based binders were also subjected to detailed DSC analysis between 30–150°C due to the presence of phenolic resole resin in these samples. The observed thermal behaviour of the binders was compared with that of the reference binder (CTht). All binders showed a transition between the pyrolysis (400–600°C) and gasification (600–800°C) regions. The carbon yield, taken as the remaining mass of sample after firing to 800°C, was recorded for each of the binders assessed.

6.1.3.1. Thermogravimetric analysis

The coal-based binders demonstrated low average mass loss, larger volatilization temperature ranges, and higher carbon yield compared with the other alternatives. The reference binder (CTht) showed a low average mass loss (0.28 g/°C) and a carbon yield of 10.6%. EcoP exhibited the closest alternative properties, with an average mass loss of 0.21 g/°C, over a temperature range of 398°C, and gave the highest carbon yield (30.2%). The CTPht-B, petroleum-based, and wood/vegetable tar binders had higher average mass loss, narrower volatilization temperature ranges, and lower carbon yield. The criteria for selecting the most favourable binder based on thermal analysis considered the smallest average mass loss over the widest temperature range: on this basis, EcoP was the most favourable and CWO the least favourable alternative to the reference binder. Glycerine and its mixtures with XG and PFR had the highest average mass losses (1.57–1.79 g/°C) and varying volatilization temperature ranges: the pure glycerine volatilized completely, with no remaining material above 800°C; its mixtures with phenolic resole resin gave carbon yields between 2.5% and 2.8%.

The binders exhibited average mass losses between 0.21–0.40 g/°C (coal-based), 0.53–0.96 g/°C (petroleum-based), 0.42–0.70 g/°C (wood/vegetable-based) and 1.57–1.79 g/°C (glycerine-based). The EcoP is considered the closest alternative to CTht in terms of small average mass loss, over a wide temperature range and relatively high carbon yield.

6.1.3.2. Differential scanning calorimetry

DSC analysis of glycerine revealed endothermic peaks between 220°C and 260°C, which were related to volatilization of the binder. The plasticized glycerine (Gly+XG) showed similar behaviour. The mixture containing phenolic resole resin exhibited distinctive exothermic peaks at 159.61°C and 163°C, which were related to the onset of dehydration condensation or start of polymerization and final curing of the resin, respectively. Mixing of the phenolic resole resin with glycerine or plasticized glycerine shifted the onset of gelation to higher temperatures.

Adding phenolic resin to glycerine results in an increase in curing temperature of the mixture from 163.0°C to 182.4°C. Plasticizing the XG with this mixture further increases the curing temperature.

6.1.4. Rheology

The viscosity flow results indicated that all binders, except CWO and the glycerine mixtures, were Newtonian fluids. Shear thinning of CWO was attributed to possible moisture in the sample that resulted in coalescence. The mixtures of glycerine (Gly+XG, Gly+XG+PFR) also showed shear-thinning behaviour. The plasticizing effect of XG on glycerine induced shear-thinning, which was enhanced when phenolic resole resin was added.

The rheological evaluation with thermal stimulus identified Tar-Veg and Tar-PW as unsuitable for THC use due to their limited thermal stability. CTht exhibited stable viscosity up to ~ 55°C, while CTPht-B had a lower initial viscosity. EcoP had the highest thermal stability of the coal-based binders. The petroleum-based binders showed the highest thermal stability when compared with the reference binder, especially the mesophase-forming pitch. The CTht+PFR mixture had the highest viscosity and thermal stability of the binder mixtures. The plasticized-glycerine mixture with phenolic resin (Gly+XG+PFR) showed similar thermal stability to the reference binder; the pure glycerine and mixture with phenolic resole resin (Gly+PFR) had the lowest viscosity and thermal stability. Glycerine showed a slight increase in viscosity between 95°C and 150°C. Most other binders reached a viscosity plateau at ~ 110°C, indicating that the glycerine mixtures did not undergo gelation-induced viscosity increases. This suggests that, for the glycerine mixtures that contained resole resin, gelation occurred above 150°C for the specific resin composition. The binder ranking prioritised viscoelasticity, lower viscosity for Newtonian fluids, and higher initial viscosity for shear-thinning binders.

All binders, except CWO, exhibited Newtonian behaviour. The Tar-PW and Tar-Veg did not exhibit good thermal stability up to 150°C and were therefore not considered as possible alternative binders for further investigation in taphole clay.

6.1.5. Overall ranking of the binders

Final ranking of the binders was achieved by calculating a contribution number (C_1) from the rankings of the three abovementioned properties using the sum of products of a significance coefficient (S_n) and massed coefficient. The significance coefficient was based on whether the ranking group (compositional, thermal, or rheology) was a primary (S_n = 2) or secondary (S_n = 1) property for the THC. The overall ranking identified the most favourable

binders to replace CTht in THC as the low-PAH pitch (EcoP) and glycerine mixed with resole resin (Gly+PFR). Beechwood tar was ranked second; Tar-PW and Tar-Veg were ranked last due to their limited thermal stability.

Despite the high PAH contents of the coal-based binders (CTPht-B and EcoP), their good thermal and rheological characteristics justify their use in THC; however, this study focused on identifying non-toxic or lower-toxicity alternatives to conventional CTht, so the petroleum-based binders were considered more favourable. CWO was ranked highest of the petroleum-based binders, followed by PWCO and MP.

The top three non-toxic alternative binders that were identified for further evaluation in THC as replacements for CTht were therefore CWO, Tar-BW, and Gly+PFR.

6.2. Evaluation of the taphole clays containing the reference and alternative binders

6.2.1. Results of non-standardized tests

The THC non-standardized tests consisted of aging, thermal aging or hardenability, strength development and the volatilization profile. The aging evaluation comprised workability and extrusion pressure (MEP) aging for 21 d, thermal aging of these properties for 48 h at a simulated elevated mud-gun barrel temperature of 60°C, and strength development at 200°C, including volatilization of the clay samples. The high-temperature properties were evaluated using the standardized CCS, AP and carbon yield tests, as well as the VOC content of clay samples produced using the reference and selected alternative binders.

6.2.1.1. Taphole clay workability and MEP aging

Mixing of the clay samples indicated that Tar-BW did not form a coherent and solid mass for extrusion purposes and had high adhesion, which is detrimental for mixing of THC. The two alternative binders used in subsequent tests were CWO and Gly+PFR. The guideline for the selected furnace application of this study requires a clay workability above 38% for up to 21 d of aging. Clay A (Gly+PFR) and Clay B (CWO) both met these requirements. The reference clay showed a 14.2% decrease in workability over the aging period. Clay A showed a 7.5% decrease after 7 d of aging, followed by an increase up to 14 d (likely due to lubrication effect of the binder), and then reached a plateau. Clay B had a greater initial decrease in workability up to 7 d (10.6%), followed by an increase (also attributed to the lubrication effect of this binder).

Clay A displayed the smallest decrease during extrusion pressure aging (MEP ageing), reaching a plateau after 14 d. The reference binder sample showed an initial increase up to 7 d, followed by a decrease. Both Clay A and Clay B exhibited relatively small increases in extrusion pressure after 14 d of aging; the reference clay continued to increase, which would impact ramming process stability.

Clay A exhibited the desired workability and MEP ageing behaviour, making it preferable to the reference clay for THC application.

6.2.1.2. Taphole clay thermal aging (hardenability)

Thermal aging analysis, or hardenability, of the clay samples showed that elevated heating (60°C) of the mud gun barrel resulted in 49.8% decrease in workability of the reference clay sample, which was a loss of half the plasticity over 48 h. This was attributed to loss of lower-temperature volatile species from the binder, which increased the viscosity and reduced workability. Clay A had the lowest decrease in workability (5%); Clay B exhibited a 22.4% decrease after the same aging period. Extrusion pressure thermal ageing of the reference sample exhibited a continuous increase up to 48 h, which was more than double that observed for Clay A. Clay A exhibited a relatively constant extrusion pressure up to 48 h; Clay B showed an increase, but not to the same extent as the reference sample. The desired extrusion pressure behaviour during thermal aging is a limited increase. This was exhibited by Clay A, which reached a plateau within 48 h. An increase in hardenability of a clay results in wastage during extrusion and shorter taphole lengths with time, causing process instabilities on furnace operations.

Clay A exhibited the desired hardenability behaviour, making it preferable to the reference clay for THC application.

6.2.1.3 Strength development of taphole clay

CCS evaluations were conducted on clay samples heated for 120 min at 200°C. The mass loss on heating was correlated with strength development of the clay. The strength development analysis revealed that the reference sample had an initial increase in CCS from 10–20 min, followed by a relaxation period, and then a continuous increase up to 120 min. This behaviour is desirable, with a conservative increase in CCS after 120 min heating, to ensure efficient and short drilling time on the taphole. A sintering strength that is too high will cause drilling difficulties that could lead to the necessity for undesired lancing practices, which are damaging to longevity of the taphole. Clay A showed similar behaviour to the reference sample, with an increase in CCS between 10–20 min of heating, followed by a relaxation period, and subsequent increase up to 120 min. Although Clay A had a relatively higher initial CCS than the reference, both had similar CCS values after 120 min of heating. In contrast, Clay B showed a reduction in CCS after 30 min of heating. This is explained by examining the volatile loss of the sample (volatilization profile), which showed continuous mass loss of the binder that contributes to strength development by increasing liquid viscosity and stiffening of the clay. Clay B did not show the same continuous mass loss as Clay A and the reference sample: after 30 min heating, the mass loss remained relatively constant, resulting in insufficient increase in CCS. This insufficient strength development of Clay B could impact various operational processes and taphole parameters, including spontaneous opening of the taphole (self-openers), lower thermomechanical strength, shorter taphole length due to clay material removal (washing) during smelting, and longer holding times on the mud gun.

Clay A showed a strength development profile that resembles that of the reference clay and is considered the preferred alternative.

6.2.2. Results of standardized tests

6.2.2.1. High-temperature properties of taphole clay

The lower strength development of Clay B was further evidenced in the high-temperature property evaluation, where the sample disintegrated on touch after firing, indicating insufficient strength development and consequent poor high-temperature strength. The reference clay achieved a compressive strength of 3.1 MPa after heating to 800°C, surpassing the specified value of 2.1 MPa for the specific furnace operation. The carbon yield was 12.4% and AP was 12% after firing. Clay A had a relatively lower CCS of 2.4 MPa, but still met the target specification. The lower CCS of Clay A was attributed to the reduced carbon yield (10.29%). The results showed that when making direct substitutions of alternative non-toxic binders to CTht, the VOC and carbon yield of the clay is lowered. The relatively small contributions of carbon for both glycerine and CWO towards the overall carbon yield of the clay, was highlighted. This suggesting a potential need for optimizing the resin/glycerine ratio. AP was slightly lower than the reference sample, but the values were comparable.

The evaluations suggest that using CWO as a binder without modification is unfavourable due to insufficient strength development related to binder volatilization. Clay A, which contained glycerine and phenolic resole resin, emerged as the most favourable alternative to conventional coal tar and resin combination. Potential optimization of the composition of Clay A by liquid ratio adjustment or use of a higher reactivity resole resin may further enhance this binder performance in THC.

Chapter 7

Conclusions

"To lose practice is to lose the battle " - Mahatma Gandhi

7. Conclusions

The aim of this study was to identify a non-toxic binder for use in THC by (i) identifying critical properties that such a binder should have, (ii) identifying which of the alternative binders have the closest compatibility with the existing benchmark binder, and (iii) evaluating taphole clays in which these identified binders were used.

This was done by selecting coal-, petroleum-, wood/vegetable tar-, and glycerine-based alternative binders, which were characterized and compared with the reference binder (CTht). The results presented in this investigation were concerned with describing the properties and performance behaviour of a conventional THC binder (high-temperature coal tar (CTht) and how this impacts its clay performance. The most suitable alternatives, selected by a ranking process following individual characterisation, were then evaluated in a THC, and the results used to identify the most suitable binder to replace CTht.

The following can be concluded from the investigation on the binders:

- Compositional and molecular structure analysis indicated that the coal-based binders comprises either cyclic aromatic hydrocarbons (aromatic benzene), chain hydrocarbons (aliphatic), or a combination of both, in the case of the EcoP. The molecular structure of the petroleum-based binders consisted primarily of alkane hydrocarbons; the other petroleum binder (MP) had a similar combined structure to that of EcoP and phenolic functional groups. The wood-based binders contained ketone/ester functional groups; the beechwood tar contained some alkyl hydrocarbons as long-chain fatty acids. The functional groups identified for the glycerine-based binders showed that no alterations occurred when glycerine was plasticized with xanthan gum or mixed with phenolic resole resin. These mixtures were all aliphatic.

- The toxicity assessment indicated that the coal-based binders had higher BE values of 0.66–1.67. The petroleum-based binders had considerably lower toxicity, with BE values of 0.03–0.24. There were no 16-EPA-PAH species present in two of the wood-based binders (Tar-BW, Tar-PW), hence these had BE values of zero. All glycerine-based binders also had a BE value of zero. Comparison of the individual 16-EPA-PAH species content in each binder showed that the binders that contained phenolic resole resin had PAH content higher than some of the 16-EPA-PAH permissible exposure limits. The general trend observed was that binders with high aromaticity showed a higher BE-value (toxicity) with some exceptions for the glycerine-based binders.

- Thermal analysis of the binders indicated that the success of CTht as binder in THC is due to its small average mass loss (0.28 g/°C) over a wide temperature range and the presence of some residual carbon after firing. Coal-based alternatives had thermal behaviours closest to that of the reference, followed by the wood-based binders (average mass loss of 0.42–0.70 g/°C), the petroleum-based binders (average mass loss of 0.55–0.96 g/°C), and the glycerine-based binders (1.57–1.79 g/°C), all of which had higher average mass losses than the reference binder. The coal-based binders had the highest carbon yield,

while the glycerine-based binders had the lowest carbon yield. The addition of glycerine to the phenolic resin resulted in an increase in curing temperature and even more so when XG was added (delayed onset of curing).

- The rheology evaluations indicated that the coal-based binders were most suitable to replace CTht, based on Newtonian behaviour and thermal stability, due to their characteristic as low-viscosity Newtonian fluids. Based on their limited rheology thermal stability, Tar-PW and Tar-Veg were disqualified as potential binder replacements for CTht.

- Overall ranking of the binders identified the three most suitable binders to replace CTht in THC as EcoP, Gly+PFR, and Tar-BW; however, the stated aim of identifying non-toxic alternatives disqualified EcoP. The next-favourable alternative was CWO.

- In application as a binder for THC, Tar-BW showed enhanced adhesion that prevented efficient mixing of the clay mass. CWO and the glycerine-phenolic mixture were therefore evaluated as alternative binders in THC.

The following can be concluded from the investigation on the taphole clays:

- Simulated clay ramming, extrusion, and strength development tests indicated that a glycerine+PFR binder caused the lowest decay in plasticity and smallest increase in extrusion pressure during aging of the THC. Thermal aging indicated that the clay containing glycerine and phenolic resin (Clay A) had lower hardenability and higher adhesion than the reference binder clay, while CWO and the phenolic resin-containing clay (Clay B) had a somewhat higher reduction in plasticity and increase in hardenability.

- Strength development of the clay samples showed that the reference THC and Clay A had similar strength development profiles. Clay B gave premature decay in strength development due to limited volatilization of the binder that assists with low-temperature stiffening of the binder and increases strength of the clay.

- High-temperature property evaluations showed that the poor strength development of Clay B resulted in insufficient strength at high temperature and sample disintegration occurred. The reference sample and Clay A achieved comparable compressive strengths after firing to 800°C, with values of 3.1 MPa and 2.4 MPa, respectively. The reference clay contained higher VOC and higher carbon yield than Clay A. Clay A and the reference THC showed comparable apparent porosities.

This investigation showed that a combination of glycerine and phenolic resole resin can potentially replace CTht as a binder in THC materials. Based on the binder characterization evaluations in Chapter 3 and clay evaluations in Chapter 4, the glycerine and phenolic resin mixture proved to be the most suitable alternative to

replace CTht in taphole clay. The Clay A sample that contained this binder had a BE-value (toxicity) of zero, workability and MEP ageing was comparable to the reference clay and within stipulated ranges. Thermal ageing of both workability and MEP was comparable to the reference clay as well as its strength development profile. Optimization of the glycerine/resole resin ratio is required to assist with the reduced carbon yield of the clay resulting from direct substitutions of the alternative non-toxic binders in the taphole clay.

Chapter 8

Recommendations for future work

"The future is completely open, and we are writing it moment by moment " ~ Pema Chöfrön

8. Recommendations for future work

Pilot-scale simulation tests for both the ramming and drilling of Clay A should be conducted to assess the holistic performance of the clay and to scale up the results from the laboratory simulation test to real-life scenarios. Optimizing the glycerine-resole resin ratio to assist with lower carbon yield as a result of direct substitution of CTht with non-toxic alternative binder. This study should also include thermomechanical testing (in inert or reducing condition) at higher temperatures (1450°C), corrosion testing to determine molten matte/slag penetration, turbulence of clay in contact with superheated matte and potentially scanning electron imaging (secondary electron image) to determine the sintering-ability and particle morphology in the microstructure. A pilot scale clay trial would be most beneficial once the clay is optimized to determine suitability.

The concept of extending the basis of the phenolic resin (phenol) into a binder phase by using a less harmful alternative such as lignin (liquid byproduct of Kraft process similar to Tar-PW or Tar-BW) is also a further research area. Resin-bonded clays are difficult to process, and as shown in this work, have associated difficulties. By using the extender (lignin), part of the harmful phenol in the phenolic resin can be replaced and potentially reduce its reactivity to allow for longer ageing periods. Using lignin as a binder could enhanced the performance of the resole resin used in the clay.

Substituting phenol and formaldehyde with lignin and furfural (produced from agricultural byproducts such as oat hulls, sugarcane bagasse and corn cobs) respectively, as non-toxic and sustainable alternatives, should be further investigated, particularly in terms of adjusting the quantity of these precursors (lignin and furfural) to achieve the desired reactivity of the resin to be used as a binder in THC. The use of resin as binders in THC (resin-bonded) has its advantages and disadvantages. Investigating the correlation between the addition of both lignin and furfural as substitutions to phenol and formaldehyde and relating that to the performance of the clay should be valuable in determining the optimal substitution of the non-toxic precursors of the resin for optimal clay performance. This could also be another route worth investigating as an alternative non-toxic green binder solution for THC.

Investigating the effect of changing reductant in the blast furnace from CO to H_2-rich gas compositions in electric arc furnace smelting on the performance of THC should also be conducted. Binders for these products, as well as their compositions, need to be assessed to determine which would perform sufficiently for this new process change for steelmaking. THC based on carbon raw materials for use in H_2 reduction smelting processes is also an idea worth investigating.

A. Bibliography

Agency for Toxic Substance and Disease Registry ATSDR, 2013. Polycyclic Aromatic Hydrocarbons (PAH): What are the Standards and Regulations for exposure?, Atlanta: ATSDR, pp. 23.

Acuna, C. & Marzin, R., 1997. Petroleum pitch, a real alternative to coal tar pitch as binder material for anode production. *Light Metals*, 38, pp. 549–554.

Agilent Technologies, 2019. Safety data sheet - Acenaphthylene Standard (1X1 mL). [Online]. Available at: https://www.agilent.com/cs/library/msds/P-620-1_NAEnglish.pdf [Accessed 12 January 2023].

Agilent Technologies, 2019. Safety data sheet - Indeno(1,2,3-cd)pyrene Standard (1X1mL). [Online]. Available at: https://www.agilent.com/cs/library/msds/P-730-1_NAEnglish.pdf [Accessed 12 January 2023].

Andreikov, E.I., Amosova, I.S. & Pervova, M.G., 2008. Determining the content of polycyclic aromatic hydrocarbons in industrial samples of coal tar and pitch. *Coke and Chemistry*, 51(8), pp. 321–325.

Apicella, B., Tregrossi, A., Stanzione, F., Ciajolo, A. & Russo, C., 2017. Analysis of Petroleum and Coal Tar Pitches as Large PAH. *Chemical Engineering Transactions*, 57, pp. 775–780.

Asmah, N., Suniatri, D. & Margono, A., 2022. Identification of active compounds in ethyl acetate, chloroform, and N-hexane extracts from peels of Citrus aurantifolia from Maribaya, West Java, Indonesia. *Journal of Advanced Pharmaceutical Technology & Research*, 11(3), pp. 107–112.

Azeem, M., Batool, F., Iqbal, N. & Haq, L., 2017. Algal-based biopolymers. In: *Algae Based Polymers, Blends and Composites*., Editor: Zia, K., Zuber, M & Ali, M., Netherlands: Elsevier, pp. 1–20.

Bae, E., Yeo, I.J., Jeong, B. & Shin, Y., Shin, K-H. & Kim, S. 2011. Study of Double Bond Equivalents and the Numbers of Carbon and Oxygen Atom Distribution of Dissolved Organic Matter with Negative-Mode FT-ICR MS. *Analytical Chemistry*, (83), pp. 4193–4199.

Baird, W., Hooven, L. & Mahadevan, B., 2005. Carcinogenic polycyclic aromatic hydrocarbon - DNA adducts and mechanism of action. *PubMed*, 2(45), pp. 106–114.

Baron, J., McKinney, S. & Wombles, R., 2016. Coal Tar Pitch-Past, Present, and Future. In: *Essential Reading in Light Metals*. Cambridge: Springer, pp. 177–181.

BBI - Bio-based industries, n.d. Viobond - Circular bio-based europe joint undertaking (CBE JU). [Online]. Available at: https://www.bbi.europa.eu/projects/viobond [Accessed 25 November 2022].

Van Beek, W. & Goff, T., 2014. An overview of the design, operation, and maintenance practices relating to tap-hole management of a PGM smelting furnace. Furnace Tapping Conference, Johannesburg: Southern African Institute of Mining and Metallurgy, pp. 27–34.

Bermudez, V., Lukubira, S. & Ogale, A., 2018. Pitch Precursor-Based Carbon Fibers. *Comprehensive Composite Materials*, II(1), pp. 41–65.

Bobrowski, A. & Grabowska, B., 2015. FTIR method in studies of the resol-type phenol resin structure in the air atmosphere over certain time intervals. *Metallurgy and Foundry Engineering*, 41(3), pp. 107–113.

Boenigk, W., Gilmet, G., Schnitzler, D., Stiegert, J & Sutton M., 2002. Production of low PAH pitch for use in Soederberg smelters. *Light Metals (Cham),* 2002, Springer Cham, Warrendale, PA, pp. 519–524.

Borrego, E., Athukorale, S., Gorla, S., Duckworth, A., Baker, M., Rosales, J., Johnson, W., Kundu, S., Toghiani, H., Farajidizaji, B., Pittmar, C. & Smith, D., 2022. High carbon yielding and melt processable bis-*ortho*-diynylarene

(BODA)-derived resins for rapid processing of dense carbon/carbon composites. *Composites Part B: Engineering*, 1(242), p. 110080.

Cameron, I., 2021. Investigating premature ageing of blast furnace taphole clay containing a resole resin and liquid pitch binder. MEng dissertation. Pretoria: University of Pretoria.

Cameron, I.J., Garbers-Craig, A.M., 2024. Understanding how the Binder System Influences the Properties and Process Performance Indicators of Taphole Clays, *Refractory Worldforum*, 16(2).

Campbell, A., Pericleous, K. & Cross, M., 2002. Modelling of freeze layer formation and refractory wear in direct smelting process. *Iron and Steelmaker*, vol. 29, no.9, pp. 41 – 45.

Cano-Barrita, P. & Leon-Martinez, F., 2016. Biopolymers with viscosity-enhancing properties for concrete. In: Biopolymers and biotech admixtures for eco-friendly construction materials. Netherlands: Elsevier, pp. 222–248.

Chandira, M., Venkataeswarlu, B. & Kumudhavalli, M., 2010. Formulation and evaluation of mouth dissolving tablets of the Etoricoxib. *Journal of Pharmaceutical Science*, 23(2), pp. 178–181.

Chen, C., Lan, G. & Tuan, W., 2000. Preparation of mullite by the reaction sintering of kaolinite and alumina. *Journal of European Ceramic Society*, 20(14), pp. 2519–2525.

Chen, J., 2003. High carbon yield phenolic resole. France, Patent No. WO2003051948A1.

Cherrie, J., Gorman, M., Jimenez, A. & van Togeren, M., 2011. Health, socio-economic and environmental aspects of possible amendments to the EU Directive on the protection of workers from the risks related to exposure to carcinogens and mutagens at work. World Health Organization: IOM Research Project, United Kingdom, pp. 2.

Choi, J., Ku, P., Cho, K. & Huh, M.-K., 2010. Comparison of Chemicals in Lagerstroemia speciosa (L.) Pers. at Growing Stage Levels by GC-MS. *Korean Journal of Crop Science*, 55(3), pp. 200–206.

Ciesinska, W., 2017. Thermo-rheological properties of coal-tar pitch modified with phenol-formaldehyde resin. *Journal of Thermal Analysis and Calorimetry*, 130, pp. 187–195.

Copetti, G., 2024. Blast Furnace Taphole Clay and Cast House - A Greener Approach. 8th International Conference on Refractories, Jamshedpur (ICRJ). Jamshedpur, India, pp. 74–80.

Coutouly, D. & Feng, S., 2007. Ecological tap hole clay for ironmaking, Beijing: TRB.

da Silva, J., Cardoso, L., Assis, D., Gomes, G., Oliveira, M., da Souza, C. & Druzian J., 2018. Xanthan Gum Production by *Xanthomonas pv. campestris* IBSBF 1866 and 1867 from Lignocellulosic Agroindustrial Waste. *Applied Biochemistry and Biotechnology*, 186, pp. 750–763.

Danish Ministry of Environment, 2014. *Risk Management Options Analysis Conclusion Document for Phenol*, Denmark: Danish Ministry of Environment.

Danish, M., Mumtaz, M., Fakhar, M. & Rashid, U., 2016. Response Surface Methodology Based Optimized Purification of the Residual Glycerol from Biodiesel Production Process. *Chiang Mai Journal of Science*, 43, pp. 1–13.

Dash, S., 2009. Development of Improved Tap Hole Clay for Blast Furnace Tap Hole. MTech Thesis. Rourkela: Department of Ceramic Engineering: National Institute of Technology, Rourkela.

de Pretto, A. & Lindstad, L., 2022. Health-friendly plugging repair paste. Furnace Tapping Conference, California: Springer International Publishing, pp. 375–388.

Delport, M., 2015. Production and sintering of mesphase pitch from anthralene oil. MEng dissertation. Pretoria: University of Pretoria.

Dembitsky, V., 2014. Naturally occurring bioactive Cyclobutane-containing (CBC) alkaloids in fungi, fungal endophytes, and plants. *Phytomedicine*, 21(12), pp. 1559–1581.

Faria, S. et al., 2011. Characterization of xanthan gum produced from sugar cane broth. *Carbohydrate Polymers*, 86(2), pp. 469–476.

Formacare, 2019. Workplace safety - Formacare. [Online]. Available at: https://www.formacare.eu/workplace-safety/ [Accessed 9 October 2021].

Fortes, D., 2019. Thermal expansion of the Al_2SiO_5 polymorphs, kyanite, andalusite and sillimanite, between 10 and 1573 K determined using time-of-flight neutron powder diffraction. *Physics and Chemistry of Minerals*, 46, pp. 687–704.

Fosu, M.-A., Ofori-Kwakye, K., Kuntworbe, N. & Bonsu, M., 2016. Investigation of Blends of Cashew and Xanthan Gums as a Potential Carrier for Colonic Delivery of Ibuprofen. *International Journal of Pharmtech Research*, 9(7), pp. 369–380.

Gargiulo, V., Apicella, B., Stanzione, F. & Tregrossi, A., 2016. Structural Characterization of Large Polycyclic Aromatic Hydrocarbons. Part 2: Solvent-Separated Fractions of Coal Tar Pitch and Naphthalene-Derived Pitch. *Energy and Fuels*, 30, pp. 2574–2583.

Geyer, P. & Halifa, Z., 2014. Blast furnace tapping practice at ArcelorMittal South-Africa, Vanderbijlpark Works. *Furnace Tapping Conference*. Johannesburg: Southern African Institute of Mining and Metallurgy, pp. 97–112.

Gupta, A., Banerjee, K., Bharath, P. & Kumar, S., 2014. Properties and Performance of a Mud Gun Mass (Tap Hole Clay) with Respect to the Stable Application of the Product in Blast Furnace, *Interceram. - Int. Ceram. Rev.* 63, pp. 307–311.

Hloben, P., 2000. Ironmaking industry. In: *Refractory Materials*. Bryanston: Rexxon Publishing, p. 136.

Hsissou, R., Seghiri, R., Benzekri, Z., Hilali, M., Rafik, M. & Elharfi, A., 2021. Polymer composite materials: A comprehensive review. *Composite Structures*, 262, pp. 2–15.

Huang, J., 2019. Lignin-Modified Thermosetting Materials. In: *Lignin Chemistry and Applications*. India: Matthew Deans, pp. 163–180.

Hundermark, R., Nelson, L., de Villiers, B., Ndlovu, J., Mokwena, D., Mukumbe, P., Pieterse, B., Seyanund, W. & van Manen, P, 2014. Redoubling Platinum Group Metals Smelting Intensity - operational challenges and solutions. *TMS: Celebrating the megascale*. Springer (Cham), pp. 189–196.

Hussein, A., Lu, Y., Mollaabbasi, R., Tessier, J. & Alamdari, H., 2020. Bio-pitch as a binder in carbon anodes for aluminum production: Bio-pitch properties and its interaction with coke particles. Fuel, 275(1), pp. 1–9.

JSS Science and Technology University, 2006. *Foundry and Forging Laboratory Manual*. Mysore: Jagadguru Sri Shivarathreeshwara (JSS).

Kageyama, T., Kitamura, M. & Tanaka, D., 2005. Eco-friendly high performance taphole mix, Tokyo: Shinagawa Technical Report, 48, pp. 41–46.

Katovic, Z., 1967. Curing of resole-type phenol-formaldehyde resin. *Journal of Applied Polymer Science*, II, pp. 85–93.

Kaushik, S., Raina, R., Bhatia, G., Verma, G. & Khandal, R., 2007. Modification of coal tar pitch by chemical method to reduce benzo(a)pyrene. *Current Science*, 93(4), pp. 540–544.

Kitamura, M., 2014. Optimizing taphole clay technology, Japan: Shinagawa refractories.

Knop, A. & Pilato, L., 1985. Degradation of Phenolic Resins by Heat, Oxygen and High Energy Radiation. In: *Phenolic Resins*., Berlin, Heidelberg: Springer, Berlin, pp. 140–146.

Krebs, V., Elalaoui, M. & Mareche, J., 1995. Carbonization of coal-tar pitch under controlled atmosphere - Part I: Effect of temperature and pressure on the structural evolution of the formed green coke. *Carbon*, 33(5), pp. 645–651.

Laza, J., Vilas, J., Rodriguez, M. & Mijangos, F., 2022. Analysis of the crosslinking process of a phenolic resin by thermal scanning rheometry. *Journal of Applied Polymer Science*, 83(1), pp. 57–65.

Lee, Y.-K. K. D.-J., Kim, H.-J. & Hwang, T.-S., 2003. Activation energy and curing behavior of resol-and novolac-type phenolic resins by differential scanning calorimetry and thermogravimetric analysis. *Journal of Applied Polymer Science*, 89, pp. 2589–2596.

Li, L., Lin, X., Zhang, Y., Dai, J., Xu, D. & Wang, Y., 2020. Characteristics of the mesophase and needle coke derived from the blended coal tar and biomass tar pitch. *Journal of Analytical and Applied Pyrolysis*, 150, pp. 1–8.

Li, M., Liu, D., Men, Z., Lou, B., Yu, S., Ding, J. & Cui, W., 2018. Effect of different extracted components from petroleum pitch on mesophase development. *Fuel*, 222, pp. 617–626.

Lindstad, L., 2018. More healthy-friendly materials for the tapping area. *Furnace Tapping Conference*. Southern African Institute of Mining and Metallurgy, pp. 95–100.

Lin, K., Shen, Z., Liang, Q., Xu, J. & Liu, H., 2020. Modelling of slag flow and prediction of corrosion state of refractory bricks in an entrained-flow gasifier. *Fuel*, 275(2), pp. 1–11.

Lui, J. et al., 2019. Study on carbonization process of coal tar pitch modified thermoplastic phenolic resin. *IOP Conference Series: Material Science and Engineering*, 631. China, pp. 1–5.

Lu, Y., Li, D., Huang, X., Picard, D., Mollaabbasi, R., Ollevier, T. & Alamdari, H., 2020. Synthesis and Characterization of Bio-Pitch from Bio-oil. *ACS Sustainable Chemistry & Engineering*, 31(8), pp. 11772–11782.

Mannweiler, U. & Perruchoud, R., 1997. Reduction of polycyclic aromatic hydrocarbons (PAH) by using petroleum pitch as binder material: A comparison of anode properties and anode behaviour of petroleum pitch and coal tar pitch anodes. *Light Metals*, Orlando, Florida: The Minerals, Metals, & Materials Society, Warrendale, pp. 555–558.

Mazumder, B., 2012. Coal-derived industrial carbons. In: *Coal Science and Engineering*. India: Woodhead Publishing, pp. 344–370.

Mc Dougall, I., 2014. Water-cooled tap-hole blocks. Furnace Tapping Conference, Johannesburg: Southern African Institute of Mining and Metallurgy, pp. 183–192.

Menendez, R., Fernandez, J. & Cabolla, V., 1996. The role of carbon black/coal-tar pitch interactions in the early stage of carbonization. *Carbon*, 34(7), pp. 895–902.

Mollaabbasi, R., Barry, T., Taghavi, S., Ziegler, D. & Alamdari, H., 2018. Rheological Characterization of Pitch and Binder Matrix. *36th International ICSOBA Conference,* Belem, pp. 511–518.

Morrell, R., 1997. Flexural strength testing of ceramics and hardmetals. Teddington: Centre of Materials Measurement and Technology: Measurement Good Practice Guide No. 7, Teddington, United Kingdom: Crown, pp. 4.

Mukhopadhyay, T., Ghatak, S. & Maiti, H., 2010. Pyrophyllite as raw material for ceramic applications in the perspective of its pyro-chemical properties. *Ceramics International*, 3(36), pp. 909–916.

Mulder, M., 2000. Membrane Preparation - Phase Inversion Membranes. In*: Encyclopedia of Separation Science*. United Kingdom: Academic Press, pp. 3331–3346.

Murilo, S., 2009. Development process of an ecological binder system for refractory mixes, USA: World International Property Organization. United States, Patent No. WO/2009/109027.

National Library of Medicine, 2023. Fluoranthene C16H10 - PubChem. [Online]. Available at: https://pubchem.ncbi.nlm.nih.gov/compound/Fluoranthene [Accessed 12 January 2023].

Nelson, L., Eatough, M. & Guay, K., 2016. Why Does Molten Aluminium Explode at Underwater or Wet Surfaces. *Light Metals: Springer, Cham*, Edward Williams, 1, pp. 1057–1067.

Nelson, L. & Hundermark, R., 2014. The 'tap-hole' - key to furnace performance. *Furnace Tapping Conference*, Johannesburg: Southern African Institute of Mining and Metallurgy, pp. 1–32.

New Jersey Department of Health, 2010. Hazardous substance fact sheet - Dibenz(a,h)anthracene. [Online]. Available at: https://nj.gov/health/eoh/rtkweb/documents/fs/0622.pdf [Accessed 12 January 2023].

New Jersey Department of Health and Senior Services, 2001. Hazardous substance fact sheet - Benzo(b)fluoranthene. [Online]. Available at: https://nj.gov/health/eoh/rtkweb/documents/fs/0208.pdf [Accessed 12 January 2023].

New Jersey Department of Health, 2016. Hazardous substance fact sheet - Benz(a)anthracene. [Online]. Available at: https://nj.gov/health/eoh/rtkweb/documents/fs/0193.pdf [Accessed 12 January 2023].

Nightingale, S. et al., 2006. Assessment of the Structural Development of Resin Bonded Taphole Clay, 4th International Congress on the Science and Technology of Ironmaking, Japan: Iron and Steel Institute of Japan, pp. 57–65.

Nolet, I., 2014. Tapping of PGM-Ni mattes: an industry survey. *Journal of Southern African Institute of Mining and Metallurgy, 116(1)*, pp. 11–16.

Otroj, S, Marzban, S., Nemati, Z., Sajadi, N. & Nilforoushan, M., 2009. Behaviour of alumina-spinel self-flowing castables with nano-alumina particles addition. *Ceramics - Silikaty*, 2(53), pp. 98–101.

Otsubo, Y., Yamasaki, A., Tanaka, Y. & Matsunaga, T., 2010. High Performance Taphole Clay for Blast Furnace, Odisha, India: TRL Krosaki Refractories Limited.

Perez, J., 2004. Development of non-polluting taphole mixture. *Refractories Applications and News*, 9(1), pp. 25–27.

Poirier, J. & Rigaud, M., 2017. Corrosion of Refractories. The Fundamentals FIRE Compendium Series Vol. 2A. Germany: Göller Verlag, pp. 2–9.

Pooladvand, H., Baghshahi, S., Mirhadi, B., Souri, A. & Arabi, H., 2011. Effect of MgO and CaO on Transformation of Andalusite to Mullite. *ASM International*, 21, pp. 1637–1644.

Roder, W., 1998. The future of coal tar pitch and alternative pitches for carbon electrodes. *Light Metals*, 48, pp. 172–183.

Rogers, D., 2007. Phenolic resin product and method of manufacturing of phenolic resin product. United States, Patent No. EP2052012A1.

Van Laar, R., van Stein Callenfels, E. & Geerdes, M., 2003. Blast furnace hearth management for safe and long campaigns. *ISSTech 2003 Conference Proceeding*. Indiana, United States: Iron & Steel Society, pp. 1079–1090.

Sako, E., Galesi, D., Leao, C., Rodrigues, F., Souza, A., Roy, J., Kitamura, M. & Horiushi, T., 2018. High-Performance Taphole Clay: A Key for Blast Furnace Hearth Protection and a Tool for Cost Reduction. *Iron and Steel Technology*, 1, pp. 1–6.

Sarika, P., Nancarrow, P., Khansaheb, A. & Ibrahim, T., 2020. Bio-Based Alternatives to Phenol and Formaldehyde for the Production of Resins. *Polymers*, 12(2237), pp. 2–24.

Sarkar, S. & Adhikari, B., 1999. Lignin-Based Phenolic Resin: Synthesis Optimisation, Adhesive Strength, and Thermal Stability. Kharagpur: Material Science Centre, Indian Institute of Technology.

Satyendra, J., 2018. Coal Tar Pitch. [Online]. Available at: https://www.ispatguru.com/coal-tar-pitch/ [Accessed 14 October 2021].

Sharp, E. & Harper, R., 1993. Resin bond taphole closure refractory product. France, Patent No. CA2124488A1.

Shmalko, V., Karchakova, V. & Zelenskyi, C. O., 2019. Determining the filler activity in the sintering of pitch composites. [Online]. Available at: https://www.intechopen.com/chapters/65603 doi: 10.5772/intechopen.82012 [Accessed 21 July 2022].

Siddiqui, H., Mahmood, N., Yuan, Z. & Crapulli, F., 2017. Sustainable Bio-Based Phenol-Formaldehyde Resoles Using Hydrolytically Depolymerized Kraft Lignin. *Molecules*, 22, pp. 1–19.

Siva, R., Raffi, M. & Srinivasa, K., 2018. Experimental Study on Environment Friendly Tap Hole Clay for Blast Furnace, *IOP Conference Series: Materials Science and Engineering*, 330, pp. 1–13.

Srivastava, M., Kumar, M., Agrawal, U. & Garg, M., 2012. Comparison of Structural Properties of Pitches Prepared from Refinery/Petrochemical Residues using NMR Spectroscopy. *The Open Petroleum Engineering Journal*, 5, pp. 14–20.

Steenkamp, J., 2014. *Chemical wear of carbon-cased refractory materials in a silicomanganese furnace taphole*, PhD Thesis. Pretoria: University of Pretoria.

Steenkamp, J., 2018. Wear analysis of tap-holes at two ferrochromium production furnaces. *Furnace Tapping Conference*. Johannesburg: Southern African Institute of Mining and Metallurgy, pp. 11–28.

Sutherland, J. & Gous, J., 2018. Managing the tap-hole life-cycle at five submerged arc furnaces producing silicomanganese at Transalloys. *Furnace Tapping Conference*. Johannesburg: Southern African Institute of Mining and Metallurgy, pp. 117–132.

Talabi, S., da Luz, A., Pandolfelli, V. & Lima, V., 2020. Graphitization of Lignin-Phenol-Formaldehyde Resins. *Materials Research*, 23(2), pp. 1–13.

Tarantino, G., Vieira, C., Pinheiro, S. & Mattedi, S., 2016. Characterization and evaluation of waxy crude oil flow. *Brazilian Journal of Chemical Engineering*, 33(4), pp. 1063–1071.

Theyab, M. & Diaz, P., 2016. Experimental Study on the Effect of Inhibitors on Wax Deposition. *Journal of Petroleum and Environmental Biotechnology*, 1(7), pp. 1–5.

Thomson, L., 2014. Monitoring, repair, and safety practices for electric furnace matte tapping. *Furnace Tapping Conference*. Johannesburg: Southern African Institute of Mining and Metallurgy, pp. 87–95.

United States Department of Labor, 2019. Permissible Exposure Limits - OSHA Annotated Table Z-1. [Online]. Available at: https://www.osha.gov/annotated-pels/table-z-1 [Accessed 12 January 2023].

United States Department of Labor, 2012. Coal Tar Pitch Volatiles | Hazard Recognition. [Online]. Available at: https://www.osha.gov/coal-tar-pitch-volatiles/hazards#:~:text=World%20Health%20Organization%20(WHO)., to%20humans%20(Group%201). [Accessed 18 November 2023].

Wang, L., Yin, Y., Qiu, W. & Liang, Y., 2017. Effects of pitch addition on the properties of environmental-friendly tap-hole clay. *Journal of the Ceramic Society of Japan*, 1(125), pp. 12–18.

Wonderstone, 2020. Technical Ceramics [Online]. Available at: https://wonderstone.co.za/technical-ceramics/ [Accessed 27 July 2021].

Xu, P. & Jing, X., 2011. High carbon yield thermoset resin based on phenolic resin, hyperbranched, polyborate and paraformaldehyde. *Polymers Advanced Technologies*, 1(22), pp. 2592–2595.

Xu, S., Li, J., Qiao, G., Wang, H. & Lu, T., 2009. Pore structure control of mesoporous carbon monoliths derived from mixtures of phenolic resin and ethylene glycol. *Carbo*n, 47, pp. 2103–2111.

Yan, M., Li, G. & Li, X., 2018. Study on the Effect of Crude Oil Composition on Waxing Characteristics of Waxy Crude Oil. *Materials Science and Engineering*, 452, pp. 1–5.

Yi, S. & Zhang, J., 2011. Relationship between Waxy Crude Oil Composition and Change in the Morphology and Structure of Wax Crystals Induced by Pour-Point-Depressant Beneficiation. *Energy & Fuels*, 25, pp. 1686–1696.

Yuan, G. & Cui, Z., 2019. Preparation, Characterization, and Applications of Carbonaceous Mesophase: A Review. In: *Liquid Crystals and Display Technology*. London: InTechOpen, pp. 101–120.

Zhang, J., Mei, G., Xie, Z. & Zhao, S., 2016. Curing Mechanism of Phenolic Resin Binder for Oxide-Carbon Refractories. *ISIJ International,* 56(1), pp. 44–49.

Zhang, Y. & Geng, X., 2020. Principle of biopolymer plasticization. In: *Processing and Development of Polysaccharide-Based Biopolymers for Packaging Applications*. Washington: American Ceramic Society, pp. 1–16.

Zhu, Y., Liu, H., Zu, Y., Hu, C., Zhao, C., Cheng, J., Chen, X. & Zhao, X., 2020. Preparation and Characterization of Coal-Pitch-Based Needle Coke (Part III): The Effects of Quinoline Insoluble in Coal Tar Pitch. *Energy & Fuels*, 34(7), pp. 8676–8684.

A. Appendix A – ASTM test methods

Standard designation	Title	Refractory test
C181-11 (2018)	Standard Test Method for Workability Index of Fireclay and High-Alumina Refractory Plastics	Taphole clay workability
C133-97 (2021)	Standard Test Methods for Cold Crushing Strength and Modulus of Rupture of Refractories	Cold crushing strength (CCS)
C571-81	Methods for Chemical Analysis of Carbon and Carbon-Ceramic Refractories	Taphole clay carbon yield
C380	-	Apparent porosity (immersion)

B. Appendix B – Auxiliary results

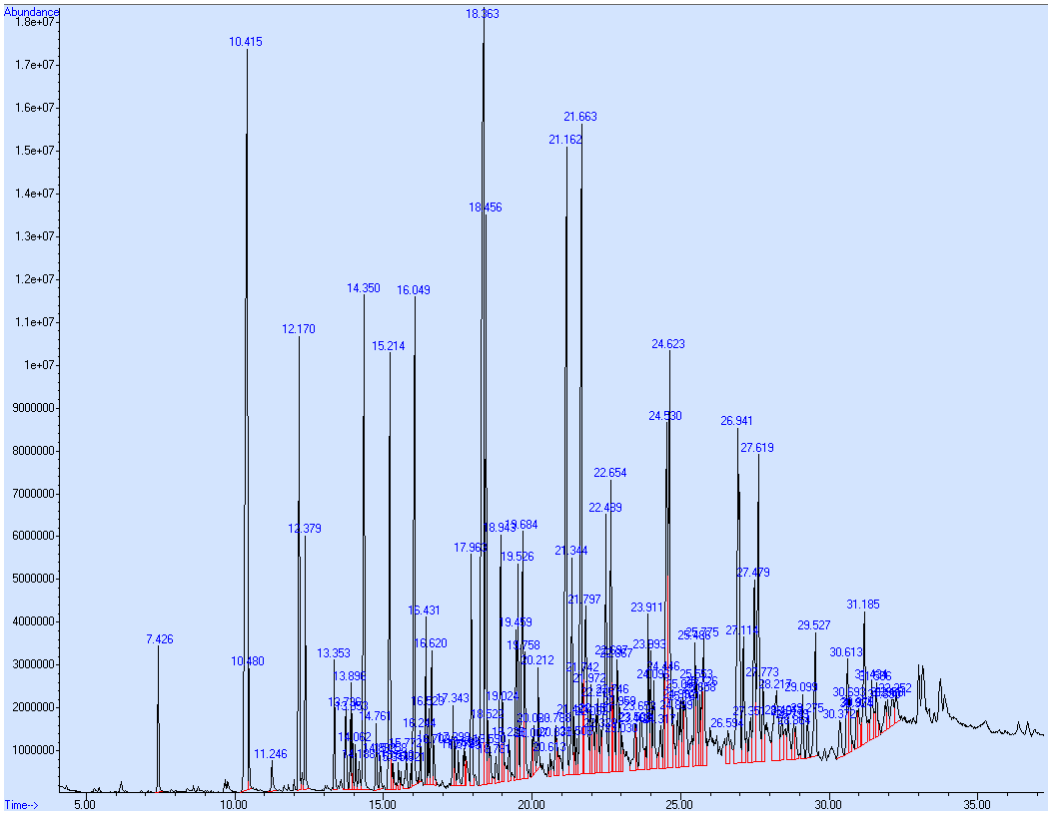

Figure B.1: Gas chromatography mass spectrometry analysis of CTht dissolved in toluene

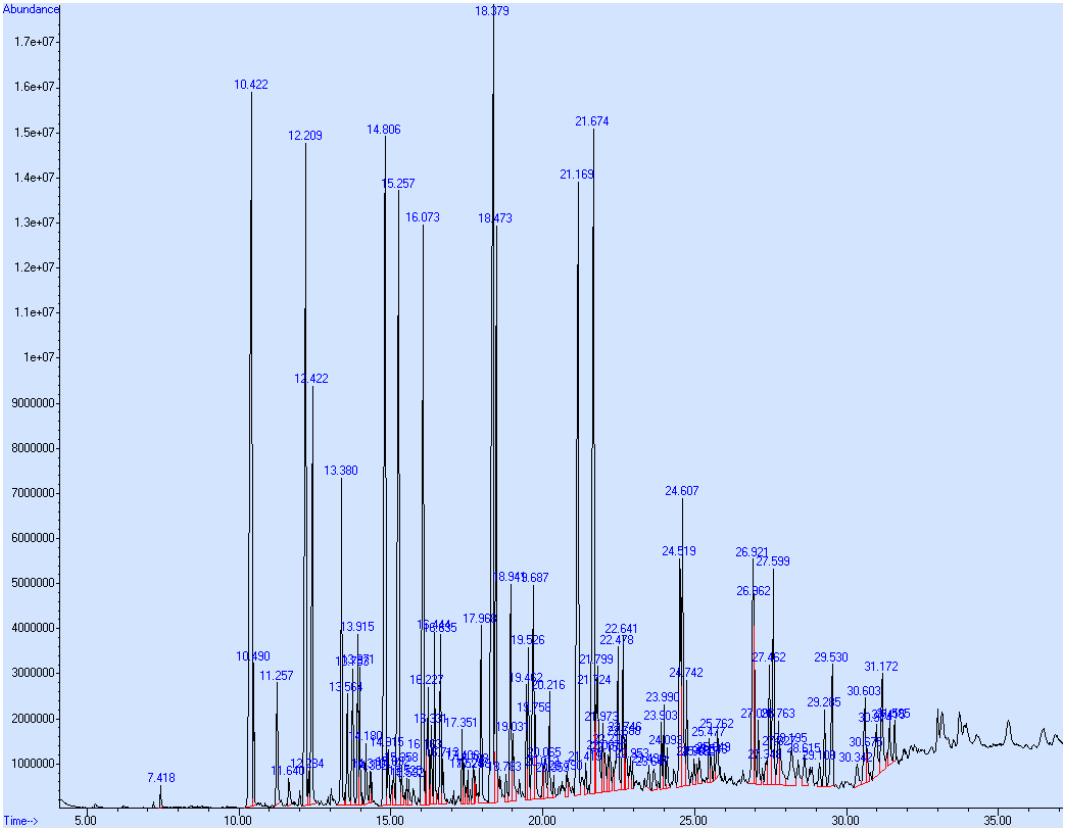

Figure B.2: Gas chromatography mass spectrometry analysis of CTPht-B dissolved in toluene

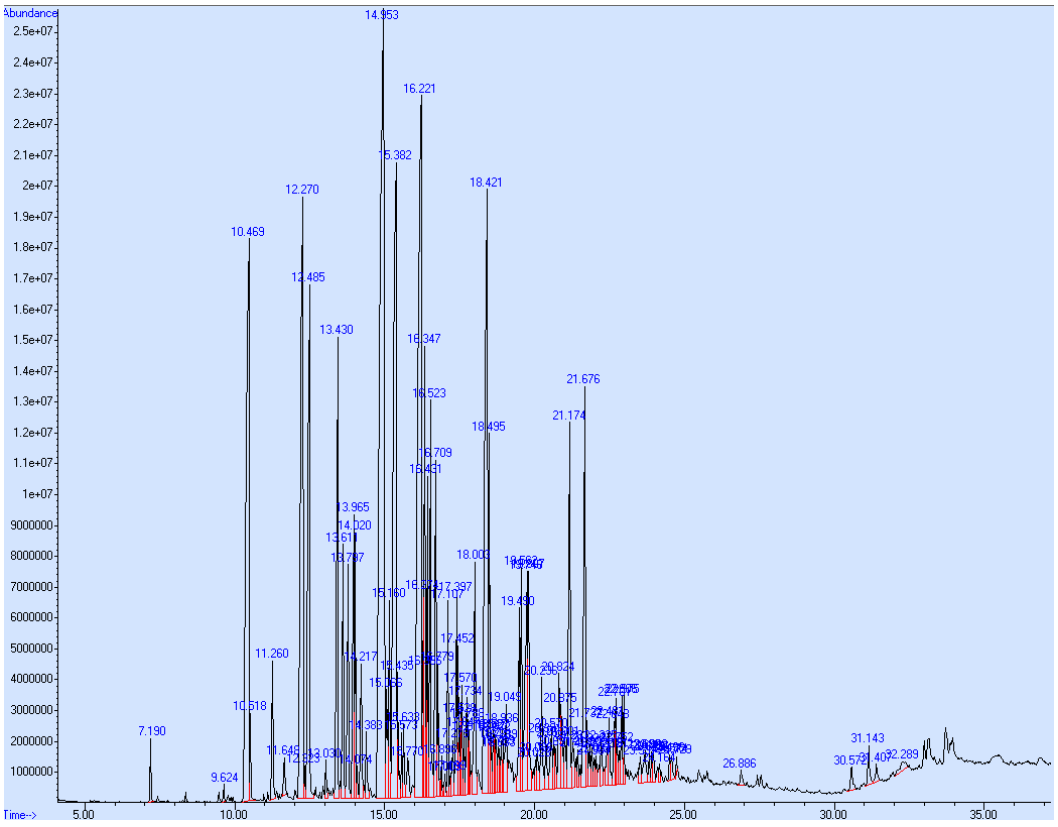

Figure B.3: Gas chromatography mass spectrometry analysis of EcoP dissolved in toluene

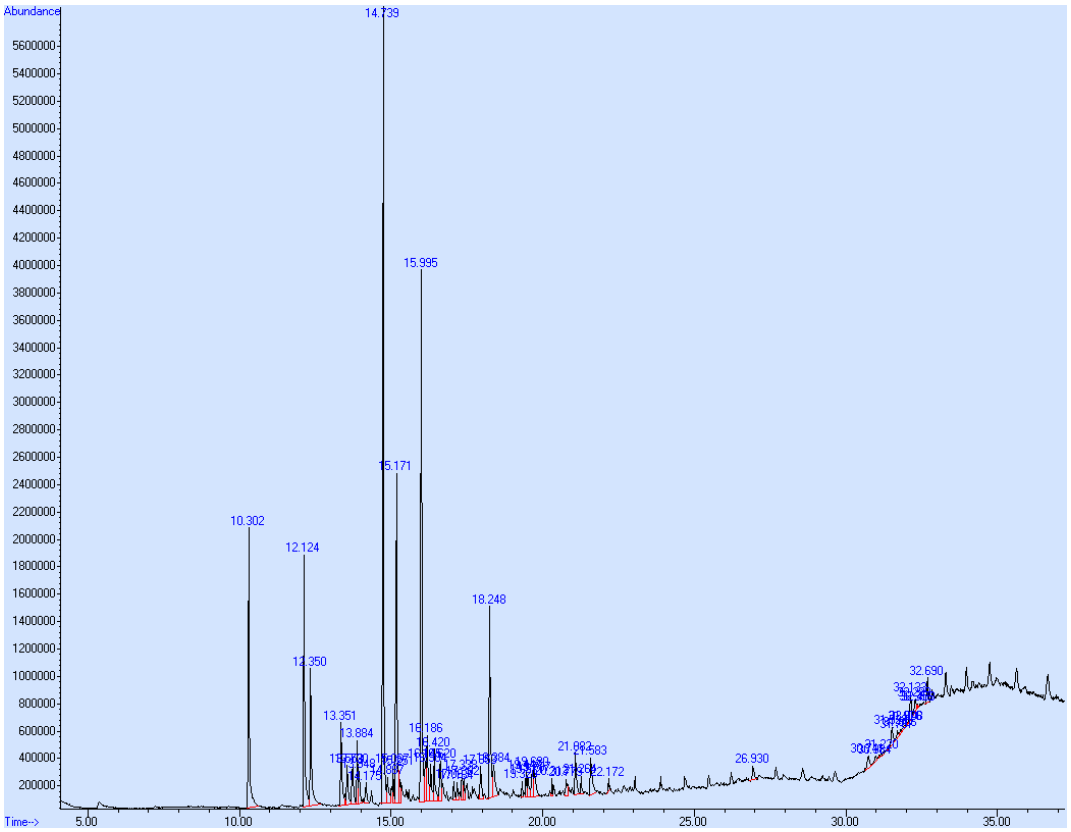

Figure B.4: Gas chromatography mass spectrometry analysis of CWO dissolved in toluene

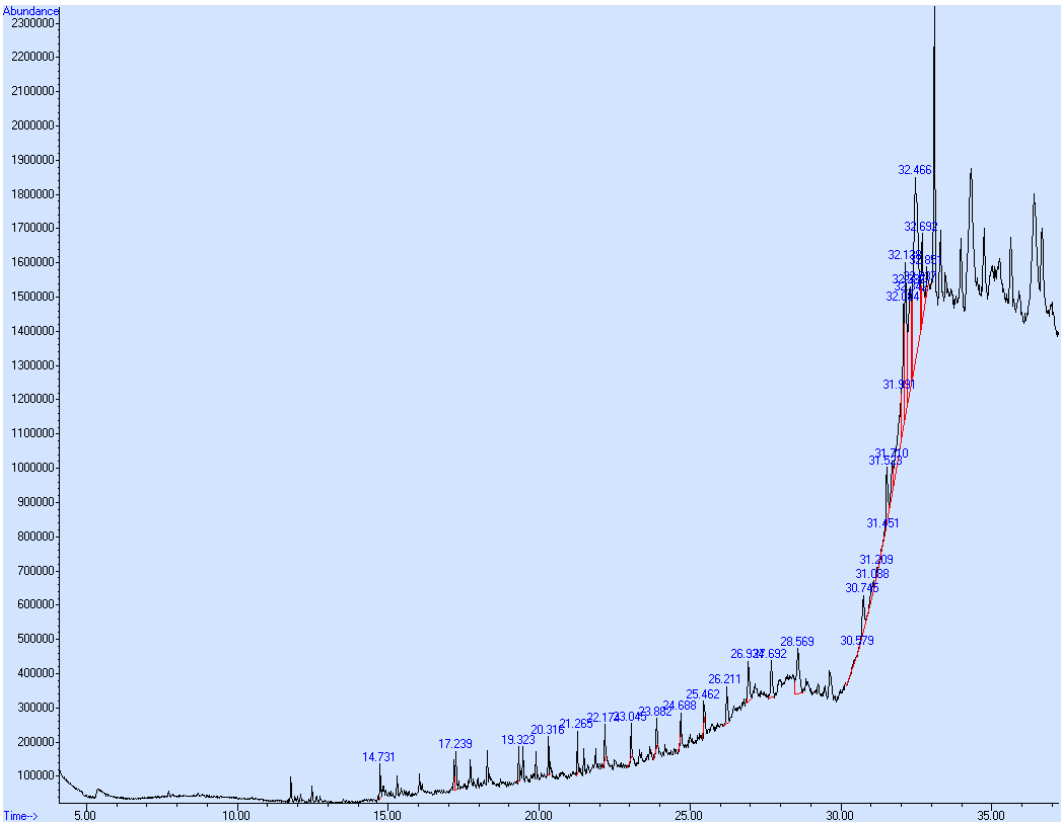

Figure B.5: Gas chromatography mass spectrometry analysis of PCWO dissolved in toluene

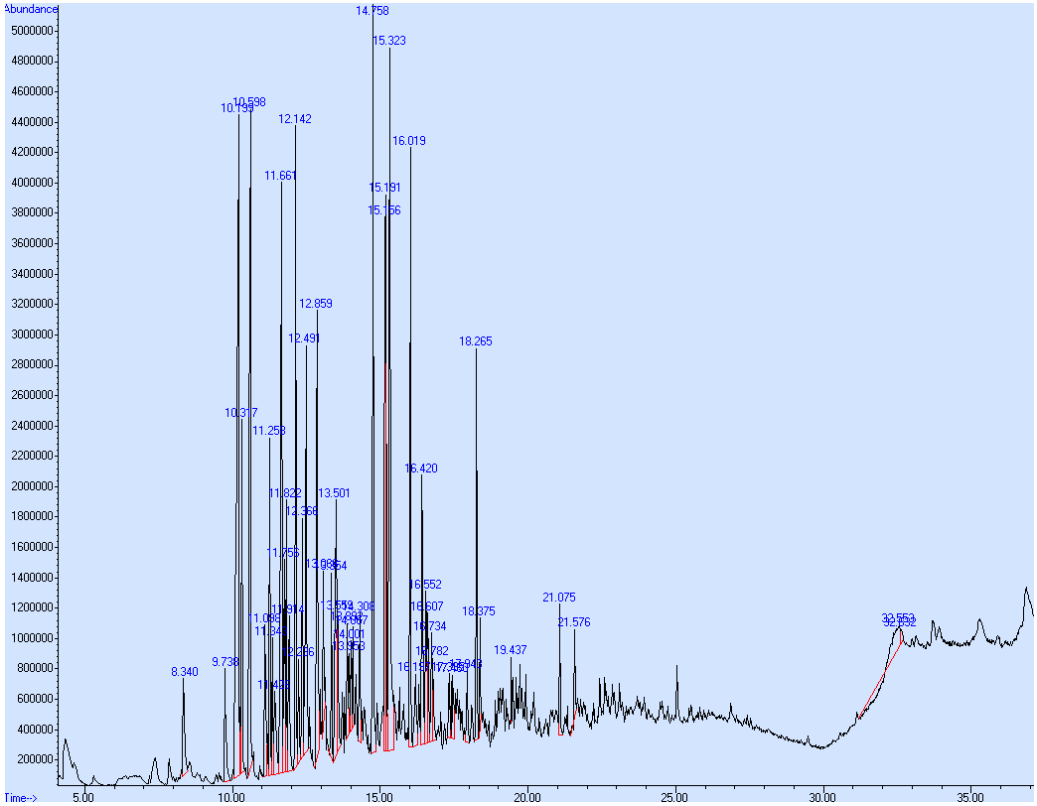

Figure B.6: Gas chromatography mass spectrometry analysis of MP dissolved in toluene

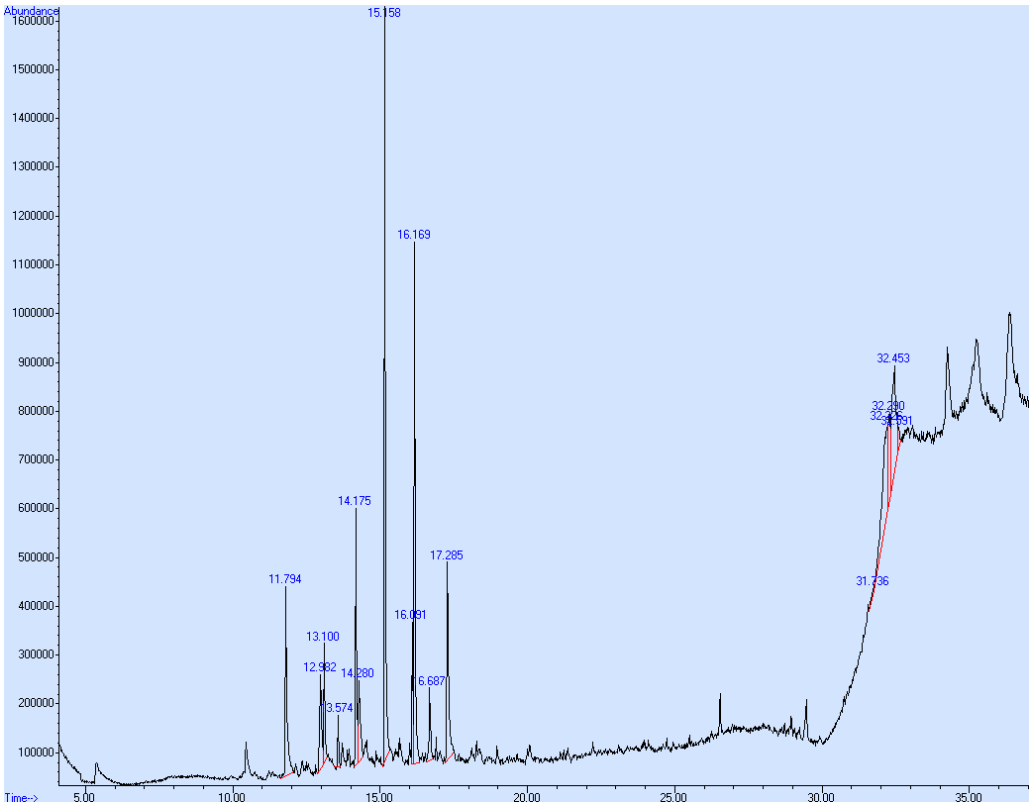

Figure B.7: Gas chromatography mass spectrometry analysis of Tar-PW dissolved in toluene

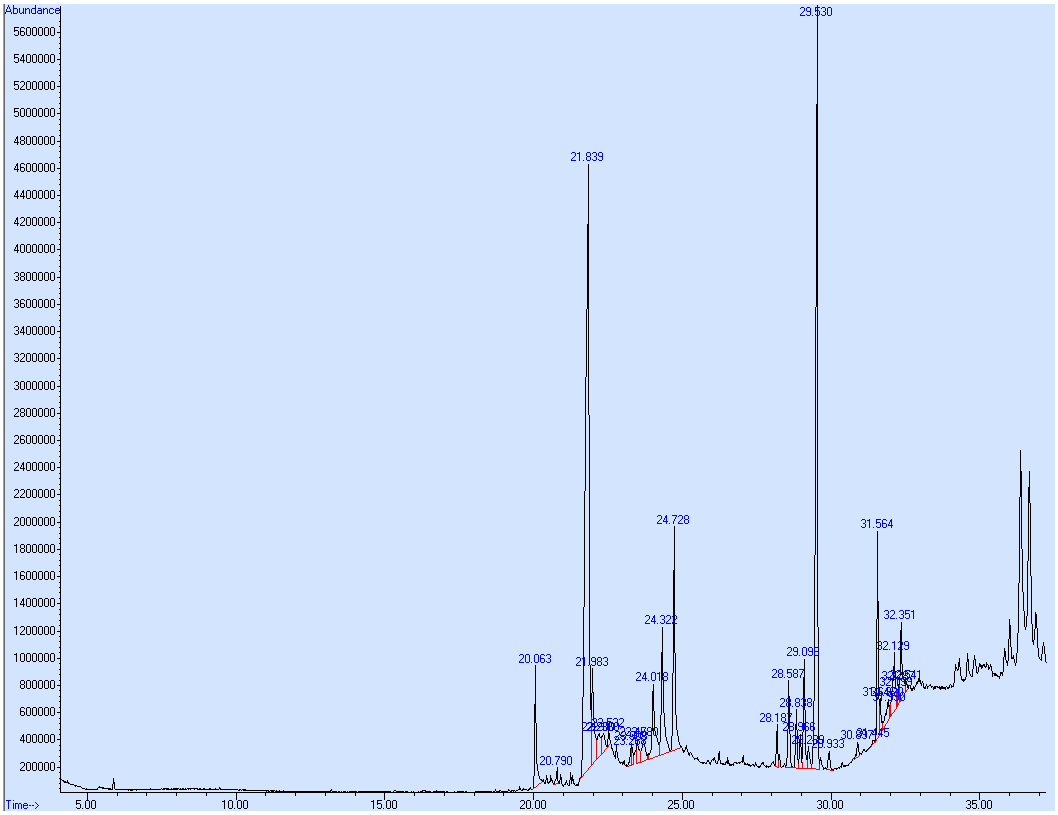

Figure B.8: Gas chromatography mass spectrometry analysis of Tar-BW dissolved in toluene

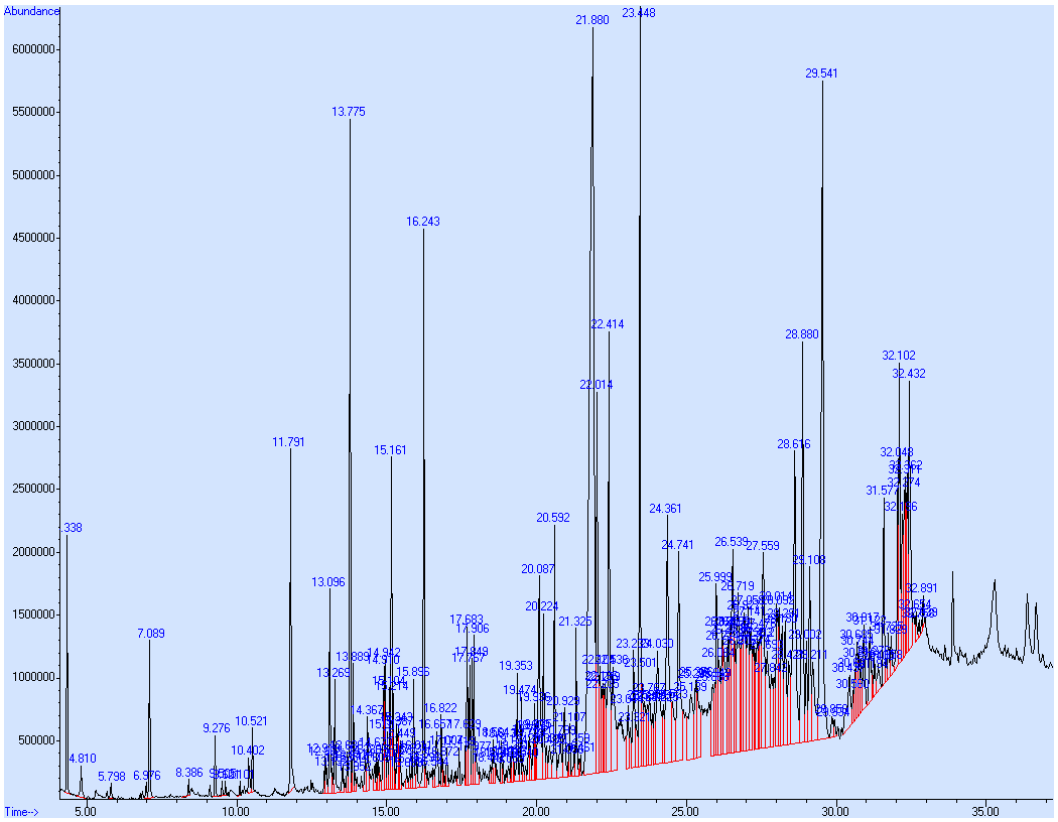

Figure B.9: Gas chromatography mass spectrometry analysis of Tar-Veg dissolved in toluene

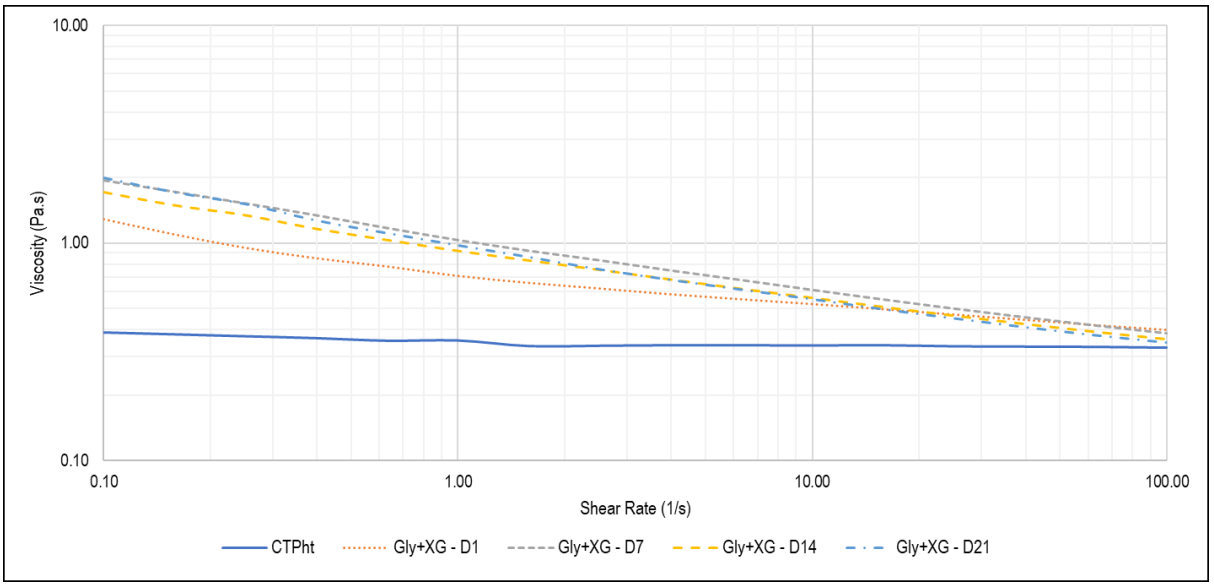

Figure B.10: Isothermal frequency sweep (45°C) after aging for 21 d to determine Newtonian behaviour of glycerine-plasticized xanthan-gum binder

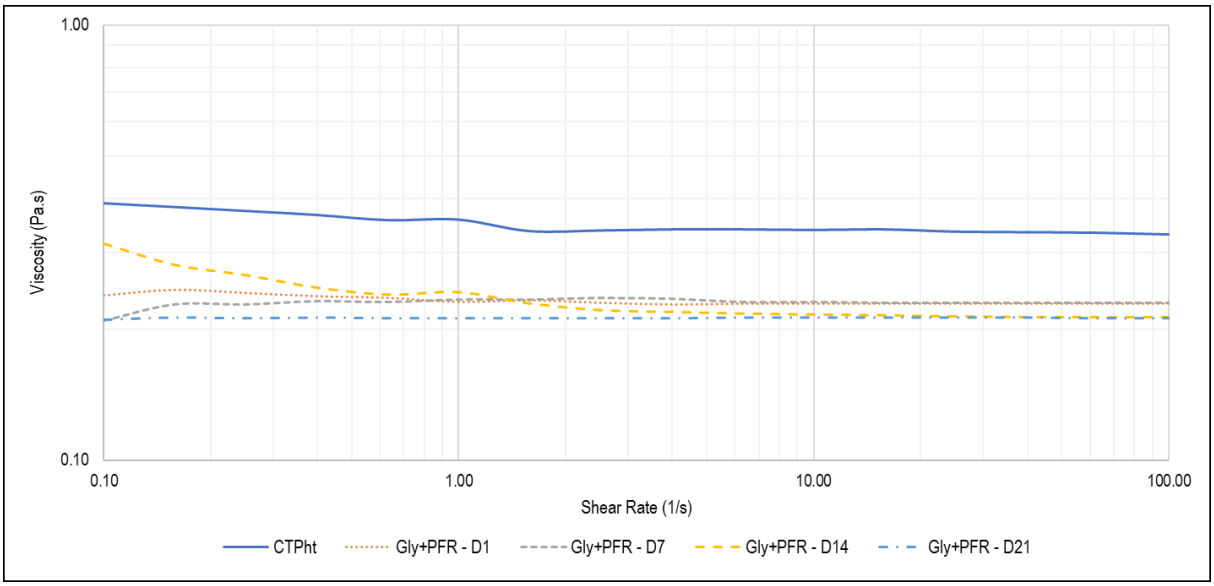

Figure B.11: Isothermal frequency sweep (45°C) after aging for 21 d to determine Newtonian behaviour of phenolic resin addition to glycerine binder

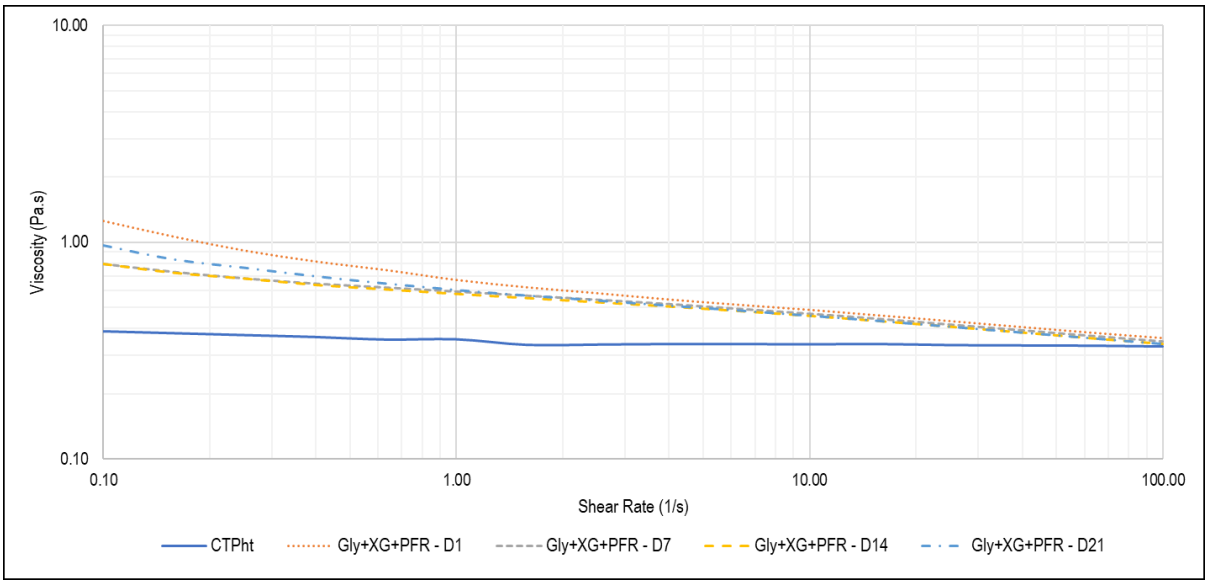

Figure B.12: Isothermal frequency sweep (45°C) after aging for 21 d to determine Newtonian behaviour of phenolic resin addition to glycerine-plasticized xanthan-gum binder

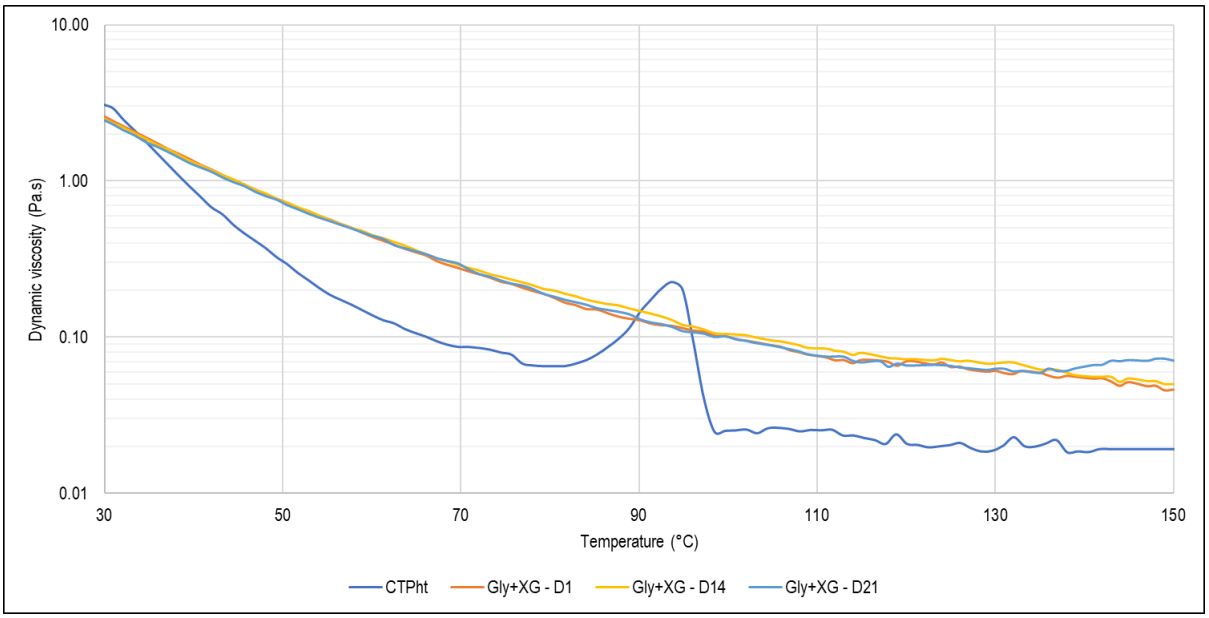

Figure B.13: Effect of temperature on dynamic viscosity of glycerine-plasticized xanthan-gum binder heated from 30–150°C

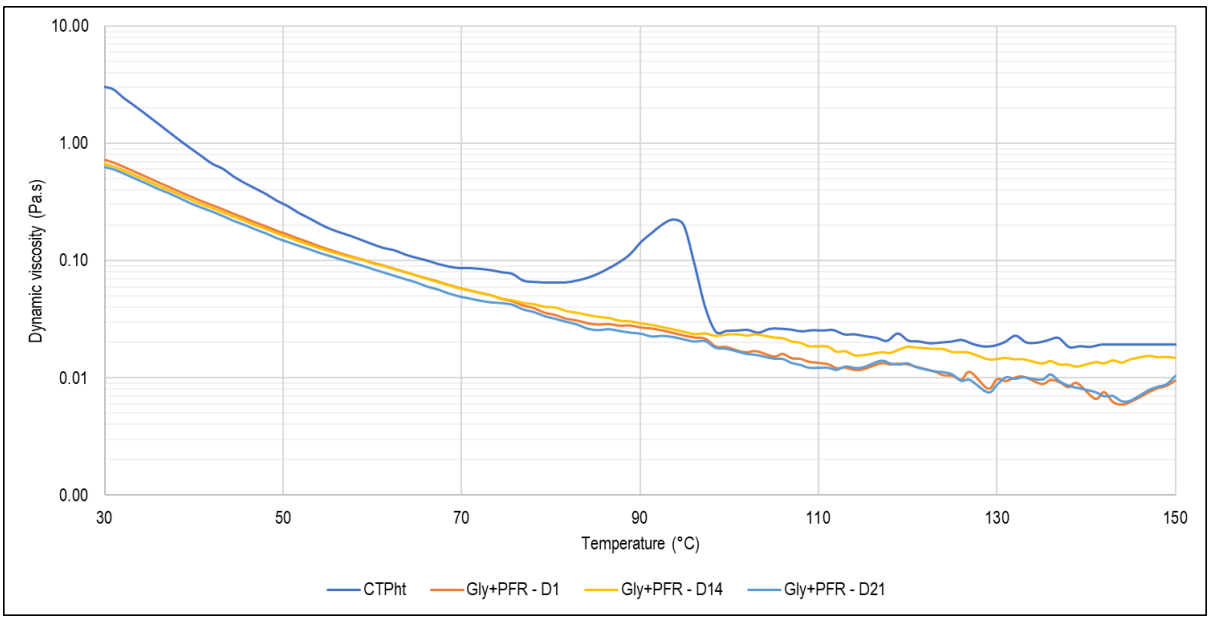

Figure B.14: Effect of temperature on dynamic viscosity of phenolic resin-containing glycerine binder heated from 30–150°C

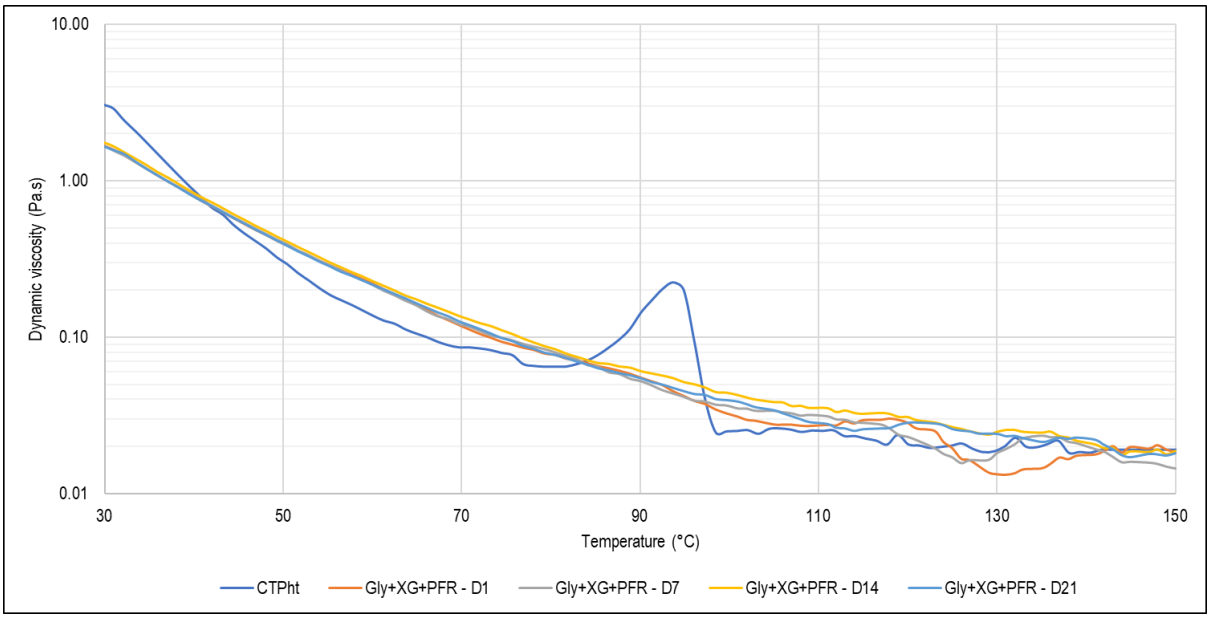

Figure B.15: Effect of temperature on dynamic viscosity of phenolic resin-containing glycerine-plasticized xanthan-gum binder heated from 30–150°C

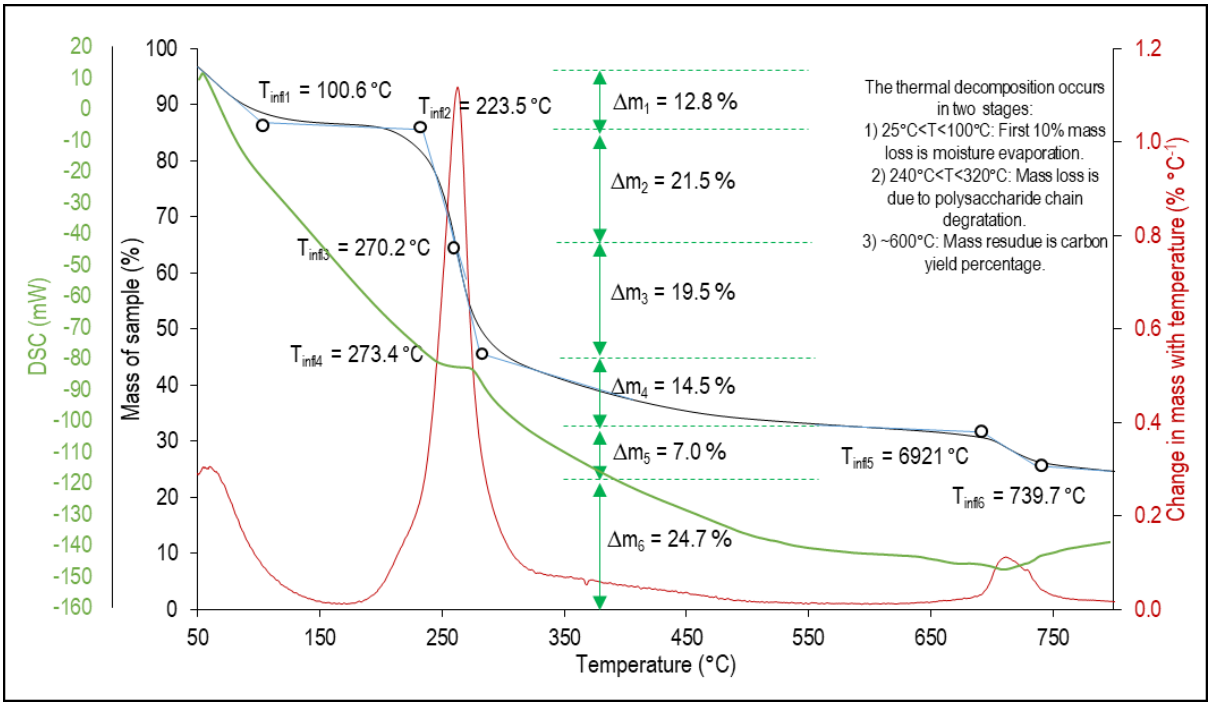

Figure B.16: Thermal analysis results for xanthan gum Source A powder, indicating inflection points and associated changes in mass

Table B.1: Untargeted GC-MS analysis of CTht showing identified compounds and area underneath each compound identification peak

Compound	Normalized Peak Area
Indene	0.96
Benzo[c]thiophene	0.56
Quinoline	0.30
1,1'-Biphenyl	2.61
Biphenylene	10.42
1,1'-Biphenyl, 2-methyl-	0.53
Dibenzofuran	3.33
1H-Phenalene	1.73
9H-Fluorene-9-carboxylic acid	0.15
3,4-Dihydropyrrolo[1',2':3,4]pyrimido[2,1,6cd]pyrrolizine	0.91
[1,1'-Biphenyl]-4-carboxaldehyde	0.25
1,1-DICYANO-2-METHYL-4-(P-METHYPHENYL)PROPENE	0.28
3-(1-methylpyrrol-2-yl)indole	0.22
Dibenzothiophene	1.88
Acridine	1.23
Benzo[h]quinoline	0.35
5,6-Benzoquinoline	0.32
9H-Carbazole	2.24
5,6-Benzoquinoline	0.32
9H-Carbazole	2.24
Dibenzothiophene, 3-methyl- (CAS)	0.35
METHYL-PHENANTHRENE	3.48
Anthracene, 9-methyl-	1.47
4H-Cyclopenta[def]phenanthrene	2.97
Anthracene, 2-methyl-	0.95
1-Methylcarbazole	0.25
1-Methylcarbazole	0.50
2-Phenylnaphthalene	0.74
4,4-dimethyl-3-ethylidene-2-(2'-methyl-1'-propenyl)cyclohexanone	0.37
Phenanthro[4,5-bcd]thiophene	0.80
Benzene, 1,1'-sulfinylbis	0.34
Benzo[b]naphtho[2,3-d]furan	14.19
9,12-Octadecadienoic acid	0.89
1-AZAPYRENE	0.77
PYRROLO(3,2,1-JK)CARBAZOLE	0.41
11H-Benzo[b]fluorene	5.72
AZULENE, 2,6-DIMETHYL-4-PHENYL-	0.76
7H-benz[de]anthracene	1.37
Benzo[b]naphtho[2,1-d]thiophene	1.83
BENZO(c)ACRIDINE	1.72
Benzo[ghi]fluoranthene	0.56
Triphenylene	9.27

Compound	Normalized Peak Area
Naphthacene	4.81
7H-Benz[de]anthracen-7-one	0.68
Phenarsazine, 5,10-dihydro-10-methyl-	0.69
Benzo(a)carbazole	1.87
2,8-BIS(FORMYL)DIBENZOTHIOPHENE	1.23
6-(2-Formylhydrazino)-N,N'-bis(isopropyl)-1,3,5-triazine-2,4-diamine	0.58
Phenol, 2,2'-[1,2-ethanediylbis(nitrilomethylidyne)]bis-	0.66
Benzo[k]fluoranthene	0.95
6-methoxy[1]benzothieno[2,3-c][1,6]naphthyridine	2.27
Benz[j]aceanthrylene, 3-methyl-	1.40
5H-Dibenzo[c,f][1,2]diazepine, 3,8-dichloro-6,11-dihydro-	0.48
3.ALPHA.,5-CYCLO-ERGOSTA-7,22-DIEN-6-ONE	0.43
2,8-diacetyl-peri-xanthenoxanthene-4,10-quinone	1.51
1,12-Benzperylene	1.92

Table B.2: Untargeted GC-MS analysis of CTPht-B showing identified compounds and area underneath each compound identification peak

Compound	Normalized Peak Area
Indene	0.16
Azulene	11.03
Benzo[b]thiophene	0.64
Isoquinoline	1.36
Benzo[b]thiophene, 5-methyl-	0.22
1,1'-Biphenyl	9.79
2-ETHYLNAPHTHALENE	0.82
Biphenylene	9.75
ACENAPHTHENE	7.56
2-Naphthalenecarbonitrile	0.59
Benzene, [1-(2,4-cyclopentadien-1-ylidene)ethyl]-	0.59
Dibenzofuran	6.21
Benzene, 1,1'-methylenebis-	1.62
1,1'-Biphenyl, 2-methyl-	0.48
Dibenzofuran, 4-methyl-	3.51
[1,1'-Biphenyl]-4-carboxaldehyde	1.39
1,1-DICYANO-2-METHYL-4-(P-METHYPHENYL)PROPENE	0.49
Dibenzothiophene	1.49
Phenanthridine	0.28
9H-Carbazole	1.89
4H-Cyclopenta[def]phenanthrene	2.54
1-Methylcarbazole	0.22
4-Methylcarbazole	0.51
2-Phenylnaphthalene	0.88
1,8-Anthracenediamine	0.24
Benzo[b]naphtho[2,3-d]furan	10.57
2-AZAFLUORANTHENE	0.54
11H-Benzo[b]fluorene	3.49
1,2,3,4-tetrahydro-1-phenyl-1,2,3-methenonaphthalene	0.55
Benzo[b]naphtho[2,1-d]thiophene	0.50
Benzo[ghi]fluoranthene	0.87
BENZO(c)ACRIDINE	0.36
Naphthacene	6.17
Triphenylene	2.80
3,4-Dihydrocyclopenta(cd)pyrene (acepyrene)	0.84
pyreno[1,2-c]furan	0.25
Benzo(c)carbazole	0.34
Triphenylene, 2-methyl-	0.56
Chrysene, 5-methyl-	0.20
4-Imidazolidinone, 5,5-diphenyl-2-thioxo-	0.32
Perylene	0.76
Benz[j]aceanthrylene, 3-methyl-	0.98

Compound	Normalized Peak Area
Bikaverin	0.52
5H-Dibenzo[c,f][1,2]diazepine, 3,8-dichloro-6,11-dihydro-	0.30
3.ALPHA.,5-CYCLO-ERGOSTA-7,22-DIEN-6-ONE	0.77
2,8-diacetyl-peri-xanthenoxanthene-4,10-quinone	1.95
2,4,6-Trimethyl-4'-chlorodiphenylsulfone	0.43
1,2:3,4-Dibenzoanthracene	0.36
14-acetyl-1,14-diazabicyclo[10.5.1]octadecane	1.00
(23S)-ethylcholest-5-en-3.beta.-ol	0.32

Table B.3: Untargeted GC-MS analysis of EcoP showing identified compounds and area underneath each compound identification peak

Compound	Normalized Peak Area
1H-Indene, 2,3-dihydro-	1.29
Benzene, 1-methyl-2-(2-propenyl)-	0.19
Benzo[b]thiophene	0.57
Isoquinoline	2.33
Quinoline	0.58
methylbenzo[b]thiophene	0.31
Quinoline, 7-methyl-	0.45
1,1'-BIPHENYL	6.95
2-ETHYLNAPHTHALENE	3.20
1-Naphthalenecarbonitrile	1.86
5-trimethylsilylfuran-2-carboxaldehyde	4.13
Dibenzofuran	26.61
Benzene, [1-(2,4-cyclopentadien-1-ylidene)ethyl]-	3.10
1,1'-Biphenyl, 2-methyl-	6.15
Dibenzofuran, 4-methyl-	11.15
[1,1'-Biphenyl]-4-carboxaldehyde	5.33
1,1-DICYANO-2-METHYL-3-PHENYLPROPENE	1.33
1,1'-Biphenyl, 2-ethyl-	0.61
Azulene, 7-ethyl-1,4-dimethyl-	0.81
Benzene, 1,1'-(1,2-ethenediyl)bis-, (E)-	1.71
CYCLOOCTATETRAENE, PHENYL-	0.87
anti-9-Methyl-1,6-methanofluorene	0.88
1,1'-Biphenyl, 4,4'-dimethyl-	0.67
4-Carbomethoxy-3-methoxy-4-methyl-2,5-cyclohexadien-1-one	1.95
3-(1-methylpyrrol-2-yl)indole	0.53
Dibenzothiophene	3.73
Acridine	0.71
5H-Indeno[1,2-b]pyridine	0.75
Benzene, 1,1'-sulfinylbis-	1.58
3-ETHOXYPHENYLACETONE HYDROXYOXIME	0.70
[2,2](9,9)ANTHRACENEOPHANE	1.78
11H-indolo[3,2-c]quinoline	1.00
Benzene, 1,2,3-trimethoxy-5-(1-propenyl)-, (E)-	0.88
NICKEL, CYCLOPENTADIENYL-(4,4-DIMETHYL-CYCLOPENTENYL)-	0.29
11H-Benzo[b]fluorene	0.52
(E)-2-Benzylidene-1-tetralone	0.80
Furosardonin A	0.42
2,5-Cyclohexadiene-1,4-dione, 2-(phenylthio)-	1.00
(z,z)-3-methyl-3h-cyclonona[def]biphenylene	0.53
1,1':2',1''-Terphenyl	0.24
Naphthacene	0.78
1,12-Benzperylene	0.74

Table B.4: Untargeted GC-MS analysis of CWO showing identified compounds and area underneath each compound identification peak

Compound	Normalized Peak Area
AZULENE	16.35
2-Methylnaphthalene	9.76
1,1'-Biphenyl	5.42
2-ETHYLNAPHTHALENE	3.04
1,1'-Biphenyl, 4-methyl-	5.12
5-trimethylsilylfuran-2-carboxaldehyde	2.00
Dibenzofuran	23.30
Benzene, [1-(2,4-cyclopentadien-1-ylidene)ethyl]-	3.57
1,1'-Biphenyl, 2-methyl-	2.84
9H-Fluoren-9-ol	6.95
Dibenzofuran, 4-methyl-	3.35
Benzene, 1,1'-(1,2-ethenediyl)bis-, (E)-	1.26
1-Heptadecene	1.73
Dibenzothiophene	2.22
1-Nonadecene	2.12
9-Hexacosene	1.35
Docosane	1.45
2-Heptadecenal, 2-tridecyl-, (E)-	0.53
TETRAACETYLADRENALINE	2.07
[1,2'-Binaphthalene]-5,5',8,8'-tetrone, 1',4-dihydroxy-2,3'-dimethyl-, (-)-	0.45
Nonadecane	2.05
6-fluoro-4,6-cholestadien-3,beta,-ol	1.01
N-METHYLDEACETYLCOLCHICINE	0.16
2-(Acetoxymethyl)-3-(methoxycarbonyl)biphenylene	0.13
Eicosane	1.79

Table B.5: Untargeted GC-MS analysis of PCWO showing identified compounds and area underneath each compound identification peak

Compound	Normalized Peak Area
Docosane	0.8963
Triacontane	1.2748
1-Nonadecene	2.4922
1-Octadecene	1.0156
1-Docosene	1.7084
Cyclotetracosane	0.4337
9-Hexacosene	4.2702
1-Octadecanethiol	2.4278
Octadecane. 1-chloro-	4.4517
TETRAACETYLADRENALINE	7.2611
Tritriacontane	2.4545
[1.2'-Binaphthalene]-5.5'.8.8'-tetrone. 1'.4-dihydroxy-2.3'-dimethyl-. (-)-	4.0168
Hexatriacontane	64.887
Pentadecane	1.2337
14-.BETA.-H-PREGNA	1.1763

Table B.6: Untargeted GC-MS analysis of MP showing identified compounds and area underneath each compound identification peak

Compound	Normalized Peak Area
Phenol, 4-methyl-	1.04
Phenol, 2,4-dimethyl-	13.67
Phenol, 3,5-dimethyl-	12.62
Azulene	10.62
Phenol, 4-(1-methylethyl)-	1.12
Phenol, 4-ethyl-3-methyl-	10.85
Phenol, 3-ethyl-5-methyl-	5.40
Isoquinoline	1.05
Phenol, 2,4,5-trimethyl-	1.49
Phenol, 2,4,6-trimethyl-	1.84
.ALPHA. TERPINENE	1.30
Benzaldehyde, 4-ethyl-	6.13
1H-Inden-5-ol, 2,3-dihydro-	3.21
(1'-butenyl)thiophene	0.91
1,1'-Biphenyl	1.22
Ethanone, 1-(3,4-dimethylphenyl)-	3.82
1H-Indole, 2-methyl-	1.00
6-Methyl-4-indanol	1.24
2-ISOPROPENYL-3,6-DIMETHYLPYRAZINE	0.44
1-Naphthalenol	2.72
Dibenzofuran	2.97
2-Naphthalenol	6.16
1,1'-Biphenyl, 4-methyl-	0.78
1-Naphthalenol, 2-methyl-	2.77
2-Methyl-3-vinylbenzofuran	1.87
Dibenzofuran, 4-methyl-	0.95
1-Naphthalenol, 4-methyl-	0.70
2-Methyl-3-vinylbenzofuran	0.61
[1,1'-Biphenyl]-3-ol	0.42
Dibenzothiophene	0.46
5-Dimethylamino-6,6-dimethyl-3,4,6,7-tetrahydro-2H-pyrrolo[2,3-d]pyrimidine-2,4-dione	0.49
Docosanoic acid, docosyl ester	0.13

Table B.7: Untargeted GC-MS analysis of Tar-PW showing identified compounds and area underneath each compound identification peak

Compound	Normalized Peak Area
Phenol, 4-ethyl-2-methoxy-	6.32
4-cyclopropyl-2-methoxyphenol	6.99
Phenol, 2-methoxy-4-propyl-	3.64
Benzene, 1,2,3-trimethoxy-5-methyl-	0.92
5-Acetyl-2-methylthiopyrimidine	5.87
CIS-ISOEUGENOL	3.26
7,8-dimethylbenzocyclooctene	14.90
Phenol, 2,6-dimethoxy-4-(2-propenyl)-	22.62
(3S)-2-chloro-1-phenyl-1-penten-3-ol	11.07
TETRAACETYLADRENALINE	11.38
22BETA-ACETOXY-3BETA,16ALPHA-DIHYDROXY-13,28-EPOXYOLEAN-29-AL	3.58
Eicosane	9.43

Table B.8: Untargeted GC-MS analysis of Tar-BW showing identified compounds and area underneath each compound identification peak

Compound	Normalized Peak Area
Hexadecanoic acid	2.74
1-TERT-BUTYL-4-(PHENYL PHENYLIMINOMETHYL)BENZENE	0.34
9-Octadecenoic acid (Z)-	32.62
Octadecanoic acid	2.94
9,12-Octadecadienoic acid (Z,Z)-	2.79
Linoleic acid	0.31
Cyclododecyne	0.51
(+-)-cis-3,4,6,9-tetrahydro-10-hydroxy-7-methoxy-1,3,8-trimethyl-1H-naphtho[2,3-c]pyran-6,9-dione[(+-)-ventilagone 7-methyl ethyl]	3.16
1-Phenanthrenecarboxylic acid, 1,2,3,4,4a,9,10,10a-octahydro-1,4a-dimethyl-7-(1-methylethyl)-, [1R-(1,alpha,,4a,beta,,10a,alpha,)]-	4.37
2,2'-Dimethyl-4,4',5,5'-tetramethoxybiphenyl	5.87
Bikaverin	2.07
7-(Trimethylsilyloxy)-3-[4-(trimethylsiloxy)phenyl]-4H-1-benzopyran-4-one	1.42
2,4-Dibenzyl-5,8-dimethoxy-6-methyl-1-naphthol	0.75
ERGOSTA-4,6,22-TRIEN-3ALPHA-OL	2.84
2,3-bis(p-methoxyphenyl)pyrazino[2,3-b]quinoxaline-1,4-dioxide	0.74
2,8-diisopropyl-peri-xanthenoxanthene-4,10-quinone	21.21
Vitamin E	4.34
Ergost-5-en-3-ol, (3,beta,)-	0.42
(23S)-ethylcholest-5-en-3,beta,-ol	3.77
(24S)-Ethyl-5,alpha,-cholestan-3,beta,-ol	0.80
5-(tert-Butyldimethylsilyl)oxy]-1,2,3,4,6,6a,12a,12b-oct\ahydro-6,9a-dimethyl-12H-benzo[a]xanthen-12-one	1.13
N-METHYLDEACETYLCOLCHICINE	0.19
Benzo[c]fluorenone	2.22
Benzenamine, 2,3,4,5,6-pentachloro-	0.30
Stigmast-4-en-3-one	2.14

Table B.9: Untargeted GC-MS analysis of Tar-Veg showing identified compounds and area underneath each compound identification peak

Compound	Normalized Peak Area
.ALPHA.-PINENE	1.79
LIMONENE	0.59
ALLO-OCIMENE	0.20
.BETA. FENCHYL ALCOHOL	0.22
Phenol, 4-ethyl-2-methoxy-	2.19
2-methoxy-4-propyl-phenol	0.74
1,2,4-Methenoazulene, decahydro-1,5,5,8a-tetramethyl-, [1S-(1.alpha.,2.alpha.,3a.beta.,4.alpha.,8a.beta.,9R*)]-	11.50
Junipene	2.18
.BETA.-CARYOPHYLLENE	0.35
.ALPHA.-HUMULENE	0.25
6,10,11,11-TETRAMETHYL-TRICYCLO[6.3.0.1(2,3)]UNDEC-1(7)ENE	0.47
.beta.-Himachalene	0.35
.gamma.-Cadinene	0.29
.delta.-cadinene (armoise-Maroc)	1.13
Naphthalene, 1,2,3,4-tetrahydro-1,6-dimethyl-4-(1-methylethyl)-, (1S-cis)-	1.17
CADINA-1,4-DIENE	0.11
.alpha.-Caryophyllene alcohol	2.22
longiborneol	1.93
.alpha.-Gurjunene	0.18
2,8-Decadiyne	0.54
.ALPHA.-GUAIENE	0.57
(2.alpha.,6.alpha.)-cis-9,10-Dimethyl-4-oxateracyclo[6.3.0.0(2,6).0(7,11)]undecane	0.30
.ALPHA.-COPAENE	0.39
2-Methyl-4-nitrosoresorcinol	0.36
2-Fluorophenyl isothiocyanate	0.27
Sandaracopimaradiene	0.26
Hexadecanoic acid	1.56
1,4a.beta.-Dimethyl-7-isopropyl-1,2,3,4,4a,9,10,10a.alpha.-octahydrophenanthrene	0.82
s-Indacen-1(2H)-one, 3,5,6,7-tetrahydro-3,3,4,5,5,8-hexamethyl-	1.04
Methyl acridine-3-carboxylate	0.53
10-Methoxybenz[a]azulen-1,4-dione	0.58
9,17-Octadecadienal, (Z)-	15.16
(+)1a7,4a,9,10,10a-dodecahydro-1,4a,7-trimethyl-7-vinyl-1-phenanthrencarbaldehydSHyl 4,azc.beta.thiomethyl](12-YL2ethylthioylenC1ethyldethyl3-YLaphthc]taoxm.beta.ano6, [ucH0alfPal[yl9	1.73
9,12-Octadecadienoic acid (Z,Z)-	0.45
Phenanthrene, 1-methyl-7-(1-methylethyl)-	1.64
4-(2'-Ethyl-5'-phenyl-pyrrol-3'-yl)pyridine	0.52
DEHYDROABIETIC ACID	2.70
Thiocyanic acid, 4-oxotricyclo[3.3.1.1(3,7)]dec-2-yl ester, (1.alpha.,2.alpha.,3.beta.,5.alpha.,7.beta.)-	2.56

Compound	Normalized Peak Area
(+-)-cis-3,4,6,9-tetrahydro-10-hydroxy-7-methoxy-1,3,8-trimethyl-1H-naphtho[2,3-c]pyran-6,9-dione[(+-)-ventilagone 7-methyl ethyl]	2.15
1-Phenanthrenecarboxylic acid, 1,2,3,4,4a,9,10,10a-octahydro-1,4a-dimethyl-7-(1-methylethyl)-, [1R-(1.alpha.,4a.beta.,10a.alpha.)]-	1.44
1,4-Dihydro-9-isopropylidene-5,6,7,8-tetramethoxy-1,4-methanonaphthalene	1.97
syn-1-(p-nitrophenyl)-2-(phenyl)-1-(methoxycarbonyl)cyclopropane	0.79
2-amino-3-(p-methoxy-phenyl-carbamoyl)-1-azirine	0.51
3,8-dimethyl-5,9-dinitrobenzo[g]isoquinoline	1.34
(E)-4-(2',4',4'-Trimethylbicyclo[4.1.0]hept-2'-en-3'-yl)-3-buten-2-one	1.50
2-Cyclohexene-1-carboxaldehyde, 2,6-dimethyl-6-(4-methyl-3-pentenyl)-	1.57
Ergosta-5,22-dien-3-ol, (3.beta.,22E)-	0.83
.delta.-tocopherol	0.95
Ergosta-4,22-diene	0.90
Bikaverin	3.03
4ALPHA-METHYLCHOLEST-7-EN-3-ONE	3.94
Cholesta-8,24-dien-3.beta.-ol, 4.beta.-methyl-	0.57
.beta.-Tocopherol	1.21
2,8-diisopropyl-peri-xanthenoxanthene-4,10-quinone	6.21
ALLO-AROMADENDRENE	0.77
CIS-CARYOPHYLLENE	0.92
3.ALPHA.,5-CYCLO-ERGOSTA-7,22-DIEN-6-ONE	0.41
Ergost-5-en-3-ol, (3.beta.)-	0.61
Stigmasta-5,23-dien-3.beta.-ol	0.51
(23S)-ethylcholest-5-en-3.beta.-ol	0.88
Xanthotoxin	0.93
Endosulfan	1.42
Nootkatone	0.84
ALLOAROMADENDRENE	1.63
(endo)-9-(t-butyl)-1,2,3,4-tetrahydro-5,6,7,8,N'-pentamethyl-1,4-iminonaphthalene-2,3-dicarboximide	0.79
3,4-DIMETHYL-5-(3,5-DIMETHYL-4-PYRIDYL)ISOXAZOLE	1.56